การประเมินฤทธิ์ต้านออกซิเดชันและการพัฒนาสูตรตำรับของสารสกัดขิงที่
บรรจุในโซลิดลิปิดนาโนพาร์ทิเคิลเพื่อนำส่งเข้าสู่ผิวหนัง

นางสาวเพชรชมพู ศิริพันธุ์

วิทยานิพนธ์นี้เป็นส่วนหนึ่งของการศึกษาตามหลักสูตรปริญญาเภสัชศาสตรมหาบัณฑิต
สาขาวิชาเภสัชกรรม ภาควิชาเภสัชกรรม
คณะเภสัชศาสตร์ จุฬาลงกรณ์มหาวิทยาลัย
ปีการศึกษา 2551
ลิขสิทธิ์ของจุฬาลงกรณ์มหาวิทยาลัย

ANTIOXIDANT EVALUATION AND FORMULATION
DEVELOPMENT OF *ZINGIBER OFFICINALE* EXTRACT
LOADED IN SOLID LIPID NANOPARTICLES FOR SKIN
DELIVERY

Miss Petchompoo Siriphan

A Thesis Submitted in Partial Fulfillment of the Requirements

for the Degree of Master of Science in Pharmacy Program in Pharmaceutics

Department of Pharmacy

Faculty of Pharmaceutical Sciences

Chulalongkorn University

Academic Year 2008

512098

Thesis Title	ANTIOXIDANT EVALUATION AND FORMULATION DEVELOPMENT OF *ZINGIBER OFFICINALE* EXTRACT LOADED IN SOLID LIPID NANOPARTICLES FOR SKIN DELIVERY
By	Miss Petchompoo Siriphan
Field of Study	Pharmaceutics
Thesis Advisor	Associate Professor Suchada Chutimaworapan, Ph.D.
Thesis Co-Advisor	Associate Professor Chaiyo Chaichantipyuth, Ph.D.

Accepted by the Faculty of Pharmaceutical Sciences, Chulalongkorn University in Partial Fulfillment of the Requirements for the Master's Degree

.......*Pornpen Pramyot C.*.........Dean of the Faculty of Pharmaceutical Sciences

(Associate Professor Pornpen Pramyothin, Ph.D.)

THESIS COMMITTEE

............*Porntip Nimmannitya*.......... Chairman

(Associate Professor Porntip Nimmannitya)

........*Suchada Chutimaworapan*....... Thesis Advisor
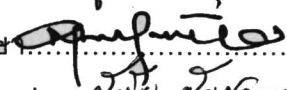
(Associate Professor Suchada Chutimaworapan, Ph.D.)

........*Chaiyo Chaichantipyuth*........ Thesis Co-advisor

(Associate Professor Chaiyo Chaichantipyuth, Ph.D.)

........*Manee Luangtana-anan*........ Member

(Associate Professor Manee Luangtana-anan, Ph.D.)

........*Waraporn Suwakul*............ Member

(Associate Professor Waraporn Suwakul, Ph.D.)

เพชรชมพู ศิริพันธุ์: การประเมินฤทธิ์ต้านออกซิเดชันและการพัฒนาสูตรตำรับของสาร
สกัดขิงที่บรรจุในโซลิดลิปิดนาโนพาร์ทิเคิลเพื่อนำส่งเข้าสู่ผิวหนัง (ANTIOXIDANT
EVALUATION AND FORMULATION DEVELOPMENT OF *ZINGIBER
OFFICINALE* EXTRACT LOADED IN SOLID LIPID NANOPARTICLES FOR SKIN
DELIVERY) อ. ที่ปรึกษา: รศ.ดร.สุชาดา ชุติมาวรพันธ์, อ. ที่ปรึกษาร่วม:รศ.ดร.ชัยโย
ชัยชาญทิพยุทธ, 237 หน้า.

การศึกษานี้มีวัตถุประสงค์เพื่อประเมินฤทธิ์ต้านออกซิเดชัน พัฒนาสูตรตำรับและประเมินลักษณะของ
สารสกัดขิงที่บรรจุในโซลิดลิพิดนาโนพาร์ทิเคิล (เอสแอลเอ็น) การประเมินฤทธิ์ของสารสกัดขิงซึ่งมีรายงานว่า
สารสำคัญหลักของขิง คือ สาร [6]- จิงเจอรอล ใช้การทดสอบการต้านอนุมูลอิสระดีพีพีเอชและไฮดรอกซิล ผล
การทดสอบดีพีพีเอชของสารสกัดด้วยอะซิโตนและสารสกัดแยก [6]-จิงเจอรอลพบว่ามีฤทธิ์ต่ำกว่าวิตามินอีและ
วิตามินซีโดยสารมาตรฐาน[6]-จิงเจอรอลมีฤทธิ์สูงสุด ผลการทดสอบฤทธิ์ต้านอนุมูลไฮดรอกซิลของสารสกัด
ด้วยอะซิโตนและสารสกัดแยก [6]-จิงเจอรอลพบว่ามีฤทธิ์ดีกว่าควอซีติน ดังนั้นสารสกัดด้วยอะซิโตนซึ่งสกัดได้
ง่ายจึงเหมาะสมที่ใช้บรรจุในเอสแอลเอ็น การเตรียมเอสแอลเอ็นใช้วิธีปั่นผสมด้วยความดันสูงโดยใช้ไขมัน 2
ชนิด คือ กลิเซอริลพาลมิโทสเตียเรต และ กลิเซอริลบีฮีเนต ใช้พอล็อกซาเมอร์ 188 หรือ ทวีน 80 ความเข้มข้น 1,
3 และ 5%เป็นสารเพิ่มความคงตัว พบว่าขนาดอนุภาคของเอสแอลเอ็นที่เตรียมจากกลิเซอริลพาลมิโทสเตียเร
ตเมื่อวัดโดยโฟตอนคอรีเลชันสเปคโทรสโคปีมีขนาดเล็กกว่าของกลิเซอริลบีฮีเนต และมีการกระจายขนาด
อนุภาคแคบ เอสแอลเอ็นที่ได้มีความคงตัวที่ 4 องศาเซลเซียสดีกว่าที่อุณหภูมิห้อง ได้คัดเลือกเอสแอลเอ็นที่คง
ตัว 6 สูตรตำรับซึ่งประกอบด้วยกลิเซอริลพาลมิโทสเตียเรตร่วมกับพอล็อกซาเมอร์ 188 หรือ ทวีน 80 ความ
เข้มข้น 3 และ 5% และ กลิเซอริลบีฮีเนตร่วมกับทวีน 80 ความเข้มข้น 3 และ 5% พบว่าขนาดอนุภาคจากกล้อง
จุลทรรศน์แบบส่องผ่านส่วนใหญ่ประมาณ 200-300 นาโนเมตร ประสิทธิภาพการกักเก็บของสาร
[6]-จิงเจอรอลของเอสแอลเอ็น 6 สูตรตำรับมีค่าระหว่าง 84.36-96.24% และเปลี่ยนแปลงเหลือ 78.91-93.26%
เมื่อเก็บไว้นาน 2 เดือน ผลจากดิฟเฟอเรนเชียลสแกนนิงแคลอรีเมทรี และพาวเดอร์เอ็กซ์เรย์ดิฟแฟรคชันแสดงให้
เห็นว่ามีการเปลี่ยนรูปของไขมันไปสู่รูปพหุสัณฐานที่คงตัวระหว่างสภาวะเก็บรักษาและทำให้เกิดการผลักสาร
สกัดขิงออกจากส่วนแกนที่เป็นไขมัน รูปแบบการปลดปล่อยสาร [6]-จิงเจอรอลออกจากเอสแอลเอ็นพบว่ามีการ
ปลดปล่อยประมาณ 25-30% ที่เวลา 24 ชั่วโมง การปลดปล่อยสาร [6]-จิงเจอรอลซึ่งออกจากระบบอย่างช้าๆ
เมื่อเวลาผ่านไปเนื่องจากการเอสแอลเอ็นมีประสิทธิภาพในการกักเก็บสารสกัดไว้ในเอสแอลเอ็นสูง การวิเคราะห์
กลไกการปลดปล่อยของสาร[6]-จิงเจอรอลพบว่าเป็นสัดส่วนกับรากที่สองของเวลา แสดงว่า [6]-จิงเจอรอลอาจ
ปลดปล่อยออกจากนาโนพาร์ทิเคิลโดยการแพร่ การศึกษาการซึมผ่านผิวหนังซึ่งใช้ผิวหนังของลูกหมูเป็นเมม
เบรนโมเดล พบว่า [6]-จิงเจอรอลซึมเข้าสู่ผิวหนังประมาณ 2.54±0.43%

ภาควิชา	เภสัชกรรม	ลายมือชื่อนิสิต..
สาขาวิชา	เภสัชกรรม	ลายมือชื่ออาจารย์ที่ปรึกษา........................
ปีการศึกษา	2551	ลายมือชื่ออาจารย์ที่ปรึกษาร่วม..................

4976586033   : MAJOR PHARMACEUTICS

KEY WORD: [6]-GINGEROL / *ZINGIBER OFFICINALE* EXTRACT / ANTIOXIDANT / SOLID LIPID NANOPARTICLES / SKIN DELIVERY

PETCHOMPOO SIRIPHAN: ANTIOXIDANT EVALUATION AND FORMULATION DEVELOPMENT OF *ZINGIBER OFFICINALE* EXTRACT LOADED IN SOLID LIPID NANOPARTICLES FOR SKIN DELIVERY. THESIS PRINCIPAL ADVISOR: ASSOC. PROF. SUCHADA CHUTIMAWORAPAN, Ph.D., THESIS COADVISOR: ASSOC. PROF. CHAIYO CHAICHANTIPYUT, Ph.D., 237 pp.

The objective of this study was to evaluate antioxidative activity of ginger extracts, to formulate and characterize solid lipid nanoparticles (SLN) containing ginger extract. Ginger extracts which were reported to contain the main principle namely, [6]-gingerol were evaluated using the DPPH method and the hydroxyl radicals scavenging assay. The DPPH-scavenging activity of acetone and isolated [6]-gingerol extracts were lower than vitamin E and vitamin C, while the standard [6]-gingerol had the greatest activity. In the hydroxyl radical scavenging test, acetone and isolated [6]-gingerol extract exhibited higher activity than quercetin. Consequently, acetone extract which was prepared by simple extraction method was selected to load in SLN. SLN were produced by high pressure homogenization technique using two lipids, glyceryl palmitostearate (GP) and glyceryl behenate (GB). Either Poloxamer 188 (P188) or Tween 80 (Tw80) of 1-5% was used as stabilizer. The sizes measured by photon correlation spectroscopy of GP-SLN were smaller than those of GB-SLN with acceptable size distribution. SLN displayed better stability profiles at 4 °C than at room temperature. Six stable SLN formulations were obtained from the GP-SLN with 3 and 5% of P188 or Tw80 and GB-SLN with 3 and 5% Tw80. The particle sizes from transmission electron electroscopy of SLN were predominantly 200-300 nm. The entrapment efficiency of [6]-gingerol of six formulations were ranged from 84.36-96.24% and changed to 78.91-93.26% at 2 months storage. Differential scanning calorimetry and powder x-ray diffraction studies revealed that lipid transformation to stable polymorph was occurred during storage and affected the expulsion of ginger extract from lipid core. The release profiles showed that [6]-gingerol released approximately 25-30% from all SLN formulations was achieved at 24 hours. The sustained release profiles were performed according to high entrapment efficiency of SLN. The release mechanism of [6]-gingerol was analyzed to be proportional to the square root of time, indicating that [6]-gingerol might be released from the nanoparticles by diffusion. The skin permeation study using porcine skin as model membrane showed that [6]-gingerol permeated into skin approximately 2.54±0.43%.

Department : Pharmacy	Student's Signature: ...Petchompoo Siriphan...
Field of Study : Pharmaceutics	Principal Advisor's Signature:...
Academic Year : 2008	Co-Advisor's Signature:...

ACKNOWLEDGEMENTS

CONTENTS

LIST OF TABLES

LIST OF FIGURES

LISTS OF ABBREVIATIONS

ANOVA	=	analysis of variance
°C	=	degree Celsius
CI	=	confidence interval
conc	=	concentration
cm	=	centimeter
CV	=	coefficient of variation
df	=	degree of freedom
DPPH	=	1,1-diphenyl-2-picryl-hydrazyl radical
DSC	=	differential scanning calorimetry
et al.	=	*et alii*, 'and others'
g	=	gram
GB	=	glyceryl behenate
GP	=	glyceryl palmitostearate
hr	=	hour
HPLC	=	high performance liquid chromatography
k	=	release rate constant
mg	=	milligram
min	=	minute
mJ	=	millijoule
ml	=	milliliter
mm	=	millimeter
MW	=	molecular weight
n	=	sample size
nm	=	nanometer
P188	=	Poloxamer® 188
pH	=	the negative logarithm of the hydrogen ion concentration
R^2	=	coefficient of determination
RI	=	reflective index
ROS	=	reactive oxygen species
rpm	=	round per minute

s	=	second
SD	=	standard deviation
SLN	=	solid lipid nanoparticles
SS	=	sum of square
TEM	=	Transmission Electron Microscopy
TLC	=	thin layer chromatography
Tw80	=	Tween® 80
μg	=	microgram
USP/NF	=	The United States Pharmacopoeia/National Formulary
UV	=	ultraviolet
w/v	=	weight by volume
w/w	=	weight by weight
XRD	=	x-ray diffractometry

CHAPTER I
INTRODUCTION

Nowadays, active substances derived from herbal plants have a major role in both pharmaceutical and cosmetic industries. Many products from natural substances were developed under new drug delivery technologies for added valuable cost. Since the sources of herbal plants are commonly found, it is possible to produce a high quantity with low cost.

Ginger (*Zingiber officinale*, Roscoe) has been used as a spice for over 2000 years. Its roots and the obtained extracts contain polyphenol compounds, gingerol derivatives. One of the major components, [6]-gingerol, has been used as a marker substance of ginger. The [6]-gingerol (1-[4´-hydroxy-3´-methyoxyphenyl]-5-hydroxy-3-decanone), a naturally occurring plant phenol, exhibits diverse pharmacological effects including high antioxidant activity (Stoilova et al., 2006), reactive oxygen species (ROS) scavenging activity (Kim et al., 2007), anti-inflammatory as a cyclooxygenases (COX-1, COX-2) inhibitor (Ippoushi et al., 2003) and skin cancer development suppressors (Park et al., 1998). The compound also reduces UVB-induced transcription factor nuclear factor (NF-kB), the important compound in the inflammation of sunburn reactions (Rabe et al, 2006).

Cumulative and prolonged exposures to ultraviolet radiations are now recognized to induce deleterious reactions in human skin, including cutaneous ageing, photo-carcinogenesis and various inflammatory skin disorders (Gilchrest, 1996). UVB and UVA are proved to generate DNA damage directly and indirectly through oxidative stress, by increasing the level of ROS. The use of photo-protecting actives increased significantly because human skin was frequently exposed to ultraviolet (UV) radiations. In addition, the water loss from the skin is also responsible for decrease in elasticity and further premature aging including the appearance of wrinkles. Cutaneous anti-oxidants play a pivotal role in the defence mechanisms against ROS generated by UV radiations, heat and air pollutants. Low-molecular weight anti-oxidants widely used for facial rejuvenation have been incorporated into lipid nanoparticles. Examples are ascorbyl palmitate (Kristl et al. 2003), α-tocopherol (Wissing and Muller 2001a), coenzyme Q10 (Bunjes et al. 2001), and α-lipoic acid (Souto, Muller and Gohla, 2005)

In recent years, considerable energy has been devoted to the formulation of colloidal drug delivery system. Many researchers have studied the preparation of solid lipid nanoparticles (SLN) in nanometer size range with narrow size distribution. The technique commonly used to produce SLN is high pressure homogenization. Concerning optimal topical formulations, SLN show distinct advantages over classical colloidal carriers such as the exhibition of high physical stability, protection of incorporated labile actives against degradation (Jenning, Schafer-Korting and Gohla, 2000c), excellent *in vivo* tolerability (Muller, Radtke and Wissing, 2002). SLN also give occlusive effect due to their solid matrix (Wissing and Muller 2003b), avoiding water loss, thus increasing skin hydration and UV blocking effect which is due to increased reflection and scattering of radiation (Wissing and Muller 2002a). In addition, they can also be added to semi-solid formulations in order to form cream, lotion or gel, so that there are various possibilities of developing a suitable formulation for different needs. Because of their particulate characters and adhesive properties, SLN can also act as physical sunscreens on their own. In addition, when incorporating free radical scavenging compound into SLN, a synergistic effect on skin photodamage protective activity will be occurred.

Although solid lipid nanoparticles are an efficient drug delivery system, compositions in their formulas had an effect on their properties. To date, there is no study that investigates the effect of solid lipid nanoparticles loaded with ginger extract on their physicochemical properties. Therefore, we need to investigate formulation factors which affect the properties of solid lipid nanoparticles loaded with ginger extract.

In this study, it has been aimed to investigate the isolated extraction of active constituents and to evaluate and compare antioxidative properties of *Zingiber officinale* extracts. This study also focused on development process and characterization of solid lipid nanoparticles containing *Zingiber officinale* extract for skin delivery.

The purposes of this study were as follows:

1. To develop the extraction of [6]-gingerol from *Zingiber officinale* extract and characterize by qualitative and quantitative analyses by chromatograph technique.
2. To investigate antioxidative activity of *Zingiber officinale* extract *in vitro*.
3. To formulate solid lipid nanoparticles and investigate the effects of types of solid lipid and types and amount of surfactant on the physicochemical properties of solid lipid nanoparticles.
4. To investigate the physical stability, entrapment efficiency, release property and skin permeation of [6]-gingerol from solid lipid nanoparticles loaded with *Zingiber officinale* extract.

CHAPTER II

LITERATURE REVIEW

A. Botanical, Chemical and Pharmacological Aspects of *Zingiber officinale* Rosc.

1. Botanical aspects of *Zingiber officinale* Rosc.

Zingiber officinale, known as ginger, is in Family Zingiberaceae which prefers tropical climate regions such as South East Asia, India, China and Jamaica. The ginger plant is an erect perennial growing from one to three feet in height. The stem is surrounded by the sheathing bases of the two-ranked leaves. A club-like spike of yellowish, purple-lipped flowers have showy greenish yellow bracts beneath. The herb develops several lateral shoots in clumps, which begin to dry when the plant matures. Leaves are 15-30 cm long and 2-3 cm broad with sheathing bases, the blade gradually tapering to a point. Flowers are rare, rather small. They have superior calyx and three toothed with opening split on one side. Three corollas are subequal oblong to lanceolate connate greenish segments. The branches arise obliquely from the rhizome, 1-3 cm length, and terminate in depressive scars or in undeveloped buds.

The unpeeled rhizome of ginger, in transverse section, shows a zone of cork tissue. The outer zone of rhizome have the irregular arranged cells, produced by cortical cells and the inner zone of cells arranged in radial rows, produced by tangential division of the cortical cells. Smoothed transversely cut surface exhibiting a narrow cortex separated by an endodermis from a much wider stele, numerous widely scattered fibrovascular bundles. No cork cambium is differentiated. The cortical cells contain abundant starch grains. There have numerous oil cells, yellowish-brown oleoresin enclosed, scattered in the cortex. It has aromatic odor and pungent taste (Kapoor, 2001). The ginger rhizomes are depicted in Figure 1

Figure 1 *Zingiber officinale* rhizomes

2. **Chemical components of *Zingiber officinale* Rosc.**

The sensory perception of ginger in the mouth and the nose arises from two distinct groups of chemicals, volatile oils and non-volatile pungent compounds.

2.1 Volatile oils

Ginger has been reported to contain usually 1-3% of volatile oil. The volatile oil components in ginger consist mainly of sesquiterpene hydrocarbons, predominantly zingeberene (35%), curcumene (18%) and farnesene (10%), with lesser amounts of bisabolene and β-sesquiphellandrene. A smaller percentage of at least 40 different monoterpenoid hydrocarbons are present with 1, 8-cineole, linalool, borneol, neral, and geraniol being the most abundant (Govindarajan, 1982). Many of these volatile oil constituents contribute to the distinct aroma and taste of ginger.

2.2 Non-volatile pungent compounds

The chemical studies on the biologically active constituents of the rhizome of *Zingiber officinale* have revealed that the major substances, non-volatile pungent principles, are gingerols, the others components are shogaols, gingediol, gingerdione and paradols. These compounds produce a ''hot'' sensation in the mouth (Jolad et al., 2004). The substances of therapeutic interest are the gingerols due to various pharmacological effects. The main constituents in ginger are series of homologous phenolic ketones known as gingerols, a series of chemical homologs differentiated by the length of their unbranched alkyl chains. The major gingerol, a maker substance of

ginger, is [6]-gingerol (1-(40-hydroxy-30-methyoxyphenyl)-5-hydroxy-3-decanone), while [8]-gingerol and [10]-gingerol occur in small quantities. The appearance of [6]-gingerol is the clearly pale yellow oil. The gingerols are thermally unstable dehydrated and are converted under high temperature to shogaols, [6]-shogaol, [8]-shogaol and [10]-shogaol (He et al., 1998). The shogaol series of compounds, even more pungent than the gingerols, are gingerol analog with a 4, 5 double bond, resulting from elimination of the 5-hydroxy group. The chemical structures of gingerols and related compounds are depicted in Figure 2 and Table1.

Compound	n	R	MW.
4-gingerol	2	H	266
6-gingerol	4	H	294
8-gingerol	6	H	322
10-gingerol	8	H	350
Me-6-gingerol	4	Me	308

Compound	n	R	MW.
6-shogaol	4	H	276
8-shogaol	6	H	304
10-shogaol	8	H	322
Me-6-shogaol	4	Me	290

Compound	n	R	MW.
6-gingediol	2	H	296
8-gingediol	4	H	324
12-gingediol	6	H	380
Me-12-gingediol	8	H	394

10-gingerdione   MW = 348
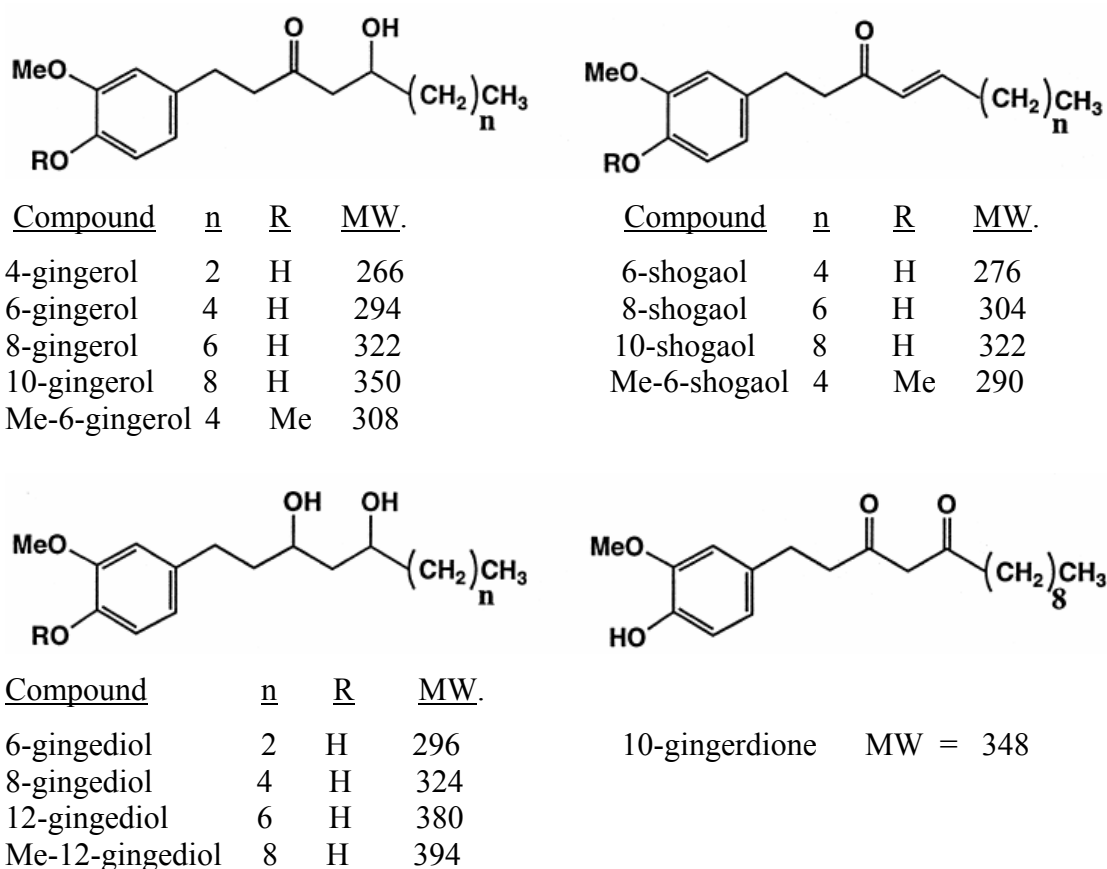
Figure 2 The chemical structures of ginger constituents.

2.3 Other constituents

In addition to the extractable oleoresins, ginger contains many fats, waxes, carbohydrates, vitamins and minerals. Ginger rhizomes also contain a potent proteolytic enzyme called zingibain.

Table 1 Chemical structures and Log P of gingerol analogues and related substances (Tjendraputra et al., 2001)
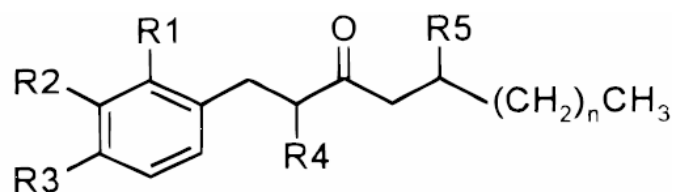
Compound	R1	R2	R3	R4	R5	Double bond	n	Log P
[6]-gingerol	H	OMe	OH	H	OH	-	4	1.8
[8]-gingerol	H	OMe	OH	H	OH	-	6	2.9
[10]-gingerol	H	OMe	OH	H	OH	-	8	3.9
[12]-gingerol	H	OMe	OH	H	OH	-	10	5.0
[6]-shogaol	H	OMe	OH	H	H	C4-C5	4	3.9
[8]-shogaol	H	OMe	OH	H	H	C4-C5	6	4.9
[6]-paradol	H	OMe	OH	H	H	-	4	4.1
[8]-paradol	H	OMe	OH	H	H	-	6	5.1
[8]-gingerdiol	H	OMe	OH	OH	OH	-	6	3.3

3. Pharmacological activities of *Zingiber officinale* Rosc.

The underground stem or rhizome of ginger has been used as a medicine in Asian, Indian, and Arabic herbal traditions since ancient times (Altman and Marcussen, 2001). There are many investigations on pharmacological activities of gingerols from *Zingiber officinale* Rosc.

3.1 Analgesic activity

The effects, of [6]-gingerol on pain receptor induced by acetic acid and formalin in mice and paw edema induced by carrageenin (CARR) in rats, were investigated (Young et al., 2005). The acetic test is normally used to study the peripheral analgesic effects of drugs. Although this test is a nonspecific (e.g., anti-cholinergic, antihistaminic and other agents also show activity in the test), it is widely used for analgesic screening and involves local cholinergic and histaminic receptors, and the mediators acetylcholine and histamine (Shibata et al., 1989) The results have shown that both of [6]-gingerol (50 mg/kg, 100 mg/kg, 250 mg/kg) and indometacin (10 mg/kg) significantly decreased the carrageenin induced the paw edema ($P < 0.001$). The carrageenan test is highly sensitive to nonsteroidal antiinflammatory drugs, it has long been accepted as a useful tool for investigating new anti-inflammatory drugs. Results indicated that activity against carrageenan-induced rat paw edema was observed with [6]-gingerol at the dose of 100 mg/kg and indomethacin at the dose of 10 mg/kg. In this study, [6]-gingerol exhibited a considerable anti-inflammatory activity (ED_{50} = 85.32 mg/kg) in comparison with drug reference.

The formalin test is a valid and reliable model of nociception and is sensitive for various classes of analgesic drugs. Formalin test produced a distinct biphasic response and different analgesics may act differently in the early and late phases of this test. Therefore, the test can be used to clarify the possible mechanism of antinociceptive effect of a proposed analgesic (Tjolsen et al., 1992). Centrally acting drugs such as opioids inhibit both phases equally (Shibata et al., 1989) but peripherally acting drugs such as aspirin, indomethacin and dexamethasone only inhibit the late phase. The late phase seems to be an inflammatory response with inflammatory pain that can be inhibited by anti-inflammatory. [6]-gingerol (25

mg/kg) produced significant ($P < 0.001$) inhibition in the late phase of formalin induced pain. The positive control indomethacin (20 mg/kg) also produced significant ($P < 0.001$) inhibition in the late phase. The effect of [6]-gingerol on the late phase of formalin test suggests that its activity may be resulted from its peripheral action when compared with indomethacin activity in this respect. Based on the results of this study, it was suggested that the antinociceptive effect of [6]-gingerol may be attributed to inhibition of prostaglandin release and other mediators involved in this test (Farsam et al., 2000).

In recent years, the vanilloid receptor (VR1) expressed in nociceptive sensory neurons, has recently been cloned and suggested to involve in chemical and thermal nociceptive stimuli of pain receptor. Therefore, direct activation or deactivation of the VR1 receptor at the site where pain is generated during inflammation and other painful conditions provides a new strategy for the development of a new class of peripheral analgesics. Vanilloid agonist binds to the pain receptor, causing inhibition of ascending pain pathway and altering the perception of and response to pain. Likewise, the morphine, narcotic agonist, binds to the opiate receptor. These findings are supported from study by Dedov (2002) was shown for the first time that gingerol constituents are relatively potent agonists of the VR1 receptor. The analgesic activity of gingerols depends on the lipophilicity of the side chain.

3.2 Cardiovascular activity

Ginger has been extensively studied for its cardiovascular activities. Ginger extract was found to exhibit a vasodilator effect through a combination of nitric oxide (NO) releasing and calcium antagonist mechanisms (Ghayur and Gilani, 2005). Apart from the crude extract, some of the known pungent principles of ginger, [6]-gingerol, 8-ginegrol, 10-gingerol and 6-shogaol were also tested on the vascular tissues and was found that the gingerols were more active than 6-shogaol for the vasodilator activity (Connell and McLachlan, 1972). The [6]-gingerol has been reported for an inhibitory response on the spontaneous contractions and Ca^{++} spikes in isolated portal veins of mice thus supporting the conclusion of a Ca^{++} antagonist action. Interestingly,

gingerols and shogaols have already been reported for their inotropic property via stimulation of SR Ca^{++}-ATPase activity (Antipenko, Spielman and Kirchberger, 1999).

3.3 Anti-inflammatory activity

During inflammation or infection, induction of COX-2 expression increases the formation of prostaglandins to promote tissue repair. Additionally, COX-2 generated prostaglandins were also reported to participate in induction of inflammatory pain, as an example, prostaglandins were found to sensitize pain fibers to mechanical and chemical stimuli. COX-2 thus responds more rapidly than COX-1 toward immune response, inflammation, tissue repair, and pain.

The ginger compounds were tested with the A549 cell line which has been known to express the COX-2 isoform in the presence of inflammatory cytokines, particularly interleukin-1β (IL-1β). After 24 h incubation with cell line, all ginger compounds exhibited a full inhibition of the COX-2 enzyme in a dose-dependent manner and structure dependent manner (Tjendraputra et al., 2001). The more lipophilic structure has the stronger activity. In the gingerol analog, the free phenolic hydroxy group is required for activity, possibly through H-bonding to the binding site of the enzyme cyclooxygenase. These findings are supported from study by Kiuchi (1992), which showed that the position of the phenolic hydroxy group adjacent to the methoxy group in gingerol and diarylheptanoids was critical for inhibition of prostaglandin biosynthesis. The gingerols and synthetic analogues exhibit a potent inhibition of COX-2 and consistent with the use of ginger in traditional medicine for the treatment of inflammation and pain.

3.4 Anti-platelet aggregation activity

In a rat model, there is evidence for an anti-platelet activity of ginger. First, it was reported that [8]-gingerol, a member of the main pungent principles of ginger selectively inhibited arachidonic acid-induced platelet aggregation and adenosine triphosphate released in rabbit washed platelet preparations. Then, [6]-gingerol and [8]-gingerols were shown to inhibit the cyclooxygenase-1/tromboxane synthase activity (Guh et al., 1995). The most recent study reported that [6]-and [8]-

gingerols, as well as other synthetic analogues, strongly inhibited human platelet aggregation and these compounds were also shown to have strong cyclooxygenase-1 (COX-1) inhibitory activity in rat basophilic leukemia cells (RBL-2H3), a cell line with COX-1 enzyme expression (Koo et al., 2001). The above pharmacological evidence has suggested that ginger constituents and related substances could be potential antiplatelet substances, like aspirin, without causing the gastric ulceration and other adverse events. In conclusion, Tjendraputra (2003) were revealed that the [8]-Paradol showed to be the most potent anti-platelet agent and COX-1 inhibitor and natural constituents of ginger and gingerol analogues were potent platelet aggregation inhibitors and more effective than aspirin.

3.5 anti-inflammatory mediator activities

The abilities of gingerols and related compounds to interact with transcription factors that regulate inflammatory gene expression were investigated. Transcription factors that have been linked to inflammatory gene expression following lipopolysaccharide (LPS) exposure include necrosis factor (NF-κB) and activator protein (AP-1). Lipopolysaccharide (LPS) induction of inflammatory mediators will activate these transcription factors leading to increased gene expression and protein for tumor necrosis factor alpha (TNF-α), interleukin-1 (IL-1), IL-12, inducible nitric oxide synthase (iNOS) and COX-2 (inducible cyclooxygenase) (Hong et al., 2002). Inhibition of these transcription factors would explain the wide range of inhibitory effects that have been ascribed to ginger. Bode et al. (2001), examined the ability of [6]-gingerol and 6-paradol to inhibit AP-1 transcriptional activity. Only [6]-gingerol was effective ($IC_{50} \pm 1.5$ mg/ml).

In the inflammatory process, LPS-induced gene expression of COX-2 and TNF-α occur primarily through activation of the NF-κB and AP-1 transcription factor pathways. If the ginger compounds are acting to inhibit one or the other of these pathways, then decreases in LPS induced TNF- α production should have been seen. It was discovered that, extracted ginger, as well as 6-, 8- or 10-gingerol are able to reduce the levels of LPS-induced COX-2 mRNA expression, so it can reduce inflammatory mediator (Lantz et al., 2007).

3.6 GI effect

3.6.1 Motion Sickness

Ginger has long been used as a remedy to decrease nausea and vomiting associated with several conditions. A randomized, double-blind, placebo-controlled study was performed to assess the effects of ginger extracts on motion sickness and gastric slow-wave dysrhythmias. Twenty two volunteers with a history of motion sickness were pre-treated with ginger 1,000 mg and 2,000 mg. Ginger improved significantly prolonging the latency period before nausea onset and shortening the recovery time after vection cessation (Riebenfeld and Borzone, 1999). The other double-blind study was performed and demonstrated a positive effect of ginger on motion sickness. The result showed ginger to be as effective as many traditional antiemetic pharmaceuticals such as dimenhydrinate, domperidone, scopolamine, cyclizine, and meclizine (Careddu, 1999).

The ginger extract also showed an antispasmodic effect, possibly due to the presence of phenolic compounds in ginger, mediated via Ca^{2-} antagonism. This study reviewed the use of ginger as a gastrointestinal prokinetic drug (Ghayur and Gilani, 2006).

3.6.2 Nausea and Vomiting

The study of nausea and vomiting in pregnancy was evaluated by women in the first trimester of pregnancy. The double-blind, placebo-controlled studies evaluated the effectiveness of ginger on morning sickness. The study of 70 pregnant women, participants received either 250 mg freshly prepared ginger powder or a placebo. Results indicated a significant reduction in nausea and number of vomiting episodes (Vutyavanich, Kraisarin and Ruangsri, 2001). Moreover, ginger also effectively reduced nausea and vomiting from post-surgical nausea and chemotherapy-induced nausea (Phillips**,** Ruggier and Hutchinson, 1993).

3.7 Cancer preventive activities

3.7.1 Gastrointestinal cancer

Helicobacter pylori is the primary etiological agent associated with peptic ulcer disease and the development of gastric and colon cancer. The *H. pylori* inhibitory effects of ginger and its constituents were tested in vitro by Mahady et al.

(2003). It was found that gingerol inhibited the growth of *H. pylori* in vitro and this activity might contribute to its chemopreventive effects against colon cancer. Yamahara et al. (1988) reported [6]-gingerol significantly inhibited gastric lesions induced by HCl and ethanol in rats. Yoshimi et al (1992) showed that gingerol, when given to male F344 rats in the diet at a concentration of 0.02% for 3 weeks, significantly reduced the multiplicity of intestinal carcinogenesis.

3.7.2 Skin cancer

The [6]-gingerol have been shown to suppress promotion of mouse skin carcinogenesis in laboratory animals (Park et al., 1998). The inhibitory activity of ginger extracts in tumor initiation and promotion is due to its pungent vanillyl ketones, including [6]-gingerol and [6]-paradol (Surh et al., 1999). Park et al. (1998) reported that [6]-gingerol inhibited TPA skin tumor promotion in addition to the inhibition of epidermal ornithine decarboxylase activity in ICR mice. In a study, Surh et al (1999) found anti-tumor-promoting properties of both [6]-gingerol and [6]-paradol. Topical application of [6]-gingerol or [6]-paradol 30 min prior to test significantly inhibited the tumor-promoter-stimulated inflammation.

3.7.3 Breast cancer

The effects of chronic treatment with hot water extract of ginger rhizome on spontaneous mammary tumorigenesis were examined in mice. In mice given free access to extract of ginger (0.125%) in drinking water, the development of mammary tumors was significantly inhibited (Nagasawa, Watanabe and Inatomi, 2002).

3.7.4 Effects on angiogenesis and metastasis

Angiogenesis, the formation of new blood vessels from pre-existing endothelium, is fundamental in a variety of physiological and pathological processes such as chronic inflammation, and tumor progression. It was reported that [6]-gingerol had potent anti-angiogenic activity in vitro and in vivo (Kim et al., 2005). These results indicated that [6]-gingerol in preventing cancers from becoming malignant, presumably by selective inhibition of angiogenesis formation at the tumor site. Gingerol suppressed experimental metastases in tumor-bearing mice and results suggested that [6]-gingerol might inhibit tumor growth and metastasis via its anti-angiogenic activity (Kim et al., 2005).

B. Reactive Species in the Biological System

Free radicals and related species are mainly derived from oxygen (reactive oxygen species/ROS) and nitrogen (reactive nitrogen species/RNS), and are generated in our body by various endogenous systems, exposure to different physicochemical conditions or pathological states (Pinnell, 2003). Free radicals can be defined as molecules or fragments of molecules, capable of independent existence, containing one or more unpaired electrons in their orbital. They tend to react very easily with various types of biomolecules, to acquire another electron and stabilize the orbital (Andreassi and Andreassi, 2004). Generally, free radicals attack the nearest stable molecules, 'stealing' its electrons. The molecule that has been attacked and loses its electron becomes a free radical itself, beginning a chain reaction. Once the process is started, it can cascade, initiating lipid peroxidation which results in destabilization and disintegration of the cell membranes or oxidation of other cellular components such as protein and DNA, finally resulting in the disruption of cells. Free radicals are generally unstable, highly reactive and energized molecules (Lee Koo and Min, 2004). Organisms constantly produce free radicals by different mechanisms. Incomplete reduction of oxygen in the mitochondrial (the major ROS source) electron transport chain releases superoxide anions into the cytoplasm (Andreassi and Andreassi, 2004) Free radicals are formed as a natural consequence of the body's normal metabolic activity and as part of the immune system's strategy for destroying invading microorganisms. Exogenous sources of free radicals include ozone, exposure to ultraviolet radiation in sunlight, and cigarette smoke. Free radicals can adversely alter lipids, proteins and DNA and have been implicated in aging and a number of human diseases. In general, free radicals and related species are very short-lived, with half-lives in milli-, micro- or nanoseconds.

1. Superoxide anion radical ($O_2^{\cdot-}$)

Superoxide anion is a reduced form of molecular oxygen created by receiving one electron. Superoxide anion is an initial free radical formed from mitochondrial electron transport systems that is the first reduction of ground state-oxygen, capable of both oxidation and reduction. Mitochondria generate energy using 4 electrons

escaping from the chain reaction of mitochondria directly react with oxygen and form superoxide anions (Lee et al., 2004).

The superoxide anion plays an important role in the formation of other reactive oxygen species such as hydrogen peroxide, hydroxyl radical, or singlet oxygen in living organism. The superoxide anion can react with nitric oxide (NO$^-$) and form peroxynitrite (ONOO$^-$), which can generate toxic compounds such as hydroxyl radical and nitric dioxide (Lee et al., 2004).

2. Hydroxyl radical (OH$^-$)

Hydroxyl radical is the most highly reactive free radical and can be formed from superoxide anion and hydrogen peroxide in the presence of metal ions such as copper or iron. Hydroxyl radicals have the highest 1-electron reduction potential (2310 mV) and can react with everything in living organisms at second-order rate constants of 109 to 1010 M-1 sec-1 (Lee et al., 2004; Halliwell et al., 1995). Hydroxyl radicals react with nearly every biomolecule such as nuclear DNA, mitochondrial DNA, proteins and membrane lipids (Keithahn and Lerchl, 2005). The rapid and nonspecific reactivity of OH$^-$ renders this free radical particularly dangerous. It may abstract hydrogen from, or hydroxylate, most biomolecules, causing cell injury or death. Hydroxyl radical is believed to be the etiological agent for several diseases and may also be involved in natural aging.

3. Hydrogen peroxide (H$_2$O$_2$)

Hydrogen peroxide is produced during normal aerobic cell metabolism and involved in enzymatic reaction, superoxide dismultase enzyme (SOD). H$_2$O$_2$ is decomposed to oxygen and water by enzyme catalase and glutathione peroxidase. Hydrogen peroxide is the least reactive molecule among ROS due to its half-life. It is stable under physiological pH and temperature in the absence of metal ions (Lee et al., 2004). In the presence of metals, H$_2$O$_2$ can be reduced to form hydroxyl radical (OH$^-$), which is highly reactive in biological effects (Keithahn and Lerchl, 2005)

C. Theory of Extrinsic Aging

1. UV induced photoaging

Photoaging primarily causes extrinsic aging by long-term effects of repeated exposure to ultraviolet light. UV radiation has numerous direct and indirect effects on the skin. It is estimated that approximately 50% of UV-induced damage is from the formation of free radicals, whereas direct cellular injury and other mechanisms consider as the remainder of UV effects (Bernstein et al., 2004).

Photoaged skin is typically dry, coarse and rough with deep lines and wrinkles and irregular pigmentation. Photoaged skin displays prominent alterations in the cellular component and the extracellular matrix of the connective tissue with an accumulation of disorganizes elastin and its microfibrillar component fibillin in the deep dermis and a severe loss of interstitial collagens. There are three principle components involved, namely, collagen fibers, the elastic fiber network and glycosaminoglycans. Collagen is the most abundant extracellular component and provides the strong tensile properties to the dermis. The elastic fiber networks provide elasticity to the skin and the glycosaminoglycan/proteoglycan macromolecules play a role in hydrating the skin and in biological signaling (Jenkins, 2002).

2. Connective tissue change

The major histopathological sign of photoaging is the massive accumulation of so called 'elastotic' material in the upper and mid dermis. The material is comprised of extracellular matrix (ECM) components that make up the normal elastic fiber network. This elastotic material involves degradation of existing elastic fibers and dysregulation of elastic and fibrillin production. The up-regulation of elastin and fibrillin gene expression in photodamaged skin and fibroblasts derived from it has been reported (Bernstein, Chen and Tamai, 1994). In contrast with elastic fiber network, components of the collagen fiber network, including collagen I and decorin are down-regulated in photodamaged skin (Varani et al., 2001). This reduction in collagen fiber production is accompanied by the degeneration of the surrounding collagenous network and leading to breakdown of the elastic fiber network. Therefore, photoaging characterized by severe connective tissue damage has been

linked to the UV-induced degeneration of different members of the extracellular matrix.

3. Molecular and genetic change

The molecular changes in DNA induced by UV radiation have been studied extensively in photocarcinogenesis. In general, UVB, more potent than UVA, can damage DNA through the generation of ROS. The mutation DNA related to specific signs of photoaging, increase in collagen damage. The molecular effects of UV light on the keratinocyte (KC) and fibroblast (FB) in the skin were investigated. UV induces reactive oxygen species (ROS) which can damage DNA or can inhibit tyrosine phosphatases, leading to increased signal transduction and ultimately up-regulation of activator protein 1 (AP-1) transcription factor. UV can also directly up-regulate c-Jun, a component of AP-1. UV radiation can also down-regulate retinoic acid (RA) receptors, which decreases RA inhibition of AP-1. Further effects of UV include direct DNA mutagenesis, up-regulation of nuclear factor-κB (NF-κB), and down-regulation of TGF-b signaling. These overall effects have been related to collagen production and breakdown, as well as to increase the inflammatory cytokine production in extracellular matrix (ECM) of the skin (Rabe et al., 2006). The diagram of UV radiation, effect on photoaged skin through the generation of ROS, is illustrated in Figure 3.

4. Role of antioxidants in photodamaged skin

The skin is equipped with enzymatic as well as nonenzymatic cutaneous antioxidants. Endogenous antioxidants include vitamin E, coenzyme Q10 (CoQ10), ascorbate, and glutathione (Shindo et al., 1994) whereas enzymatic antioxidants include superoxide dismutase, catalase, and glutathione peroxidase (Leccia et al., 2001). These provide protection from ROS produced during normal cellular metabolism. Excessive exposure to UV radiation is thought to deplete antioxidant level, leading to a state of oxidative stress. UV radiation can influence endogenous antioxidant enzyme levels because of the up-regulation of superoxide dismutase and glutathione peroxidase (Pinnell, 2003). Concentrations of carotenoids are lower in human cutaneous malignancies, such as basal cell carcinoma, suggesting that these

antioxidants are important in the skin's defense against UV radiation and photocarcinogenesis (Hata et al., 2000). The molecular structures of endogenous antioxidants are shown in Figure 4 (Yamamoto, 2001).

Antioxidants protect the skin against damage produced by UV irradiation in several pathways. Low-molecular-weight, nonenzymic antioxidants include L-ascorbic acid in the fluid phase, glutathione in the cellular compartment, vitamin E in membranes and ubiquinol in mitochondria (Lin et al., 2003).

When ROS is generated in a lipophilic structure, it is reduced by α-tocopherol which reduces lipid peroxidation in lipid structures of the stratum corneum and for protecting stratum corneum proteins from oxidation. Topical α-tocopherol protected UV-induced erythema and protected against UV-induced photoaging changes (Jurkiewicz, Bissett and Buettner, 1995).

Topical L-ascorbic acid protected skin from UVB- and UVA-phototoxic injury as measured by erythema and sunburn cell formation. Topical L-ascorbic acid protected against UVB-induced immunosuppression and slightly enhanced levels of messenger RNA for procollagens I and III in skin (Darr et al., 1992).

Coenzyme Q (CoQ) refers to ubiquinone and its reduced form, ubiquinol, has potential antioxidant functions similar to those of vitamin E. It prevents lipid peroxidation by reducing peroxyl radicals (Takahashi et al., 1993)

Tea polyphenols have anti-inflammatory effects. Topical green tea polyphenols reduced UV-induced erythema and sunburn cell formation in human skin and reduced UVB-induced inflammatory responses and infiltration of leukocytes in human skin. Moreover, tea polyphenols also have immune-modulating effects, protected human skin from UV-induced Langerhans cell depletion (Elmet et al., 2001)

Figure 3 Effects of UV light on the keratinocyte (KC) and fibroblast (FB) cell in the skin layer (Rabe et al., 2006)

Figure 4 The molecular structure of endogenous antioxidants (Yamamoto, 2001).

5. Application of gingerol compounds on UV-induced photodamage

In normal condition, ROS play a very important physiological role as secondary messengers (Valko et al., 2007). Long exposing to the UVB radiation increases the cellular level of ROS which results in oxidative stress to the cells and ROS have been shown to initiate cellular damage leading to apoptosis (Vile and Tyrrell, 1995). In addition, ROS have been suggested to play a role as second-messenger molecules in signaling pathways and in the regulation of gene expression related to the biological effects elicited by UVB. NF-κB, a redox-regulated transcription factor, is involved in regulating cellular processes such as inflammation and apoptosis, and is upregulated by UVB in vivo and in vitro (Saliou et al., 2001). In addition, ROS are known to play an important role in UVB-induced expression of cyclooxygenase-2 (COX-2). This in turn augments the production of a variety of inflammatory mediators such as prostaglandins and leukotriens (Hruza and Pentland, 1993).

In recently research, it was found that [6]-gingerol inhibited UVB-induced expression of COX-2 mRNA and protein in human keratinocyte. Furthermore, [6]-gingerol down-regulated UVB-induced DNA binding activity of NF-κB, a transcription factor involved in expression of pro-inflammatory genes. The increasing of ROS participates in UVB induction of COX-2 expression and transactivation of NF-κB. The mechanism of inhibitory effect of [6]-gingerol on UVB-induced COX-2 expression is due to inhibition of NF-kB signaling by preventing ROS accumulation in vitro (human keratinocyte HaCaT cells) and in vivo (mouse skin) (Kim et al., 2007).

Another effect of UV irradiation is inducing apoptosis which is regulated by a number of molecular processes, including activation of the cell death receptor CD95 (Fas/APO-1). Activation of Fas by UVB irradiation results in activation of caspase-3. The [6]-gingerol significantly down-regulated the activation of caspase-3, caspase -8, caspase -9 and expression of Fas. However, [6]-gingerol did not reduce DNA damage from UVB. The study observed that [6]-gingerol did not repair or rescue cells from DNA damage, but inhibited activation of apoptotic signal (Kim et al., 2007). The various mechanisms of [6]-gingerol involve in the UV-induced photodamage.

Therefore, these results suggest that [6]-gingerol have a protective effect against UVB-induced photodamage.

D. Solid Lipid Nanoparticles

Solid lipid nanoparticles are particles with an average diameter in the nanometer range. The SLN were realized by simply exchanging the liquid lipid (oil) of the emulsions by the lipid that solidified at room temperature and also at body temperature. It was stabilized by surfactant in the aqueous phase. The lipid compositions in SLN formulation can be highly purified triglycerides, complex glyceride mixtures or even waxes (Mehnert and Mader, 2001). In general, SLN prepared from triglycerides. These triglycerides seem promising for the preparation of solid lipid nanoparticles because their melting points are above body temperature but sufficiently low to allow melt-homogenization in an aqueous phase

It has been claimed that SLN combine the advantages and avoid the disadvantages of other conventional colloidal system. Compared to liposomes and emulsions, solid particles possess some advantages because the particles are in the solid state. Therefore, the mobility of incorporated drugs is reduced, which is a prerequisite for controlled drug release and also protect the incorporated active compounds against chemical degradation (Jenning and Gohla, 2001). A clear advantage of SLN is the lipid matrix is made from physiological biodegradable lipids which decrease the danger of acute and chronic toxicity (Muller et al., 1995). In addition, the production processes not participate with organic solvents and they also easily be produced on a large scale.

There are two basic production methods for SLN, the high pressure homoge nization technique and the microemulsion technique.

1. SLN preparation

1.1 High pressure homogenization method

High pressure homogenization (HPH) is a reliable and powerful technique for the preparation of SLN. HPH has been used for years for the production of nanoemulsions for parenteral nutrition. The advantage of this technique is scaling up represent no problem in most cases. High pressure homogenizers push a liquid with

high pressure (100–2000 bar) through a narrow gap (in the range of a few microns). The fluid accelerates on a very short distance to very high velocity (over 1000 km/h). Very high shear stress disrupts the particles down to the submicron range. Typical lipid contents are in the range 5–10% and represent no problem to the homogenizer. Even higher lipid concentrations (up to 40%) have been homogenized to lipid nanodispersions (Lippacher, Muller and Mader, 2000). Two general approaches of the homogenization step, the hot homogenization and the cold homogenization techniques, can be used for the production of SLN. In both cases, the beginning step involves the drug incorporation into the bulk lipid by dissolving or dispersing the drug in the lipid melt.

Hot homogenization is performed at temperatures above the melting point of the lipid. The solid lipid and drug were melt at 5-10 °C above the melting point of lipid and were dispersed in the aqueous emulsifier phase (same temperature). A pre-emulsion of the drug loaded is obtained by high speed stirrer device. The primary product of the hot homogenization is a nanoemulsion due to the liquid state of the lipid. Solid particles are expected to be formed by cooling of the sample to room temperature. The hot homogenization technique is also suitable for drugs showing some temperature sensitivity because the exposure to an increased temperature is short. In case of highly temperature sensitive compounds the cold homogenization technique can be applied. The cold homogenization technique is also necessary to use when formulating hydrophilic drugs because they would partition between the melted lipid and the water phase during the hot homogenization process. For the cold homogenization technique the drug-containing lipid melt is cooled. The high cooling rate favors a homogenous distribution of the drug within the lipid matrix. The solid lipid was ground to lipid microparticles and these lipids are dispersed in a cold surfactant solution yielding a pre-suspension. Then this pre-suspension is homogenized at room temperature (Muller, Lippacher and Gohla 2000). In general, compare to hot homogenization, larger particle size and broader size distribution are observed in cold technique. The method of cold homogenization minimizes the thermal exposure of the sample, but it does not avoid it due to the melting of the mixture of drug and lipid in the initial step (Mehnert and Mader, 2001).

1.2 Solvent emulsification /evaporation method

This production method prepares nanoparticle dispersions by precipitation in o/w emulsions (Sjostrom and Bergenstahl, 1993). The lipophilic lipid is dissolved in a water-immiscible organic solvent (cyclohexane, chloroform) that is emulsified in an aqueous phase. The organic solvent was removed from the emulsion by evaporation under reduced pressure. Then, nanoparticle dispersion is formed by precipitation of the lipid in the aqueous medium. An important advantage of this method is the avoidance of heat during the preparation, which makes it suitable for the incorporation of thermolabile drug. However, the residue of organic solvent may retain and contaminate the nanoparticles in the formulation.

1.3 Microemulsion method

Microemulsion contains two-phase systems composed of an inner and outer phase (o/w-microemulsion). Solid lipid nanoparticles are prepared by stirring an optically transparent mixture at 65–70 $^{\circ}$C which is typically composed of a low melting fatty acid (e.g. stearic acid) and emulsifier. The hot microemulsion is dispersed in cold water (2–3 $^{\circ}$C) under stirring. Typical volume ratios of the hot microemulsion to cold water are in the range of 1:25 to 1:50. The dilution process is critically determined by the composition of the microemulsion. The droplet structure is already obtained in the microemulsion and therefore, no energy is required to achieve submicron particle size (Ma et al., 2007).

2. Models for incorporation of active compounds into SLN

There are basically three different models for the incorporation of active ingredients into SLN (Muller,Radtke and Wissing, 2002).

(I) Homogeneous matrix model

(II) Drug-enriched shell model

(III) Drug-enriched core model.

The structure obtained is a function of the formulation composition (lipid, active compound, surfactant) and of the production conditions.

A homogeneous matrix with molecularily dispersed drug or drug being present in amorphous clusters is thought to be mainly obtained when applying the cold homogenization method and when incorporating very lipophilic drugs in SLN with the hot homogenization method. In the cold homogenization method, the bulk lipid

contains the dissolved drug in molecularily dispersed form, mechanical breaking by high pressure homogenization leads to nanoparticles having the homogeneous matrix structure (Figure 5a). The same will happen when the oil droplet produced by the hot homogenization method is being cooled, crystallized and no phase separation between lipid and drug occurs during this cooling process. This model is assumed to be valid for incorporation of, e.g. the drug prednisolone, which can show release from 1 day up to weeks (Muhlen and Mehnert, 1998)

An outer shell enriched with active compound can be obtained (Figure 5b) when phase separation occurred during the cooling process from the liquid oil droplet to the formation of a solid lipid nanoparticle. According to the diagram, the lipid can precipitate first forming a practically compound-free lipid core. At the same time, the concentration of active compound in the remaining liquid lipid increases continuously during the forming process of the lipid core. Finally, the compound-enriched shell crystallizes comparable to the eutecticum in the diagram. This model is assumed, for example, for coenzyme Q10 which the enrichment leads to a very fast release.

A core enriched with active compound can be formed when the opposite occurs, which means the active compound starts precipitating first and the shell will have distinctly less drug (Figure 5c). This leads to a membrane controlled release governed by the Fick law of diffusion. The three models presented each represent the ideal type. There can also be mixed types which can be considered as a fourth model.
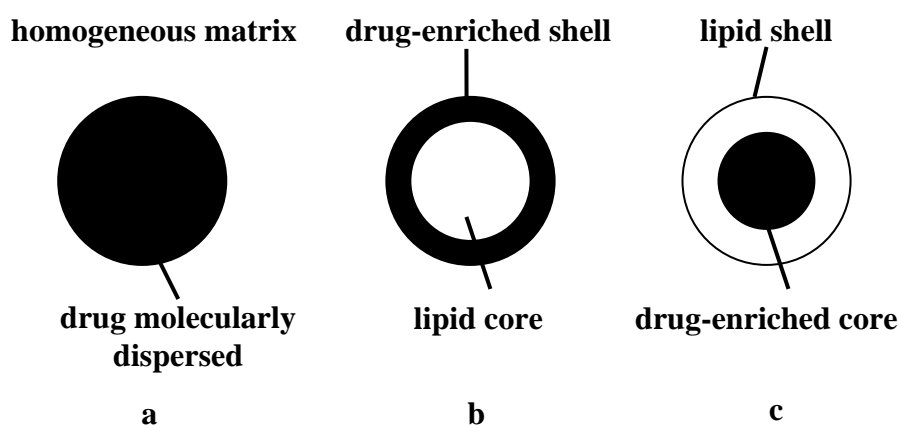
Figure 5 Models of incorporation of active compounds into SLN: homogeneous matrix (a), core-shell models with drug-enriched shell (b), drug-enriched core and lipid shell (c)

3. Release of active compounds from SLN

The release profile characterization of SLN may play a significant role on the application. The effect of formulation parameters and production conditions on the release profile from SLN was intensively investigated by Muhlen, Schwarz and Mehnert (1998). For example, they investigated the release profile as a function of production temperature. It can be summarized that the release was followed by a prolonged release. The burst release was highest when producing at high temperatures and applying the hot homogenization method. It decreased with decreasing temperature and was almost non-existent when applying the cold homogenization method. The extent of burst release could also be controlled by the amount of surfactant used in the formulation. High surfactant concentration leads to high burst release, low surfactant concentration to minimization of the burst. This was explained by redistribution effects of the compound between the lipid and the water phase during the cooling down process after production of the hot oil in water emulsion during the hot homogenization process. Heating the lipid and water mixture leads to an increased solubility of the active compound in the water phase, the compound partitions from the melted lipid droplet to the water phase. After homogenization, the oil in water emulsion is cooled, the lipid core starts crystallising with still a relatively high amount of active compound in the water phase. Further cooling leads to supersaturation of the compound in the water phase, the compounds tries to partition back into the lipid phase; a solid core has already started forming leaving only the liquid outer shell for compound accumulation. The production condition and composition of formulation affected to model of incorporation drug and the release profile.

4. Characterization of physical stability of solid lipid nanoparticles

4.1. Lipid modification

4.1.1 Crystallization of glycerides

SLN suspensions consequently presented complex additional stability aspects compared to other lipid systems due to their crystallization kinetics and the polymorphism of the dispersed lipid. Crystalline solids show definite melting points, passing from the solid to the liquid state. This should be considered in SLN

formulation. Comparable to the bulk lipid, the melting point of SLN was used to determine the SLN from hot high pressure homogenization and warm microemulsion methods which formulate SLN from melt lipid dispersed in aqueous phase. SLN were frequently made from glycerides which are solid at room temperature. It is noted that the fusion temperature of bulk lipids is 73 °C, 64 °C, 56 °C, and 47 °C for tristearin, tripalmitin, trimyristin, and trilaurin, respectively. In general, the melting points of lipid nanocrystals were lower than the bulk material due to the increasing of defects in the crystal lattice of drug loaded lipid. Consequently, nanoparticles prepared from triglycerides which are solid at room temperature did not necessarily crystallize on cooling to storage temperatures. The particles can remain liquid for several months without crystallization. Westesen and Bunjes (1995) observed that colloidal dispersion of trimyristin and trilaurin particles remain in the liquid state for at least several months of storage at room temperature. Cooling the dispersion below a critical crystallization temperature did not result in particle crystallization. The particles can remain in a supercooled liquid state for a long period of time. Supercooled melts are not lipid nanosuspensions but emulsions. In case of, the emulsions of supercooled melts were formulated instead of SLN. The supercooled state of the droplets was not thermodynamically stable and the advantages of these systems for sustained drug release could not be achieved due to it rely on the solid state of the lipid matrix. For these reasons, the solidification of the particles after melt-homogenization must be ensured.

4.1.2 Polymorphism of glycerides

Polymorphism is defined as the ability to reveal different unit cell structures in crystals, originating from a variety of molecular conformations and molecular packing (Sato and Garti, 1988). Polymorphism is one of the important physical degradation routes which affect the stability of solid dosage forms because polymorphs generally have different thermodynamic properties such as melting points, X-ray diffraction patterns, and solubility.

The main polymorph forms in glycerides are the α, β' and β forms described by Sato and Garti (1988).

α: Hexagonal (H) subcell with a lattice spacing of 0.42 nm.

β': Orthorhombic perpendicular (O) subcell with wide lattice spacings of 0.42–0.43 and 0.37–0.40 nm.

β: Triclinic parallel (T) subcell with a wide lattice spacing of 0.46 nm.

The α form has the tendency to be transformed quickly to the more stable β' form. The most stable form is the β form (Jenning, Schafer and Gohla, 2000). Therefore, the transition of liquid (melt) from α to β' via β was the pathway for triglycerides to the optimum packing form of the molecules (Westesen et al., 1993). This unstable form gradually transformed toward the most stable form during storage at elevated temperatures while losing the initial spherical surface structures. This led to crystalline aggregate growth (Eldem, Speiser and Altorfer, 1991). Polymorphism influenced to the drug content of nanoparticles due to the rearrangement of the crystal lattice might occur in thermodynamically stable form and connected with expulsion of the drug molecules. Drug expulsion during polymorph transition was explained by a reduction of amorphous regions in the carrier lattice due to a β' to β polymorph transition (Jenning, Mader and Gohla, 2000). By changing to the more stable modifications, the lattice became more perfect and the number of imperfections decreased (Lippacher, Muller and Mader, 2000). To cope with this problem, a medium chain triglyceride containing oil was incorporated in a matrix of a solid long chain glyceride (glyceryl behenate) to obtain the imperfect lattice SLN based on binary mixtures (Jenning, Thunumann and Gohla, 2000). In this case, the highly disordered state in the glyceryl behenate nanoparticles due to liquid medium chain triglycerides delayed crystallization that led to long-term physical stability and influenced the release mechanism that depended on the transformation rate. The release mechanism of active substances from the cetyl palmitate matrix was influenced by the crystal structure (Lukowski et al., 2000).

4.1.3 Gelation phenomena

Gelation phenomena describe the transformation of low-viscosity SLN dispersion into a viscous gel. This process may occur very rapidly and unpredictably. In most cases, gel formation is an irreversible process which involves the loss of the colloidal size. It was suggested that gel formation is connected with crystallization processes. Strange surfaces induce crystallization or change of modification of the lipid crystals. This process is connected with an increase of the particle surface due to the preferred formation of platelets (in β-modification). The surfactant molecules cannot longer provide sufficient coverage of the new surfaces and therefore, aggregation is observed (Siekmann and Westesen, 1994b) SLN systems do not completely recrystallize during the storage time and contain several lipid modifications (unstable α and more stable β') (Freitas and Muller, 1999)

The presence of liquid phases promotes the crystallization in the stable form because unstable crystals may redissolve and crystallize in the stable modification. In this way, it is possible to accelerate the α to β' transformation during storage at RT without melting of the Compritol.

Westesen demonstrated by TEM that tripalmitin and tristearin crystals have a spherical shape in the α modification. The β' modification is built up from stapled spheroids and the stable b redistribution of the drug. Of course, increasing the modification is built up from long, coagulated platelets (Westesen and Siekmann, 1997).

4.2 Stability measurement

In the destabilization phenomena, most of cases can visually observed (coalescence, gelling). The final product becomes a non-homogeneous system and change in viscosity. However, the beginning of the destabilization process could be detected earlier by the measurement below.

4.2.1. Crystallization of solid lipid
4.2.1.1 Differential scanning calorimetry

The characterization of the degree of lipid crystallinity and the modification of lipid is the critical topics for physical stability investigation. These

parameters are strongly correlated with drug incorporation and release profile. Thermoanalysis of the SLN provides information about crystallization behavior, the timing of polymorphic transitions, fusion temperature, enthalpy, and the degree of crystallinity of melt-homogenized glyceride nanoparticle dispersions (Siekmann and Westesen, 1994a)

4.2.1.2 Synchrotron radiation X-ray diffraction

The X-ray diffraction pattern is photographed on a sensitive plate arranged behind the crystal. In this method, the structure of a crystal was investigated. It has become possible to determine the distances of the various planes of the crystal lattice. The structure of various compounds can be determined in this way. The patterns of X-ray scattering possible to assess the length of the long and short spacing of the lipid lattice. X-ray scattering (SAXS) often completes the study. These techniques were used to investigate crystallization tendency and polymorphic transitions of triglyceride nanoparticles (Bunjes, Westesen and Koch, 1996)

4.2.2. Modification of size

Photon Correlation Spectroscopy (also known as dynamic light scattering) is the most powerful technique for routine measurements of nanoparticle size and most of the studies of lipid systems use PCS for size determination. PCS measures the fluctuation of the intensity of scattered light caused by particle movement. However, PCS is not able to detect particles over 3 μm. The calculations of size with PCS are made by considering particles as spherical systems. This characteristic should be verified by other techniques like microscopy before measurement.

In general, uncertainties of physical stability may result from non-spherical particle shapes. For example, platelet structures commonly occur during lipid crystallization. Therefore, additional techniques might be useful. For example, light microscopy is recommended, although it is not sensitive to the nanometer size range. It gives a fast indication of the presence and character of microparticles (microparticles of unit form or microparticles consisting of aggregates of smaller

particles). Electron Microscopy provides, in contrast to PCS, direct information on the particle shape (Mehnert and Mader, 2001).

4.3 Destabilization inductors

4.3.1 Compositions of SLN formulation

4.3.1.1 Lipid matrix

There are many types of lipids used for preparation of SLN. The overview of lipid ingredients are listed below,

Triglyceride　　　:　Trilaurin, Trimyristin, Tristearin

Partial glyceride　:　Glyceryl monostearate, Glyceryl palmitostearate, Glyceryl behenate

Wax　　　　　　:　Cetyl palmitate, Beeswax

These materials display dissimilarities in crystal lattice order. Glycerides crystallise in different subcell arrangements (hexagonal, orthorhombic and triclinic). They exhibit marked polymorphism with three and often more individual forms. In contrast, the polymorphism of waxes is drastically reduced. Mainly, an orthorhombic subcell prevails and the polymorphic transition rate is low (Jenning and Gohla, 2000).

Considering the evolution of the crystallized structure from metastable to stable polymorphs and this influence on drug content and release, the choice of the initial crystal lattice is primarily important.

The measurements of particle sizes of wax SLN displayed excellent long term stability of size and size distribution, whereas glyceride particles showed particle growth and micrometer aggregates. The pure triglyceride tripalmitate, possessing a higher ordered crystal packing, expeled the drug upon solidification, similar to wax SLN. For this reason, the content of incorporated drug during storage time was lower in wax and pure solid lipids than partial glyceride SLN (Compritol) (Jenning and Gohla, 2000).

4.3.1.2 Surfactant

A variety of different emulsifiers has been used for the preparation of SLN dispersion. In parenteral formulations, only a very limited number of surfactants can be used due to the irritative, hemolytic action of the amphiphilic

surfactants. Surfactants used in parenteral route include phospholipids, bile salts, poloxamers and polysorbate 80 (Singla, Garg and Aggarwal, 2002). Other routes of administration are less critical in this topic. The type of emulsifier in the formulation affects the physical stability by changing the kinetics of polymorphic transitions in recrystallization process of bulk triglycerides (Siekmann and Westesen, 1994b). In dispersion, type and amount of surfactant may influence the crystallization temperature. The polymorphic transition and crystallization temperature are important parameters for lipid nanoparticles. If the crystallization temperature much lower than its melting temperature, the particles remain in liquid state, supercooled lipid. The SLN dispersion with optimized stabilizer composition is physically stable for years.

4.3.2 Storage parameters

4.3.2.1 Influence of light

The light exposure of the SLN caused changes in the system leading to a reduction of the zeta potential due to a modification of the crystallization form. With sufficient reduction of repulsive forces, particles can interact to form a gel network. Freitas and Muller (1998) showed rapid gelling of the initial SLN suspension (composed of glyceryl behenate) when it was stored in white glass under artificial light. Data indicated that light radiation had a destabilizing effect. Furthermore, increase in the intensity of light radiation accelerated particle growth and gelling. Moreover, high energetic radiation (UV, short wavelengths) increased destabilization. The mechanism implied was related to the modification of the zeta potential. The light exposure of the SLN causes changes in the system leading to a reduction of the zeta potential and consequently the physical stability.

4.3.2.2 Influence of temperature

The correspond to high energy input, high temperature and light exposure, can lead to changes in the crystalline structure of lipids. The destabilization process was generally induced by high temperatures due to changes in zeta potential. Freitas and Muller (1998) observed rapid growth of particles when stored at high temperature, 50 °C, associated with a decrease in zeta potential value. The temperature at 4°C was generally the most favorable storage temperature.

However, in some cases, long-term storage at 20 °C did not result in drug-loaded SLN aggregation or drug loss, compared to 4 °C storage conditions (Heiati, Tawashi and Phillips, 1998). At lower temperature, a high film rigidity of the emulsifier (microviscosity) avoids fusion of the film layers after particle contact. Microviscosity is a temperature dependent factor. Temperature increase causes a microviscosity decrease leading to destabilization of SLN dispersion.

Zeta potential is an important and useful indicator of particle surface charge, which can be used to predict and control the stability of colloidal suspensions or emulsions. The measurement of zeta potential is often the key to understanding dispersion and aggregation processes in applications. Higher temperatures as well as light increase the kinetic energy of a system, in combination with a reduced zeta potential, this leads to SLN aggregation and gelation. This energy input can lead to changes in the crystalline structure of the lipid. An increased formation of β modification was reported during the storage of tripalmitate SLN (Siekmann and Westesen, 1992). Crystalline re-orientation can result in changes of the charges on the particle surface (Nernst potential) and subsequently the measured zeta potential. In addition, different sides of a crystal can possess a different charge density. During one-dimensional growth of a crystal, the surface ratio of differently charged crystal sides changes and consequently the measured zeta potential changes.

4.4 Application of lipid nanoparticles in dermatological aspect
4.4.1 Occlusive property and skin hydration

Solid lipid nanoparticles (SLN) have been introduced as an attractive carrier system for various pharmaceutical drugs and cosmetic active ingredients. The hydrophobic lipid composition has the distinct occlusive property in vitro depending on their size, crystalline status and lipid concentration (Wissing and Muller, 2002b)

The occlusion factor can be determined in vitro using the test by Vringer (1992). Briefly, the evaporation of water from a beaker covered with a cellulose acetate filter to which the formulation is applied is determined as a function of time. A beaker covered with the filter paper only is used as reference and the occlusion factor can be calculated. It was experimentally observed that the occlusion factor of high

crystallinity lipid was larger than the non-crystalline lipid. The small size of particle and high lipid content promoted the degree of crystallinity of lipid and also the occlusive property.

The first film formation model of SLN on the skin was developed by Muller and Dingler (1998) a hexagonal packaging in a monolayer was assumed. The models of particle packaging of microparticles and nanoparticles are shown in Figure 6.

When applying lipid particles onto the skin, the pressure leads to fusion of the particles forming a dense film, having a surface area which is dependent on the particle size. The space filled with air in a layer of optimal packing density is independent on the particle size, which is considered to be 24% if assuming a three-dimensional hexagonal packing of ideal spherical-like particles. However, comparing a layer of nanoparticles (Figure 6, upper) with a layer of microparticles (Figure 7, lower), the dimensions of the air channels will be much smaller in the former; thus, the hydrodynamic evaporation of water will decrease. In contrast, larger pores will facilitate the water loss from the surface of the skin and enhance the moisture loss. In addition, recent investigations by electron microscopy showed that after evaporation of the water from SLN dispersion, a continuous, pore-less film was formed (Figure 6 lower and Figure 8)

The capillary forces of the nanometer pores between the SLN particles are contractive promoting fusion and dense pore-less film formation. This film promotes skin hydration. The data from vivo study showed that the formulation with additional SLN was able to significantly increase skin hydration within 4 weeks of treatment compared to the conventional cream (Wissing and Muller, 2003b).

4.4.2 SLN as novel UV sunscreen system

Due to the reduction of the ozone layer, the harmful effect of UV radiation is rising. There is an increasing need for effective UV protection systems with minimized side-effects. The two basic UV protection systems are molecular UV blockers (sunscreens) and particulate compounds such as titanium dioxide. Side-effects of molecular blockers are photoallergies and phototoxic effects. For this reason, the particulate blockers are used as an alternative in order to avoid side effect from the molecular blockers. The mechanism of protection is simply scattering of UV

rays. Wissing and Müller (2001a) discovered that highly crystalline solid lipid nanoparticles could also act as particulate UV blockers by scattering the UV light. The incorporation of the molecular sunscreen into the SLN matrix led to a synergistic UV protective effect (Wissing and Müler, 2001b). This means the total amount of molecular sunscreen in the formulation can be reduced and minimized the side effects. In addition, the release of sunscreen from particle matrix was controlled and prolonged, so the penetration through skin during application time was limited (Wissing and Muller, 2003a).
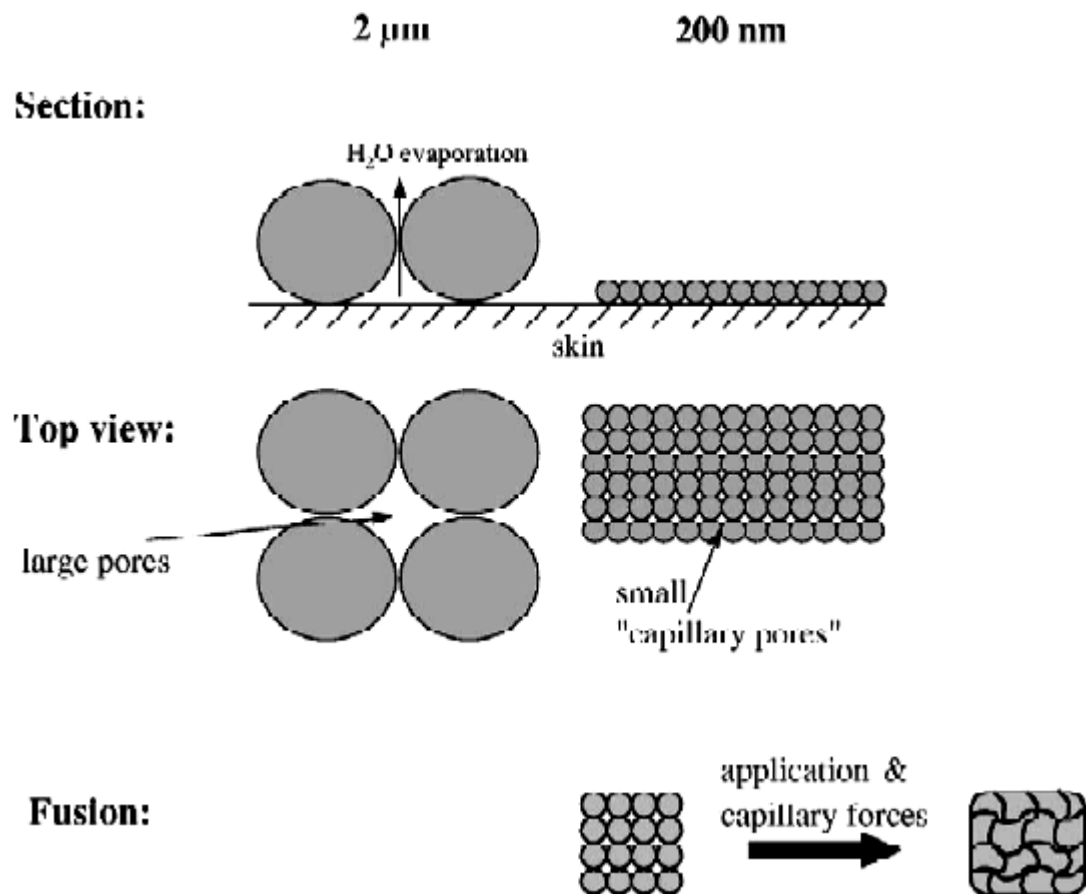
Figure 6   Model of film formation on the skin for lipid 2-mm particles and lipid 200 nm particles shown as section (upper) and from the top (middle), and a new model of fusion of the nanoparticles to a pore-less film (lower).
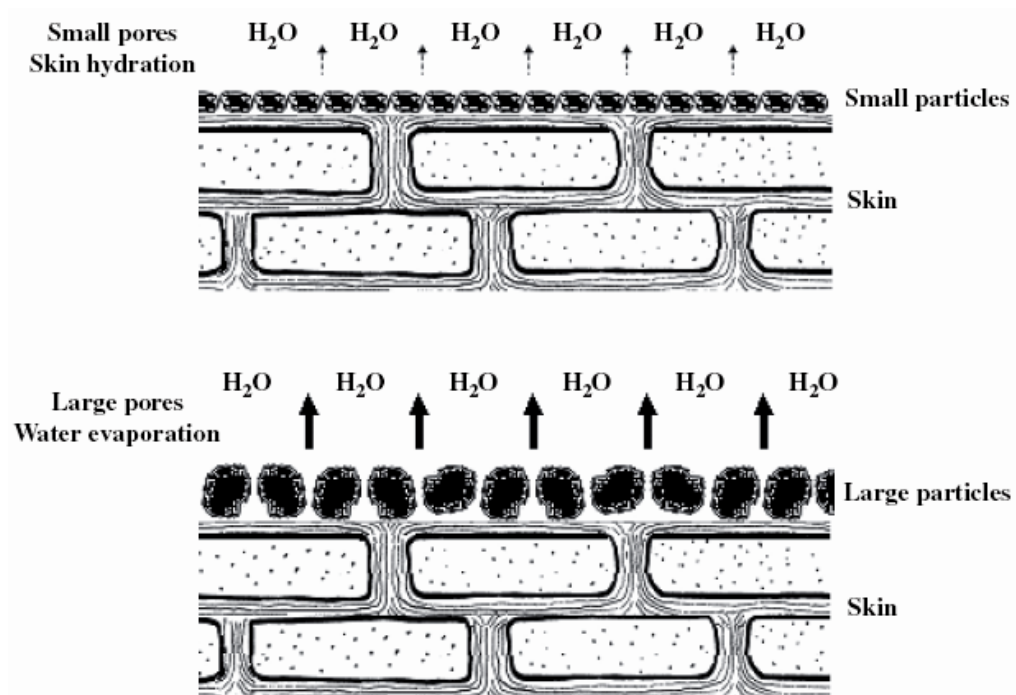
Figure 7 Occlusion effects of particles depending on their size. An aqueous solid lipid nanoparticles or nanostructured lipid carrier dispersion (diameter 500 nm, upper) in comparison with a solid lipid microparticle dispersion (diameter 1 μm, lower) (Souto and Muller, 2008).
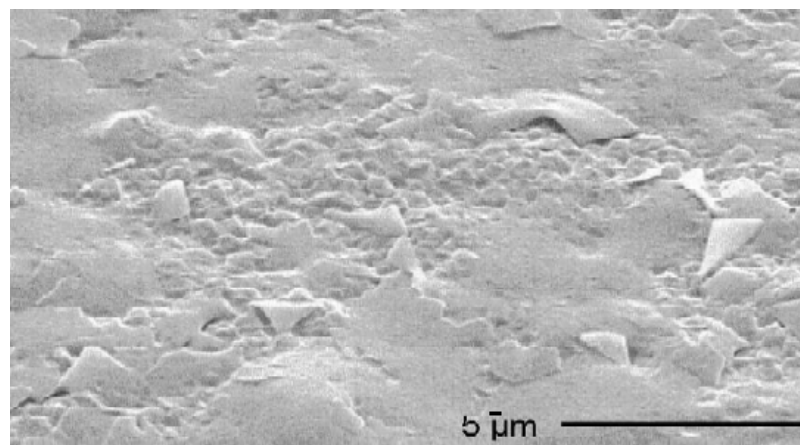
Figure 8 Electron micrograph of an air-dried SLN dispersion (Wissing and Muller, 2001b).

4.4.3 Penetration of active compounds into the skin

Skin permeation studies were investigated by many researchers. The composition of SLN also influenced on the penetration profiles. Modulation of release and active penetration into the skin could be achieved using the creation of supersaturated systems (Muller, Radtke and Wissing, 2002). These systems can be created by incorporation of lipid nanoparticles into topical formulations (creams, ointments, emulsions, gels). The increase in saturation solubility will lead to an increased diffusion pressure of the active into the skin. During shelf life, the active remains entrapped into the lipid matrix because this latter preserves its polymorphic form. After application of lipid dispersion onto the skin, and because of an increase in temperature and water evaporation, increasing the thermoactivity, the lipid matrix transforms from unstable polymorph into a more ordered polymorph leading to the release of active compound into a system already saturated with the same active, and thus creating a supersaturation effect. Penetration studies using several interesting cosmetic ingredients have been performed such as retinoids (Jenning and Gohla, 2001; Pople and Singh, 2006), coenzyme Q10 (Teeranachaideekul et al., 2007b), ascobyl palmitate (Teeranachaideekul et al., 2007a) and tocopherol (Wissing and Muller, 2001a; Worle et al., 2006).

CHAPTER III

MATERIALS AND METHODS

Crude Drugs

1. Fresh rhizomes of *Zingiber officinale* (purchased from Pak klong Talad Market, Bangkok, Thailand, 2006)

Materials

1. Absolute Ethanol, AR grade (Merck, Germany)
2. Acetonitrile, HPLC grade (Lab Scan Co., Ltd., Thailand)
3. L-ascorbic acid (Merck, Germany, lot no. F891427513)
4. Chloroform, AR grad (Labscan Asia, Thailand)
5. 1,1-diphenyl-2-picryl-hydrazyl radical (DPPH), Lot no. 51K1419, Sigma-Aldrich, Inc., USA
6. 2-Deoxyribose (Fluka, South Korea, lot no. 1266223)
7. Disodium hydrogen phosphate (Merck, lot no. F1021786 125)
8. Disodium ethylene diamine tetraacetic acid (EDTA) (T Chemical, Thailand)
9. Ethanol (Merck, Germany)
10. Ferrous ammonium sulphate (Merck, Germany)
11. [6]-Gingerol Standard (generous gift from the GPO, Thailand)
12. Glyceryl behenate (Compritol$^®$ ATO 888) (Gattefosse', France, lot no 103100)
13. Glyceryl palmitostearate (Precirol$^®$ATO5) (Gattefosse', France, lot no102456)
14. Glyceryl myristate (Dynasan$^®$ 114) (Gattefosse', France, lot no104248)
15. Hydrogen peroxide solution (30%w/v) (Merck, Germany, lot no. 602)
16. Methanol, HPLC grade (Lab Scan Co., Ltd., Thailand)
17. Poloxamer 188 (Lutrol$^®$ F68) (Lot No WPAB524C , BASF, Germany)
18. Potassium dihydrogen phosphate (Merck, Germany, lot no. A315973 127)
19. Quercetin (Sigma-Aldrich, Inc., USA, lot no. 2085730)
20. Sodium chloride (Merck, Germany, lot no.K32104204 324)
21. Sodium hydroxide (Merck, Germany, lot no. UN106498)
22. Prednisolone Standard 100.07 % (DMSc reference standard, lot no.145052)
23. 2-Thiobarbituric acid (Sigma-Aldrich, Germany, lot no. 066K0750)

24. α-Tocopherol (Fluka, Germany, lot no. 4486991)

25. Trichloroacetic acid (Fluka, Germany, lot no. 1222401)

26. Tween® 80 (East Asiatic Company, Thailand, lot no. 55055)

Apparatuses

1. Analytical balance (Model AX105, Mettler Toledo, Switzerland)

2. Centrifuge (Hitachi himac CR20B3, Japan)

3. Differential scanning calorimeter (DSC822^e, Mettler Toledo, Switzerland)

4. Dry cabinet (Model GH-197, Ampore House, Taiwan)

5. Freeze dryer (Model FD-6-850MPO, Dura-Dry™, FTS System Inc., USA)

6. High performance liquid chromatography system

    - Automatic sample injector (SIL-10A, Shimadzu, Japan)

    - Communications bus module (CBM-10A, Shimadzu, Japan)

    - Column (BDS Hypersil C18, 5μm, 250mm x 4.6mm, lot no.6596)

    - Liquid chromatograph pump (LC-10AD, Shimadzu, Japan)

    - Precolumn (μBondapack C18, 10 μm, 125 Aº, Water Corporation, Ireland)

    - UV-VIS detector (SPD-10A, Shimadzu, Japan)

7. High pressure homogenizer (Model EmulsiFlex C5, Avestin, Canada)

8. High speed stirrer (WiggenHouser, Germany)

9. Homogenizer (Model EURO-D, Memmert, Germany)

10. Micropipette (Biohit, Finland)

11. Modified Franz Diffusion cells (Crown Glass Company, USA)

12. Magnetic stirrer (Model RCT basic, KIKA® Works Guangzhou, China)

13. Photon Correlation Spectrometer (Zetapals, Brookhavern Instrument, USA)

14. pH meter (Orion model 420A, Orion Research Inc., USA)

15. Rotary evaporator (Buchi heating bath B-490, Switzerland)

16. Sonicator (Model TP680DH, Elma, Germany)

17. Stability cabinet (Eurotherm Axyos, Germany)

18. Stopwatch (Heuer, Switzerland)

19. Transmission Electron Microscope (Model JEM-1230, Jeol, Japan)

20. Ultracentrifuge (Model L80, Beckman, USA)

21. Ultrasonicator (Crest Ultrasonics, Malaysia)

22. UV-Visble Spectophotometer (UV-1601, Shimadzu, Japan)

23. Vacuum pump (CB 169 Vacuum System, Buchi, Switzerland)

24. Vortex mixer (Vortex Ginies-2, Scientific Industries, USA)

25. Water bath (Model WB22, Becthai Co., Ltd., Thailand)

26. X-ray diffractometer (Model JDX-3530, Jeol, Japan)

Accessories

1. Centrifuge bottles polycarbonate (10.4 ml) (Beckman Instruments, USA)

2. Disposable syringe filter nylon 13 mm, 0.45 μm (Chrom Tech, USA)

3. Parafilm (American National Can TM, USA)

4. Polycarbonate centrifuge bottles (Beckman, USA, lot no. A60519)

5. Regenerated cellulose membrane, MWCO 12,000-14,000 (CelluSep T4, Canada, lot no. 8764)

6. Porcine skin (donated by S.Y farm, Ratchaburi, Thailand)

7. TLC Alumina sheet silica gel 60F 254 20x20 cm (E. Merck, Germany)

8. Whatman filter paper No.1, 150 mm (Whatman International Ltd. England)

Methods

A. Preparation of Crude Extracts from Rhizomes of *Zingiber officinale*

  1. **Preparation of crude dry ginger**

Fresh rhizomes of ginger (20.2 kg) were perchased from local market in Bangkok, Thailand. They were dried in a hot air oven under 60ºC and milled into dried coarse powder.

  2. **Extraction process**

Dried coarse powder of ginger (2 kg) was extracted with various solvent of different polarities. Coarse powder was marcerated with hexane at ambient temperature for 3 days. The filtration of the extracted liquid was made through filter paper (Whatman no.1) under vacuum. Then, the defatted residue was re-extracted using either acetone or 20% ethanol in water as the solvent. The marc was successively extracted until exhausted. Each extracted solution was dried using rotary evaporator to obtain crude acetone extract and ethanol extract, respectively. The extraction process was performed according to diagram shown in (Figure 9). The crude extracts were allowed to stand overnight in a desiccator until constant weight to obtain solvent free extract. The percentage yield was also calculated.

  3. **Isolation of [6]-gingerol from crude extracts of *Zingiber officinale***

The acetone crude extract was mixed with adsorbent and fractionated by column chromatography on silica gel. The mixture of n-hexane:acetone (4:1) was used as a developing solvent. Multiple column chromatography fractions were collected and were identified by TLC profiled using standard [6]-gingerol as reference. Fractions which had the same characteristic with reference were combined and evaporated. The retention time of isolated [6]-gingerol crude extract and standard [6]-gingerol were checked by HPLC for identification.
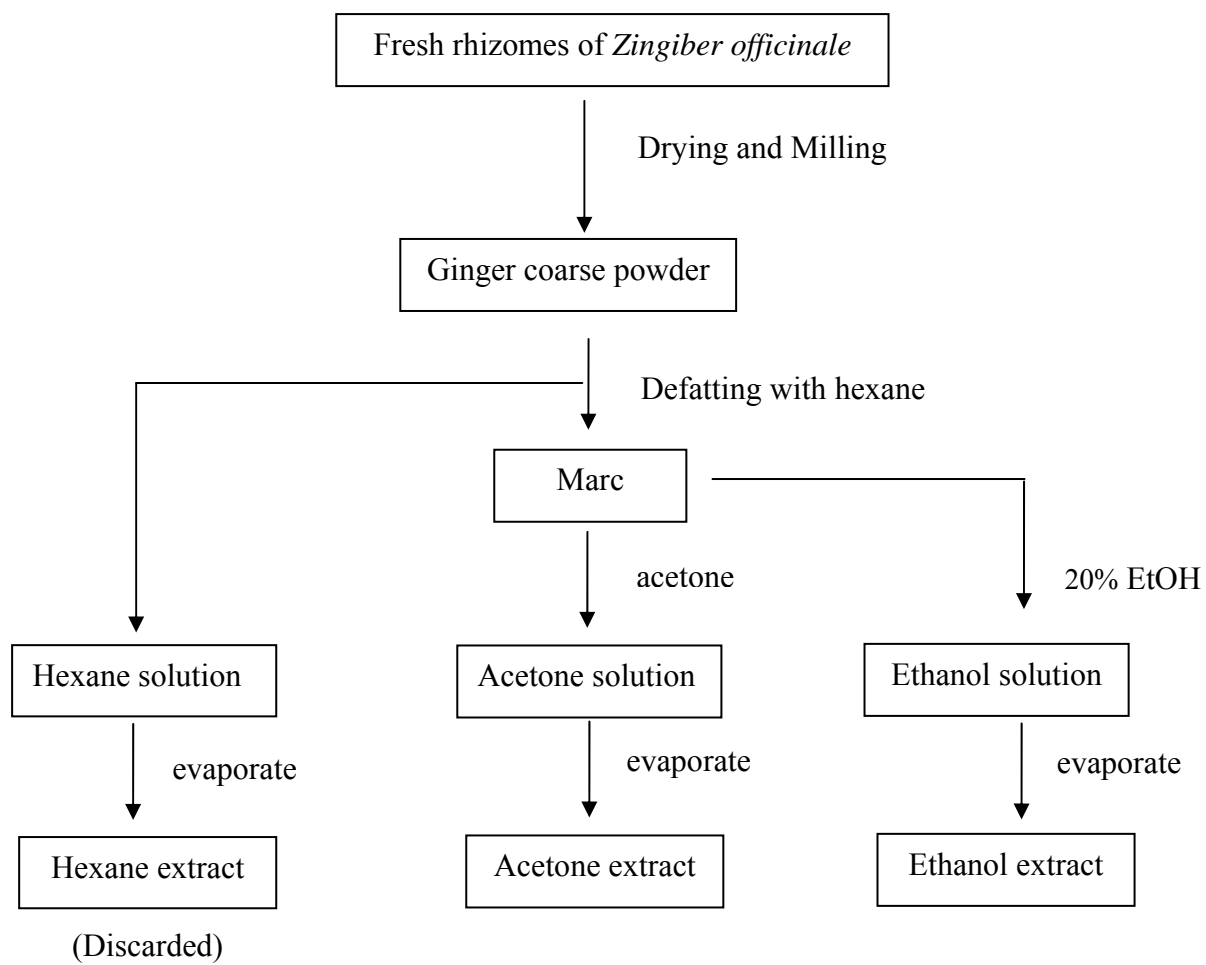
Figure 9 Diagram of the solvent extraction process of *Zingiber officinale*

B. Determination of Active Constituents from *Zingiber officinale*

1. Thin Layer Chromatographic (TLC) Method

TLC method was used for identification of [6]-gingerol in crude extract from *Zingiber officinale*. The method was rapid and available for a number of samples to be identified. Sample and standard could be applied in a single plate.

The fractionated extractions from silica column chromatography were spotted on TLC Alumina sheet compared with standard solution of [6]-gingerol. Afterthat, the plate was placed into equilibrated mobile phase, hexane:acetone (4:1) (He et al., 1998) inside a close chamber. When the mobile phase has moved to an appropriated distance, the plates have been removed and dried. The plates were visualized by vaporing of iodine sublimation. The basic parameter used to describe migration is the Rf value, where

$$Rf = \frac{\text{Distance moved by the solute}}{\text{Distance moved by mobile phase front}}$$

2. High Performance Liquid Chromatographic (HPLC) Method

The identification of [6]-gingerol in crude extracts from *Zingiber officinale* was performed by HPLC method because of its specificity and high sensitivity.

2.1 Chromatographic Condition

The chromatographic conditions for the analysis of active constituents from *Zingiber officinale* were investigated and modified from the method reported by (Jolad et al, 2004):

Column	:	BDS Hypersil C18, 5 µm, 250 mm x 4.6 mm
Precolumn	:	µBondapack C18, 10 µm, 125A°
Mobile phase	:	Acetonitrile:Methanol:Water (52:5:43)
Injection volume	:	20 µl
Flow rate	:	1 ml/min
Detector	:	UV detector at 282 nm
Temperature	:	ambient
Runtime	:	15 min

The mobile phase was freshly prepared, filtered through 0.45 µm membrane filter and then degassed by sonication for 30 min before use.

2.2   Standard Solution

2.2.1 Preparation of standard solutions

The 1 mg part of standard [6]-gingerol was accurately weighed and transferred into a 10 ml volumetric flask, diluted and adjusted to volume with methanol. The stock solution had the final concentration of [6]-gingerol was 100 µg/ml.

The solutions of 500 µl of [6]-gingerol standard stock solution was added into 5 ml volumetric flasks. The dilution to volume with methanol gave final concentrations of 10 µg/ml of [6]-gingerol.

2.2.2 Preparation of sample solutions

The sample solution of isolated [6]-gingerol and acetone crude extract was prepared and the concentrations of both acetone extract and isolated [6]-gingerol extract were 10 µg/ml.

3. UV Spectrophotometric Method

UV spectrophotometric method was used for the identification and determination of [6]-gingerol content of crude extracts from *Zingiber officinale* because it was convenient and rapid.

3.1 Validation of the UV spectrophotometric method

3.1.1 Preparation of standard [6]-gingerol solutions

The 1 mg part of [6]-gingerol was accurately weighed and transferred into a 10 ml volumetric flask, diluted and adjusted to volume with methanol. This stock solution had the final concentration of [6]-gingerol of 100 µg/ml.

The solutions of standard [6]-gingerol stock solution were added into 5 ml volumetric flasks. The dilution to volume with methanol gave final concentrations of 5, 10, 15, 20, 25, 30 and 35 µg/ml of [6]-gingerol, respectively.

The standard solutions were freshly prepared and analyzed. As a result, the standard curve between concentration and absorbance was plotted.

3.1.2 Preparation of sample solutions

The sample solution of isolated [6]-gingerol and acetone crude extract was prepared in the same concentration as the standard solutions. The final concentration was in range 5-35 µg/ml

3.1.3 Validation of the UV spectrophotometric method

The analysis of parameters in the assay validation for the UV spectrophotometric method was specificity, linearity, precision and accuracy.

3.1.2.1 Specificity

Under the conditions used, the absorbance of [6]-gingerol must not be interfered by the absorbance of other components in the sample

3.1.2.2 Linearity

Three sets of seven standard solutions of [6]-gingerol ranging from 5 to 35 µg/ml were prepared and analyzed. Linear regression analysis of the absorbance versus their concentrations was performed. The linearity was determined from the coefficient of variation (R^2).

3.1.2.3 Accuracy

The accuracy of an analytical method is the closeness of test results obtained by that method to the true value. The accuracy of the method was determined from the percentage of recovery. Five sets of three concentrations (low, medium, high) of [6]-gingerol at 7, 17, 27 µg/ml were prepared and analyzed, respectively. The percentage of recovery for each concentration was calculated from the ratio of inversely estimated actual concentration multiplied by 100.

3.1.2.4 Precision

a) **Within run precision**

The within run precision was determined by analyzed five sets of three concentrations of [6]-gingerol at 7, 17, 27 µg/ml in the same day. The percent coefficient of variation (%CV) of [6]-gingerol of each concentration was determined.

b) **Between run precision**

The between run precision was determined by analyzing three concentrations of [6]-gingerol at 7, 17, 27 µg/ml on five different days. The percent coefficient of variation (%CV) of [6]-gingerol of each concentration was determined.

Acceptance criteria:

In order to get high accuracy, the percentage of recovery should be within 98-102% for each nominal concentration, whereas the different coefficient percentage for both within run precision and between run precision should be less than 2%.

C. Evaluation of Different *Zingiber officinale* Extracts for Antioxidant Activities

Various evaluation methods for antioxidant activity have been used to monitor and compare the antioxidant activity of plant. In recent years, oxygen radical absorbance capacity assays have been used to evaluate antioxidant activity.

Anti-oxidative properties of ginger extracts were determined using 2 different methods as follows:

1. Hydrogen-donating activity (DPPH radical scavenging activity)

Hydrogen-donating activity of the ginger extracts; acetone, ethanol, isolated [6]-gingerol extracts and standard [6]-gingerol, were determined using the free radical generator 1,1-diphenyl-2-picryl-hydrazyl (DPPH). DPPH free radical has been used to assess the ability of phenolic compounds to transfer labile hydrogen atoms to radicals (Stoilova et al., 2006). Total hydrogen atom donating capacities were evaluated in the IC_{50} index, defined as the concentration needed to reduce 50% of DPPH radical.

The diphenylpicrylhydrazyl (DPPH) method is a simple calorimetric assay of antioxidant activity based on the decrease in absorbance at 517 nm. The addition of antioxidant (RH) results in the changing of purple color to yellow. The reaction of DPPH and its reduction product are shown as follows:

DPPH· + RH ⟶ DPPH-H + R·
(purple)   (yellow)
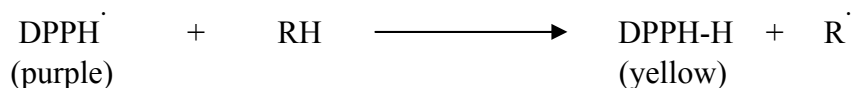
1.1 Preparation of 0.1 mM DPPH radical solution

DPPH was accurately weighed 3.943 mg and dissolved in 100 ml of methanol

1.2 Preparation of test samples

The test samples were prepared with initial concentration of 1 mg/ml. The stock solution was diluted with methanol until a suitable range of concentration (μg/ml). The DPPH solution (1ml) was added into the test sample solution (1ml). The final concentrations are shown in Table 2

Table 2. The initial and final concentrations (μg/ml) of the test samples

Initial concentration (μg/ml)	200	140	100	60	20	15	10	5	2	1
Final concentration (μg/ml)	100	70	50	30	10	7.5	5	2.5	1	0.5

1.3 Measurement of activity

A methanolic solution (1 ml) of the sample at various concentrations (final concentration 0.5–100 μg/ml) were added to 1 ml of DPPH (0.1 mM) solution. The mixture was left to stand at ambient temperature for 30 min in the darkness. The absorbance was measured by a UV–Vis spectrophotometer at 517 nm. The L-ascorbic acid and α-tocopherol were used as the positive control (Castro et al, 2006 and Lee et al, 2008). The ability to scavenge the DPPH radical was calculated using the follow equation: (Xu et al, 2008)

$$\% \text{ Inh.} = \frac{\text{Abs.control} - \text{Abs.sample}}{\text{Abs.control}} \times 100$$

Where the Abs. control is the absorbance of the control (DPPH solution without sample), the Abs. sample is the absorbance of the test sample (DPPH solution plus test sample).

1.4 Calculation of IC $_{50}$

After calculation of % inhibition for each concentration of the test sample, a graph showing concentration versus % inhibition was plotted. The concentration at 50% inhibition (IC $_{50}$) of each test sample was calculated from the equation of polynomial regression of the initial linear portion of the graph. All tests and analyses were performed in triplicate and averaged.

1.5 Statistic analysis

The mean ± SD values were obtained from triplicate experiments. Statistical comparison of the IC $_{50}$ values among different ginger extracts and other antioxidants was made using one-way ANOVA and Duncan test ($\alpha = 0.05$).

2. Hydroxyl radical scavenging activity

The hydroxyl radical scavenging ability was evaluated based on its ability to inhibit deoxyribose degradation. The degradation of deoxyribose caused by hydroxyl radical (reaction 1). The hydroxyl radicals attack deoxyribose to form malondialdehyde (MDA) under heat and acid conditions (reaction 2). MDA is reacted with thiobarbituric acid (TBA) and form a pink chromogen (reaction 3). This calorimetric reaction can be detected and measured at 532 nm. The addition of hydroxyl radical scavenger results in the decreasing of deoxyribose fragment and MDA formation. Lower absorbance of the pink chromogen in the reaction mixture indicated higher free radical scavenging activity (Halliwell et al.,1987)

$$Fe^{2+}\text{-EDTA} + H_2O_2 \longrightarrow Fe^{3+}\text{-EDTA} + OH^{\cdot} + OH^{-} \quad (1)$$

$$OH^{\cdot} + \text{deoxyribose} \longrightarrow \text{fragment} \qquad MDA \quad (2)$$

$$TBA + MDA \longrightarrow \text{pink chromogen} \qquad (3)$$
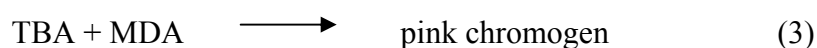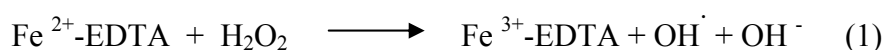
2.1 Preparation of the reaction mixture (Ardestani and Yazdanparast, 2006)

2.1.1 Preparation of phosphate buffer (pH 7.4)

Potassium dihydrogen phosphate (KH_2PO_4, MW. 136.09) and di-Sodium hydrogen phosphate (Na_2HPO_4, MW. 141.96) (2.38 and 0.19 g) were dissolved in distilled water. Sodium Chloride (NaCl, MW. 58.44) (8 g) was dissolved in water. Then, solutions were mixed to volume 1000 ml and adjusted to pH 7.4.

2.1.2 Preparation of 28 mM 2-deoxy-D-ribose (deoxyribose)

Deoxyribose (M.W. = 134.13) (18.75 mg) was dissolved in 5 ml of phosphate buffer pH 7.4.

2.1.3 Preparation of 1.04 mM EDTA

EDTA (M.W. = 292.25) (3.04 mg) was dissolved in 10 ml of phosphate buffer pH 7.4.

2.1.4 Preparation of 1 mM hydrogen peroxide (H_2O_2)

EDTA (30% w/v, M.W. = 34.01) (1 ml) was dissolved in 10 ml of phosphate buffer pH 7.4.

2.1.5 Preparation of 2 mM Ferrous ammonium sulphate ($Fe(NH_4)_2(SO_4)_2$)

$Fe(NH_4)_2(SO_4)_2$ (M.W. = 251.84) (5.04 mg) was dissolved in 10 ml of phosphate buffer pH 7.4.

2.1.6 Preparation of 1% 2-thiobarbituric acid (TBA)

Thiobarbituric (0.50 mg) was dissolved in 50 ml of 50 mM of NaOH solution.

2.1.7 Preparation of 2.8% trichloroacetic acid (TCA)

Thiobarbituric (1.40 mg) was dissolved in 50 ml of ultrapure water.

2.2 Preparation of test samples

The stock solution of acetone, isolated [6]-gingerol, ethanol extract and standard [6]-gingerol were prepared and dissolved in phosphate buffer pH 7.4 with initial concentration of 1 mg/ml. Then, the stock solutions were dilute with buffer until the range of final concentrations (10-400 μg/ml) was obtained. The concentrations of ginger extracts were 10, 50, 100, 150, 200, 300 and 400 μg/ml.

2.3 Measurement of activity

The reaction mixtures contained $Fe(NH_4)_2(SO_4)_2$ (100 μl), EDTA (100 μl), H_2O_2 (100 μl), deoxyribose (100 μl) and different concentrations of the test extracts (10-400 μg/ml) (100 μl). The final volume of reaction mixtures was made to 1.0 ml with PBS (20 mM, pH 7.4). The final concentration of test extracts was 1-40 μg/ml. After incubation at 37 °C for 1 hr, the color was developed by adding 1 ml of 2.8% TCA (w/v in water) and 1 ml of 1% TBA (w/v). The mixture was heated in a boiling water bath for 15 min and then cooled. Quercetin was used as the positive control and PBS as the blank. The absorbance of the resulting solution was measured spectrophotometrically at 532 nm. All the analyses were done in triplicates and average values were taken. Inhibition of deoxyribose degradation in percent was calculated according to the equation: (Mathew and Abraham, 2006)

$$\% \text{ Inh.} = \frac{\text{Abs.control} - \text{Abs.sample}}{\text{Abs.control}} \times 100$$

2.4 Calculation of IC $_{50}$

After calculation of % inhibition for each concentration of the test sample, a graph showing concentration versus % inhibition was plotted. The concentration at 50% inhibition (IC $_{50}$) of each test sample was calculated from the equation of polynomial regression of the initial linear portion of the graph. All tests and analyses were performed in triplicate and averaged.

2.5 Statistic analysis

The mean ± SD values were obtained from triplicate experiments. Statistical comparison of the IC $_{50}$ values among different ginger extracts and other

antioxidants was made using one-way analysis of variance (ANOVA) ($\alpha = 0.05$). The Duncan test was used for multiple comparisons using SPSS 11 for Windows.

D. Determination of Solubility of *Zingiber officinale* Extract in Solid Lipids

The important factor that determines the loading capacity of the extract in the lipid is the solubility of extract in melted lipid (Kumar et al., 2007). glyceryl palmitostrarate (GP, Precirol[®] ATO 5), glyceryl behenate (GB, Compritol[®] ATO 888), glyceryl myristate (Dynasan[®] 114) and cetyl palmitate were screened for their potential to solubilize ginger extract. Briefly, the amount 5% of ginger extract of solid lipid was taken in screwcapped test tubes. The corresponding amount of molten lipid required in the formula was added to solubilize the extract. Mixture of lipid and extract was heated above its melting point. The end point of the solubility study was the formation of clear, homogeneous dispersion of ginger extract in both molten lipid and solidified lipid. The solid lipid was selected on the basis of the solubilizing potential and the safety for topical route.

E. Preparation of Solid Lipid Nanoparticles (SLN)

1. Preparation of extract-free solid lipid nanoparticles

There are different approaches for the production of solid lipid nanoparticles (SLN). In this study, hot high pressure homogenization (HPH) technique was applied for the preparation of aqueous SLN dispersions, according to Muller et al. (2000). The oil and aqueous phases were prepared separately. The oil phase consisted of melted solid lipid and aqueous phases consisted of hydrophilic surfactant dispersed in water. The solid lipid was melted at a temperature 5 °C above its melting point. Under mechanical stirring at 10000 rpm using a high speed stirrer (WiggenHouser, Germany) the melted lipid phase was dispersed in a hot aqueous surfactant solution of identical temperature for 1 min. The obtained pre-mix emulsion was homogenized at 500 bar 3 cycles using the EmulsiFlex C5[®] (Avestin, Canada). The obtained o/w nanoemulsion was allowed to cool down to room temperature and the lipid in hot dispersion recrystallized forming aqueous SLN dispersions. The aqueous SLN was stored at different conditions, room temperature and 4 °C .The ingredient used in the

formulation were 5% of the selected lipids in topic D as solid lipid with 1-5% of Tween® 80 (Tw80) and Poloxamer® 188 (P188) as stabilizer. Each formulation was formulated in triplicate batches.

The effect of types of solid lipid and types and amount of surfactant were evaluated on the characteristics of SLN. The appearances of the extract-free SLN prepared by HPH method were observed visually i.e. color change, phase separation, coalescence and gel formation. The particle size and size distribution (polydispersity index, PI) were also investigated. For physical stability, they were assessed after preparations for 14, 30 and 60 days under storage conditions, RT and 4 °C. The physically stable composition was selected for further study.

2. Preparation of *Zingiber officinale* extract loaded solid lipid nanoparticles

The extract free formulations that had good physical stability were chosen to load ginger extract. The ginger extract which exhibited the best antioxidant activities in both tests would selected for loaded in SLN. Five percent of ginger extract calculated as a percentage of lipid matrix (0.25%) was added to the melt lipid and followed by the same procedure as in drug-free SLN.

F. Evaluation of Solid Lipid Nanoparticles

The characteristics such as appearance, surface morphology, shape, size and size distribution and the percentage of entrapment efficiency of each formulation were investigated.

1. Determination of physicochemical properties of extract-free SLN

The physicochemical properties of solid lipid nanoparticles drug delivery system before incorporation of ginger extract were determined as following:

1.1 Physical appearances

The physical appearances of the formulations such as color, coalescence, gel formation and phase separation were visually observed.

1.2 Particle size analysis

Particle size analysis was performed by photon correlation spectroscopy, PCS (Brookhaven, UK). A sample was dispersed and diluted in distilled water to

weak opalescence before use. The SLN dispersion was put in a quartz cuvette and be placed into instrument. PCS yields the mean particle size and the polydispersity index (PI) as the measure of the distribution. Each obtained value from each formulation was the average of 3 measurements.

The formulations which were stable during a period of 2 months of storage at room temperature and at 4 °C were selected for further study.

2. Determination of physicochemical properties of ginger-loaded SLN

The physicochemical properties of solid lipid nanoparticles drug delivery system after incorporation of ginger extract were determined as following:

2.1 Physical appearances

Physical appearances of SLN containing ginger extract were investigated as the same procedure in topic F1.

2.2 Particle size analysis

Particle size analysis of SLN containing ginger extract was investigated as the same procedure in topic F1.

3. Morphology

The morphological feature of ginger loaded SLN was investigated using transmission electron microscope (TEM), (JEM-1230, Jeol, Japan). The samples were placed on a specimen mesh coated with collodion film, being stained by 2% phosphotungstic acid and dried under room temperature.

4. Entrapment efficiency of ginger loaded SLN

The ginger loaded SLN formulations which were stable during a period of 2 months of storage at room temperature and at 4 °C were selected for entrapment efficiency study.

4.1 Assay of the entrapment efficiency study

The determination of amount of entrapped [6]-gingerol was performed by UV spectrophotometry due to rapidity and convenience.

4.1.1 Preparation of standard [6]-gingerol solutions

The 1 mg part of [6]-gingerol was accurately weighed and transferred into a 10 ml volumetric flask, diluted and adjusted to volume with chloroform: methanol (1:1). This stock solution had the final concentration of [6]-gingerol of 100 μg/ml.

The solutions of 250, 350, 450, 550, 650, 750 and 850 μl of standard [6]-gingerol stock solution were added into 5 ml volumetric flasks. The dilution to volume with chloroform: methanol (1:1) gave final concentrations of 5, 7, 9, 11, 13, 15 and 17 μg/ml of [6]-gingerol, respectively.

The standard solutions were freshly prepared and analyzed. As a result, the standard curve between concentration and absorbance was plotted.

4.1.2 Validation of the UV spectrophotometric method

The analysis of parameters in the assay validation for the UV spectrophotometric method was specificity, linearity, precision and accuracy.

a) Specificity

Under the conditions used, the absorbance of [6]-gingerol must not be interfered by the absorbance of other components in the sample

b) Linearity

Three sets of seven standard solutions of [6]-gingerol ranging from 5 to17 μg/ml were prepared and analyzed. Linear regression analysis of the absorbance versus their concentrations was performed. The linearity was determined from the coefficient of variation (R^2).

c) Accuracy

c1) Accuracy of analysis of solution

The accuracy of an analytical method is the closeness of test results obtained by that method to the true value. The accuracy of the method was determined from the percentage of recovery. Five sets of three concentrations (low, medium, high) of [6]-gingerol at 8, 12, 16 µg/ml were prepared and analyzed, respectively. The percentage of recovery for each concentration was calculated from the ratio of inversely estimated actual concentration multiplied by 100.

c2) Accuracy of analysis of SLN formulation

The accuracy formulation of an analytical method is the closeness of test results obtained by that method to the true value. The accuracy of the method was determined from the percentage of recovery. Five sets of three concentrations (low, medium, high) of [6]-gingerol at 8, 12, 16 µg/ml that spiked into selected formulation of SLN in topic F1.2 were prepared and analyzed, respectively. The percentage of recovery for each concentration was calculated from the ratio of inversely estimated actual concentration multiplied by 100.

d) Precision

d1) Within run precision

The within run precision was determined by analyzed five sets of three concentrations of [6]-gingerol at 8, 12, 16 µg/ml in the same day. The percent coefficient of variation (%CV) of [6]-gingerol of each concentration was determined.

d2) Between run precision

The between run precision was determined by analyzing three concentrations of [6]-gingerol at 8, 12, 16 µg/ml on five different days. The percent coefficient of variation (%CV) of [6]-gingerol of each concentration was determined.

Acceptance criteria:

In order to get high accuracy, the percentage of recovery should be within 98-102% for each nominal concentration, whereas the different coefficient percentage for both within run precision and between run precision should be less than 2%.

4.2 The entrapment efficiency study

One gram of loaded SLN dispersion was weighed into the microcentrifuge assembly. The encapsulated ginger extract was separated by ultracentrifugation at 65,000 rpm at 4 °C for 7 hours. The precipitated pellet containing ginger extract were lyzed by adding solution of chloroform: methanol (1:1). The clear solution was analyzed for entrapped [6]-gingerol content by UV-Vis spectrophotometry. The absorbance were monitored at 282 nm and compared with the standard curve of standard [6]-gingerol solution. The supernatants were freezed dried and dissolved in solution of chloroform: methanol (1:1). The obtained solution was analyzed for content of untrapped [6]-gingerol. All analyses were determined in five measurements and calculated the percentage of recovery. The entrapment efficiency and recovery were calculated by equations below. Drug-free SLN was used as blank.

$$\% \text{ entrapment efficiency} = \frac{\text{Amount of drug encapsulated}}{\text{Total loading amount}} \times 100$$

$$\% \text{ recovery} = \frac{A + B}{\text{Total loading amount}} \times 100$$

where A is amount of drug entrapped in solid lipid of SLN ; B is amount of free drug in supernatant.

Statistical analysis of differences in the Entrapment efficiency was performed by using Analysis of Variance (ANOVA). A *P*-value of 0.05 was taken as the level of significance.

5. Thermal analysis by differential scanning calorimetric method

The differential scanning calorimetric (DSC) thermogram was determined by using differential scanning calorimeter (DSC822, Mettler Toledo, Switzerland). A highly sensitive ceramic sensor in the DSC instrument was used to measure the difference between the heat flows to the sample and reference crucibles. The samples (3-5 mg) were accurately weighed into standard aluminum pans (40 µl) and then sealed. The DSC runs were conducted over a temperature range 25-125 ºC at rate of 10ºC/min. All tests were performed under a nitrogen atmosphere of 2 ml/min.

6. Powder X-ray Diffractogram

Powder X-ray diffractograms were carried out by using powder X-ray diffractometer (Bruker AXS model D8 Discover, Germany) with Cu-K radiation as the source of X-rays. The measurement conditions were set as voltage of 40 kV, current of 40 mA, scanning speed of 0.2 ° sec/step in the 0.02º angle range of 3-45°.

7. The analysis of [6]-gingerol in release and permeation study

The determination of [6]-gingerol content was performed by high performance liquid chromatography, HPLC.

7.1 Chromatographic Condition

The chromatographic conditions for the analysis content of [6]-gingerol from *Zingiber officinale* were investigated and modified from the method reported by (Jolad et al, 2004):

Column	:	BDS Hypersil C18, 5 µm, 250 mm x 4.6 mm
Precolumn	:	µBondapack C18, 10 µm, 125Aº
Mobile phase	:	Acetonitrile:Methanol:Water (40:10:50)
Injection volume	:	20 µl
Flow rate	:	0.8 ml/min
Detector	:	UV detector at 282 nm
Temperature	:	ambient
Runtime	:	15 min
Internal standard	:	prednisolone

The mobile phase was freshly prepared, filtered through 0.45 μm membrane filter and then degassed by sonication for 30 min before using.

7.2. The determination of [6]-gingerol content in 20% isopropanol in PBS buffer pH 7.4

The determination of [6]-gingerol content in 20% isopropanol in PBS buffer pH 7.4 was performed for analysis of [6]-gingerol in receiver medium of Franz cell in release study.

7.2.1 Preparation of internal standard solution

A stock solution of internal standard was prepared by accurately weighed 2.5 mg of prednisolone into a 25 ml volumetric flask, diluted and adjusted to volume with methanol. The final concentration of prednisolone stock solution was 100 μg/ml.

7.2.2 Preparation of standard solutions

The 1 mg parts of standard [6]-gingerol was accurately weighed and transferred into a 10 ml volumetric flask, diluted and adjusted to volume with methanol. These stock solutions have the final concentrations of [6]-gingerol was 100 μg/ml.

The solutions of 12.5, 25, 50, 150, 250, 350 μl of [6]-gingerol standard stock solution, and 250 μl of internal standard stock solution were added into 5 ml volumetric flasks. The dilution to volume with 20% isopropanol in PBS buffer pH 7.4 gave final concentrations of 0.25, 0.5, 1, 3, 5, 7 μg/ml of [6]-gingerol, respectively.

The standard solutions were freshly prepared and used for the HPLC determination. As a result, the standard curve between concentration and peak area was plotted.

7.3 Validation of the HPLC method

The analytical parameters used in the validation of the HPLC assay method were specificity, linearity, accuracy and precision (USP 24, 2000). The validation procedure was performed as follows:

7.3.1 Specificity

The specificity of the method was determined by comparing the test results from analyses of [6]-gingerol in 20% isopropanol in PBS buffer pH 7.4 with standard solutions. Under the chromatographic conditions used, the peak of [6]-gingerol must be completely separated from and not be interfered by the peaks of methanol and prednisolone.

7.3.2 Linearity

The linearity was determined from the coefficient of determination (R^2). Six concentrations of standard solutions and three replicates of each concentration were prepared and analyzed. The relation between the peak area and concentrations were plotted and the least square linear regressions were calculated.

7.3.3 Accuracy

The accuracy of an analytical method is the closeness of test results obtained by that method to the true value. Five sets of three concentrations (low, medium, high) of [6]-gingerol at 2, 4, 6 µg/ml were prepared and analyzed, respectively. The accuracy of the method was determined from the percentage of recovery. The percentage of recovery of each concentration was calculated from the estimated concentration to know concentration multiplied by 100.

7.3.4 Precision
a) Within run precision

The within run precision was determined by analyzed five sets of three concentrations (low, medium, high) of [6]-gingerol at 2, 4, 6 µg/ml in the same day. Peak area of [6]-gingerol was calculated and the percent of coefficient of variation (%CV) of each concentration was determined.

b) Between run precision

The precision during the operation run was determined by analyzing three concentrations (low, medium, high) of [6]-gingerol at 2, 4, 6 µg/ml on

five different days. Peak area of [6]-gingerol was calculated and the percent of coefficient of variation of each concentration was determined.

Acceptance criteria:

For accuracy, the percentage of recovery should be within 98-102% of each nominal concentration, whereas the percent coefficient of variation for both within run precision and between run precision should be less than 2%.

7.4 The determination of [6]-gingerol content in PBS buffer pH 7.4

The determination of [6]-gingerol content in PBS buffer pH 7.4 was performed for analysis of [6]-gingerol in receiver medium of Franz cell in permeation study. The following topics were performed as the same concentration and same condition as topic 7.2 and 7.3.

7.4.1 Preparation of internal standard solution

7.4.2 Preparation of standard solutions

7.4.3 Validation of the HPLC method

7.5 The determination of [6]-gingerol content in methanol

The determination of [6]-gingerol content in methanol was performed for analysis of [6]-gingerol in new born pig skin.

7.5.1 Preparation of internal standard solution

A stock solution of internal standard was prepared by accurately weighed 2.5 mg of prednisolone into a 25 ml volumetric flask, diluted and adjusted to volume with methanol. The final concentration of prednisolone stock solution was 100 µg/ml.

7.5.2 Preparation of standard solutions

The 1 mg parts of standard [6]-gingerol was accurately weighed and transferred into a 10 ml volumetric flask, diluted and adjusted to volume with methanol. These stock solutions have the final concentrations of [6]-gingerol was 100 µg/ml.

The solutions of 100, 200, 300, 400, 500, 600, 700 µl of [6]-gingerol standard stock solution, and 250 µl of internal standard stock solution were added into 5 ml volumetric flasks. The dilution to volume with methanol gave final concentrations of 2, 4, 6, 8, 10, 12, 14 µg/ml of [6]-gingerol, respectively.

The standard solutions were freshly prepared and used for the HPLC determination. As a result, the standard curve between concentration and peak area was plotted.

7.5.3 Validation of the HPLC method

The analytical parameters used in the validation of the HPLC assay method were specificity, linearity, accuracy and precision (USP 24, 2000). The validation procedure was performed as follows the topic 7.3.

8. In vitro release study of solid lipid nanoparticles containing *Zingiber officinale* extract

The *in vitro* release study was performed by using modified Franz diffusion cell, which consisted of donor and receiver compartments. The dialysis membrane was placed between two compartments of modified Franz diffusion cell. The membrane was soaked in distilled water for 24 hours, then washed by hot distilled water and soaked in isotonic phosphate buffer saline buffer pH 7.4 for an hour before use. The receiving compartment contained about 14 ml of 20% isopropanol in isotonic phosphate buffer saline pH 7.4 which was maintained at 37±0.5°C by a circulating water jacket. The receptor fluid and membranes were equilibrated to the desired temperature for 1 hr before this study. After equilibration, the sample of film (diameter 1.8 cm) was carefully placed into the donor compartment and 100 μl of ginger extract loaded SLN was dropped into donor compartment then covered with parafilm to prevent evaporation. The hydroalcoholic solution (80% ethanol) of acetone extract was used as control. The receptor fluid was continuously mixed by magnetic stirring bar throughout the time of study. A volume of 1 ml were taken from receiver medium at certain time intervals of 2, 4, 6, 8, 10, 12, 14, 16, 20 and 24 hours. The receptor compartment was replaced with receptor solution to keep the constant volume during the experiment. The examination was performed in 5 replicates. The samples were analyzed for amount of [6]-gingerol released from the SLN by HPLC method.

The amount of drug released was calculated by multiplying the drug concentration with medium volume. The percentage of drug release was calculated by the following equation:

$$\% \text{ drug release} \quad = \quad (A_t / A_0) \times 100$$

where A_t is cumulative released amount of drug at a particular time; A_0 is the initial amount of drug.

9. Skin permeation study of solid lipid nanoparticles containing *Zingiber officinale* extract

Permeation experiments were performed by using modified Franz diffusion cell, which consisted of donor and receiver compartments. The porcine skin was placed between two compartments of modified Franz diffusion cell. The porcine skin was soaked in isotonic phosphate buffer saline buffer pH 7.4 for an hour before use. The receiving compartment contained 14 ml of isotonic phosphate buffer saline buffer pH 7.4 which was maintained at 37 ± 0.5°C by a circulating water jacket. The receptor fluid and porcine skin were equilibrated to the desired temperature for 1 hr before the permeation study. After equilibration, the sample of pig skin (diameter 1.8 cm) was carefully placed into the donor compartment and 100 μl of ginger extract loaded SLN was also dropped into donor compartment. The hydroalcoholic solution (80% ethanol) of acetone extract was used as control. The receptor fluid was continuously mixed by magnetic stirring bar throughout the time of study. A volume of 1 ml were taken from receiver medium at certain time intervals of 2, 4, 6, 8, 10, 12, 14, 16, 20 and 24 hours. The receptor compartment was replaced with receptor solution to keep the constant volume during the experiment. The samples were analyzed for amount of [6]-gingerol permeated through the skin into the receptor compartment by HPLC method as mentioned below. Additionally, at the end of study, the remaining portion of the loaded SLN in the donor compartment and the porcine skin were removed and analyzed for [6]-gingerol in methanol extract. The pig skin was cut into small pieces and soaked in methanol. Then, the amount of [6]-gingerol in methanol was analyzed by HPLC. The examination was performed in 5 replicates.

G. Statistical Analysis

The data of % DPPH inhibitor, % hydroxyl radical inhibitor, % Entrapment efficiency, rate constant of release and rate constant of permeation were analyzed by statistically using one-way analysis of variance (ANOVA). When a significant difference ($p<0.05$) was indicated, the data were subjected to multiple comparison by Duncan test to compare the difference. The statistical package for the social sciences (SPSS) program version 11.0 was used in this study.

CHAPTER IV

RESULTS AND DISCUSSION

A. Preparation of Crude Extracts from Rhizome of *Zingiber officinale*

1. Ginger crude extract from solvent extraction

Extraction of natural plants can be done by using variety of solvents depending on the polarity of required active compound. In this study, hexane, acetone and 20% ethanol were used as the solvent for *Zingiber officinale*. The crude hexane extract of *Zingiber officinale* was obtained by maceration of two kilograms of the dried coarse powder with hexane for extraction of nonpolar compounds, such as volatile oils and other nonpolar compounds. The dried defatted coarse powder (Figure 10) was directly extracted by individual solvents either acetone or 20% ethanol. As 20% ethanol was relatively more polarity than acetone, the ethanol extract was composed of semipolar and polar compounds. All obtained extracts, acetone extract and ethanol extract, had thick dark-brown color. The percentage of yield of ginger extracts with different solvent extractions are showed in Table 3

Figure 10 Dried defatted coarse powder of *Zingiber officinale*.

Table 3 The percentages of yield of ginger extracts

Ginger extract	Dried ginger (g)	Weight of extract (g)	% Yield
Acetone	2000	92.91	4.65
20% Ethanol	1000	146.14	14.61
Isolated [6]-gingerol	2000	5.03	0.25

2. Isolation of [6]-gingerol from crude extracts of *Zingiber officinale*

From the preliminary study by UV spectrophotometry, the UV absorption spectrum of standard [6]-gingerol exhibited maximum absorption at 282 nm. Acetone extract showed maximum absorption at 282 nm with much more intensified peak than ethanol extract (Figure A1). Thus, acetone extract was selected to the next purification process by column chromatography.

The acetone crude extract was mixed with adsorbent and isolated by column chromatography on silica gel. Many fractions were collected and were identified by TLC profiled using standard [6]-gingerol as reference. The characteristic of standard [6]-gingerol and fractions are shown in Figure 11

The fractions 16-37, which showed the same characteristic with reference, were combined and evaporated. Then, the concentrated fraction was purified by column chromatography on silica gel and fractions were identified by TLC as showed in Figure 12. The fractions 4-6, which had the same characteristic with reference, were combined and used as isolated [6]-gingerol extract. The isolated [6]-gingerol extract obtained as dark brown color similar to acetone and ethanol extracts as showed in Figure 13
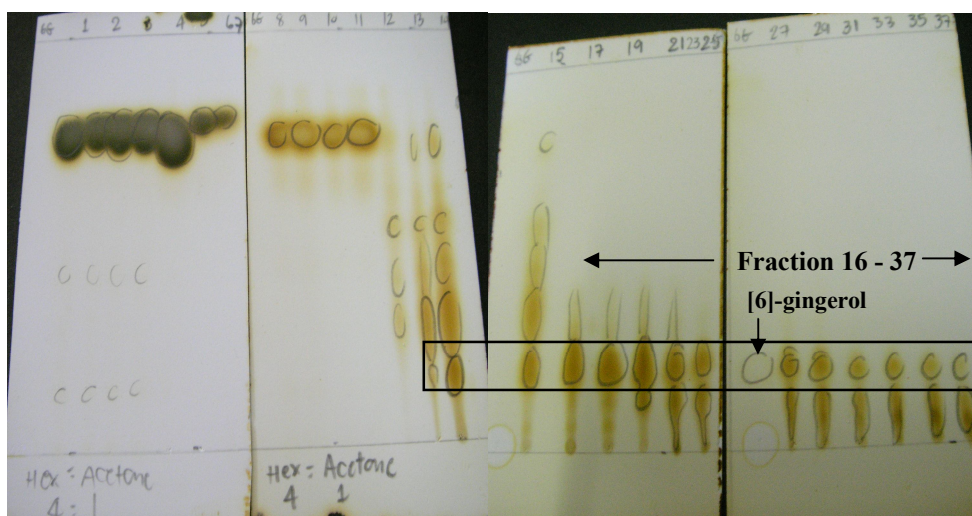
Figure 11 TLC chromatograms of standard [6]-gingerol and ginger extract with hexane:acetone (4:1) as mobile phase.
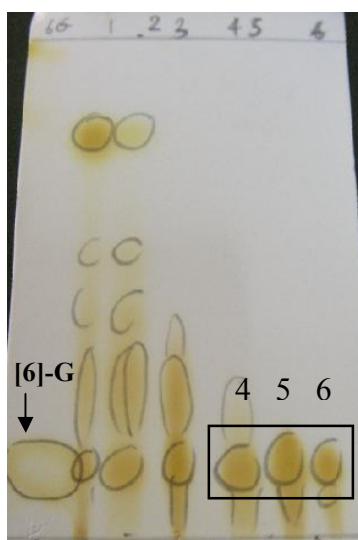
Figure 12 TLC chromatogram of standard [6]-gingerol and refractionated fractions

(a)   **(b)**   **(c)**
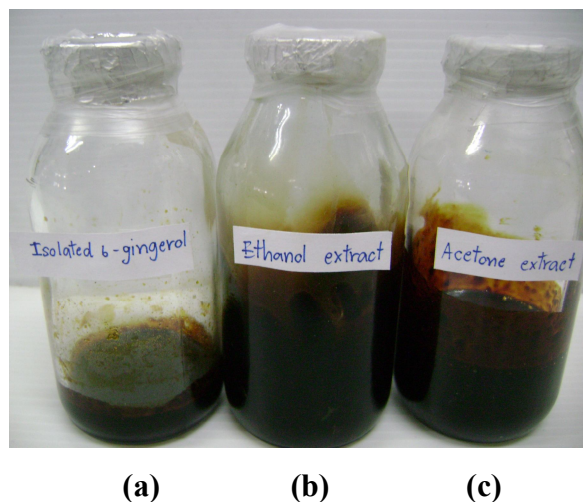
Figure 13 Three fractions of ginger extracts: (a) isolated-[6]-gingerol, (b) ethanol extract and (c) acetone extract

B. Identification and Determination of Active Constituents from *Zingiber officinale*

I. Identification of [6]-gingerol in ginger extracts

1. Thin Layer Chromatographic (TLC) Method

TLC is the most versatile and flexible chromatographic method. It is rapid and available for a number of samples to be identified. Samples and standard can be applied in a single plate and separated at the same time.

The isolated compound from crude extract was identified by TLC using mixture of n-hexane:acetone (4:1) as a developing solvent (He et al., 1998). The chromatogram of the compound was compared to the standard [6]-gingerol. From chromatogram in Figure 12, the calculation of distance of standard [6]-gingerol and compound in TLC sheet was found that the R_f value of the extract was equal to the standard [6]-gingerol at the value of 0.24. The finding was similar to the result reported by He et al. (1998) as $R_f = 0.25$. From the data obtained, it was confirmed that isolated [6]-gingerol crude extract had the same characteristics as standard [6]-gingerol. Based on the data, the major composition of this extract was [6]-gingerol.

2. High Performance Liquid Chromatographic (HPLC) Method

The developed HPLC system was applied to identify the extract from rhizomes of ginger. It was found that the extract had similar chromatogram to the standard [6]-gingerol. The identical retention time of extract and standard [6]-gingerol were 6.308-6.318 min as shown in Figure 14. From the data obtained, it was found that acetone and isolated [6]-gingerol crude extract had the same chromatogram characteristics as standard [6]-gingerol.

II. Determination of [6]-gingerol in ginger extract by UV Spectrophotometric Method

1 Validation of the UV spectrophotometric Method

The validation of analytical method is the process by which it is established that the performance characteristics of the method meet the requirements for the intended analytical applications. The performance characteristics are expressed in term of analytical parameters. For UV spectrophotometric method validation, these include linearity, accuracy and precision.

1.1 Linearity

The calibration curve data of standard [6]-gingerol are shown in Table 4. The plot of standard [6]-gingerol concentrations versus absorbance (Figure 15) displayed the linear correlation in the concentration range studied of 5-35 μg/ml. The coefficient of determination (R^2) of this line was 0.9998. These results indicated that UV spectrophotometric method was acceptable for quantitative analysis of [6]-gingerol in the range studied.
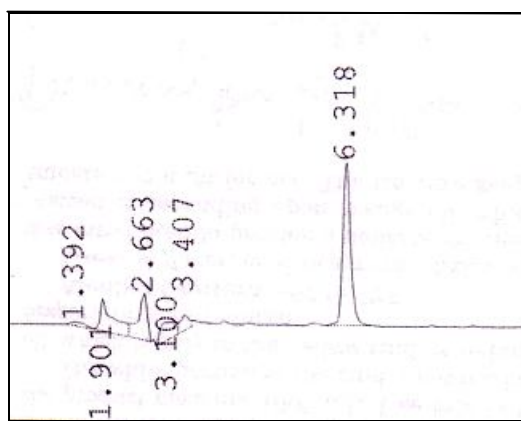
(a)
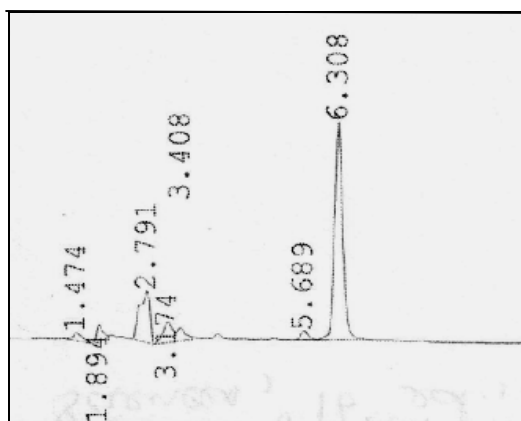
(b)
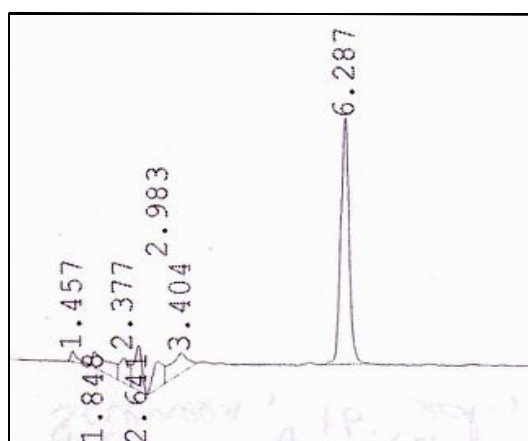
(c)

Figure 14 HPLC chromatogram of ginger extracts, (a) standard [6]-gingerol, (b) acetone extract, (c) isolated-[6] gingerol

1.2 Accuracy

The accuracy of an analytical method is the closeness of test results obtained by the method to the true value. The determination of accuracy was performed by analyzing five sets of three concentrations (7, 17, 27 μg/ml). The inversely estimated concentrations and percentages of analytical recovery of each drug concentration are shown in Table 5 and Table 6, respectively. All percentages of analytical recovery were in the range of 99.13 – 102.67 %, which indicated that this method could be used for analysis of [6]-gingerol in all concentrations studied with high accuracy.

1.3 Precision

The precision of [6]-gingerol analyzed by UV spectrophotometric method were determined both within run precision and between run precision as illustrated in Tables 7 and 8. All coefficients of variation values were small, as 0.10-0.12% and 0.11-0.35%, respectively. The coefficient of variation of an analytical method should generally be less than 2%. Therefore, the UV spectrophotometric method was precise for quantitative analysis of [6]-gingerol in the range studied.

Table 4 Data of calibration curve of [6]-gingerol by UV spectrophotometric method

Concentration (μg/ml)	Absorbance			Mean	SD	%CV
	Set1	Set2	Set3			
5	0.1952	0.1952	0.1945	0.1950	0.0004	0.2073
10	0.3005	0.3002	0.3014	0.3007	0.0006	0.2077
15	0.4091	0.4088	0.4082	0.4087	0.0005	0.1121
20	0.5032	0.5032	0.5032	0.5032	0.0000	0.0000
25	0.6099	0.609	0.6082	0.6090	0.0009	0.1396
30	0.7179	0.7179	0.7176	0.7178	0.0002	0.0241
35	0.8235	0.8223	0.8202	0.8220	0.0017	0.2032
R^2	0.9998	0.9998	0.9998	0.9998	-	-
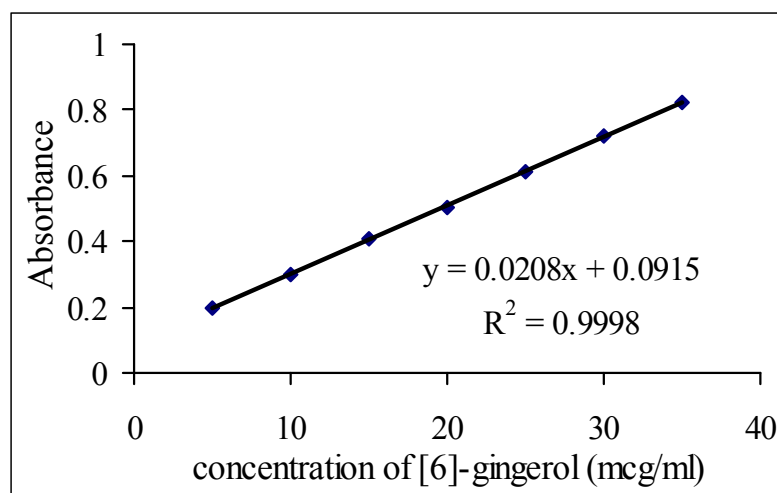
Figure 15 Calibration curve of [6]-gingerol by UV spectrophotometric method

Table 5 The inversely estimated concentrations of [6]-gingerol

Concentration (μg/ml)	Inversely estimated concentration (μg/ml)					Mean ± SD
	1	2	3	4	5	
7	6.9087	6.9231	6.9663	6.9952	6.9038	6.9394 ± 0.04
17	17.4279	17.4183	17.4712	17.4712	17.4808	17.4538 ± 0.03
27	27.2500	27.2548	27.3269	27.2837	27.2500	27.2731 ± 0.03

Table 6 The percentages of analytical recovery of [6]-gingerol

Concentration (μg/ml)	%Analytical recovery					Mean ± SD
	1	2	3	4	5	
7	98.69	98.90	99.52	99.93	98.63	99.13 ± 0.57
17	102.52	102.46	102.77	102.77	102.83	102.67 ± 0.17
27	100.92	100.94	101.21	101.05	100.92	101.01 ± 0.12

Table 7 Data of within run precision by UV spectrophotometric method

Concentration (µg/ml)	Absorbance					Mean	SD	%CV
	Set1	Set2	Set3	Set4	Set5			
7	0.2353	0.2357	0.2356	0.2358	0.2353	2.4749	0.002	0.10
17	0.4541	0.4541	0.4543	0.4548	0.4554	4.9369	0.006	0.12
27	0.6584	0.658	0.6593	0.6577	0.6585	6.5159	0.006	0.10

Table 8 Data of between run precision by UV spectrophotometric method

Concentration (µg/ml)	Absorbance					Mean	SD	%CV
	Set1	**Set2**	**Set3**	**Set4**	**Set5**			
7	0.2353	0.2356	0.2365	0.2371	0.2352	0.2359	0.008	0.35
17	0.4541	0.4539	0.455	0.455	0.4552	0.4546	0.006	0.13
27	0.6584	0.6585	0.66	0.6591	0.6584	0.6589	0.007	0.11

In conclusion, the analysis of [6]-gingerol by UV spectrophotometric method developed in this study showed good specificity, linearity, accuracy and precision. Thus this method was used for the determination of the content of [6]-gingerol in this investigation.

2. Determination of [6]-gingerol content in ginger crude extract

The [6]-gingerol content of acetone extract and isolated [6]-gingerol extract are depicted in Table 9. The results also showed that both extracts were composed of [6]-gingerol as the major compound as 67.84% in acetone extract and 74.51% in isolated [6]-gingerol extract. Despite of the slightly higher content of [6]-gingerol in the isolated [6]-gingerol extract, the isolation process was complicated and time-consuming. It was interesting that the acetone extract contained a slightly lower content of [6]-gingerol, but it was prepared by a simple solvent extraction method.

Table 9 Concentration and percent content of [6]-gingerol in acetone and isolated [6]-gingerol extract (mean ± SD, n=3)

Sample Conc.(μg/ml)	Acetone extract		Isolated [6]-gingerol	
	Measured conc. (μg/ml)	% content	Measured conc. (μg/ml)	% content
10	6.82 ± 0.03	68.23 ± 0.32	7.42 ± 0.04	74.26 ± 0.51
15	10.30 ± 0.14	68.65 ± 0.92	11.23 ± 0.08	74.84 ± 0.63
20	13.40 ± 0.04	67.03 ± 0.19	14.99 ± 0.07	74.94 ± 0.43
25	16.96 ± 0.04	67.86 ± 0.16	18.40 ± 0.05	73.62 ± 0.24
30	20.43 ± 0.03	68.11 ± 0.10	22.43 ± 0.04	74.75 ± 0.16
35	23.50 ± 0.08	67.42 ± 0.22	26.14 ± 0.11	74.68 ± 0.39
Mean % [6]-gingerol		67.84 ± 0.63		74.51 ± 0.49

C. Evaluation of Antioxidant Activity of Different *Zingiber officinale* Extracts

Two different evaluation methods for antioxidant activity were used in this study. The methods based on different antioxidative mechanisms. One based on the hydrogen-donating activity and the other hydroxyl radical scavenging activity. These methods have been used and gave reliable results in many investigations (Halliwell, Gutteridge and Aruoma, 1987 and Bondet, Williams and Berset, 1997).

1. Hydrogen-donating activity (DPPH radical scavenging activity)

One of the antioxidant mechanisms is to remove free radical by donating free hydrogen to free radical. The hydrogen-donating activity of acetone, ethanol, isolated-[6]-gingerol extracts as well as L-ascorbic acid and α-Tocopherol were determined in term of their DPPH scavenging activities. The degree of DPPH discoloration is attributed to the hydrogen donating potential of the test compounds. The change in color of DPPH, measured at 517 nm, was compared with a control sample without test extract. The DPPH method measured the antioxidative activity of any compounds on basis of the decrease of absorbance at 517 nm. The antioxidant which had hydrogen-donating activity resulted in the change of purple to yellow (Stilova et al., 2006). Because l-ascorbic acid and α-tocopherol were potent antioxidants and were widely used to compare the antioxidant activity, they were selected as positive control in this study (Castro et al., 2006 and Lee et al., 2008). The result indicated that all ginger extracts and the positive control, L-ascorbic acid and α-tocopherol had varying degree of free radical scavenging activities.

The plot of percentages of DPPH scavenging activity (% inhibition) at various concentrations (0.5, 1, 2.5, 5, 7.5, 10, 30, 50, 70 and 100 μg/ml) of the test samples are shown in Figure 16. The result revealed that, maximum inhibitory activities of ginger extracts were 50-93%. It was found that scavenging effect increased with increasing concentration of antioxidants and the plot reached plateau and the inhibition became steady. The clear relationship between inhibition and concentration of individual antioxidants is shown in Figure 17. The DPPH-scavenging activity of acetone and isolated [6]-gingerol extracts were quite similar and lower than vitamin E and vitamin C, whereas standard [6]-gingerol exhibited the highest scavenging

activity. The ethanol extract showed the lowest scavenging activity as seen in Figure 16. However, the maximum activity of ethanol extract was not found from the studied concentration range.
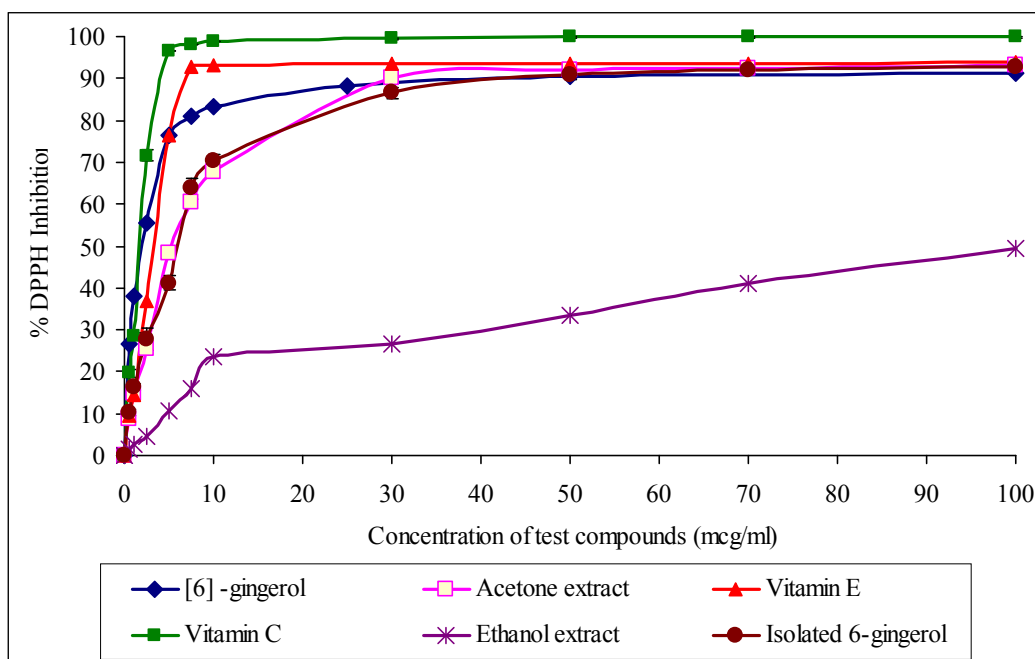
Figure 16 DPPH radical inhibition of various ginger extracts compared to standard [6]-gingerol and positive controls (Mean ± SD, n = 3)

The concentration at 50% inhibition (IC_{50}) of each sample was calculated from the equation of the partial polynomial plot and given in Table 10. The polynomial regression equation for determining the IC_{50} and the regression coefficient (R^2) are also provided for the individual antioxidants in Figure B1. The estimated IC_{50} values can be ranked from the lowest to the highest, as follow: standard [6]-gingerol (1.45 µg/ml ± 0.04), vitamin C (1.62µg/ml ± 0.03), Vitamin E (3.18 µg/ml ± 0.05), acetone extract (5.42 µg/ml ± 0.03), isolated-[6]-gingerol (5.67 µg/ml ± 0.35) and ethanol extract (101.33 µg/ml ± 1.15). The IC_{50} values in Table 10 correlated with data in Figure 16. Standard [6]-gingerol exhibited the highest antioxidant potency because of the lowest IC_{50} and confirmed that [6]-gingerol was the major antioxidant in ginger rhizome. The acetone and isolated [6]-gingerol extracts were quite similar in activity because the radical scavenging activities of extracts were correlated with [6]-gingerol

content. The [6]-gingerol content in acetone extract was not different from isolated [6]-gingerol extract (Table 9).
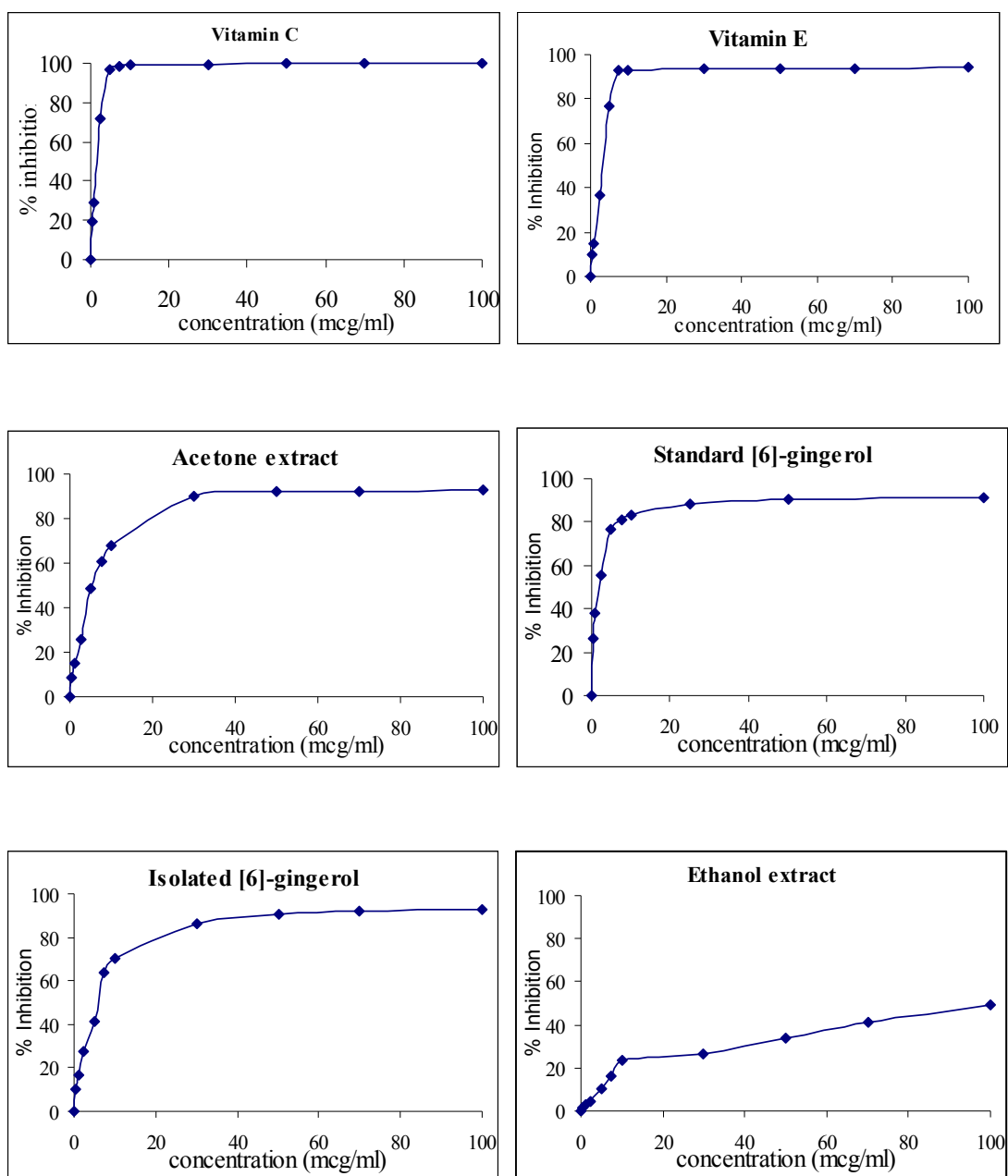
Figure 17 Relationship between percent DPPH radical inhibition and the concentration of the individual antioxidants (Mean ± SD, n = 3)

Table 10 The IC50 values calculated from polynomial equations for DPPH radical scavenging activity of each antioxidants

Sample	Polynomial equation			
	IC50 (μg/ml)	Mean (μg/ml)	SD	R^2
Standard [6]-gingerol	1.49	1.45	0.0451	0.9922
	1.45			0.9890
	1.40			0.9934
Isolated [6]-gingerol	5.95	5.67	0.3483	0.9906
	5.28			0.9863
	5.78			0.9806
Acetone ext.	5.44	5.42	0.0265	0.9970
	5.39			0.9962
	5.43			0.9969
Ethanol ext.	102	101.33	1.1547	0.9997
	102			0.9987
	100			0.9992
Vitamin C	1.66	1.62	0.0351	0.9957
	1.62			0.9960
	1.59			0.9950
Vitamin E	3.18	3.18	0.0551	0.9940
	3.23			0.9945
	3.12			0.9943

The IC_{50} data were subsequently analyzed by one-way analysis of variance (ANOVA) at 95% confidence followed by LSD method which results are depicted in Table B8 and B9, respectively. It was found that there were significant differences among the antioxidants studies ($p < 0.05$). According to Duncan method (Table B10), the antioxidants could be divided into 4 groups regarding their abilities to inhibit or scavenge DPPH radicals. The IC_{50} ranking is as follow:

ethanol extract < isolated [6]-gingerol = acetone extract < vitamin E < vitamin C = standard [6]-gingerol.

The DPPH radical scavenging activity of isolated [6]-gingerol extract exhibited no significant different from the acetone extract. This result might be due to the [6]-gingerol contents in both extracts were not much different (Table 9) and the radical scavenging activities of extracts were correlated with [6]-gingerol content. Ethanol extract, in contrast, showed the lowest antioxidant activity. It was noticed that the inhibition could be increased as the extract concentration increased. This implied that the result was attributed to the low content of [6]-gingerol in the ethanol extract and much lower than acetone extract. Acetone which was relatively nonpolar than 20% ethanol in water could extract higher [6]-gingerol content.

2. Hydroxyl radical scavenging activity

Antioxidants that are able to inhibit free radical chain reaction can be evaluated by their abilities to prevent damage of 2-deoxy-D-ribose, a DNA sugar, by hydroxyl radical. The degradation of deoxyribose could be measured by pink color at 532 nm. The hydroxyl radical scavenger resulted to the decrease of pink color (Halliwell, Gutteridge and Aruoma, 1987).

The effect of various solvent extracts of *Zingiber officinale* on the inhibition of free radical-mediated DNA-sugar damage was assessed by deoxyribose method. The hydroxyl radical scavenging activity of various solvent extracts were compared with positive control, quercetin, as depicted in Figure 18. The degree of discoloration was attributed to the hydroxyl radical scavenging potential of the test compounds. The change in color of pink chromogen, measured at 532 nm, was compared with a

control sample without antioxidants. As presented in Figure 18, it was found that as the concentration was increased, the extent of antioxidant activity (% inhibition of hydoxyl radical) also increased for all test compounds. The result showed that the presence of higher concentrations of all test compounds prevented the oxidation of deoxyribose.
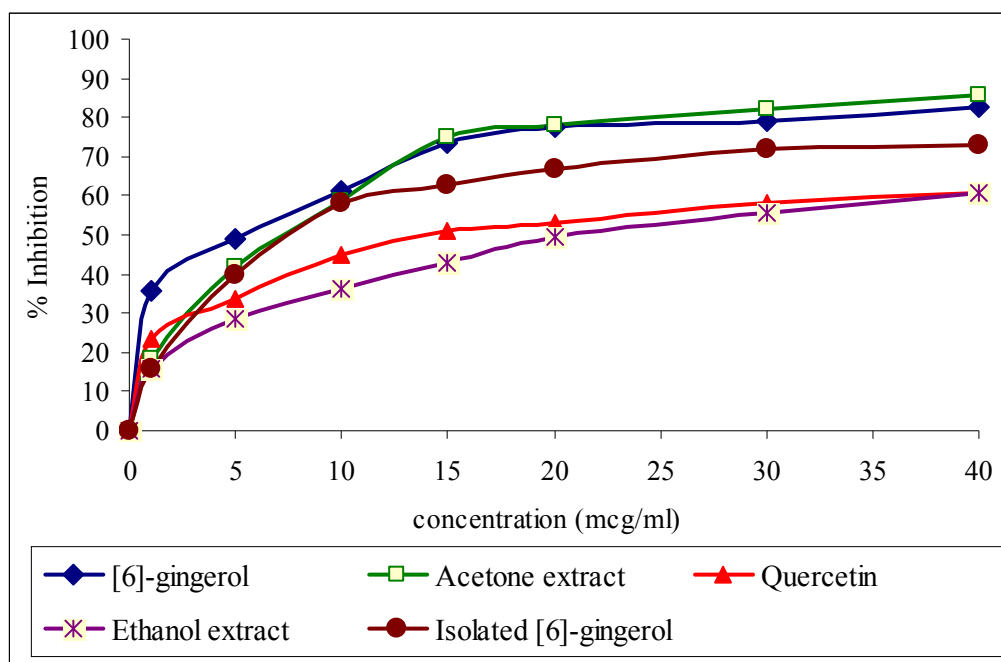
Figure 18 The extent of hydroxyl radical inhibition of various ginger extracts compared to standard [6]-gingerol and positive control (Mean ± SD, n = 3)

The clear relationship between inhibition of hydroxyl radical and concentration of individual antioxidants is shown in Figure 19. The concentration at 50% inhibition (IC_{50}) of each sample was calculated from the equation of the partial polynomial plot and given in Table 11. The polynomial regression equation for determining the IC_{50} and the regression coefficient (R^2) are also provided for the individual antioxidants in Figure C1. The estimated IC_{50} values can be ranked from the lowest to the highest, as follow: standard [6]-gingerol (5.63 μg/ml ± 0.03), isolated-[6]-gingerol (6.87 μg/ml ± 0.05), acetone extract (7.31 μg/ml ± 0.03), quercetin (14.23 μg/ml ± 0.15) and ethanol extract (21.47 μg/ml ± 0.51). The IC_{50} values in Table 11 correlated with data in Figure 18. Standard [6]-gingerol exhibited the highest antioxidant potency because of the lowest IC_{50}, whereas ethanol extract showed the lowest scavenging activity. The result correlated with the result by the DPPH, hydrogen-donating activity method.
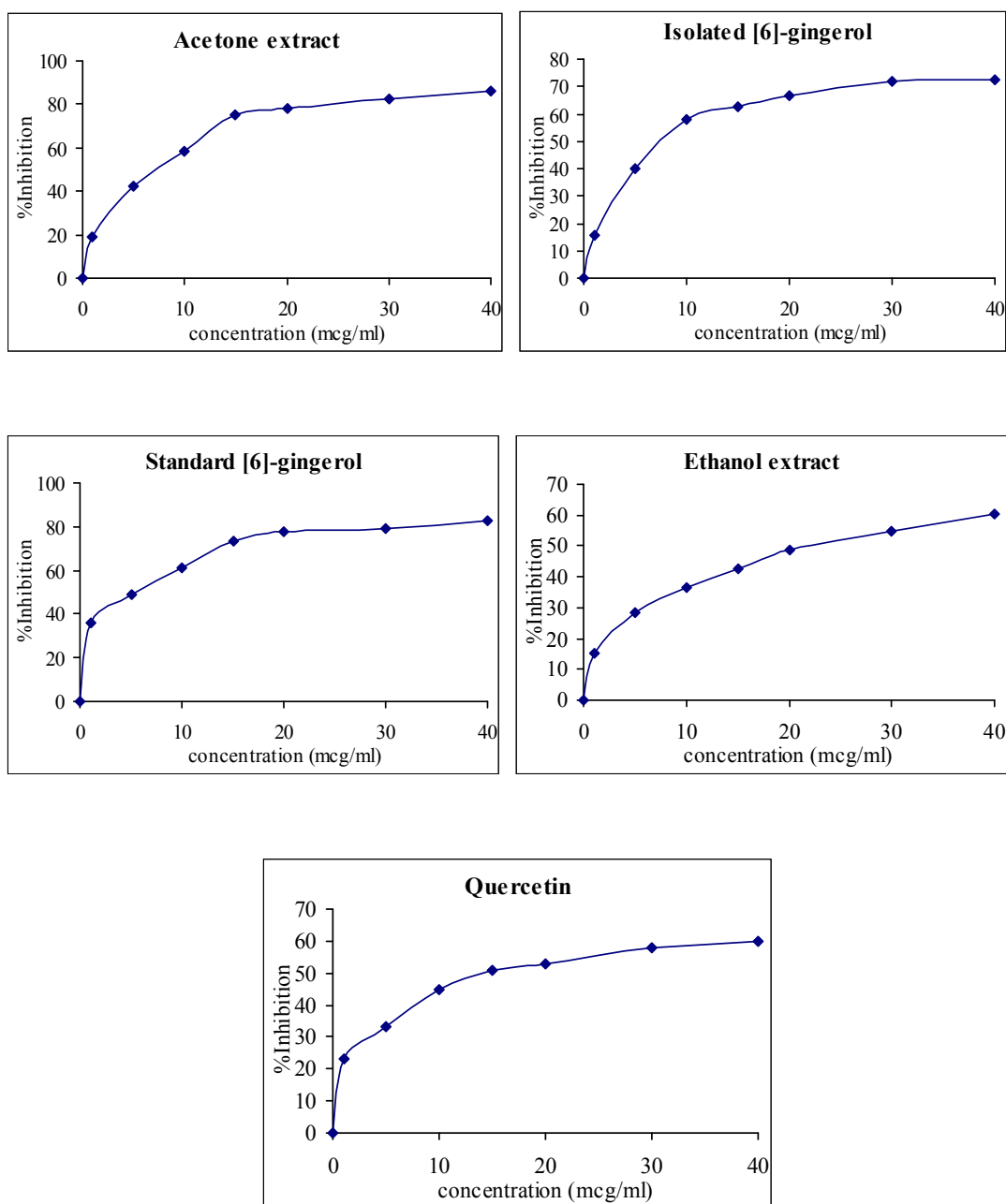
Figure 19 Relationship between percent hydroxyl radical inhibition and the
concentration of the individual antioxidants (Mean ± SD, n = 3)

Table 11 The IC50 values calculated from polynomial equations for hydroxyl radical scavenging activity of each antioxidants

Sample	Polynomial equation			
	IC50 (µg/ml)	Mean (µg/ml)	SD	R^2
Standard [6]-gingerol	5.60	5.63	0.0252	0.9988
	5.65			0.9992
	5.63			0.9988
Isolated [6]-gingerol	6.88	6.87	0.0503	1.0000
	6.92			0.9999
	6.82			1.0000
Acetone ext.	7.24	7.31	0.0265	0.9954
	7.27			0.9955
	7.41			0.9954
Ethanol ext.	21.72	21.47	0.5096	0.9931
	21.80			0.9925
	20.88			0.9966
Quercetin	14.40	14.23	0.1528	0.9986
	14.20			0.9991
	14.10			0.9999

The IC_{50} data were subsequently analyzed by one-way analysis of variance (ANOVA) at 95% confidence followed by LSD method. It was found that there were significant differences among the antioxidants studies ($p < 0.05$). According to Duncan method (Table C9), the antioxidants could be divided into 4 groups regarding their abilities to inhibit or scavenge hydroxyl radicals. The IC_{50} ranking is as follow:

ethanol extract < quercetin < isolated [6]-gingerol = acetone extract < standard [6]-gingerol.

The hydroxyl radical scavenging activity of isolated [6]-gingerol extract exhibited no significant different from the acetone extract (P>0.05). This result may be due to the [6]-gingerol content in both extracts were not much different (Table 9) and the radical scavenging activities of extracts were correlated with [6]-gingerol content.

Similar to the DPPH method, ethanol extract exhibited the lowest hydroxyl radical scavenging activity. This might be due to the lower [6]-gingerol content in the extract than in the acetone extract. It was noticed that all plots in Figure 16 did not show the plateau. It revealed that the increase of concentration of extract used in the study might give the higher activity.

The evaluation of antioxidant activities of different solvent fractions of natural plants were investigated in many researches (Pandey et al., 2007; Tiwari and Tripathi, 2007 and Singh et al., 2007). In general, the free radical scavenging activity in different assays can be linked to the presence of phenolic compounds in solvent fractions because these compounds exhibit important mechanisms of antioxidative activities (Yildirim et al., 2000). Tiwari et al (2007) suggested that polar fraction possessed more antioxidant phytomolecules than antioxidant in non-polar fraction because polar fraction may have more polyhydroxy phenolic molecules and Singh et al., (2007) reported that water fraction exhibit stronger antioxidant activity than ethyl acetate fraction. In this study, the antioxidant activities of gingerols compounds, natural phenolic compound, were evaluated by comparing with different solvent fractions. In contrast to both previous researches reported, the acetone fraction exhibit more potent activity than ethanol extract. Because of the lipophilic property of

gingerol analogues, [6]-gingerol and related phenolic substances could be extracted by sparingly non-polar solvent. The lipophilic structures and log P of ginger substances are displayed in Table 1. From the data obtained, it was found that [6]-gingerol, mainly compound, has the lowest lipophilic property (the lowest log P, log P=1.8) when comparing with other lipophilic substances (paradol and shogaol series), which possess the higher log P (log P=2.9-5.1). For this reason, it was clearly explained that both of major and minor phenolic substances prefered to dissolve in acetone more than polar solvent. This might be attributed to the higher phenolic content in the non polar fraction.

The ethanolic extract presented the lowest activities in both DPPH and deoxyribose assays, so it was not considered to apply for loading in SLN. Whereas, according to easily obtained by solvent extraction and comparable antioxidative activities with isolated [6]-gingerol extract, the acetone extract exhibited high potential for use as radical scavenger and for loading in SLN in the further investigation.

D. Determination of Solubility of *Zingiber officinale* Extract in Solid Lipids

Kumar et al. (2007) reported that the important factor that determined the loading capacity of the extract in the lipid was the solubility of extract in melted lipid. In this study, glyceryl palmitostearate (GP, Precirol® ATO 555), glyceryl behenate (GB, Compritol® 888 ATO), glyceryl myristate (Dynasan® 114) and cetyl palmitate were screened for their potential to solubilize ginger extract. The end point of the solubility study was the formation of clear and homogeneous of ginger extract in lipids both in molten state and solidified state. The characteristics of ginger extract in different lipids at molten state (85°C) and solidified state (room temperature) are displayed in Figure 20.

In this study, it was found that glyceryl palmitostearateate (GP) and glyceryl behenate (GB) demonstrated the effectively solubilizing potential of ginger extract. At both high and room temperature, ginger extract was well soluble in both selected lipids. Homogeneous matrices were obtained in solidified lipids.

The result might be due to the lipophilic property of ginger extract, which likely dissolved in the lipophilic long chain mixed triglyceride, GP (C16-C18) and GB (C22), whereas it precipitated in glyceryl myristate (C14) and cetyl palmitate.

In addition, as respected by Muller et al., 1997, the selected lipids possessed biocompatibility and safety for topical use, so they were selected for the present study.

E. Preparation of Solid Lipid Nanoparticles (SLN)

1. Preparation of extract-free solid lipid nanoparticles

There are different approaches for the production of solid lipid nanoparticles (SLN). In this study, hot high pressure homogenization (HPH) technique was applied for the preparation of aqueous SLN dispersions. Using the hot high-pressure homogenization (HPH) technique, it was able to produce physically stable SLN formulations under storage condition (Muller et al., 2000).

From the solubility potential of ginger extract in lipids from Topic D, glyceryl palmitostearate (GP, Precirol® ATO 555) and glyceryl behenate (GB, Compritol® 888 ATO) at 5% concentration of the formula were selected and used in the formulation of SLN. With the amount of 1, 3 and 5% of either Tween® 80 (Tw80) or Poloxamer® 188 (P188) as stabilizer, 12 formulations could be prepared (Table 12). The products obtained were visually observed for their appearances and physical stability.

2. Preparation of ginger extract loaded solid lipid nanoparticles

The extract-free SLN that had good physical stability were chosen to load ginger extract. Five percent of ginger extract calculated as percentage of lipid matrix (0.25% of total formulation) was added to the melted lipid and followed by the same procedure as in extract-free SLN.

(a)   (b)

(c)   (d)

Figure 20 Photographs of ginger extract in different lipids at molten state at 85°C and
solidified state at room temperature (RT);

    (a) cetyl palmitate   (85°C)   (b) cetyl palmitate   (RT)

    (c) glyceryl myristate (85°C)   (d) glyceryl myristate (RT)

(e)   (f)

(g)   (h)

Figure 20 (continued) Photographs of ginger extract in different lipids at molten state
at 85°C and solidified state at room temperature (RT);

    (e) glyceryl palmitostearate (85°C)   (f) glyceryl palmitostearate (RT)

    (g) glyceryl behenate   (85°C)   (h) glyceryl behenate   (RT)

Table 12 Formulations of extract-free solid lipid nanoparticles

Code	Lipid 5%	Stabilizer	
GPT1	glyceryl palmitostearate	Tween 80	1%
GPT3	glyceryl palmitostearate	Tween 80	3%
GPT5	glyceryl palmitostearate	Tween 80	5%
GPP1	glyceryl palmitostearate	Poloxamer 188	1%
GPP3	glyceryl palmitostearate	Poloxamer 188	3%
GPP5	glyceryl palmitostearate	Poloxamer 188	5%
GBT1	glyceryl behenate	Tween 80	1%
GBT3	glyceryl behenate	Tween 80	3%
GBT5	glyceryl behenate	Tween 80	5%
GBP1	glyceryl behenate	Poloxamer 188	1%
GBP3	glyceryl behenate	Poloxamer 188	3%
GBP5	glyceryl behenate	Poloxamer 188	5%

F. Evaluation of Solid Lipid Nanoparticles (SLN)

1. Determination of physicochemical properties of extract-free SLN

The physicochemical properties of solid lipid nanoparticles drug delivery system before incorporation of ginger extract were determined as following:

1.1 Appearances and physical stability of extract-free SLN

The physical appearances of the formulations such as color, coalescence, gel formation and phase separation were visually observed.

The visual observations of SLN containing both 5% GP and GB with either 1-5% of Poloxamer 188 (P188) or Tween 80 (Tw80) were investigated. The visual appearances of drug-free SLN are depicted in Table 13. SLN with 1-5% Tw80 as stabilizer showed bluish white clear dispersion and SLN with 1-5% P188 using as stabilizer showed white translucent fluid dispersion.

Under storage conditions, RT and 4°C, all SLN formulations prepared from glyceryl palmitostearate (GP) showed stable fluid dispersion at 14, 30, 60 and 180

days period. The SLN dispersions exhibited no change of physical appearances. Contrarily, SLN formulations prepared from glyceryl behenate (GB) gave stable dispersions along storage period till 180 days only at storage temperature of 4°C or refrigerated temperature. At room temperature, SLN formulations with GB as lipid and P188 as stabilizer showed physical unstability. The change could be observed as gel formation. The worst change was found in the SLN with P188 of 3% concentration with phase separation. However, the GB-SLN formulations gave stable dispersion in the formulations using Tween 80 of 3 and 5% as stabilizer. Color change was not detected during storage condition till 6 months. All formulations gave white dispersion along the study period.

The processing procedure also affected the physical stability of SLN. In most cases, 3–5 homogenization cycles at 500–1500 bar were sufficient to produce SLN dispersion. In this study, 3 homogenization cycles at 500 bar was used as the optimum homogenization condition. This optimum condition was widely conducted in many reports (Lippacher et al., 2001; Wissing and Muller, 2002a). Increasing the homogenization pressure or the number of cycles often resulted in an increase of the particle size due to the breaking of the emulsion droplet and particle coalescence during high energy input homogenization (Schwarz et al., 1994).

Both GP-SLN and GB-SLN formulations displayed good physical appearance for more than 6 months at storage temperature 4°C. The possible explanation was attributed to the optimal producing condition and to the optimal compositions of lipid and stabilizer. The result also confirmed the quality of raw materials using in this investigation. From the results, all formulations were selected for loading ginger extract and were investigated in further study.

At low temperature, 4°C was generally the most favorable storage temperature. The physical stabilities of SLN were maintained at 4 °C longer than at room temperature. High temperatures increased the kinetic energy of a system and led to SLN aggregation and gelation. These findings agreed with previous research by Freitas and Muller (1998).

Table 13 The physical appearance and physical stability of extract-free solid lipid nanoparticles at various time intervals under storage conditions.

Formulation	Day 0	Day 14		1 Month		2 Months		6 Months	
		4 °C	RT	4 °C	RT	4 °C	RT	4 °C	RT
GPP1	+++	+++	+++	+++	+++	+++	+++	+++	+++
GPP3	+++	+++	+++	+++	+++	+++	+++	+++	+++
GPP5	+++	+++	+++	+++	+++	+++	+++	+++	+++
GPT1	+++	+++	+++	+++	+++	+++	+++	+++	++
GPT3	+++	+++	+++	+++	+++	+++	+++	+++	++
GPT5	+++	+++	+++	+++	+++	+++	+++	+++	++
GBP1	+++	+++	+++	+++	+++	+++	+	+++	+
GBP3	+++	+++	+++	+++	+++	+++	-	+++	-
GBP5	+++	+++	+++	+++	+++	+++	+	+++	+
GBT1	+++	+++	+++	+++	+++	+++	+	+++	+
GBT3	+++	+++	+++	+++	+++	+++	+++	+++	+++
GBT5	+++	+++	+++	+++	+++	+++	+++	+++	+++

+++, ++, +, - : stable dispersion, viscosity increasing, gel formation, phase separation

GP, Glyceryl palmitostearate; GB, Glyceryl behenate; P, Poloxamer 188; T, Tween 80: 1, 3, 5 as 1%, 3%, 5% of stabilizer

1.2 Particle size analysis

The particle sizes determined by PCS of extract-free GP-SLN and GB-SLN containing 1-5% of P188 or Tw80 are shown in Table 14. The mean diameters of all preparations were in nanometer range. Particle size analysis of developed formulations was monitored during 2 months at different storage temperatures, 4 °C and RT. The concentration of P188 and Tw80 was varied from 1% to 5% for obtaining the stable and smaller SLN particles. The effect of types of solid lipid and types and amount of surfactant were evaluated on the characteristics of SLN.

Particle size and particle size distribution as measured by polydispersity index (PI) of extract-free SLN formulations at 4 °C during 2 months are illustrated in Table 14. The effect of formulation on particle size of SLN might be demonstrated from the histogram of particle size and SLN formulation in Figure 21 and plots between particle size and surfactant concentrations of freshly prepared SLN formulations are showed in Figure 22.
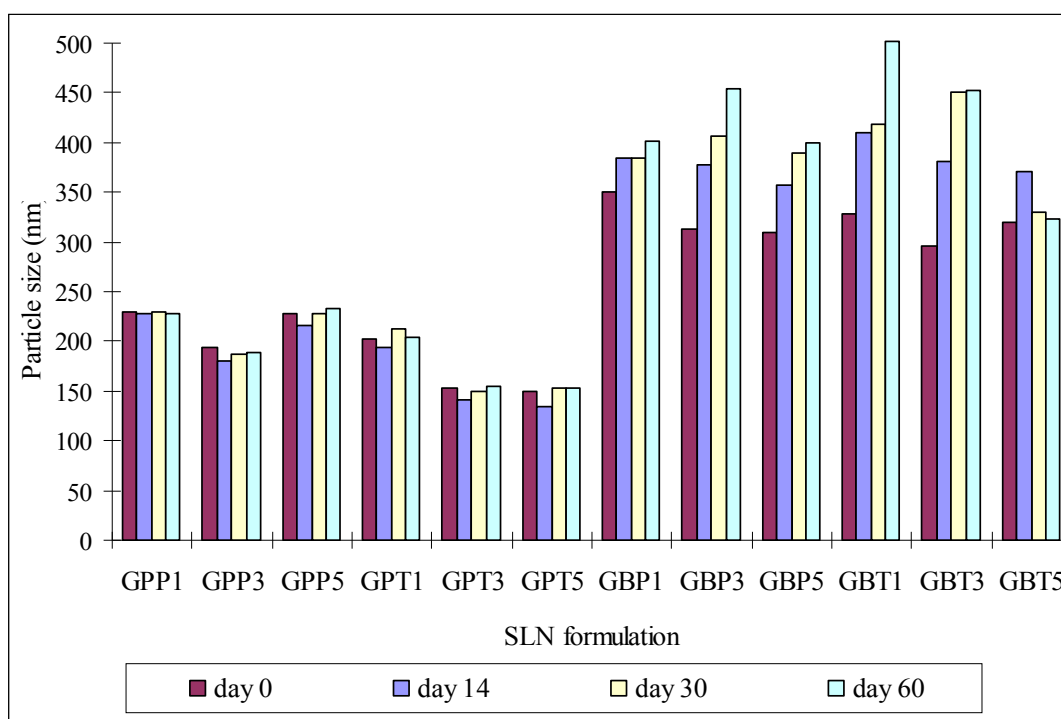
Figure 21 Histogram of particle sizes and extract-free SLN formulations at 4 °C during 2 months

Table 14 Particle size and polydispersity index of ginger extract-free SLN under storage conditions at day 14, day 30 and day 60 (Mean, n = 3)

| | Day 0 | | Day 14 | | | | Day 30 | | | | Day 60 | | | |
| | | | 4 C | | RT | | 4 C | | RT | | 4 C | | RT | |
SLN	size (nm)	PI	size (nm)	PI	size (nm)	PI	size (nm)	PI	size (nm)	PI	size (nm)	PI	size (nm)	PI
GPP1	230.2	0.261	227.5	0.227	220.6	0.200	229.6	0.093	253.8	0.214	227.7	0.275	351.2	0.355
GPP3	193.7	0.211	181.0	0.255	179.5	0.252	186.8	0.266	186.2	0.288	189.0	0.287	219.9	0.240
GPP5	228.6	0.284	215.6	0.318	217.1	0.293	228.1	0.303	237.5	0.216	232.6	0.287	247.8	0.210
GPT1	202.4	0.254	194.2	0.252	203.0	0.208	212.2	0.256	228.1	0.303	204.5	0.240	237.9	0.286
GPT3	152.5	0.241	140.7	0.233	147.7	0.233	149.5	0.286	155.3	0.232	154.4	0.270	300.5	0.211
GPT5	150.0	0.256	134.0	0.261	149.4	0.229	152.3	0.243	159.8	0.279	153.1	0.232	468.6	0.241
GBP1	350.6	0.005	384.8	0.036	400.7	0.030	384.1	0.005	406.1	0.005	400.6	0.367	Gel formation	
GBP3	313.3	0.074	377.6	0.026	378.0	0.032	407.1	0.005	418.7	0.005	454.8	0.351	Phase seperation	
GBP5	309.5	0.037	356.3	0.260	375.2	0.195	390.3	0.005	400.2	0.005	400.5	0.255	Gel formation	
GBT1	328.0	0.077	409.6	0.093	390.3	0.025	419.0	0.005	437.9	0.005	504.8	0.355	Gel formation	
GBT3	295.9	0.170	381.4	0.258	314.8	0.017	451.0	0.005	375.6	0.005	452.1	0.342	368.1	0.277
GBT5	320.5	0.395	371.1	0.337	314.8	0.201	329.5	0.005	298.5	0.005	322.7	0.236	305.8	0.336

GP, Glyceryl palmitostearate; GB, Glyceryl behenate; P, Poloxamer 188; T, Tween 80: 1, 3, 5 as 1%, 3%, 5% of stabilizer

From the result in Table 14, Figure 21 and Figure 22, it showed that particle size of GP-SLN and GB-SLN gradually decreased with increasing surfactant concentration from 1% to 3%. Increasing the concentration of P188 and Tw80 from 3% to 5% did not significant different in reducing the particle size. Thus, the optimal concentration of both P188 and Tw80 was 3% that produced small particle size and narrow size distribution of SLN.
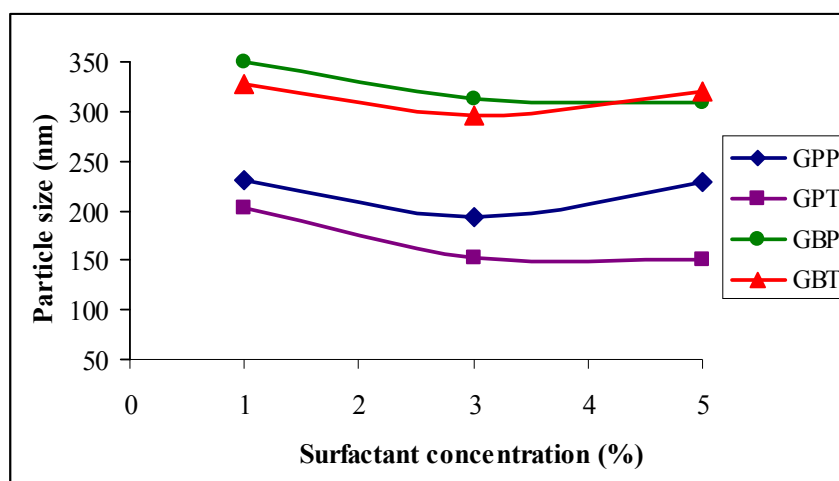
Figure 22 Plots between particle size and surfactant concentrations at day 0

GP, glyceryl palmitostearate; GB, glyceryl behenate; P, Poloxamer 188;

T, Tween 80

The primary role of surfactant was stabilization of the nanoparticles in the colloid state and prevention of particle size growth during storage. The 3% of P188 and 3% of Tw80 were sufficient to cover the surface of nanoparticles effectively and also prevent agglomeration during the homogenization process. At low concentration of surfactant, uncovered interface of oil droplet easily fused and large particles were obtained in recrystallization process. High concentration of surfactant could not reduce particle size and PI due to excess surfactants caused bridging between particles. This result is consistent with previous studies by Vivek, Reddy and Murthy (2007) and Kumar et al (2007).

From Figure 22, it was clearly shown that glyceryl palmitostearate as lipid in the SLN formulations gave smaller particle sizes, regardless on surfactant type and concentration.

The lipophilic property of lipid influenced to the emulsifying capacity of surfactant during hot homogenization. At the same concentration of surfactant, the

reducing in surface tension and droplet size of molted GB, the more lipophilic lipid, was more difficult than the molted GP. For this reason, average size of GP-SLN was smaller than GB-SLN because GP contained mixture of C_{16} and C_{18} carbon chains which were shorter than C_{22} of GB. This finding agreed with the previous report of Jansook (2005).

Regarding physical stability, data from Figure 21 showed that the sizes of GB-SLN were gradually increased during storage, whereas sizes of GP-SLN were not different from the initial sizes under the same concentration of surfactant and storage condition. This result revealed that physicochemical properties of lipid such as lipophilicity and degree of crystallinity strongly influenced on particle size and short term stability of SLN dispersions.

The solid lipid with high melting point possessed high degree of crystallinity (Muhlen and Mehnert, 1998). Freitas and Muller (1998) reported that SLN dispersion with high recrystallization index of lipid phase showed an increased particle size growth. For this reason, GB-SLN, with higher melting temperature than GP-SLN, proned to have particle size growth during storage time.

2. Evaluation of *Zingiber officinale* extract loaded SLN

After incorporation of ginger extract, the physicochemical properties of solid lipid nanoparticles drug delivery system were determined as following: appearance, size and size distribution, surface morphology, shape, and the percentage of entrapment efficiency.

2.1 Physical appearances

The physical appearances of SLN containing ginger extract of both GP-SLN and GB-SLN with either 1-5% of Poloxamer® 188 (P188) or Tween® 80 (Tw80) such as color, coalescence, gel formation and phase separation were visually examined and as depicted in Table 15.

Table 15 The physical appearance and physical stability of ginger extract loaded solid lipid nanoparticles at various time intervals under storage conditions.

Formulation	Day 0	Day 14		1 Month		2 Months		6 Months	
		4 °C	RT	4 °C	RT	4 °C	RT	4 °C	RT
GPPG1	+++	+++	+++	++	++	+	+	+	+
GPPG3	+++	+++	+++	+++	++	+++	++	+++	-
GPPG5	+++	+++	+++	+++	++	+++	++	+++	-
GPTG1	+++	+++	+++	+++	+	++	+	++	+
GPTG3	+++	+++	+++	+++	+++	+++	++	+++	+
GPTG5	+++	+++	+++	+++	+++	+++	+++	+++	+
GBPG1	+++	+++	+	+	+	+	+	+	+
GBPG3	+++	+++	++	+++	+	+	+	+	+
GBPG5	+++	+++	+++	+++	+	+	+	+	+
GBTG1	+++	+++	+	+	+	+	+	+	+
GBTG3	+++	+++	+++	+++	+++	+++	+++	+++	+
GBTG5	+++	+++	+++	+++	+++	+++	+++	+++	+

+++, ++, +, - : stable dispersion, viscosity increasing, gel formation, phase separation
GP, Glyceryl palmitostearate; GB, Glyceryl behenate; P, Poloxamer 188; T, Tween 80: 1, 3, 5 as 1%, 3%, 5% of stabilizer

The stable dispersion of GP-SLN was also obtained at storage temperature 4°C and RT during 2 months. However, gelatinous dispersion occurred with the dispersion containing low surfactant concentration at 1% of P188 and Tw80 after storage at room temperature especially in the GP-SLN. Low concentration of surfactant was not sufficient to cover the surface of nanoparticles effectively and could not prevent agglomeration during the storage time.

In case of GB-SLN, stable physical appearance was observed in 3% and 5% of Tw80. The gel forming, irreversible physically unstable, was occurred mostly in P188 stabilized GB-SLN. The physicochemical property of stabilizer affected stability of SLN. The use of P188, a gelling agent with block copolymer, as stabilizer of SLN and the ability to form network structures was reported (Harland and Peppas, 1993). Because of the gelling property of P188, the bridging effects between molecules

appeared so possible and could promote the gel formation (Frisbee and McGinity, 1994). Another possible reason for the gelation process was structural changes occurring during storage. Transformation of the polymorph forms and recrystallization of the lipid from spherical to platelet form caused new and unprotected interfaces which not stabilized with covered surfactant molecules (Westesen and Siekmann, 1997). Indeed, ginger extract in lipid phase increasing in nonpolar property which needed more capacity in emulsification process and caused limited free stabilizer molecules for the new surfaces of platelet form when comparing with extract free SLN.

At low temperature, 4°C was generally the most favorable storage temperature. The physical stabilities of SLN were maintained at 4 °C longer than at room temperature. High temperatures increased the kinetic energy of a system and led to SLN aggregation and gelation. The high temperature exposure could lead to change in the crystalline structure of lipids to more stable β form. This stable form showed the platelet form which had more surface area and caused insufficient stabilizer capacity of surfactant in system and the unstable gel formation was ocurred. These findings agreed with previous research by Freitas and Muller (1998).

From the result obtained, six formulations which obviously were stable during a period of 2 months of storage at room temperature and at 4 °C were selected for further study. The formulations were GP-SLN with 3% and 5% of either P188 or Tw80 of and GB-SLN with 3% and 5% of Tw80.

2.2 Particle size analysis

The particle sizes determined by PCS of ginger extract loaded GP-SLN and GB-SLN containing 1-5% of P188 and Tw80 are shown in Table 16. As shown in Figure 23, an increase in particle size was observed for all ginger extract loaded SLN formulations as compared to blank SLN, suggesting the presence of ginger extract in the matrix of nanoparticles. In addition, the lipophilicity of extract also increased viscosity and lipophilicity of lipid phase which resulted in decreasing in emulsification performance and decreasing in the homogenization efficiency (Mehnert and Mader, 2001). The mean diameters of all preparations were in nanometer range and polydispersity index of these particle were in between 0.1-0.4, which demonstrated narrow size distribution.

The effect of type of surfactant on particle size of SLN was evaluated. SLN containing P188 gave larger particle size than Tw80 because P188 was a block copolymer stabilizer which could cause bridging effect and led to coalescence (Freitas and Muller, 1998). Additionally all GP-SLN formulations gave smaller particle size than all GB-SLN formulations as depicted in Figure 23.

For stability study, particle size analysis of developed formulations was monitored during 2 months at different storage temperatures, 4 $^{\circ}$C and RT. The relationship between particle size and extract-loaded SLN formulations at 4 $^{\circ}$C during 2 months is illustrated in Table 16 and Figure 24.

The results showed that particle size of GP-SLN and GB-SLN gradually decreased with increasing surfactant concentration from 1% to 3%. High concentrations of the emulsifier reduced the surface tension and facilitated the particle partition during homogenization. The decrease in particle size was connected with a tremendous increase in surface area during homogenization and occurred very rapidly. However, the process of a primary coverage of the new surfaces competed with the agglomeration of uncovered lipid surfaces. The primary dispersion had to contain excessive emulsifier molecules, which should rapidly cover the new surfaces (Mehnert and Mader, 2001). From this reason, the formulations which contained high concentration of stabilizer exhibited more stable than low concentration of surfactant.
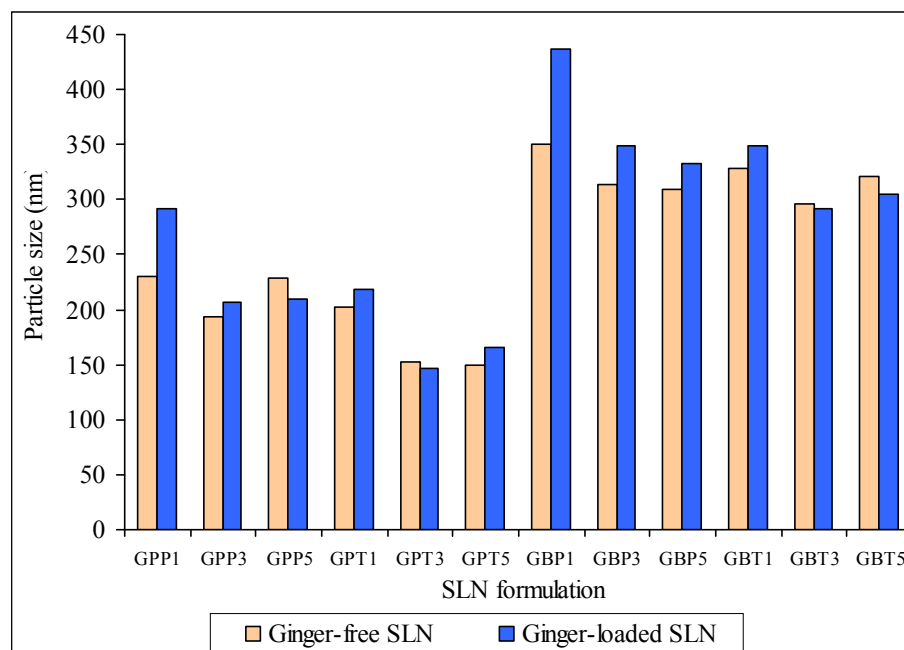
Figure 23 The relationship between particle size and extract-free SLN and extract-loaded SLN formulations, freshly prepared

Table 16 Particle size and polydispersity index of ginger extract-loaded SLN under storage conditions at day 14, day 30 and day 60 (Mean, n = 3)

| SLN | Day 0 | | Day 14 | | | | Day 30 | | | | Day 60 | | | |
| | | | 4 C | | RT | | 4 C | | RT | | 4 C | | RT | |
	size (nm)	PI	size (nm)	PI	size (nm)	PI	size (nm)	PI	size (nm)	PI	size (nm)	PI	size (nm)	PI
GPPG1	291.7	0.344	272.1	0.267	286.3	0.306	336.2	0.337	429.8	0.361	Gel formation		Gel formation	
GPPG3	207.2	0.291	187.3	0.274	199.1	0.262	183.8	0.287	190.0	0.249	191.0	0.275	202.8	0.254
GPPG5	209.9	0.178	193.1	0.193	209.8	0.232	206.6	0.269	222.4	0.199	204.3	0.272	230.0	0.271
GPTG1	218.3	0.260	193.2	0.193	210.3	0.295	210.5	0.241	204.9	0.286	688.6	0.368	Gel formation	
GPTG3	146.8	0.254	146.5	0.220	145.7	0.200	157.3	0.241	254.7	0.193	177.6	0.284	273.6	0.216
GPTG5	165.9	0.217	171.4	0.217	168.5	0.235	190.3	0.263	204.9	0.240	201.1	0.275	226.1	0.257
GBPG1	436.7	0.175	365.9	0.254	Gel formation		Gel formation		Gel formation		Gel formation		Gel formation	
GBPG3	348.6	0.045	367.0	0.258	383.2	0.248	398.8	0.399	Gel formation		Gel formation		Gel formation	
GBPG5	332.6	0.005	324.2	0.199	354.9	0.187	357.1	0.321	Gel formation		Gel formation		Gel formation	
GBTG1	349.0	0.230	489.1	0.261	Gel formation		Gel formation		Gel formation		Gel formation		Gel formation	
GBTG3	291.6	0.139	338.1	0.257	332.1	0.275	324.7	0.271	330.6	0.401	355.7	0.311	379.2	0.337
GBTG5	304.7	0.166	318.8	0.293	302.8	0.204	344.2	0.285	340.1	0.273	372.1	0.261	328.7	0.305

GP, Glyceryl palmitostearate; GB, Glyceryl behenate; P, Poloxamer 188; T, Tween 80: 1, 3, 5 as 1%, 3%, 5% of stabilizer
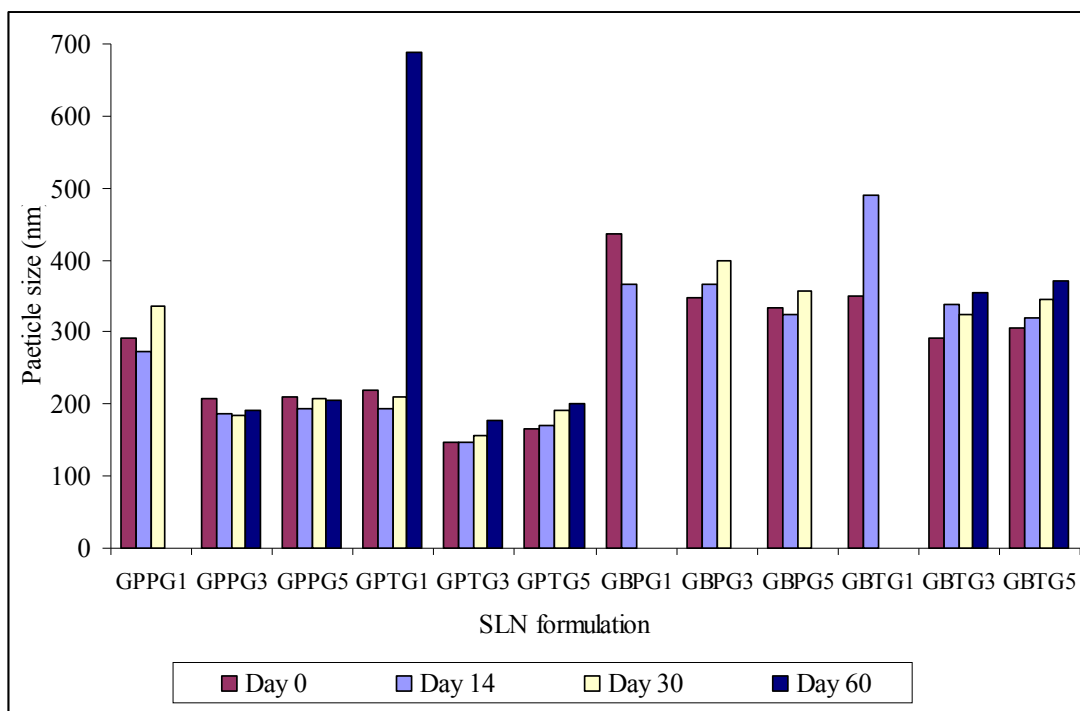
Figure 24 Histogram of particle size and ginger extract-loaded SLN formulations at 4 °C during 2 months (not available data in some observations due to phase separation or gel formation)

As shown in Figure 24, the unstable physical stability was found in SLN formulations which contained low concentration of stabilizer. Moreover, the dramatically increased in particle size was also detected in GPTG1 and GBTG1. The measurements of particle sizes and size distribution of SLN displayed prediction of long term stability of SLN formulations. The developed formulations which sharply increased in particle size could be developed to gel formation or phase separation during storage time.

2.3 Morphology

The morphological feature of ginger loaded SLN was investigated using transmission electron microscope (TEM). The observation of size, shape and surface topography were done by transmission electron microscopy (TEM). Figure 25 shows the transmission electron photomicrographs of ginger extract loaded SLN at day 0 and day 60. The particle topography of all formulations showed regular, spherical and uniform nanospheres. The nanoparticles exhibited spherical shaped and homogenous in size distributions. During storage for 2 months, the nanoparticles were observed

with no change of particle morphology. The particle sizes of particles were approximately around 200 nm. With respect to the particle size determination, the TEM studies supported the basic conclusion drawn from particle size measurements that the dispersion consisted predominantly of particles with dimension below 200-300 nm.

(day 0)   **(a)**   (day 60)

(day 0)   **(b)**   (day 60)
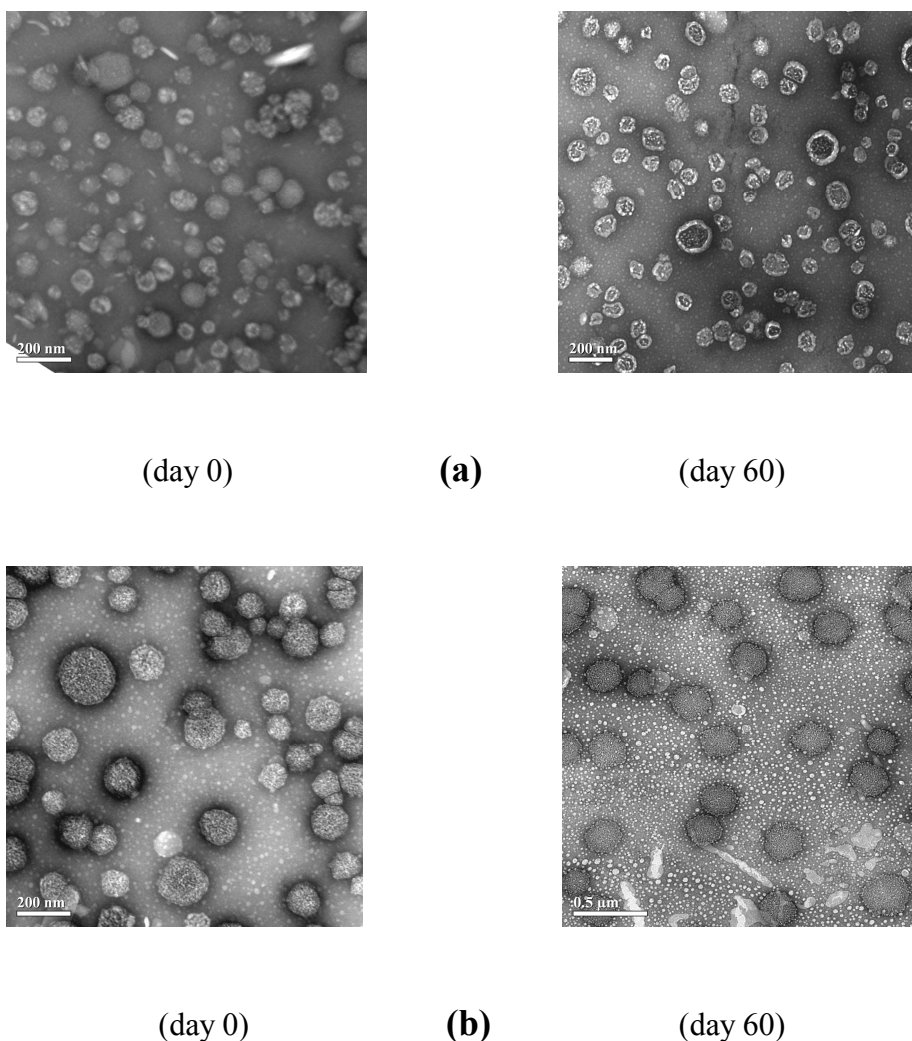
Figure 25 Transmission electron photomicrographs of ginger extract loaded SLN at day 0 and day 60; (a) GPG 5% P188, (b) GPG 3% Tw80, (c) GPG 5% Tw80, (d) GBG 3% Tw80 and (e) GBG 5% Tw80

(day 0)   **(c)**   (day 60)

(day 0)   **(d)**   (day 60)

(day 0)   **(e)**   (day 60)
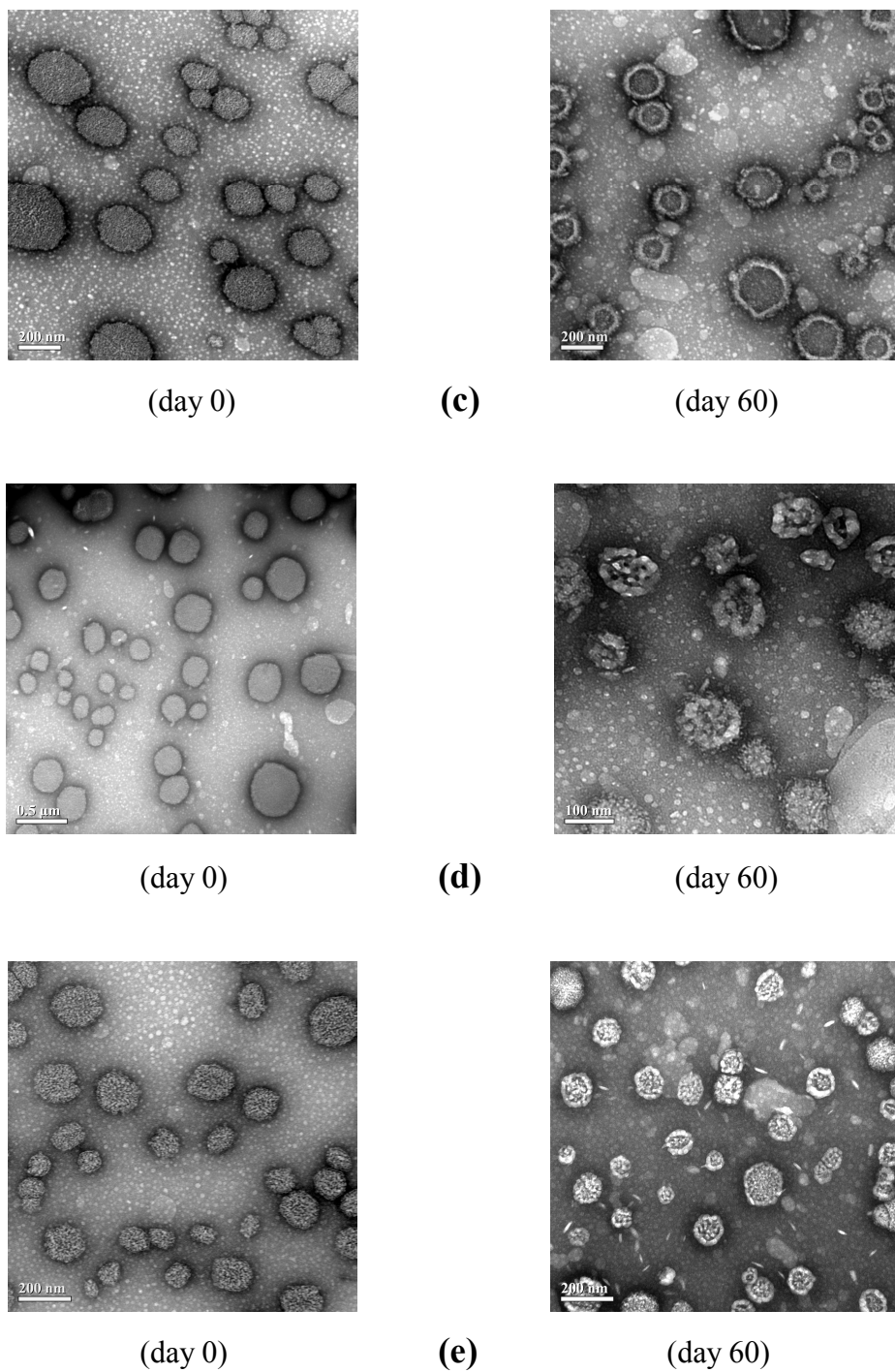
Figure 25   (continued) Transmission electron photomicrographs of ginger extract loaded SLN at day 0 and day 60; (a) GPG 5% P188, (b) GPG 3% Tw80, (c) GPG 5% Tw80, (d) GBG 3% Tw80 and (e) GBG 5% Tw80

2.4 Entrapment efficiency

The six ginger loaded SLN formulations which obviously stable during a period of 2 months of storage at room temperature and at 4 °C were selected and analyzed for entrapment efficiency. The formulations were GP-SLN with 3% and 5% of either P188 or Tw80 of and GB-SLN with 3% and 5% of Tw80.

2.4.1 Validation of the UV Spectrophotometric method for assay of the entrapment efficiency study

The determination of amount of entrapped [6]-gingerol was performed by UV spectrophotometry due to rapidity and convenience. The validation of analytical method was the process for evaluation that the method was suitable and reliable for the intended analytical applications. The analytical parameters used for the UV spectrophotometric assay validation were specificity, linearity, accuracy and precision.

1) Specificity

The UV validation absorption spectrum of [6]-gingerol showed the maximum absorbance at the wavelength of 282 nm. Therefore, the detection of [6]-gingerol was performed at this wavelength, which also was used by He et al. (1998).

2) Linearity

The calibration curve of [6]-gingerol in chloroform: methanol (1:1) is shown in Figure 26. Linear regression analysis of the absorbances versus the corresponding concentrations was performed and the coefficient of determination (R^2) was calculated as 0.9999 as depicted in Table 17. The calibration data were found to be linear with excellent coefficient of determination. These results indicated that UV spectrophotometric method was acceptable for quantitative analysis of [6]-gingerol in the concentration range studied.

Table 17 Data for calibration curve of [6]-gingerol by UV spectrophotometric method

Concentration (µg/ml)	Absorbance			Mean	SD.	% CV
	Set 1	Set 2	Set 3			
5	0.2909	0.2909	0.2908	0.2909	0.002	0.69
7	0.3357	0.3363	0.3363	0.3361	0.004	1.19
9	0.3795	0.3792	0.3796	0.3794	0.002	0.53
11	0.4248	0.4247	0.4243	0.4246	0.003	0.71
13	0.4715	0.4715	0.4717	0.4716	0.002	0.42
15	0.5166	0.5172	0.5165	0.5168	0.004	0.77
17	0.5593	0.5592	0.5590	0.5592	0.002	0.36
R^2	0.9999	0.9998	0.9999	0.9999	-	-
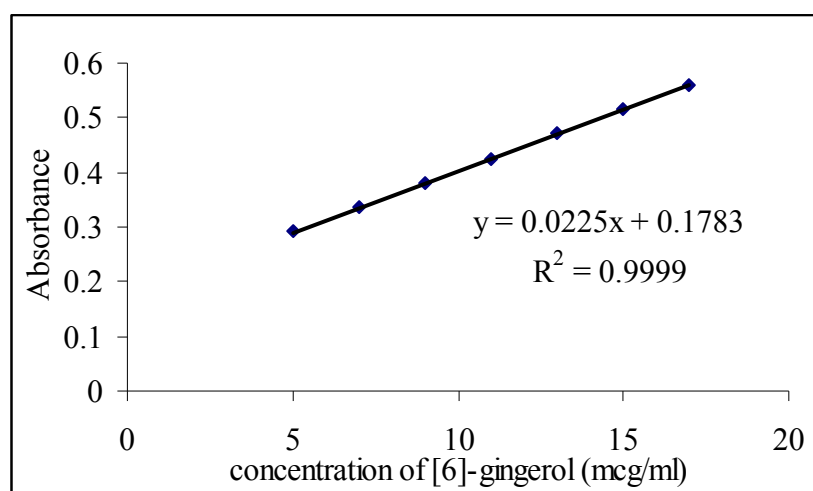
Figure 26 Calibration curve of [6]-gingerol by UV spectrophotometric method.

3) Accuracy

a) Accuracy of [6]-gingerol solution

Three [6]-gingerol solutions were prepared at the concentration of 8, 12, 16 µg/ml in five sets. Each individual sample was analyzed by UV spectrophotometer. The inversely estimated concentrations and percentages of analytical recovery of [6]-gingerol solution are shown in Tables 18 and 19, respectively. All percentages of analytical recovery were in the range of 99.39-100.50%, which indicated the high accuracy of this method. Thus, it could be used for analysis of [6]-gingerol in all concentrations studied.

b) Accuracy of [6]-gingerol in SLN formulation

The percentages of analytical recovery of SLN formulation for GP-SLN and GB-SLN are displayed in Tables 20 and 21. All percentages of analytical recovery were in the range of 98.10-100.32% and 98.62-101.73%, which indicated the high accuracy of this method. Thus, it could be used for analysis of [6]-gingerol in all concentrations studied.

Table 18 The inversely estimated concentrations of [6]-gingerol solution by UV spectrophotometric method

Concentration (µg/ml)	Inversely estimated concentration (µg/ml)					Mean ± SD
	Set 1	Set 2	Set 3	Set 4	Set 5	
8	7.9911	8.0133	7.9511	8.0400	7.9689	7.9929 ± 0.4406
12	11.9822	12.0133	11.9733	12.0444	11.9511	11.9929 ± 0.3040
16	16.0000	16.0400	15.9689	16.0800	15.9778	16.0133 ± 0.2891

Table 19 The percentage of analytical recovery of [6]-gingerol solution by UV spectrophotometric method

Concentration (µg/ml)	%Analytical recovery					Mean ± SD
	Set 1	Set 2	Set 3	Set 4	Set 5	
8	99.89	100.17	99.39	100.50	99.61	99.91 ± 0.4403
12	99.85	100.11	99.78	100.37	99.59	99.94 ± 0.3038
16	100.00	100.25	99.81	100.50	99.86	100.08 ± 0.2891

Table 20 The percentage of analytical recovery of [6]-gingerol in GP-SLN by UV spectrophotometric method

Concentration (µg/ml)	%Analytical recovery					Mean ± SD
	Set 1	Set 2	Set 3	Set 4	Set 5	
8	99.29	98.58	98.10	98.22	98.34	98.51±0.4710
12	99.10	99.21	100.32	99.92	99.56	99.62±0.5062
16	98.49	99.67	99.44	99.29	99.76	99.33±0.5064

Table 21 The percentage of analytical recovery of [6]-gingerol in GB-SLN by UV spectrophotometric method

Concentration (μg/ml)	%Analytical recovery					Mean ± SD
	Set 1	Set 2	Set 3	Set 4	Set 5	
8	99.65	101.73	101.19	100.99	99.36	100.58±1.0254
12	100.20	100.92	101.48	101.25	100.79	100.93±0.4810
16	100.05	101.46	101.33	100.62	98.62	100.42±1.1555

4) Precision

The precision of [6]-gingerol analyzed by UV spectrophotometric method were determined both within run precision and between run precision as illustrated in Tables 22 and 23. All coefficient of variation values were very low, as 0.04-0.08% and 0.09-0.38%, respectively. The coefficient of variation of an analytical method should generally be less than 2%. Therefore, the UV spectrophotometric method was precise for quantitative analysis of [6]-gingerol in the range studied.

Table 22 Data of within run precision by UV spectrophotometric method

Concentration (μg/ml)	Absorbance					Mean	SD	% CV
	Set 1	Set 2	Set 3	Set 4	Set 5			
8	0.3580	0.3579	0.3573	0.3575	0.3579	0.3577	0.0003	0.0848
12	0.4478	0.4479	0.4478	0.4476	0.4475	0.4477	0.0002	0.0367
16	0.5382	0.5385	0.5377	0.5384	0.5381	0.5382	0.0003	0.0579

Table 23 Data of between run precision by UV spectrophotometric method

Concentration (μg/ml)	Absorbance					Mean	SD	% CV
	Set 1	Set 2	Set 3	Set 4	Set 5			
8	0.3580	0.3581	0.3581	0.3574	0.3583	0.3580	0.0003	0.0956
12	0.4478	0.4479	0.4440	0.4477	0.4477	0.4470	0.0017	0.3781
16	0.5382	0.5375	0.5383	0.5375	0.5379	0.5379	0.0004	0.0701

In conclusion, the analysis of [6]-gingerol by UV spectrophotometric method developed in this study showed good specificity, linearity, accuracy and precision. Thus, this method was used for the determination of the content of [6]-gingerol in the entrapment efficiency study of SLN.

2.4.2 The entrapment efficiency study of SLN

Determination of the amount of entrapped [6]-gingerol in SLN dispersion was carried out by using centrifugation method. The entrapment efficiency study of ginger loaded SLN was observed during storage time of 2 months, (day 0, day 30 and day 60). The results in Table 24 clearly showed that the preparation by hot high pressure homogenization gave high entrapment efficiency of [6]-gingerol. The finding was consistent with previous studies that claimed for higher encapsulation efficiency of lipophilic compound by the same method (Kumar et al., 2007; Muhlen et al., 1998).

Table 26 shows the percentages of recovery of entrapment efficiency study which included the content of entrapped [6]-gingerol and unentrapped [6]-gingerol in Table 25. The high percentage of recovery, more than 97 %, depicted the accuracy of analytical method used in the study.

After statistical analysis with one-way ANOVA and Duncan test at 5% significant level, there were significant differences between varied compositions of SLN dispersions as depicted in Tables E7 and E8. These results reveal that type and amount of surfactant affected loading capacity of SLN.

It was noticed that the higher entrapment efficiency was obtained with decreasing surfactant concentration from 5% to 3% (compared with the same type of lipid and surfactant). This result was consistent with Muller et al. (2000). The explanation might be attributed to the high producing temperature and surfactant concentration which increased the solubility of the extract in the water phase and increasing in partitioning from lipid droplet to water phase. In the cooling process, the solidified lipid was started before the repartitioning of gingerol molecules to lipid core.

Formulations of GP-SLN prepared with P188 have shown less loading capacity compared with Tw80. It might be due to the block copolymer of P188 which highly increased the solubility of extract in water phase in the homogenization.

The high compatibility between extract and lipid might result in high %entrapment efficiency. Because of high lipophilicity and well solubilizing potential of GP and GB, there were no significant differences between both lipids in entrapment efficiency study ($P>0.05$) (Table E8).

Table 24 Entrapment efficiency of ginger extract loaded SLN at 4 ºC for 2 months

No.	Loaded SLN	% Entrapment efficiency		
		Day 0	Day 30	Day 60
1	GPTG3	96.27±0.7743	96.24±1.0918	93.26±0.1677
2	GPTG5	90.33±1.1895	90.12±1.2884	88.49±1.0107
3	GBTG3	95.50±1.4283	95.27±1.2667	93.28±2.1004
4	GBTG5	90.44±1.2091	90.40±0.7812	87.24±0.7872
5	GPPG3	88.59±1.1381	88.66±0.5267	86.25±0.9521
6	GPPG5	84.52±0.7669	84.36±0.5591	78.91±1.3066

Table 25 Percent free [6]-gingerol in supernatant of ginger extract loaded SLN at storage temperature 4 ºC for 2 months

No.	Loaded SLN	% Free [6]-gingerol		
		Day 0	Day 30	Day 60
1	GPTG3	3.18±0.3581	3.24±0.2784	5.91±0.1619
2	GPTG5	9.56±0.4330	9.47±0.1068	11.43±0.1464
3	GBTG3	3.59±0.5550	5.30±0.6166	7.68±0.5385
4	GBTG5	9.69±0.6644	9.84±0.2540	13.32±1.6673
5	GPPG3	10.85±0.2458	9.59±0.1871	12.76±0.2166
6	GPPG5	14.13±0.4099	15.62±0.1322	18.18±1.0372

Table 26 Percent recovery of [6]-gingerol content in entrapment efficiency study of ginger extract loaded SLN at storage temperature 4 ºC for 2 months

No.	Loaded SLN	% Recovery of [6]-gingerol		
		Day 0	Day 30	Day 60
1	GPTG3	99.45±0.5638	99.48±0.9198	99.17±0.2295
2	GPTG5	99.89±0.9279	99.59±1.2626	99.92±1.1360
3	GBTG3	99.09±0.8827	100.57±0.7577	100.95±2.3889
4	GBTG5	100.12±0.6216	100.24±0.6853	100.56±1.4315
5	GPPG3	99.44±1.0329	98.25±0.5314	99.01±0.9100
6	GPPG5	98.65±0.4443	99.98±0.5035	97.10±0.8636

Although %EE values decreased with an increase in storage duration, the acceptable %EE was obtained in all formulation, 78.91-93.26%. The slightly decreased %EE might be due to the transformation of solid lipid. Bunjes et al (1996) and Jenning, Thunemann and Gohla (2000) reported that polymorphism influenced the nanoparticles drug content and drug expulsion during polymorph transition to more stable form, β form. The perfect lattice caused the expulsion of incorporated drug from lipid matrix leaded to lower percentage of entrapment efficiency.

From the result in this study, the GPPG5, with the lowest %EE (lower than 85%), was not selected to study in the next topics.

2.5 Thermal analysis by differential scanning calorimetric method

Differential scanning calorimetric (DSC) analysis was performed for all selected formulations and the recorded DSC parameters are presented in Table 27.

The DSC thermograms of bulk lipids, GP and GB showed endothermic peaks at 75.31 °C while the thermogram of GB exhibited the melting peak at 58.66 °C. These results were corresponding to the investigation of Jansook (2005).

From data obtained in Table 27, all formulations of loaded SLN dispersions had reduction in enthalpies and width in melting range comparable with bulk solid lipid, GP and GB. The increasing melting range could be correlated with the impurities or less ordered crystal, so the melt of the substance required less energy than perfect crystalline material. Comparing to the bulk lipid and extract free-SLN, the impurities lattice of SLN formulation were occurred by the presence of ginger

extract and molecules of surfactant. The imperfection lattice was offered space to the accommodated extract. These results were corresponding to the high entrapment efficiency of ginger extract in lipid core of SLN dispersion.

Comparing to the formulation of GP-SLN and GB-SLN at day 0, the melting range of both SLN formulations were broadening and lower enthalpy were obtained with increasing storage time. It also demonstrated the modification of lipid. The results were accordance to the research of Westesen, Siekmann and Koch (1993).

Table 27 DSC results of bulk lipid and developed ginger extract loaded SLN

Sample		Enthalpy (J/g)	Peak (°C)	Onset (°C)	End set (°C)
Precirol		143.11	58.66	52.30	63.51
Compritol		133.12	75.31	71.20	77.99
GPTG 3	Blank	98.66	60.57	54.94	62.20
	day 0	94.57	61.86	57.31	63.75
	day 30	87.06	60.07	55.99	61.70
	day 60	92.61	58.31	50.35	60.06
GPTG 5	Blank	87.97	60.23	57.49	61.59
	day 0	83.95	62.41	60.28	64.37
	day 30	67.83	59.88	47.86	61.23
	day 60	72.81	58.41	52.68	60.14
GBTG 3	Blank	109.69	73.15	69.65	75.73
	day 0	104.56	74.64	70.02	76.67
	day 30	100.39	71.84	65.60	75.48
	day 60	96.35	72.64	66.06	75.84
GBTG 5	Blank	105.54	72.97	68.74	74.96
	day 0	99.64	76.43	72.63	78.28
	day 30	68.28	73.84	66.85	75.37
	day 60	83.52	71.99	66.18	74.59
GPPG3	Blank	118.77	50.41	43.77	55.26
	day 0	99.45	47.06	42.01	49.55
	day 30	123.70	52.55	51.21	66.26
	day 60	112.46	57.65	48.15	62.41

The amount of surfactant also affected the arrangement of crystal lattice. As depicted in Table 27, the lower enthalpy obtained with increasing surfactant concentration from 3% to 5%. This results were agreed with Soukharev (2007) reported that the surfactants were distributed to the melted lipid phase during the production process and distorted the crystallization process.

The effect of loaded ginger extract on thermal behavior of SLN was monitored and recorded. The melting point depression and lower enthalpy of ginger loaded SLN might be due to the oily like compound of acetone extract. The presence of liquid or non- crystallizing active substances has been found to decrease the crystallization temperature of glyceride nanoparticles in a similar way as the loading with tocopheryl acetate and ubidecarinone (Bunjes et al., 2001)
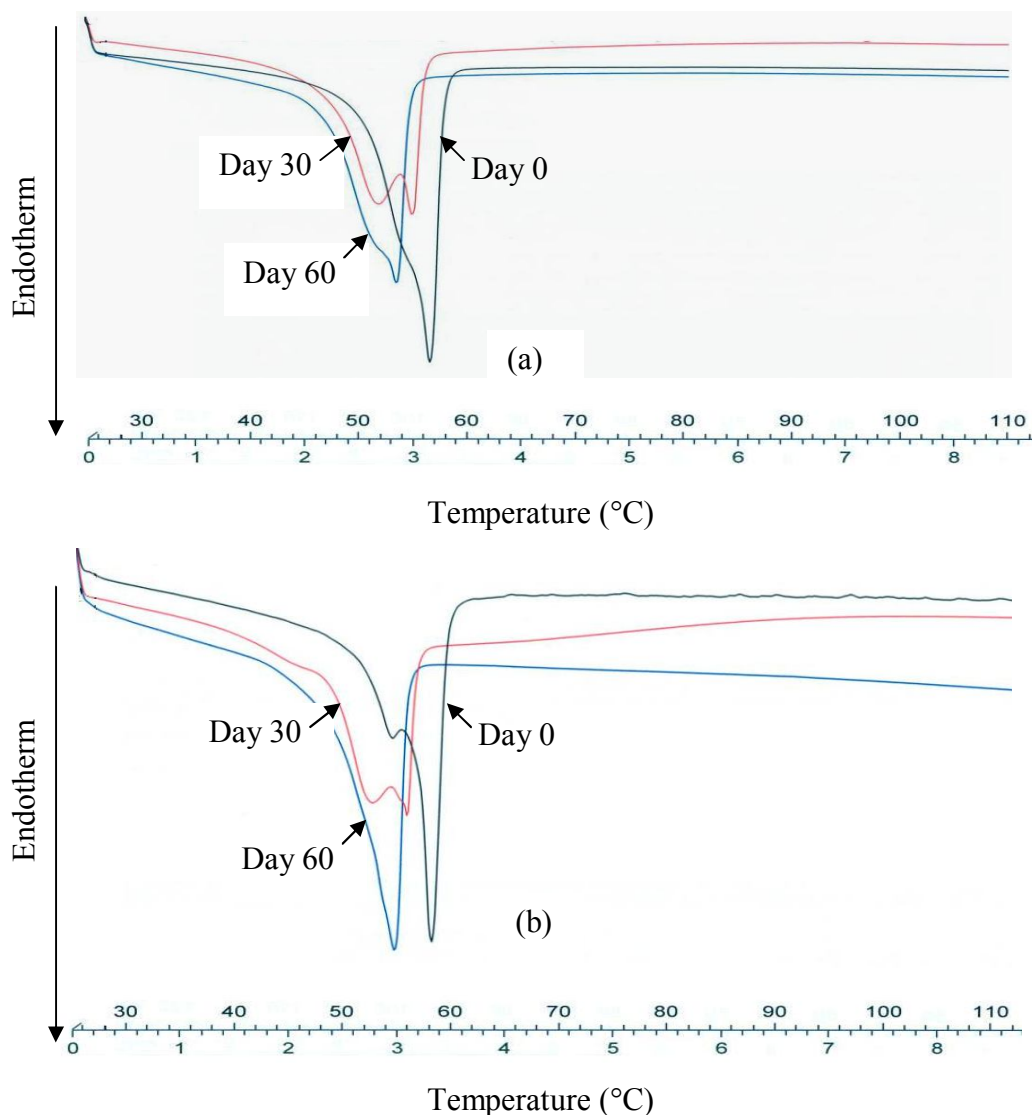
Figure 27 DSC thermograms of ginger extract loaded SLN formulations during storage time, (a) GPTG3, (b) GPTG5, (c) GBTG3 and (d) GBTG5 and (e) GPPG3
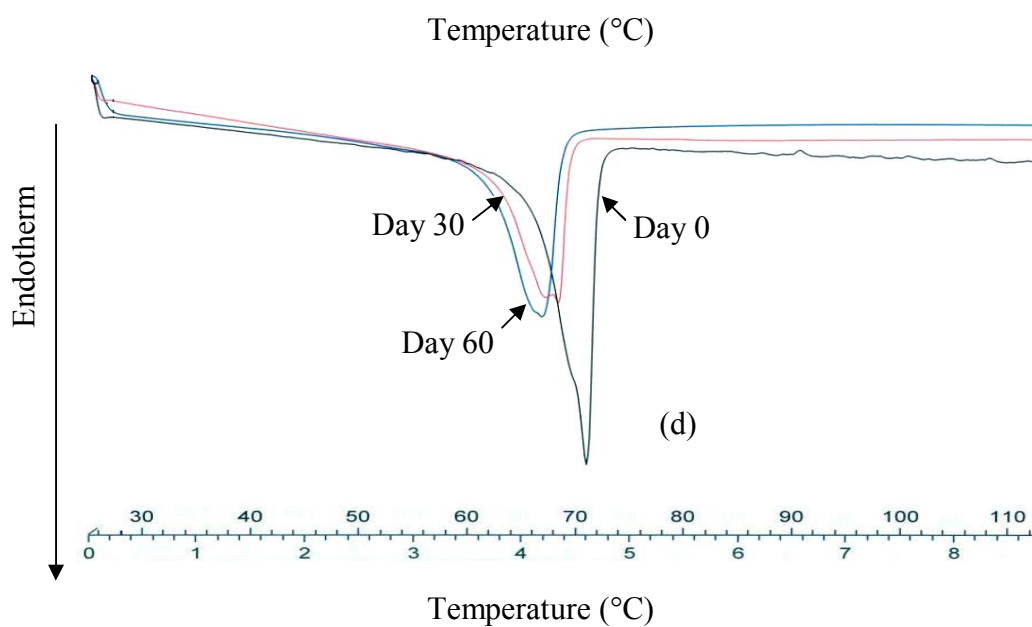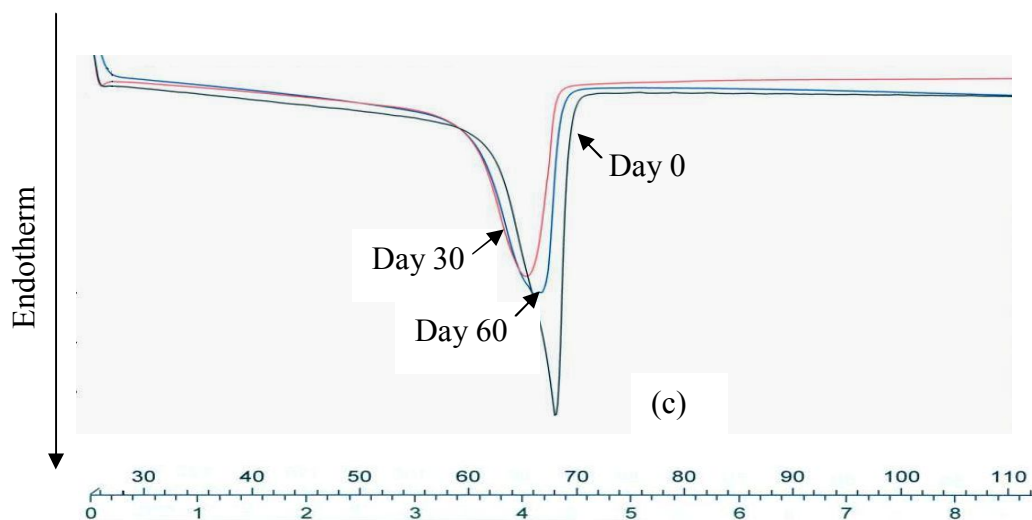
Figure 27 (continued) DSC thermograms of ginger extract loaded SLN formulations during storage time, (a) GPTG3, (b) GPTG5, (c) GBTG3, (d) GBTG5 and (e) GPPG3
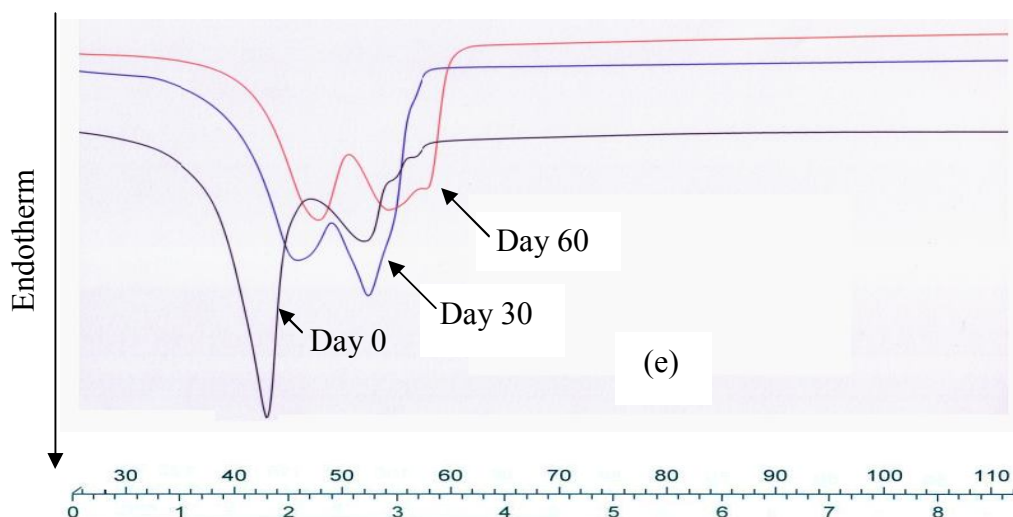
Figure 27 (continued) DSC thermograms of ginger extract loaded SLN formulations during storage time, (a) GPTG3, (b) GPTG5, (c) GBTG3, (d) GBTG5 and (e) GPPG3

2.6 Powder X-ray Diffractogram

Powder X-ray diffractometry has been widely used to determine the degree of crystallinity of pharmaceutical excipients. In this study, the crystalline state of lipid and SLN were investigated by wide angle X-ray diffraction (WAXD).

The X-ray diffractograms of bulk GP and GP-SLN are shown in Figure 28 while the X-ray diffractograms of bulk GB and GB-SLN are shown in Figure 29.

The diffractogram of GP (Figure 28a) showed the characteristic peaks at 0.46, 0.42 and 0.38 nm which was in accordance with the investigation by Jansook, 2005. These signals of bulk GP corresponded to the β modification of triglyceride (Jenning and Gogla, 2000 and Heurtault et al., 2003). The principal peak of diffractogram of GPTG3 and GPTG5 at day 0 (Figure 28b and 28d) had a reduced intensity at 0.46 nm while increased intensity at 0.42 and 0.38 nm. It might be due to the incorporation of ginger extract and lipid modification to β' form. The presence of three dominated peaks clearly revealed that GP-SLN transformed to β' form during storage. From the result obtained, the β/β' form was influenced to the lower enthalpy in thermal analysis. The result confirmed the observation that obtained from the DSC thermograms. In contrast, the diffractogram of GPPG3 showed the characteristic peaks similarly to the diffractogram of GP.

The diffractogram of bulk GB (Figure 29a) showed two main typical signals of triglyceride, occurring high intensity at 0.42 nm and low intensity at 0.38

nm, which corresponded to β' form (Souto, Mehnert and Muller, 2006). From this result, the difference in polymorph of bulk lipid between GP and GB, the β form of GP required more energy in melting process than the β' form of GB. In this study, the observation of lipid transformation was investigated by both DSC and XRD techniques. The principal peaks of diffractogram of GBTG3 and GBTG5 at day 0 and day 60 were depicted strongly intensity at 0.46, 0.42 and 0.38 nm which means the presence of β and β' form of lipid.

From Figure 28, it was revealed that GP-SLN, GPTG3 and GPTG5, clear exhibited β peak at 0.46 at storage time day 60, while GB-SLN, GBTG3 and GBTG5, showed β peak at 0.46 at day 0 (Figure 29). The type and characteristic of lipid affected lipid transformation. Glyceryl palmitostearate gradually changed from β' to β, while glyceryl behenate turned to β immediately after hot homogenization process. The modification of lipid to stable polymorph influenced the capacity of incorporated substance in lipid core because stable polymorph had perfect crystal lattice which the number of imperfections in the crystal lattice is reduced thus leading to drug expulsion. The results from XRD study confirmed lipid modification and also explained the stability and entrapment efficiency of SLN formulations. Lipid modification leaded to drug expulsion during storage time caused slightly decrease in entrapment efficiency. Moreover, lipid changed from spherical form (β' form) to platelet form (β form) which easily aggregated and formed particle growth during storage time. GB exhibited high crystallinity so the stability of GB-SLN slightly shorter than GP-SLN.
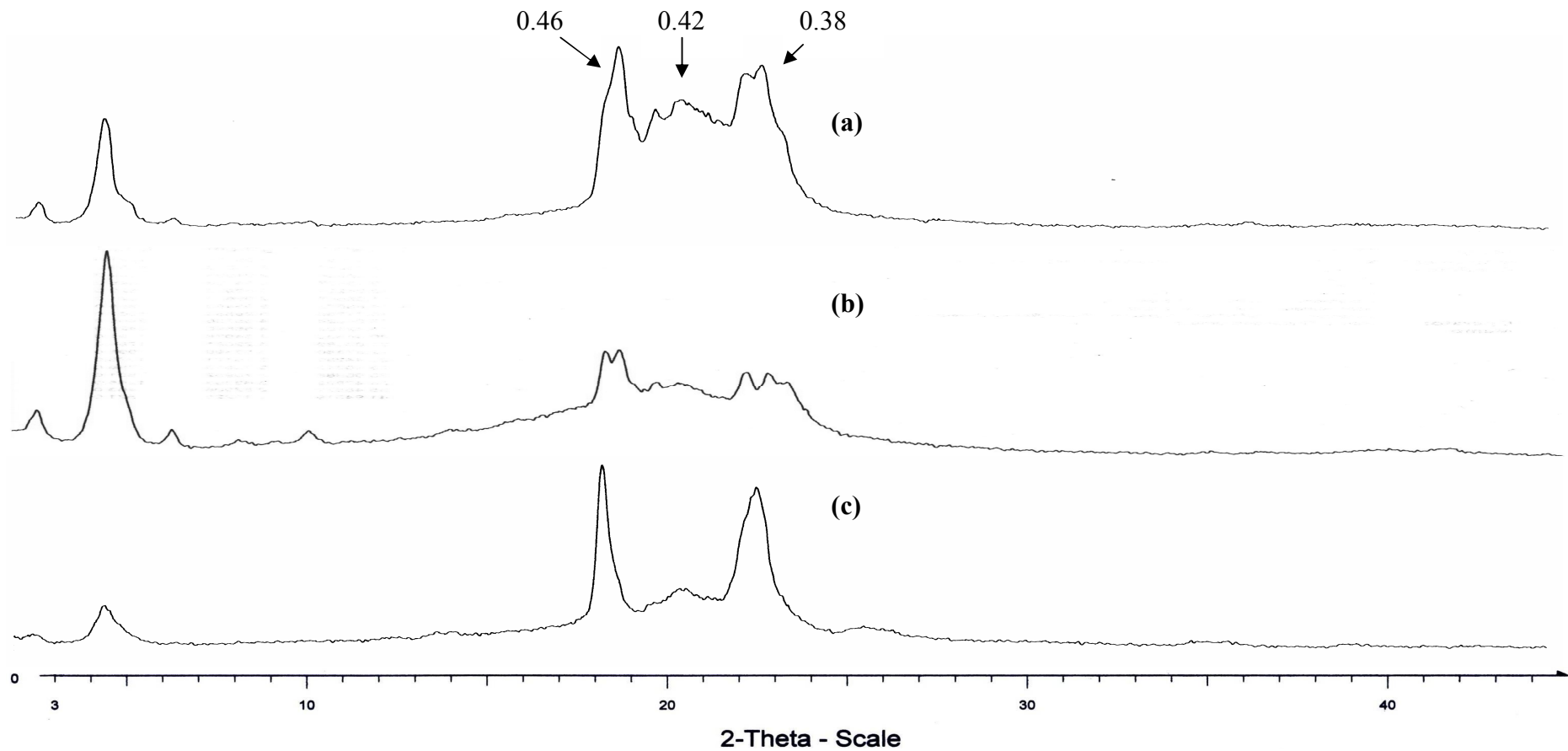
Figure 28   X-ray diffractograms of ginger extract loaded GP-SLN ; (a) glyceryl palmitostearate (GP), (b) GPTG3_day0 , (c) GPTG3_2 months ,(d) GPTG5_day0 , (e) GPTG5_2 months , (f) GPPG3_day0 and (g) GPPG3_2 months

Figure 28 (continued) X-ray diffractograms of ginger extract loaded GP-SLN ; (a) glyceryl palmitostearate (GP), (b) GPTG3_day0 , (c) GPTG3_2 months ,(d) GPTG5_day0 , (e) GPTG5_2 months , (f) GPPG3_day0 and (g) GPPG3_2 months
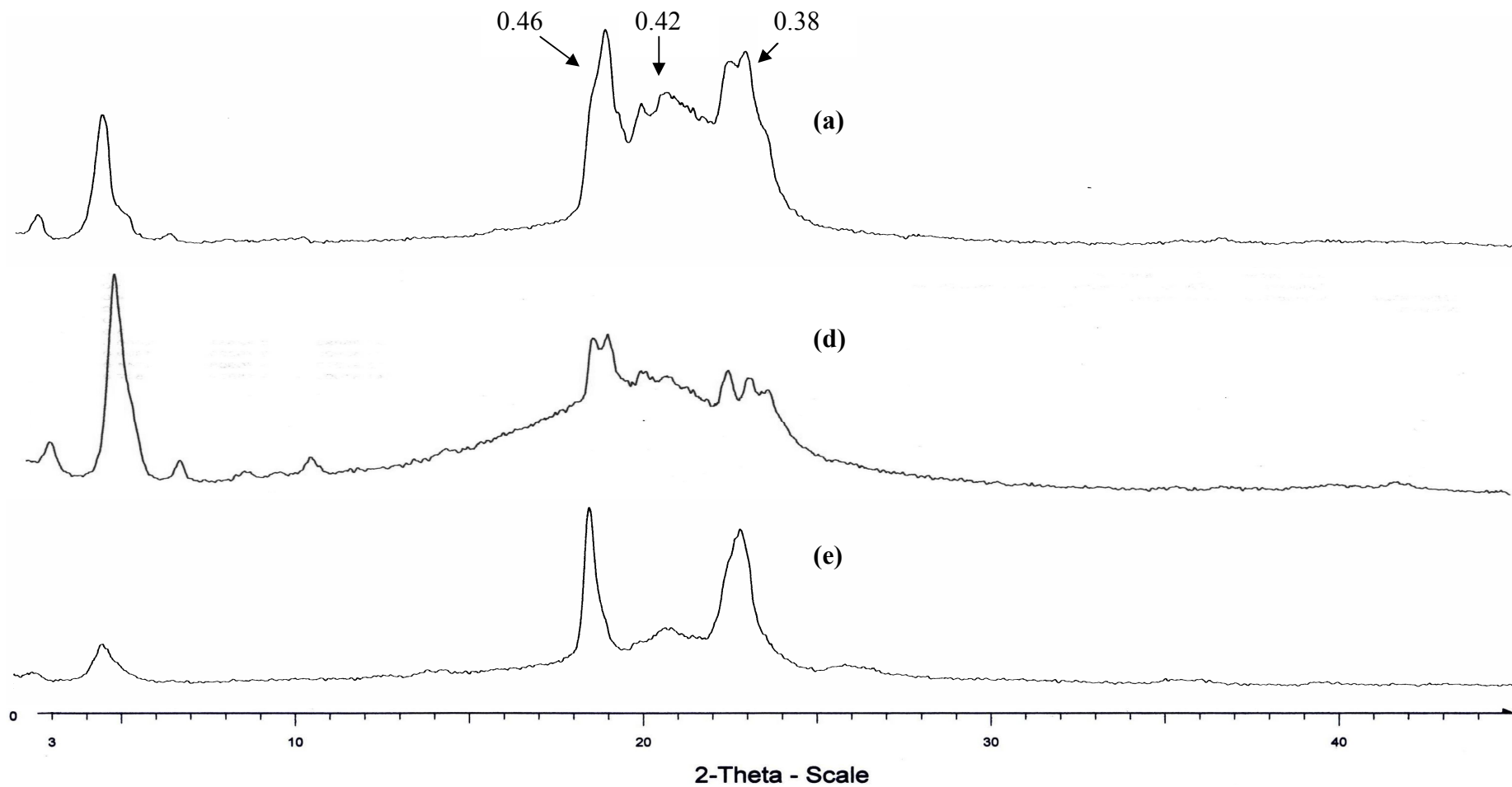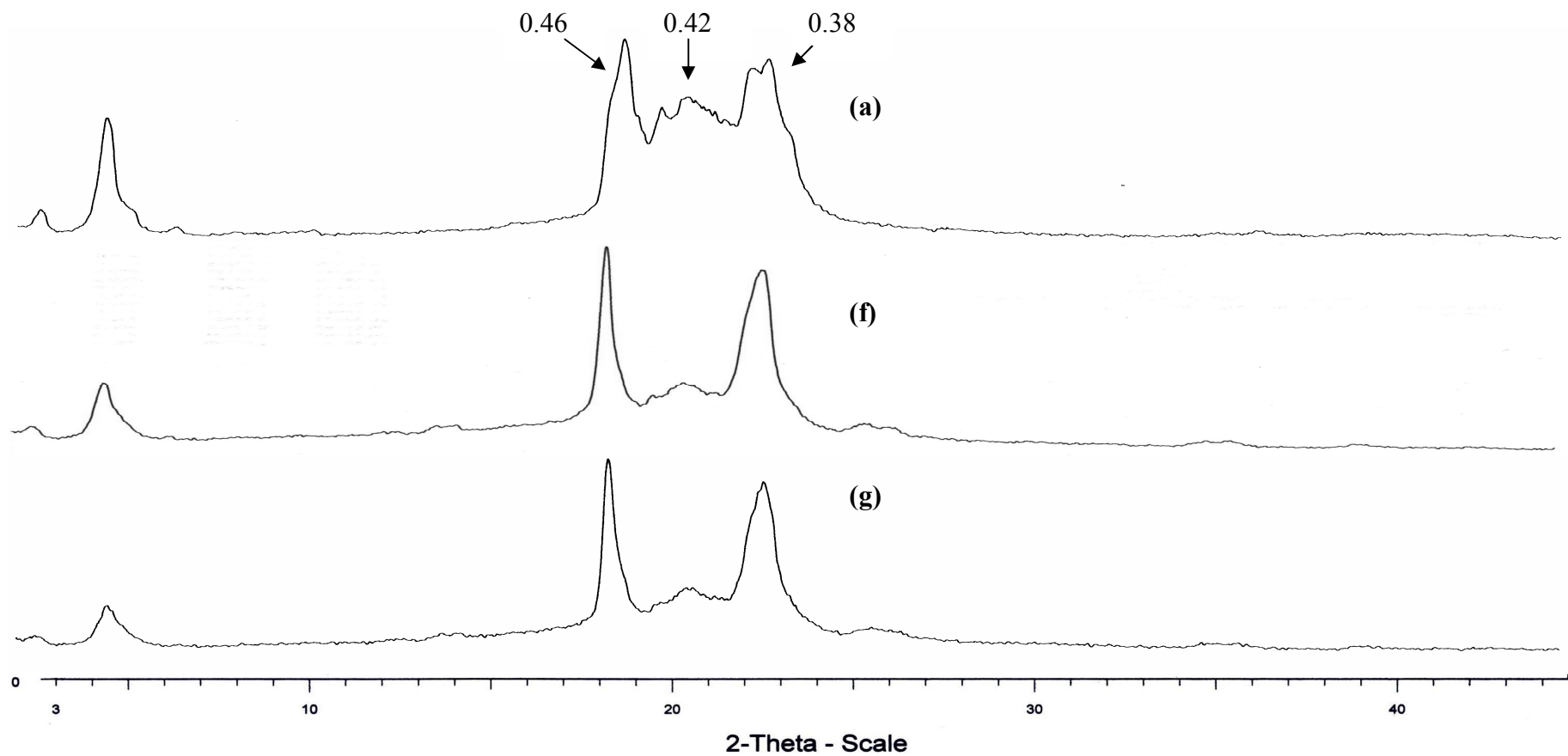
Figure 28 (continued) X-ray diffractograms of ginger extract loaded GP-SLN; (a) glyceryl palmitostearate (GP), (b) GPTG3_day0 , (c) GPTG3_2 months ,(d) GPTG5_day0 , (e) GPTG5_2 months , (f) GPPG3_day0 and (g) GPPG3_2 months
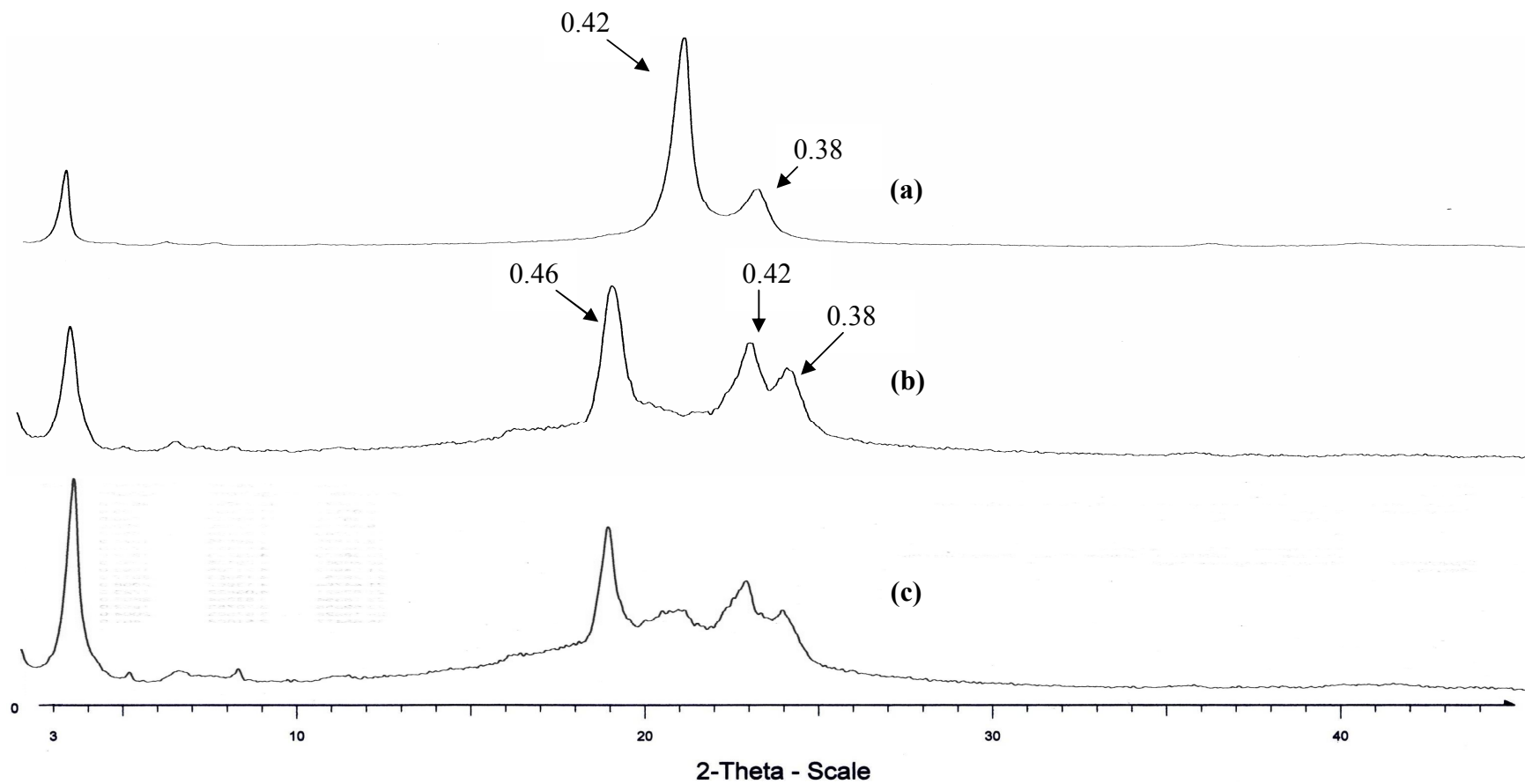
Figure 29 X-ray diffractograms of ginger extract loaded GB-SLN; (a) glyceryl behenate (GB), (b) GBTG3_day0, (c) GBTG3_2 months, (d) GBTG5_day0 and (e) GBTG5_2 months
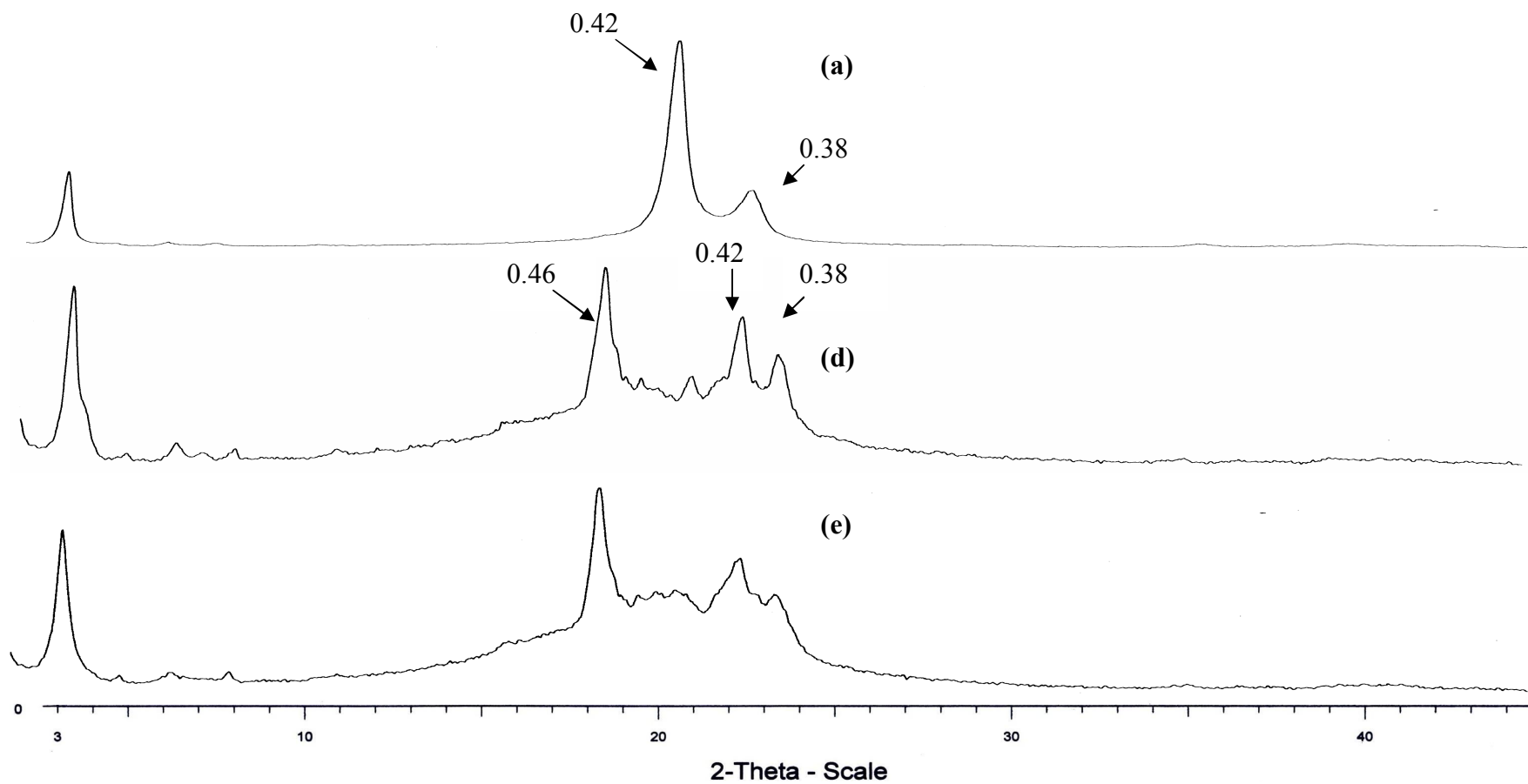
Figure 29 (continued) X-ray diffractograms of ginger extract loaded GB-SLN; (a) glyceryl behenate (GB), (b) GBTG3_day0, (c) GBTG3_2 months, (d) GBTG5_day0 and (e) GBTG5_2 months

2.7 The analysis of [6]-gingerol content in release and permeation study

The determination of [6]-gingerol content was performed by high performance liquid chromatography, HPLC. The following topics were performed as the same chromatographic condition as topic F7.2. The validation procedure was performed in all system. The analytical parameters used in the validation of the HPLC assay method were specificity, linearity, accuracy and precision (USP 24, 2000).

2.7.1 The determination of [6]-gingerol content in 20% isopropanol in PBS buffer pH 7.4

The determination of [6]-gingerol content in 20% isopropanol in PBS buffer pH 7.4 was performed for analysis of [6]-gingerol in receiver medium of Franz cell in release study.

2.7.2 The determination of [6]-gingerol content in PBS buffer pH 7.4

The determination of [6]-gingerol content in PBS buffer pH 7.4 was performed for analysis of [6]-gingerol in receiver medium of Franz cell in permeation study.

2.7.3 The determination of [6]-gingerol content in methanol

The determination of [6]-gingerol content in methanol was performed for analysis of [6]-gingerol in new born pig skin.

All of data obtained from topics above are displayed in Appendix G. From the result, it indicated that all analytical systems could be used for analysis of [6]-gingerol content in all solvent system for release and permeation study with high accuracy.

2.8 In vitro release study of solid lipid nanoparticles containing *Zingiber officinale* extract

In this study, five formulations which stable over 2 months and entrapment efficiency over 85% were selected to investigate in release study. From the result in entrapment efficiency study, the GPPG5, with the lowest %EE (lower than 85%), was not selected to study in this topic.

In vitro release studies are important to understand the in vivo performance of the dosage form. Release studies help in evaluation of sustained and prolonged release of dispersion system.

The prepared formulations were evaluated the release pattern of [6]-gingerol from SLN by using Franz diffusion cell with barrier-free cellulose membrane. The release study was performed not more than 24 h according to the realistic application time. The sink condition was maintained by using 20% isopropanol in PBS in the receptor compartment. HPLC method was selected to determine the amount of [6]-gingerol in receptor compartment due to accuracy and specificity. The experiment was conducted in five replicates, n=5.

Figure 30 presented the release data and release profiles of [6]-gingerol from loaded SLN formulations. The amount released of [6]-gingerol was exhibited approximately 20-30% within 24 hours from SLN formulation. The release profiles of [6]-gingerol from each formulation and acetone extract solution, using as control, are clearly depicted in Figure 31. To validate of the release system, the release of [6]-gingerol from the solution of acetone extract was performed. The release profile showed a short lag time of 2 hours and reached the plateau of 100% release at 8 hours (Figure 31a)

The release data over the whole time period were explained according to the treatment proposed by Higuchi for [6]-gingerol release from SLN formulation. To quantitate the release data for comparison, the release profiles were plotted according to Higuchi's equation.

$$Q_t \quad = \quad k_H\, t^{1/2}$$

where:

Q_t is the amount of drug release at time t

k_H is the release rate constants of Higuchi

t is the release time

Figure 32 depicted the Higuchi plots of the release of [6]-gingerol from SLN formulations. Plots of the cumulative amount Q_t of drug released versus the square root of time were a short lag period. The coefficient of determination of the relationship between cumulative amount releases versus square root of time (R^2) of [6]-gingerol in each formulation are presented in Figure E1-E5. The release rate constants of SLN formulations are displayed in Table 28.
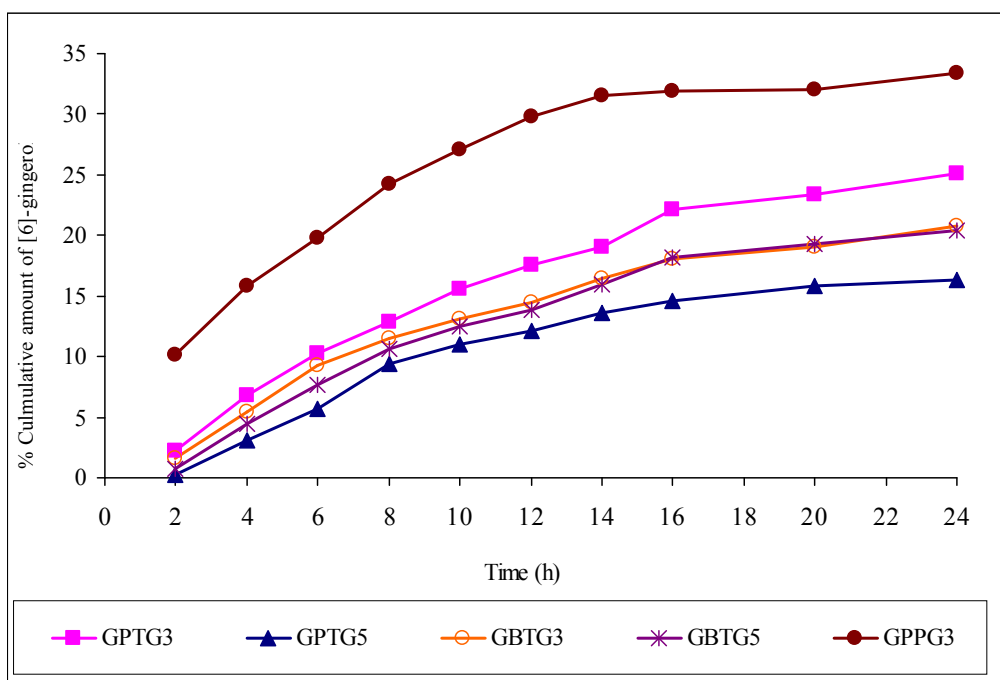
Figure 30 The release profiles of [6]-gingerol from SLN formulations; GPTG3, GPTG5, GBTG3, GBTG5 and GPPG3, (mean ± SD, n=5)

In this study**,** the release profiles of [6]-gingerol from SLN formulations best fit with the Higuchi equation which describes the diffusion of drug from homogeneous and granular matrix system. This finding was corresponded with the report of Vivex, Reddy and Murthy (2007).

After statistical analysis with one-way ANOVA and Duncan test at 5% significant level, there were significant differences ($P<0.05$) in release profiles among varied compositions of SLN dispersions as depicted in Table G8. These results in Table 28 reveal that the formulation of GPPG3 had the highest release rate constant at 4.6058 $\mu gcm^{-2}h^{-1/2}$.
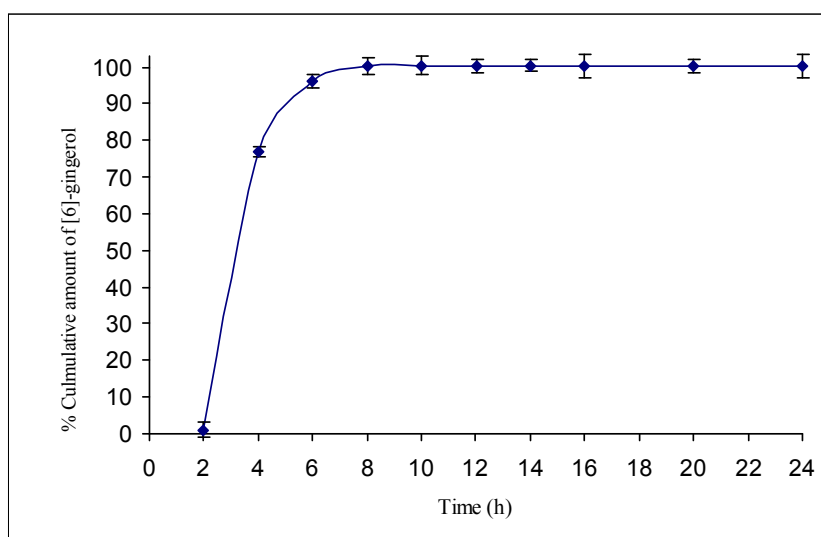
(a)
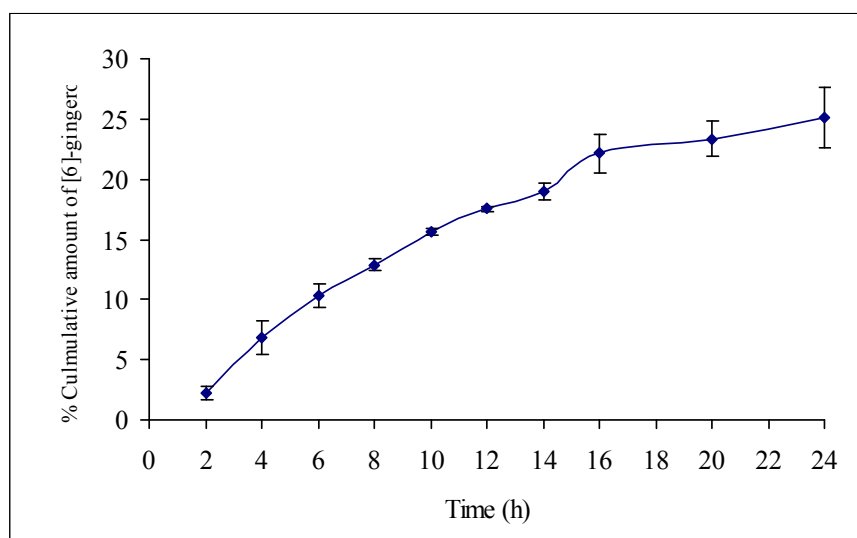
(b)

Figure 31 The release profiles of [6]-gingerol from (a) acetone extract solution, (b) GPTG3, (c) GPTG5, (d) GPPG3, (e) GBTG3 and (f) GBTG5 (mean ± SD, n=5)
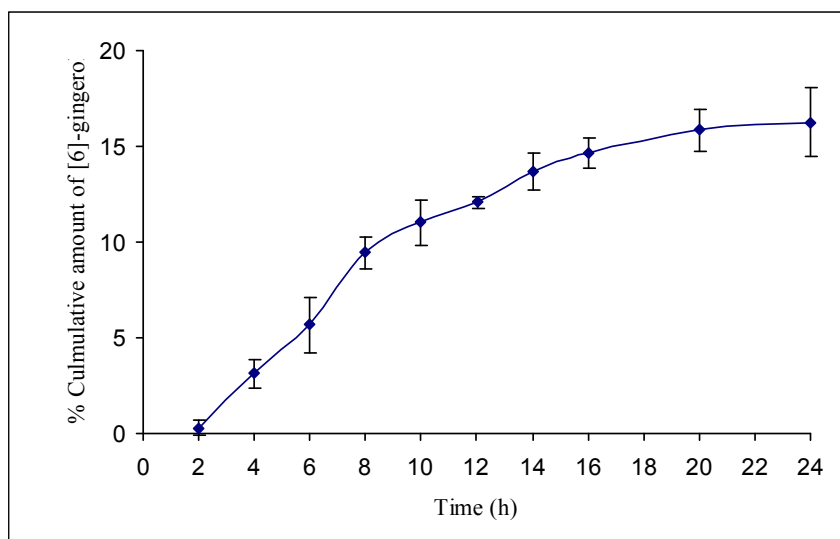
(c)
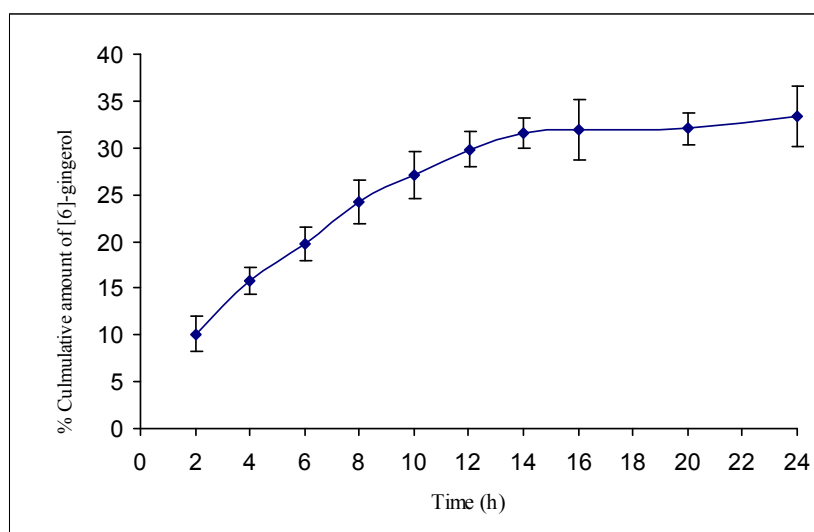
(d)

Figure 31 (continued) The release profiles of [6]-gingerol from (a) acetone extract solution, (b) GPTG3, (c) GPTG5, (d) GPPG3, (e) GBTG3 and (f) GBTG5 (mean ± SD, n=5)
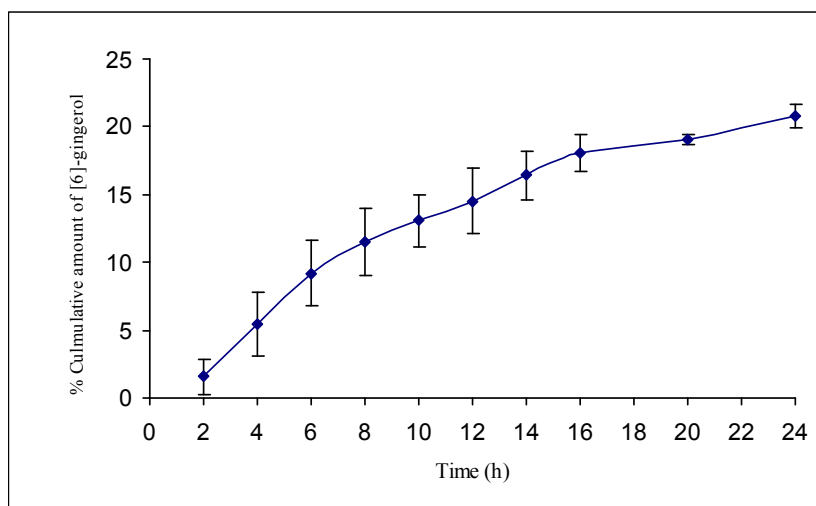
(e)
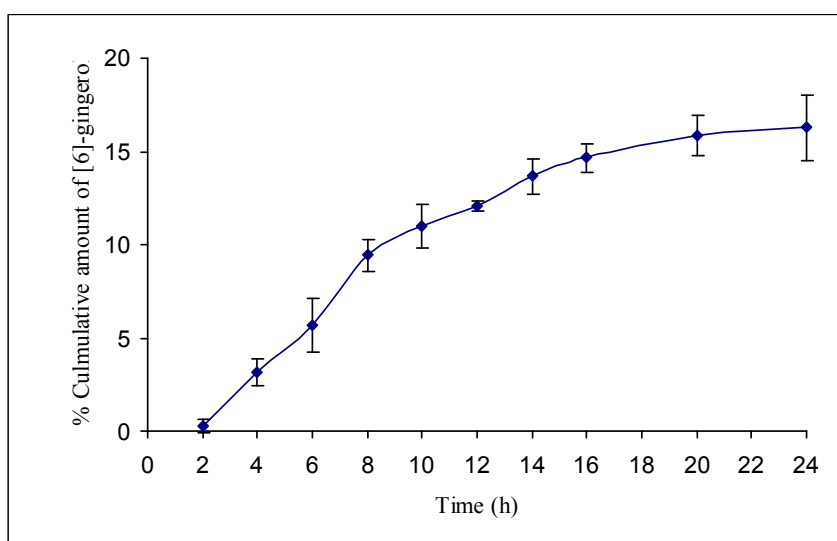
(f)

Figure 31 (continued) The release profiles of [6]-gingerol from (a) acetone extract solution, (b) GPTG3, (c) GPTG5, (d) GPPG3, (e) GBTG3 and (f) GBTG5 (mean ± SD, n=5)

(a)

(b)

(c)

(d)

(e)
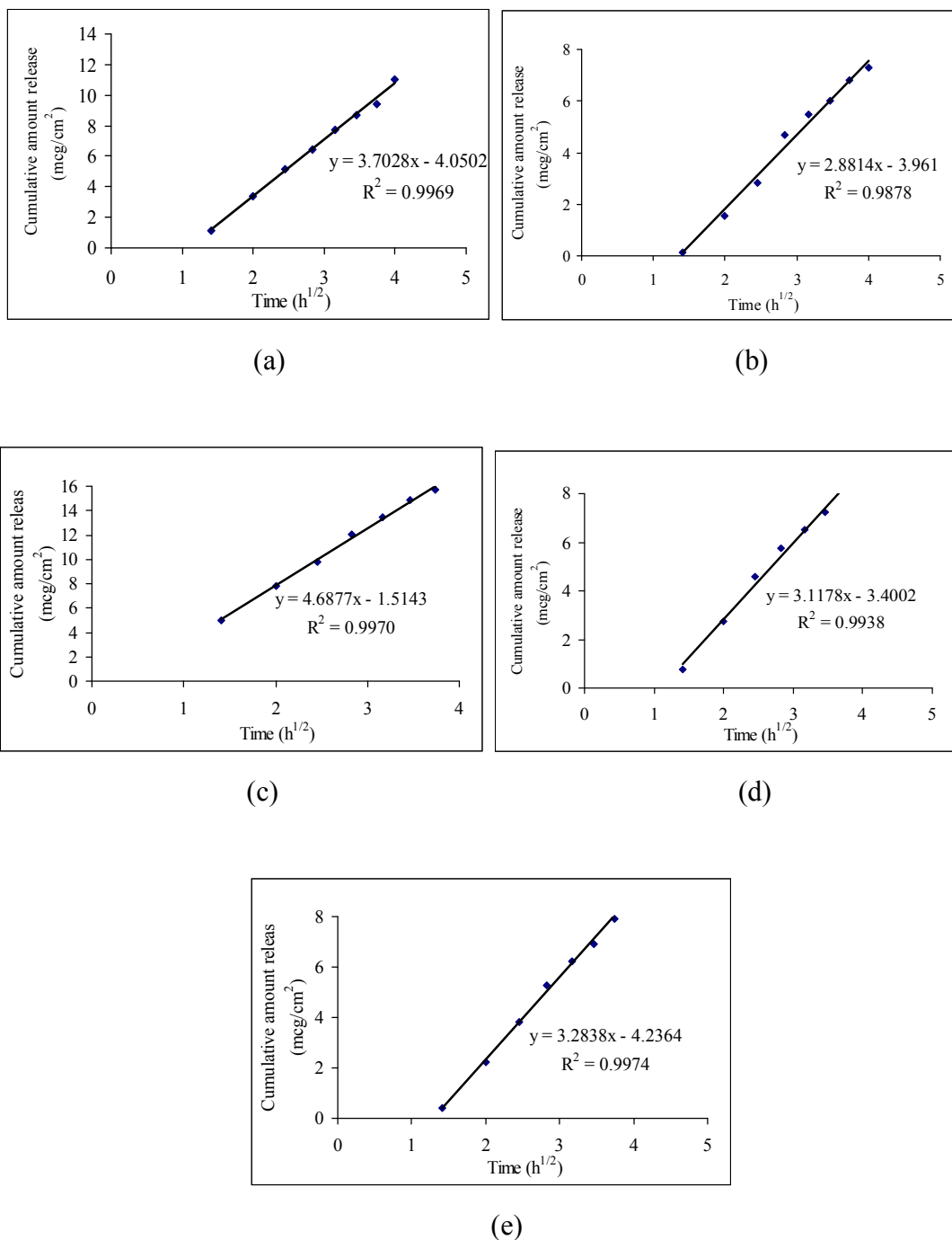
Figure 32 Higuchi plots of release profiles of [6]-gingerol from SLN formulations, (a) GPTG3, (b) GPTG5, (c) GPPG3, (d) GBTG3, (e) GBTG5, and, (mean, n=5)

Table 28 The release rate constant of [6]-gingerol from SLN formulations, (n=5)

Release rate constant ($\mu gcm^{-2}h^{-1/2}$)							
Formulation	N1	N2	N3	N4	N5	mean	SD
GPTG3	3.7776	3.4425	3.8842	3.9144	3.4951	3.7028	0.2203
GPTG5	2.7998	2.7903	2.8804	2.9980	2.9404	2.8818	0.0895
GPPG3	4.6576	4.4673	4.8836	4.3037	4.7168	4.6058	0.2251
GBTG3	3.1794	3.2868	3.1224	3.0284	2.9717	3.1177	0.1242
GBTG5	3.3316	3.2349	3.2595	3.1413	3.4592	3.2853	0.1187

The result in Figure 30 showed that the composition of SLN influenced release profiles. Moreover, the release profile of GPPG3 was corresponded with entrapment efficiency study. The GPPG3, the lowest entrapment efficiency, was performed the highest release profile. It might be due to more free [6]-gingerol in aqueous dispersion, which freely passed through the membrane, than the highly entrapped formulation. However, the formulations GPPG3, GBTG3 and GPTG5 which the %EE were not significantly different at 88%, 90% and 91%, were performed mark different in release profiles. This data revealed that the composition of SLN influenced the release profiles. For the similar finding, the effect of composition and entrapment efficiency of SLN formulations on release characteristics were also discussed in report of Jain et al (2005).

It was noticed that SLN with poloxamer 188 as stabilizer exhibited higher release profile than formulations with Tween 80 as stabilizer. Similar finding with poloxamer 188, the SLN which composed of poloxamer 407 as a surfactant performed burst release in drug enrich shell model comparable with another formulation (Jansook, 2005). However, the characterization of the drug location needed to be further investigated by NMR technique (Wang, Sun and Zhang, 2002) and also determined by fluorescence and paraelectric spectroscopy (Lombardi, 2005).

In this study, the occluded condition was performed by covering the donor part which was aqueous dispersion system with parafilm. Since the water evaporation was not occurred, the film formation and lipid transformation during experiment were not included in mechanism of drug release, whereas both processes played important roles in the release in vivo. Thus, the discovered result in this study might be attributed to the main mechanism of controlled release of [6]-gingerol which diffused through the lipid carrier (Wissing and Muller, 2002a).

Indeed, the release profiles of [6]-gingerol from SLN formulations showed an interesting biphasic release. Figure 30 shows the in vitro release profile of [6]-gingerol from SLN. There was lag time in the first initial 2 hours. After 2 hours, the release rate increased with time until 12-14 hours following. Afterward, the release rate declined in a steady pattern. This biphasic release was in accordance with the previous study of Pople and Singh (2006) on the release of vitamin A palmitate from SLN produced with compritol. The release pattern of oxybenzone from SLN described by Wissing and Muller, (2002a) also showed an interesting biphasic release with total percentage release of 40% after 24 h.

In case of SLN, the different drug incorporation and release mechanism models were existed (Muller, Mader and Gohla, 2000), the drug-enriched shell model and the drug-enriched core model. In this study, the SLN formulations containing 5% ginger extract with respect to the lipid matrix correspond to the both of drug-enriched shell model and the drug-enriched core model. From the release profiles, it might be interpreted that the high release rate of [6]-gingerol was caused by drug adsorbed on the surface of SLN, while the sustained release rate was corresponded with the diffusion of molecule from the core of lipid.

The release profiles indicated that SLN dispersions showed retarded release of [6]-gingerol from the lipid matrix when compared with acetone extract solution. The sustained release was probably due to diffusion of [6]-gingerol molecules from the lipid matrix. In addition, the highly entrapped [6]-gingerol in solid lipid core was also included in the slow release profiles (20%-30% over 24 h). This finding was similarly observed in release profile of prednisolone from GB-SLN approximately 30 % over 24 h (Muhlen, Schwarz and Mehnert, 1998) and release profiles of clotrimazole approximately 25 % over 24 h (Souto et al., 2004). In this study, the sustained release property of SLN was corresponded with many reports (Pople and Singh, 2006 and Wissing and Muller, 2002a), which revealed that the prolonged drug release could be attributed to embedment of drug in solid lipid matrix.

In order to study the correlation between release profiles and permeation profiles, the formulations which displayed different in release rate constant which showed the highest and the lowest release rate constant were selected to investigate in permeation study. Three formulations, GPPG3, GPTG3 and GPTG5 were chosen to permeation study.

2.9 In vitro permeation study of solid lipid nanoparticles containing *Zingiber officinale* extract

In vitro percutaneous absorption methods have become widely used for measuring the absorption of compounds that come in contact with skin. In this study, the in vitro skin permeation study of different formulations was performed using modified Franz diffusion cell through new born pig skin. New born pig skin was used because it had similar permeation characteristics to human skin in term of lipid composition and hair follicle density (Bronaug, Stewart and Congdon, 1982). However, the mean diameter of hair follicle and thickness of skin are different from human skin (Mestres et al., 2007). To overcome this problem, the new born pig skin was used due to the similarity thickness with human skin (Cilurzo, Minghetti and Sinico, 2007). In order to obtain the acceptability of data from in vitro study, the procedure should simulate in vivo conditions. Franz diffusion apparatus was widely used in permeation study due to the simulation to the in vivo application of topical dosage form. Circular specimen of skin was mounted between donor and receiver compartments with stratum corneum side facing the ambient temperature.

The cumulative amounts of [6]-gingerol permeated through newborn pig skins were plotted as function of time. The permeation rate constant (Flux, J, $\mu g/cm^2 h$) of [6]-gingerol at steady state was calculated from the slope of linear portion of the cumulative amount permeated per unit area versus time plot. The permeation profiles of [6]-gingerol incorporated in SLN formulations are depicted in Figure 33.

For further comparing and understanding the membrane permeability of these formulations, the membrane permeability coefficients (P_{app}, cm/h) were calculated. These coefficients were calculated from the slope, which obtained from the linear plot as in Figures 33. The slopes were divided by the concentration in the donor phase (C_d, $\mu g/ml$) (Reichling et al., 2006). The values of flux and apparent permeation coefficient of [6]-gingerol were calculated accordind to Fick's law of diffusion and are summarized in Table 29.
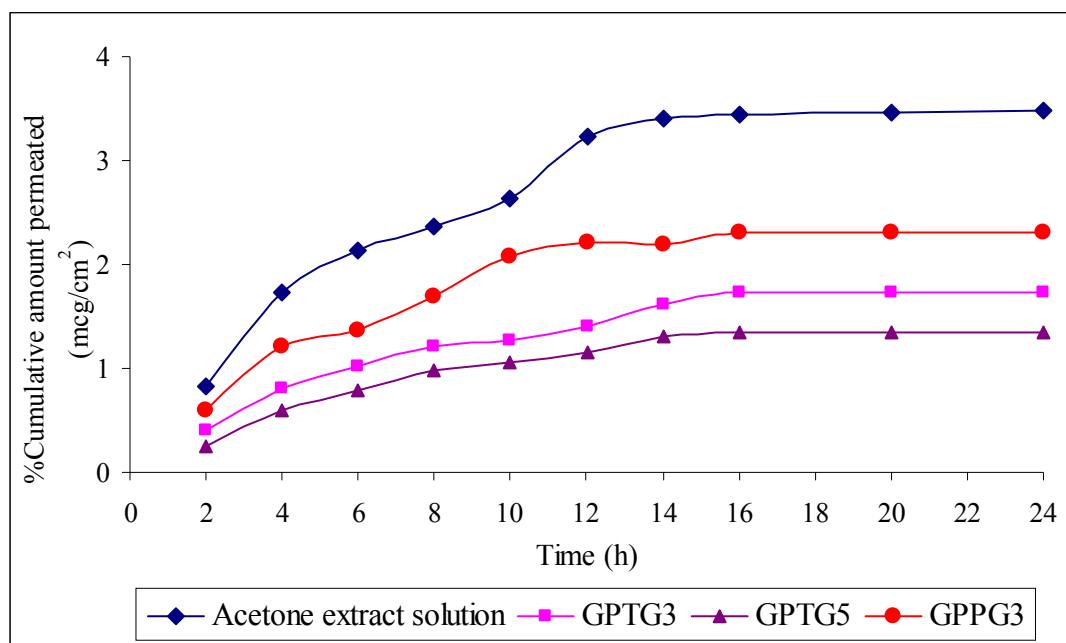
Figure 33 The skin permeation profiles of [6]-gingerol from SLN formulations; GPTG3, GPTG5, GPPG3 and acetone extract solution, (mean ± SD, n=5)

Data from Figure 33 revealed that depending on the composition of SLN, different penetration profiles were obtained. This finding also agreed with the report of penetration profiles of SLN containing flurbiprofen (Jane et al., 2007). However,

The high permeation rate of [6]-gingerol from acetone extract solution due to the significant permeation enhancement effect of solvent ethanol. The permeation result was related to release study that GPPG3 performed the highest release rate and the highest permeation rate. From data obtained in Table 29 and 30, the highest skin permeation rate constant of GPPG3 was found to be 0.1769 $\mu g/cm^2h$ and the permeation rate constant of GPTG3 and GPTG5 were not clearly different at 0.1227 and 0.1270 $\mu g/cm^2h$. In addition, the amount of [6]-gingerol and percentage of [6]-gingerol permeated pig skin also show in Tables 30 and 31. The permeation profile per unit area of [6]-gingerol from SLN are showed in Figure 34.

The small amount of penetrated [6]-gingerol was detected due to the main barrier function of stratum corneum. However, many researches reported that SLN enhance the penetration and transport active substances particularly lipophilic agents (Muller, Radtke and Wissing, 2002; Pople and Singh, 2006; Puglia et al., 2008).

In this study, high permeation rate constant of control was observed and it was higher than permeation rate of [6]-gingerol from SLN formulation. Acetone extract in 80% ethanol was used as control which contained high concentration of alcohol might denature protein in skin and alcohol was well known permeation enhancer. This was the key factor that made control exhibited higher potential in skin delivery than SLN formulation. However, many researches above were used conventional gel or emulsion as control which not had permeation enhancer effect as alcohol, so the permeation rate of SLN higher than control.

After statistical analysis with one-way ANOVA and Duncan test at 5% significant level, there were not significant differences ($P>0.05$) in permeation profiles among varied compositions of SLN dispersions as depicted in Table H5. It might be due to the variation in thickness and number of hair follicle of biological new born pig skin in this experiment.

(a)

(b)

(c)

(d)
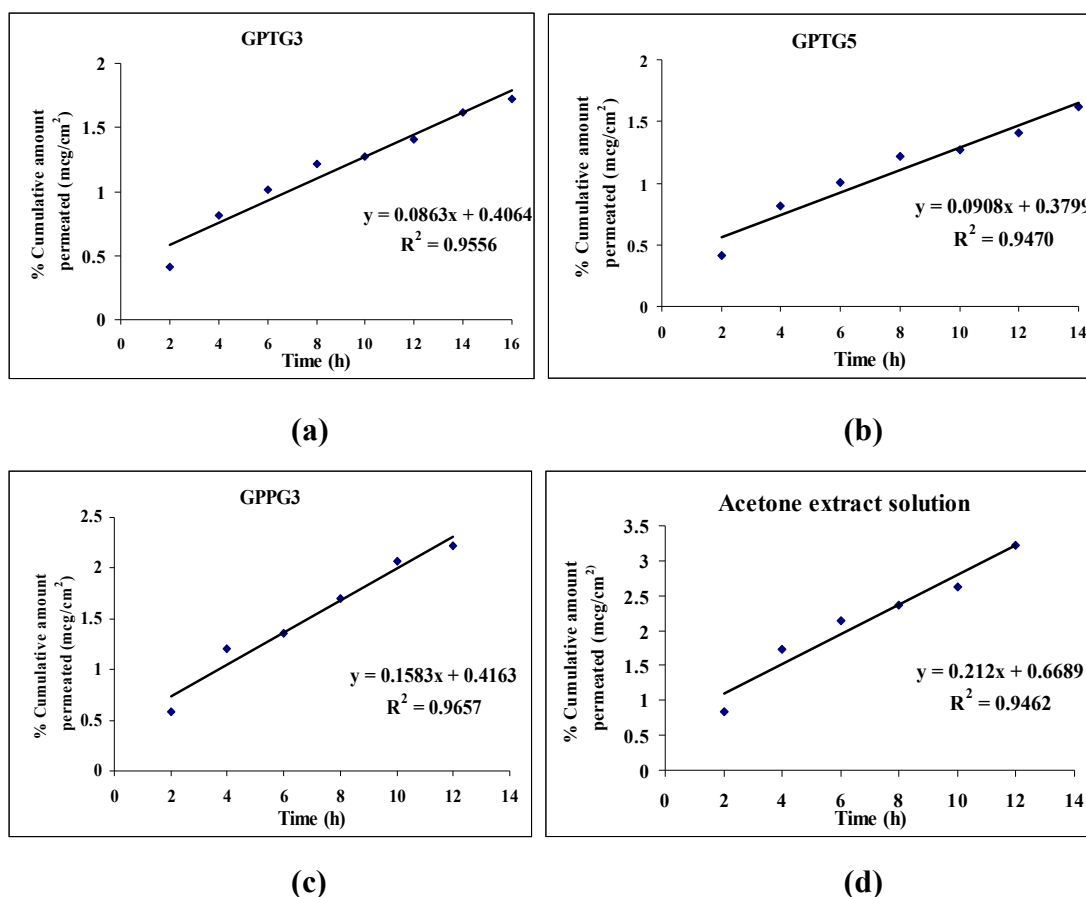
Figure 34 The permeation profile per unit area of [6]-gingerol from (a) GPTG3, (b) GPTG5, (c) GPPG5 and (d) acetone extract solution, (mean ± SD, n=5)

Table 29 The mean values of flux and apparent permeation coefficient of [6]-gingerol from skin permeation profiles of [6]-gingerol

Formulation	Flux (μg/cm^{2}h)	P (cm/h)	SD
GPTG3	0.1227	0.0733	0.0678
GPTG5	0.1270	0.0758	0.0498
GPPG3	0.1769	0.1056	0.0915
acetone extract solution	0.2079	0.1241	0.0991

Table 30 The permeation rate constant of [6]-gingerol from SLN formulations, (n=5)

Formulation	Permeation rate constant (μg/cm^{2}h)					mean	SD
	N1	N2	N3	N4	N5		
GPPTG3	0.0655	0.0391	0.1894	0.2122	0.1073	0.1227	0.0678
GPPTG5	0.0934	0.0487	0.1630	0.1870	0.1427	0.1270	0.0498
GPPPG3	0.0999	0.0539	0.2605	0.2943	0.1760	0.1769	0.0915
Acetone extract	0.0791	0.0962	0.2896	0.3064	0.2681	0.2079	0.0991

Table 31 Amount of [6]-gingerol permeated in pig skin extracted by methanol (n=5)

Formulation	Amount of [6]-gingerol in extracted skin (mcg)					mean	SD
	N1	N2	N3	N4	N5		
GPTG3	1.9995	1.7929	1.7872	1.9528	1.8466	1.8758	0.0959
GPTG5	1.6962	1.7776	1.7337	1.2556	1.9214	1.6769	0.2505
GPPG3	3.9168	3.7408	3.6463	4.6327	5.3364	4.2546	0.7179
Acetone extract	9.8792	10.4554	11.572	13.7346	14.0311	11.9345	1.8828

Table 32 Percentage of [6]-gingerol permeated in pig skin (n=5)

Formulation	Percentage of [6]-gingerol in extracted skin					mean	SD
	N1	N2	N3	N4	N5		
GPTG3	1.1937	1.0704	1.0670	1.1659	1.1024	1.1199	0.0573
GPTG5	1.0127	1.0613	1.0350	0.7496	1.1471	1.0011	0.1496
GPPG3	2.3384	2.2333	2.1769	2.7658	3.1859	2.5401	0.4286
Acetone extract	5.8980	6.2420	6.9087	8.1998	8.3768	7.1251	1.1240

In this study, the cumulative amount of [6]-gingerol permeated from SLN (express as % dose) after 24 h was in range 1-3% and the flux value of [6]-gingerol were in range 0.1227-0.1769 $\mu g/cm^2 h$.

In the permeation process, besides the main mechanism, diffusion through the solid lipid, there were another factors involved in drug penetration. During the experiment, water evaporation occurred in all formulations. This induced lipid transformation of SLN into rigid semisolid gel which induced drug expulsion from stable polymorph of lipid. The film formation on the skin surface also enhanced skin hydration and occluded condition promoted penetration into the deeper skin (Jenning et al., 2000; Wissing and Muller, 2002 and Kumar et al., 2007).

From data in Tables 31 and 32, [6]-gingerol was detected in skin during 24 h. It could be implied that local effect antioxidative property in skin might occurred. However, the further indirect antioxidant evaluation assay needs to confirm this benefit potential.

In general, skin absorption depends on the physicochemical properties of active compound, in particular, molecular weight and lipophilicity. The permeation required both lipid and aqueous solubility (Mestres et al., 2007). The physicochemical properties of [6]-gingerol (MW. 182, log P 1.85) were able to compatible with both aqueous and lipid layer in skin structure. From this result, [6]-gingerol was detected in the receiver compartment. This might be lead to the systemic absorption after permeated through skin layer. However, the benefit effects in systemic absorption of [6]-gingerol were widely investigated and reported in previous chapter. In this study, the systemic inflammatory effect, COX-inhibitor and the important role in photodamage suppressor of [6]-gingerol would be the synergist benefit for skin application. Moreover, the sustained release of [6]-gingerol SLN might effort the free radical scavenging activity over application time.

The existence of stratum corneum reservoir for drugs has been expressed for many years. The skin was recognized to be a depot of skin (Malkinson and Ferguson, 1955). The interaction between drug and skin reservoir was complicated by effects such as binding of drug to keratin in stratum corneum and viable epidermis, lipophilicity of compound and the nature of formulation used (Miselnicky et al., 1988 and Heard and Monk, 2003). This could explain the slow diffusion of drug through the skin and the time to desorb after removal of the application.

From data obtained in this study, it revealed that the application of ginger extract loaded SLN for antioxidative property for skin delivery is feasible due to the interested permeation profiles of [6]-gingerol from SLN dispersions. In addition, [6]-gingerol could be locally distributed in the skin layer. Because of the in vitro study, the realristic factor such as, mechanically apply, dosage form per unit area of skin, the biological systemic clearance of skin were not involved, whereas, it exhibited the important factors for skin delivery. It attributed that the real effect of these preparations as antioxidant for topical preparation needed in vivo further investigations.

CHAPTER V

CONCLUSIONS

The present study was aimed to develop solid lipid nanoparticles containing *Zingiber officinale* extract. The investigation of antioxidative activities of *Zingiber officinale* extract were performed by DPPH and deoxyribose assay. Hot homogenization method was used in SLN production. The composition of SLN formulations and the physicochemical properties of free-SLN and ginger extract loaded SLN were investigated. The results of this study could be concluded as follows:

1. The dark brown resinous viscous liquid of *Zingiber officinale* extract was obtained by maceration. Acetone and ethanol extract were prepared by defatting with hexane and macerating with acetone or 20% ethanol, respectively. The isolated-[6] gingerol extract was obtained by silica gel column chromatography. The [6]-gingerol in crude extract exhibited the same characteristics as standard [6]-gingerol as shown by TLC and HPLC chromatograms.

2. The content of [6]-gingerol in acetone extract and isolated-[6] gingerol extract was not significantly different. The quantitative analysis of [6]-gingerol content in both extracts by UV spectrophotometric method were approximately 68% and 74% w/w, respectively.

3. The hydrogen-donating activities of acetone, ethanol, isolated-[6]-gingerol extracts as well as L-ascorbic acid and α-Tocopherol were determined in term of their DPPH scavenging activities. The DPPH-scavenging activity of acetone and isolated [6]-gingerol extracts were not significantly different and lower than vitamin E and vitamin C, whereas standard [6]-gingerol exhibited the highest scavenging activity. The ethanol extract showed the lowest scavenging activity. Standard [6]-gingerol exhibited the highest antioxidant potency because of the lowest IC_{50} and confirmed that [6]-gingerol was the major antioxidative compound from ginger rhizome. The acetone and isolated [6]-gingerol extracts were quite similar in activity because the radical scavenging activities of extracts were correlated with [6]-gingerol content.

4. The hydroxyl radical scavenging property of acetone, ethanol, isolated-[6]-gingerol extracts and quercetin were evaluated by deoxyribose assay. The hydroxyl scavenging activity of acetone and isolated [6]-gingerol extracts were not significantly different but higher than quercetin, whereas standard [6]-gingerol exhibited the highest scavenging activity. The ethanol extract showed the lowest scavenging activity. It was confirmed that the radical scavenging activities of extracts were correlated with [6]-gingerol content. According to easily obtained by solvent extraction and comparable antioxidative activities with isolated [6]-gingerol extract, the acetone extract of ginger exhibited high potential for loading in the SLN formulations.

5. The solid lipids were evaluated for their potential to solubilize ginger extract. In both molten and solidified state, ginger extract was well soluble in glyceryl palmitostearateate (GP) and glyceryl behenate (GB) and the homogeneous matrix was obtained.

6. Solid lipid nanoparticles (SLN) were prepared from GP and GB as lipids and Tween 80 and Poloxamer 188 as stabilizer by high pressure homogenizer technique and displayed good physical appearances and stability for more than 6 months at storage temperature 4°C. The type of lipid and amount of surfactant influenced the physical stability, particle size and size distribution of free-SLN.

7. The type of lipid, amount of surfactant and lipophilic property of ginger extract influenced the physical stability, particle size and size distribution of ginger extract loaded-SLN. Six formulations which were obviously stable during a period of 2 months of storage at room temperature (25 °C) and at 4 °C were selected for further study, GP-SLN with 3%, 5% Poloxamer 188 or Tween 80 and GB-SLN with 3%,5% Tween 80.

8. The morphological feature of ginger loaded SLN was investigated using TEM. The nanoparticles showed spherical shaped and homogenous in size distribution and showed no change during 2 months storage. The particle sizes were approximately around 200-300 nm which correlated with particle size measurement by PCS.

9. The SLN prepared by hot high pressure homogenization gave high entrapment efficiency (EE) of [6]-gingerol. The type and amount of surfactant affected loading capacity of SLN. Although %EE values decreased with an increase of storage duration, the acceptable %EE was obtained in all formulation, 78.91-93.26%.

10. All formulations of loaded SLN dispersion had reduction in enthalpy and width in melting range comparable with bulk solid lipid, GP and GB. The increasing melting range could be correlated with the impurities or less ordered crystal. Comparing to the formulation of at freshly prepared GP-SLN and GB-SLN, the melting range of SLN were broadening with increasing storage time. It also demonstrated the modification of lipid.

11. In both GP-SLN and GB-SLN, lipid transformation from β' form to more stable β form during storage time was demonstrated. The more ordered lattice leaded to the expulsion of loaded ginger extract. This finding was correlated with the entrapment efficiency study.

12. The release profiles of [6]-gingerol from SLN formulations were best fit into the Higuchi equation which described the diffusion of drug from homogeneous and granular matrix system. The release profiles indicated that SLN dispersions showed retarded release of the [6]-gingerol from the lipid matrix when compared with acetone extract solution. The sustained release was probably due to diffusion of [6]-gingerol molecules from the lipid matrix.

13. The permeation profiles of [6]-gingerol incorporated in SLN formulations were corresponded with the release study. GP-SLN with 3% P188 exhibited the highest skin permeation rate constant which was found to be 0.1583 $\mu g/cm^2h$. The cumulative amount of [6]-gingerol was detected in pig skin (expressed as % dose) after 24 h was in range 2.54±0.43%. It could be implied that local antioxidative effect in skin might occurred. In the permeation process, it was influenced by many mechanisms involved in drug penetration, such as diffusion through the solid lipid, lipid transformation induced by water evaporation, enhanced skin hydration, which promoted penetration into the deeper skin.

REFERENCES

Altman, R.D. and Marcussen, K.C. 2001. Effects of a ginger extract on knee pain in patients with osteoarthritis. Arthritis and Rheumatism 44: 2531–2538.

Andreassi, M. and Andreassi, L. 2004. Antioxidants in dermocosmetology: from the laboratory to clinical application. Journal of Cosmetic Dermatology 2: 153-160.

Antipenko, A.Y., Spielman, A.I. and Kirchberger, M.A. 1999. Interactions of [6]-gingerol and ellagic acid with the cardiac sarcoplasmic reticulum Ca^{++}-ATPase. Journal of Pharmacology and Experimental Therapy 290: 227– 234.

Ardestani. A, and Yazdanparast, R. 2006. Antioxidant and free radical scavenging potential of *Achillea santolina* extracts. Food Chemistry 92: 111-119.

Bernstein, E.F., Chen, Y.Q. and Tamai, K. 1994. Enhanced elastin and fibrillin gene expression in chronically photodamaged skin. Journal of Invest Dermatology 103: 182–186.

Bernstein, E.F., Brown, D.B., Schwartz, M.D., Kaidbey, K., Ksenzenko, S.M. 2004. The polyhydroxy acid gluconolactone protects against ultraviolet radiation in an in vitro model of cutaneous photoaging. Dermatological Surgery 30:189-196.

Bronaug, R. L., Stewart, R. F. and Congdon, E. 1982. Method for in vitro percutaneous absorption studies II. Animal model for human skin. Toxicology Apply and Pharmacology 62: 481-488.

Bode, A.M., Ma, W.-Y., Surh, Y.-J. and Dong, Z. 2001. Inhibition of epidermal growth factor-induced cell transformation and activator protein-1 activation by [6]-gingerol. Cancer Research 61: 850–853.

Bondet, V., Williams, W. B. and Berset, C. 1997. Kinetics and mechanisms of antioxidant activity using the DPPH• free radical method. LWT 30(6): 609-615.

Bunjes, H., Westesen, K. and Koch, MHJ. 1996. Crystallization tendency and polymorphic transitions in triglyceride nanoparticles. International Journal of Pharmaceutics. 129: 159–75.

Bunjes, H., Drechsler, M., Koch, M.H.J. and Westesen, K. 2001. Incorporation of the model drug ubidecarenone into solid lipid nanoparticles. Pharmaceutical Research.18: 287–293.

Careddu, P. 1999. Motion sickness in children: results of a double-blind study with ginger (Zintona,) and dimenhydrinate. Healthnotes Reviews 6: 102-107.

Castro, I. A., Rogero, M. M., Junqueira, R. M. and Carrapeiro, M. M., 2006. 2,2 -Diphenyl-1-picrylhydrazil free radical scavenging activity of antioxidant mixtures evaluated by response surface methodology. International Journal of Food Science and Technology. 41 (Supplement 1): 59–67.

Cilurzo, F., Minghetti, P. and Sinico, C. 2007. Newborn pig skin as model membrane in in vitro drug permeation studies: A technical note. AAPS PharmSciTech 8(4): E1-E4.

Connell, D.W. and McLachlan, R. 1972. Natural pungent compounds: examination of gingerols, shogaols, paradols and related compounds by thin-layer and gas chromatography. Journal of Chromatography 67: 29–35.

Darr, D, Combs, S., Dunston, S., Manning, T. and Pinnell, S. 1992. Topical vitamin vitamin C protects porcine skin from ultraviolet radiation-induced damage. British Journal of Dermatology 127: 247-253.

Dedov, V.N., Tran, V.H., Duke, C.C., Connor, M., Christie, M.J., Mandadi, S. and Roufogalis, B.D. 2002. Gingerols: a novel class of vanilloid receptor (VR1) agonists British Journal of Pharmacology 137: 793 – 798.

Eldem, T., Speiser, P. and Altorfer, H. 1991. Polymorphic behavior of sprayed lipid micropellets and its evaluation by differential scanning calorimetry and scanning electron microscopy. Pharmaceutical Research 8:178–84.

Elmets, C.A., Singh, D., Tubesing, K., Matsui, M., Katiyar, S. and Mukhtar, H. 2001. Cutaneous photoprotection from ultraviolet injury by green tea polyphenols. Journal of American Acadamy of Dermatology 44: 425-432.

Farsam, H., Amanlou, M., Dehpour, A.R. and Jahaniani, F. 2000. Antiinflammatory and analgesic activity of Biebersteinia multifida DC. Root [6]-gingerol. Journal of Ethnopharmacology 71: 443–447.

Freitas, C. and Muller, R.H. 1998 Effect of light and temperature on zeta potential and physical stability in solid lipid nanoparticle (SLN) dispersions. International Journal of Pharmaceutics.168: 221–229.

Freitas, C. and Muller, R.H. 1999. Correlation between long-term stability of solid lipid nanoparticles (SLN) and crystallinity of the lipid phase. European Journal of Pharmaceutics and Biopharmaceutics 47: 125–132.

Frisbee, S.E. and McGinity, J.W. 1994. Influence of nonionic surfactants on the physical and chemical properties of a biodegradable pseudolatex. European Journal of Pharmaceutics and Biopharmaceutics 40: 355-363.

Ghayur, M.N.and Gilani, A.H. 2005. Ginger lowers blood pressure through blockade of voltage-dependent calcium channels. Journal of Cardiovascular Pharmacology 45: 74– 80.

Ghayur, M.N. and Gilani, A.H. 2006. Species differences in the prokinetic effects of ginger. International Journal of Food Sciences and Nutrition 57: 65-73.

Gilchrest, B.A. 1996. A review of skin ageing and its medical therapy. British Journal of Dermatology.135: 867–875.

Govindarajan, V., 1982. Ginger-chemistry technology and quality evaluation: Part-I CRC. Critical Reviews in Food Science and Nutrition. 17: 1–96.

Guh, J.H., Ko, F.N., Jong, T.T. and Tenf, C.M. 1995. Antiplatelet effect of gingerol isolated from *Zingiber officinale*. Journal of Pharmacy and Pharmacology 47:329–332.

Halliwell, B.,Gutteridge, J.M.C., and Aruoma, O.I. 1987. The deoxyribose method: A simple "test-tube" assay for determination of rate constants for reaction of hydroxyl radicals. Analytical Biochemistry. 165: 215-219.

Halliwell,B., Aeschbach, R., Loliger, J. and Aruoma, O.I. 1995. The characterization of antioxidant. Food Chemistry and Toxicity 33(7): 601-617.

Harland, R.S. and Peppas, N.A. 1993. Drug transport in and release from controlled delivery devices of hydrophilic/hydrophobic block and graft copolymers. European Journal of Pharmaceutics and Biopharmaceutics 39: 229-233.

Hata, T.R., Scholz, T.A., Ermakov, I.V., McClane, R.W., Khachik, F. and

Gellermann, W. 2000. Non-invasive raman spectroscopic detection of carotenoids in human skin. Journal of Invest Dermatology 115: 441-448.

He, X., Matthew, W.B., Lian, L., and Lin, L. 1998. High–performance liquid chromatography-electrospray mass spectrometric analysis of pungent constituents of ginger. Journal of Chromatography A 796 : 327-334.

Heard, C. M., Monk. B. V. and Modley, A. J. 2003. Binding of primaquine to epidermal membranes and keratin. International Journal of Pharmaceutics. 257: 237-244.

Heiati, H., Tawashi, R. and Phillips, N.C. 1998. Drug retention and stability of solid lipid nanoparticles containing azidothymidine palmitate after autoclaving, storage and lyophilization. Journal of Microencapsulation. 15:173–84.

Heurtault, B., Sualnier, P., Pech, B., Proust, J. E. and Benoit, J. P. 2003. Physico-chemical stability of colloidal lipid particles. Biomaterials 24: 4283-4300.

Hong, C.H., Hur, S.K., Oh, O.-J., Kim, S.S., Nam, K.A., Lee and S.K. 2002. Evaluation of natural products on inhibition of inducible cyclooxygenase (COX-2) and nitric oxide synthase (iNOS) in cultured mouse macrophage cells. Ethnopharmacology 83, 153–159.

Hruza, L.L. and Pentland, A.P. 1993. Mechanisms of UV-induced inflammation. Journal of Invest Dermatology 100: 35S–41S.

Ippoushi, K., Azuma, K., Ito, H., Horie, H., and Higashio, H. 2003. 6-Gingerol inhibit nitric oxide synthesis in activated J774.1 mouse macrophages and prevent peroxynitrite-induced oxidation and nitration reactions. Life Science. 73: 3427-3437

Jane, S. K., Chourasia, M. K., Masuriha, R., Soni, V., Jain, A., Jain, N. K. and Gupta, Y. 2005. Solid lipid nanoparticles bearing Flurbiprofen for transdermal delivery. Drug Delivery 12: 207-215.

Jansook Phasavee. 2005. Development of solid lipid nanoparticles and nanostructured lipid carriers containing amphotericin B. Master's Thesis. Department of Manufacturing Pharmacy, Faculty of Pharmaceutical Science, Chulalongkorn University.

Jenning, V. and Gohla, S. 2000. Comparison of wax and glyceride solid lipid nanoparticles (SLN®). International Journal of Pharmaceutics 196: 219–222.

Jenning, V., Gysler, A., Schafer, M.K. and Gohla, S. 2000a. Vitamin A loaded solid lipid nanoparticles for topical use: occlusive properties and drug targeting to the upper skin. European Journal of Pharmaceutics and Biopharmaceutics. 49: 211–218.

Jenning, V., Mader, K.and Gohla, S. 2000b. Solid lipid nanoparticles (SLN) based on binary mixtures on liquid and solid lipid: a(1)H-NMR study. International Journal of Pharmaceutics. 205: 15-21.

Jenning, V., Schafer, M. K.and Gohla, S. 2000c. Vitamin A-loaded solid lipid nanoparticles for topical use: drug release properties. Journal of Controlled Release 66: 115–126.

Jenning, V. Thunemann, A. F. and Gohla, S. 2000d. Characterization of a novel solid lipid nanoparticles carrier system based on binary mixtures on liquid and solid lipids. International Journal of Pharmaceutics. 199: 167-177.

Jenning, V. and Gohla, S. 2001. Encapsulation of retinoids in solid lipid nanoparticles (SLN). Journal of Microencapsulation. 18: 149–158.

Jenkins, G. 2002. Molecular mechanisms of skin ageing. Mechanisms of Ageing and Development 123: 801–810.

Jolad, S.D., Lantz, R.C., Solyom, A.M., Chen, G.J., Bates, R.B. and Timmermann, B.N. 2004. Fresh organically grown ginger (*Zingiber officinale*): composition and effects on LPS-induced PGE2 production. Phytochemistry 65: 1937-1954.

Jurkiewicz, B.A., Bissett, D.L. and Buettner, G.R. 1995 Effect of topically applied tocopherol on ultraviolet radiation-mediated free radical damage in skin. Journal of Invest Dermatology 104: 484-488.

Kapoor, L.D. 2001. Handbook of Ayurvedic Medicinal Plants CRC Press, New York, USA, pp 341-342.

Keithahn, C. and Lerchl, A. 2005. 5-Hydroxytryptophan is a more potent in vitro hydroxyl radical scavenger than melatonin or vitamin C. Journal of Pineal Research 38: 62-66.

Kim, J.K., Kim, Y., Na, K.M., Surh, Y.J., and Kim, T.Y., 2007. [6]-Gingerol prevents UVB-induced ROS production and COX-2 expression in vitro and in vivo. Free Radical Research. 41(5): 603–614

Kim, E.C., Min, J.K., Kim, T.Y., Lee, S.J., Yang, H.O., Han, S., Kim, Y.M. and Kwon, Y.G. 2005. [6]-Gingerol, a pungent ingredient of ginger inhibits angiogenesis in vitro and in vivo. Biochemical and Biophysical Research Communications 335: 300–308.

Koo, K.L.K., Ammit, A.J., Tran, V.H., Duke, C.C. and Roufogalis, B.D. 2001. Gingerols and related analogues inhibit arachidonic acid-induced human platelet serotonin release and aggregation. Thrombosis Research 103: 387–397.

Kristl, J., Volk, B., Gasperlin, M., Sentjurc, M. and Jurkovic, P. 2003. Effect of colloidal carriers on ascorbyl palmitate stability. European Journal of Pharmaceutics and Biopharmaceutics. 19: 181–189.

Kumar, A.S., Abhijit, A.D., Medha, D.J. and Vandana, B.P. 2007. Solid lipid nanoparticles (SLN) of tretinoin: Potential in topical delivery. International Journal of Pharmaceutics. 350: 11-21.

Lantz, R.C., Chen, G.J., Sarihana, M., Solyom, A.M., Jolad, S.D., and Timmermann, B.N. 2007. The effect of extracts from ginger rhizome on inflammatory mediator production. Phytomedicine 14:123-128

Lin, J.Y., Selim, M.A., Shea, C.R., Grichnik, J.M., Omar, M.M., and Monteiro-Riviere, N.A. 2003. UV photoprotection by combination topical antioxidants vitamin C and vitamin E. Journal of American Acadamy of Dermatology.48(6): 866-874.

Lippacher, A., Muller, R.H., Mader, K., 2000. Investigation on the viscoelastic properties of lipid based colloidal drug carriers. International Journal of Pharmaceutics 196: 227–230.

Lippacher, A., Muller, R.H., Mader, K., 2001. Preparation of semisolid drug carriers for topical application based on solid lipid nanopaeticles. International Journal of Pharmaceutics 214: 9-12.

Leccia, M.T, Yaar, M., Allen, N., Gleason, M. and Gilchrest, B.A. 2001. Solar simulated irradiation modulates gene expression and activity of antioxidant enzymes in cultured human dermal fibroblasts. Experimental Dermatology 10: 272-279.

Lee, J., Koo, N. and Min, D.B. 2004. Reactive oxygen species, aging, and antioxidative nutraceutical. Comprehensive Reviews of Food Sciences and Food Safety 3: 21-33.

Lee, Y. L., Yang, J.H., and Maua, J.L., 2008. Antioxidant properties of water extracts from Monascus fermented soybeans. Food Chemistry. 106: 1128–1137.

Lombardi, B.S. 2005. Lipid nanoparticles for skin penetration enhancement-correlation to drug localization within the particle matrix as determined by fluorescence and paraelectric spectroscopy. Journal of Controlled Release. 110: 151-163.

Lukowski, G., Kasbohm, J., Pflegel, P., LLLing, A. and Wulff, H. 2000. Crystallographic investigation of cetylpalmitate solid lipid nanoparticles. International Journal of Pharmaceutics 196: 201-205.

Ma, Q.H., Xia, Q., Lu, Y.Y., Hao, X.Z., Gu, N., Lin, X.F. and Luo, D. 2007. Preparation of tea polyphenols-loaded solid lipid nanoparticles based on the phase behaviors of hot microemulsions. Solid State Phenomena 121-123: 705-708.

Mahady, G.B., Pendland, S.L., Yun, G.S., Lu, Z.Z. and Stoia, A., 2003. Ginger (Zingiber officinale Roscoe) and the gingerols inhibit the growth of Cag A$^+$ strains of Helicobacter pylori. Anticancer Research 23: 3699–3702.

Malkinson, F. D. and Ferguson, E. H. 1955. Percutaneous absorption of hydrocortisone-4-C14 in two human subjects. Journal of Invest Dermatology. 25: 281-283.

Mathew, S. and Abraham, T. E. 2006 In vitro antioxidant activity and scavenging effects of *Cinnamomum verum* leaf extract assayed by different methodologies. Food and Chemical Toxicology . 44: 198–206.

Mehnert, W. and Mader, K. 2001. Solid lipid nanoparticles-Production, characterization and applications. Advanced Drug Delivery Reviews 47: 165-196.

Mestres, G. M., Mestres, J. P., Bres, J., Martin, S., Ramos, J. and Vian, L. 2007. The in vitro percutaneous penetration of three antioxidants compound. International Journal of Pharmaceutics 331: 139-144.

Miselnicky, S. R., Lichtin, J. L., Sakr, A. and Bronaugh, R. L. 1988. The influence of solubility, protein binding and percutaneous absorption on reservoir formation in skin. Journal of Social Cosmetic Chemistry 39(3): 169-177.

Muhlen, A. and Mehnert, W. 1998. Drug release and release mechanism of prednisolone loaded solid lipid nanoparticles. Pharmazie 53: 552.

Muhlen, A., Schwarz, C., Mehnert, W. 1998. Solid lipid nanoparticles (SLN) for controlled drug delivery: drug release and release mechanism. European Journal of Pharmaceutics and Biopharmaceutics 45: 149–155.

Muller, R.H., Mehnert, W., Lucks, J.S., Schwarz, C., Muhlen, A., Weyhers, H., Freitas, C. and Ruhl, D. 1995 Solid lipid nanoparticles (SLN) – an alternative colloidal carrier system for controlled drug delivery. European Journal of Pharmaceutics and Biopharmaceutics. 41: 62-69.

Muller, R.H, Ruhl, D., Runge, S., and Mehnert, W. 1997. Cytotoxicity of solid lipid nanoparticles as a function of the lipid matrix and the surfactant. Pharmaceutical Research 14(4): 458-460.

Muller, R.H. and Dingler, A. 1998. The next generation after the liposomes: solid lipid nanoparticles (SLN, Lipopearls) as dermal carrier in cosmetics. Eurocosmetics 7–8: 19– 26.

Muller, R. H. , Lippacher, A. and Gohla, S. 2000. Solid lipid nanoparticles (SLN) as a carrier system for the controlled release of drugs. Handbook of Pharmaceutical Controlled Release Technology Marcel Dekker, New York, USA. pp. 377-392.

Muller, R.H., Mader, K. and Gohla, S. 2000. Solid lipid nanoparticles (SLN) for controlled active delivery – a review of the state of art. European Journal of Pharmaceutics and Biopharmaceutics. 50: 161–177.

Muller, R.H., Radtke, M. and Wissing, S.A. 2002. Solid lipid nanoparticles (SLN) and nanostructured lipid carriers (NLC) in cosmetic and dermatological preparations. Advanced Drug Delivery Reviews. 54(1): S131–S155.

Nagasawa, H., Watanabe, K. and Inatomi, H. 2002. Effects of bitter melon (Momordica charantia l.) or ginger rhizome (Zingiber offifinale rosc) on spontaneous mammary tumorigenesis in SHN mice. American Journal of Chinese Medicine 30: 195–205.

Pandey, N., Chaurasia, J.K., Tiwari, O.P., Tripathi, Y.B. 2007. Antioxidant properties of different fractions of tubers from *Pueraria tuberosa* Linn. Food Chemistry 101: 215-218.

Park, K.K., Chun, K.S., Lee, J.M., Lee, S.S., and Surh, Y.J. 1998. Inhibitory effects of [6]-gingerol, a major pungent principle of ginger, on phorbol ester-induced inflammation, epidermal ornithine decarboxylase activity and skin tumor promotion in ICR mice. Cancer Letters. 129: 139–144.

Phillips, S., Ruggier, R. and Hutchinson, S.E. 1993. *Zingiber officinale* (Ginger) – an antiemetic for day case surgery. Anaesthesia 48: 715-717.

Pinnell, S. R. 2003. Cutaneous photodamage, oxidative stress, and topical antioxidant protection. Journal of American Acadamy of Dermatology 48(1): 1-13.

Pople, P.V. and Singh, K.K. 2006. Development and evaluation of topical formulation containing solid lipid nanoparticles of vitamin A. AAPS Pharmaceutical Science Technology 7: 91.

Puglia, C., Blasi, P., Rizza, L., Schoubben, A., Bonona, F., Rossi, c. and Ricci, M. 2008. Lipid nanoparticles for prolonged topical delivery: an in vitro and in vivo investigation. International Journal of Pharmaceutics 357: 295-304.

Rabe, J.H., Mamelak, A.J., McElgunn, P.J.S., Morison, W.L. and Sauder, D.N. 2006. Photoaging: Mechanisms and repair. Journal of American Acadamy of Dermatology 55(1): 1-13.

Reichling, J., Landvatter, U., Wagner, H., Kostka, K. H. and Schaefer, F. 2006. In vitro release and human skin permeation of Australian teas tree oil (TTO) from topical formulations. European Journal of Pharmaceutics and Biopharmaceutics. 64: 222-228.

Riebenfeld, D and Borzone, L. 1999. Randomized double-blind study comparing ginger (Zintona,) and dimenhydrinate in motion sickness. Healthnotes Reviews 6: 98-101.

Saliou, C., Rimbach, G., Moini, H., McLaughlin, L., Hosseini, S., Lee, J., Watson, R.R. and Packer, L. 2001. Solar ultraviolet-induced erythema in human skin and nuclear factor-kappa-B dependent gene expression in keratinocytes are modulated by a French maritime pine bark extract. Free Radical and Biological Medicine 30: 154–160.

Sato, K. and Garti, N. 1988. Crystallization and polymorphism of fats and fatty acids. Marcel Dekker, New York, USA. pp. 3–87.

Schwarz, C., Mehnert, W., Lucks, J.S. and Muller, R.H. 1994. Solid lipid nanoparticles (SLN) for controlled drug delivery. I. Production, characterization and sterilization Journal of Controlled Release 30: 83-96.

Shibata, M., Ohkubo, T., Takahashi, H. and Inoki, R. 1989. Modified formalin test: characteristic biphasic pain response. Pain 38: 347–352.

Shindo, Y., Witt, E., Han, D., Epstein, W. and Packer, L. 1994. Enzymic and non-enzymic antioxidants in epidermis and dermis of human skin. Journal of Invest Dermatology 102:122-124.

Siekmann, B. and Westesen, K. 1992. Submicron-sized parenteral carrier systems based on solid lipids. Pharmacy and Pharmacology Letter 1: 123–126.

Siekmann, B. and Westesen, K. 1994a. Electron-microscopic characterization of melt-homogenised solid lipid nanoparticles. European Journal of Pharmaceutics Sciences. 2: 190.

Siekmann, B. and Westesen, K. 1994b. Thermoanalysis of the recrystallization process of melt-homogenized glyceride nanoparticles. Colloids and Surface sciences B. 3: 159–175.

Singh, R., Singh, S., Kumar, S. and Arora, S. 2007. Free radical-scavenging activity of acetone extract/fractions of *Acacia auriculiformis* A. Cunn. Food Chemistry 100: 1509-1516

Singla, A.K., Garg, A. and Aggarwal, D. 2002. Paclitaxel and its formulations. International Journal of Pharmaceutics 235: 179-192.

Sjostrom, B. and Bergenstahl, B. 1993. Preparation of submicron drug particles in lecithin-stabilized o/w emulsions. I. Model studies of the precipitation of cholesteryl acetate International Journal of Pharmaceutics. 88: 53–62.

Souto, E. B., Wising, S. A., Barbosa, C. M. and Muller, R. H. 2004. Development of a controlled release formulation based on SLN and NLC for topical clotrimazole delivery. International Journal of Pharmaceutics 278: 71-77.

Souto, E.B., Muller, R.H. and Gohla, S. 2005. A novel approach based on lipid nanoparticles (SLN®) for topical delivery of *a*-lipoic acid. Journal of microencapsulation. 22(6): 581–592.

Souto, E. B., Mehnert, W. and Muller, R. H. 2006. Polymorphic behavior of Compritol® 888 ATO as bulk lipid and as SLN and NLC. Journal of Microencapsulation 23(4): 417-433.

Souto, E. B. and Muller, R. H. 2008. Cosmetic features and applications of lipid nanoparticles (SLN®, NLC®). International Journal of Cosmetic Science 30: 157–165.

Stoilova, I., Krastanov, A., Stoyanova, A, and Denev, P. 2006. Antioxidant activity of a ginger extract (*Zingiber officinale*). Food Chemistry.107: 1-7.

Surh, Y.J., Park, K.K., Chun, K.S., Lee, L.J., Lee, E. and Lee, S.S. 1999. Anti-tumor-promoting activities of selected pungent phenolic substances present in ginger. Journal of Environmental Pathologyb Toxicology and Oncology 18: 131–139.

Takahashi, T., Okamoto, T., Mori, K., Sayom H, and Kishi, T. 1993. Distribution of ubiquinone and ubiquinol homologues in rat tissues and subcellular fractions. Lipids 28: 803

Teeranachaideekul, V., Muller, R.H. and Junyaprasert, V.B. 2007a. Encapsulation of ascorbyl palmitate in nanostructured lipid carriers (NLC)-effects of formulation parameters on physicochemical stability. International Journal of Pharmaceutics. 340: 198–206.

Teeranachaideekul, V., Souto, E.B., Junyaprasert, V.B. and Muller, R.H. 2007b. Cetyl palmitate-based NLC for topical delivery of Coenzyme Q(10) - development, physicochemical characterization and in vitro release studies. European Journal of Pharmaceutics and Biopharmaceutics. 67: 141–148.

Tiwari, O.P., Tripathi Y.B. 2007. Antioxidant properties of different fractions of *Vitex negundo* Linn. Food Chemistry 100: 1170-1176.

Tjendraputra, E.N., Tran, V.H., Brenan, D.L., Roufogalis, B.D. and Duke, C.C. 2001.

Effect of Ginger Constituents and Synthetic Analogues on Cyclooxygenase-2 Enzyme in Intact Cells <u>Bioorganic Chemistry</u> 29:156–163.

Tjendraputra, E.N., Ammit, A.J., Roufogalis, B.D., Tran, V.H., and Duke, C.C. 2003. Effective anti-platelet and COX-1 enzyme inhibitors from pungent constituents of ginger. <u>Thrombosis Research</u> 111: 259–265.

Tjolsen, A., Berge, O.G., Hunskaar, S., Rosland, J.H. and Hole, K. 1992. The formalin test: an evaluation of the method. <u>Pain </u>51: 5–17.

Valko, M., Leibfritz, D., Moncol, J., Cronin, M.T.D., Mazur, M. and Telser, J. 2007. Free radicals and antioxidants in normal physiological functions and human disease The International Journal of Biochemistry & Cell Biology 39: 44–84.

Varani, J., Spearman, D., Perone, P., Fligiel, S.E., Datta, S.C., Wang, Z.Q., Shao, S., Fisher, G.J. and Voorhees, J.J., 2001. Inhibition of type I procollagen synthesis by damaged collagen in photoaged skin and by collagenase-degraded collagen in vitro. <u>American Journal of Pathology.</u> 158: 931–942.

Vile, G.F. and Tyrrell, R.M. 1995. UVA radiation-induced oxidative damage to lipids and proteins in vitro and in human skin fibroblasts is dependent on iron and singlet oxygen. <u>Free Radical and Biological Medicine</u> 18: 721–730.

Vivek, K., Reddy, H. and Murthy, R.S.R. 2007. Investigations of the effect of the lipid matrix on drug entrapment, in vitro release, and physical stability of olanzapine-loaded solid lipid nanoparticles. <u>AAPS PharmSciTech</u> 8(4): E1-E9.

Vringer, T. 1992. Topical preparation containing a suspension of solis lipid particles. European Patent Application No.91200664.

Vutyavanich, T., Kraisarin, T. and Ruangsri, R. 2001. Ginger for nausea and vomiting in pregnancy: randomized, double-masked, placebo-controlled trial. <u>Obstetic Gynecology</u> 97: 577-582.

Wang, J. X., Sun, X. and Zhang, Z. R. 2002. Enhance brain targeting by synthesis of 3' 5'- Dioctanoyl -5- fluoro – 2' – deoxuridine and incorporation into solid lipid nanoparticles. <u>European Journal of Pharmaceutics and Biopharmaceutics</u>. 54: 285-290

Westesen, K., Siekmann, B. and Koch, M.H.J. 1993. Investigations on the physical state of lipid nanoparticles by synchrotron radiation X-ray diffraction. <u>International Journal of Pharmaceutics</u>. 93: 189-199.

Westesen, K. and Bunjes, H. 1995. Do nanoparticle prepared from lipids solid at room temperature always posses a solid lipid matrix. International Journal of Pharmaceutics. 115: 129-131.

Westesen, K. and Siekmann, B. 1997. Investigation of the gel formation of phospholipid-stabilized solid lipid nanoparticles. International Journal of Pharmaceutics. 151: 35–45.

Wissing, S.A. and Müler, R.H. 2001a. A novel sunscreen system based on tocopherol acetate incorporated into solid lipid nanoparticles (SLN). International Journal of Cosmetic Science. 23: 233–243.

Wissing, S.A. and Muller, R.H. 2001b. Solid lipid nanoparticles (SLN_)—a novel carrier for UV blockers. Pharmazie 56: 783–786.

Wissing, S.A.and Muller, R.H., 2002a. Solid lipid nanoparticles as carrier for sunscreen: in vitro release and in vivo skin permeation. Journal of Controlled release 81: 225-233.

Wissing, S.A.and Muller, R.H., 2002b.The influence of the crystallinity of lipid nanoparticles on their occlusive properties. International Journal of Pharmaceutics. 242: 377–379.

Wissing, S.A. and Müller, R.H. 2003a. Cosmetic applications for solid lipid nanoparticles (SLN). International Journal of Pharmaceutics 254: 65–68

Wissing, S.A. and Muller, R.H. 2003b. The influence of solid lipid nanoparticles (SLN) on skin hydration and viscoelasticity: in vivo study. European Journal of Pharmaceutics and Biopharmaceutics 56: 67-72.

Worle, G., Siekmann, B. and Bunjes, H. 2006. Effect of drug loading on the transformation of vesicular into cubic nanoparticles during heat treatment of aqueous monoolein/poloxamer dispersions. European Journal of Pharmaceutics and Biopharmaceutics. 63: 128–133.

Xu, G., Liu, D., Chen, J., Ye, X., Maa, Y., and Shi, J. 2008. Juice components and antioxidant capacity of citrus varieties cultivated in China. Food Chemistry. 106: 545–551.

Yamahara, J., Mochizuki, M., Rong, H.Q., Matsuda, H. and Fujimura, H., 1988. The anti-ulcer effect in rats of ginger constituents. Journal of Ethnopharmacology 23: 299–304.

Yamamoto, Y. 2001. Role of active oxygen species and antioxidants in photoaging. Journal of Dermatological Science 27(1): S1– S4.

Yildirim, A., Mavi, A., Oktay, M., Kara, A.A., Algur, O.F. and Bilaloglu, V. 2000. Comparison of antioxidant and antimicrobial activities of tilia (*Tilia argentea*), sage (*Salvia triloba* L.) and black tea (*Camellia sinensis*) extracts. Journal of Agricultural and Food Chemistry 48: 5030-5034.

Yoshimi, N., Wang, A., Morishita, Y., Tanaka, T., Sugie, S., Kawai, K., Yamahara, J. and Mori, H. 1992. Modifying effects of fungal and herb metabolites on azoxymethane-induced intestinal carcinogenesis in rats. Japanese Journal of Cancer Research 83: 1273–1278.

Young, H.Y., Luo, Y.L., Cheng, H.Y., Hsieh, W.C., Liao, J.C., and Peng, W.H. 2005. Analgesic and anti-inflammatory activities of [6]-gingerol. Journal of Ethnopharmacology. 96:207–210

Appendix A

Preliminary study
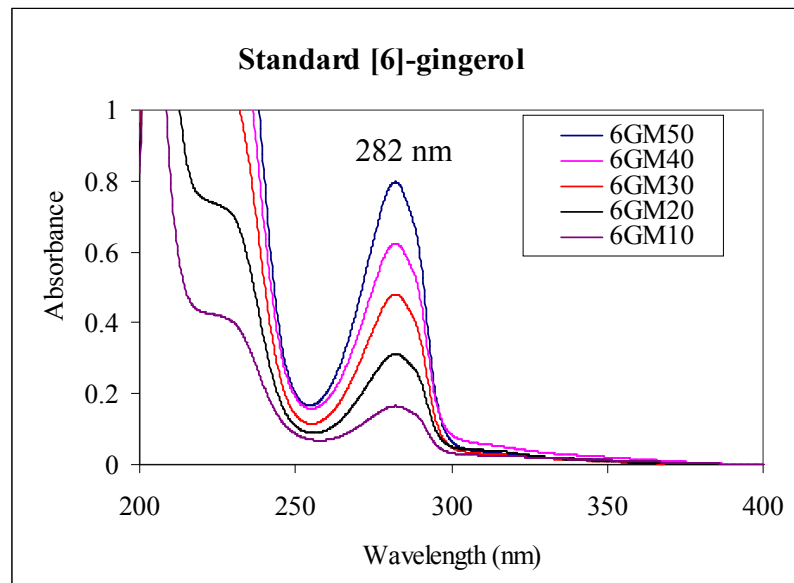
(a)
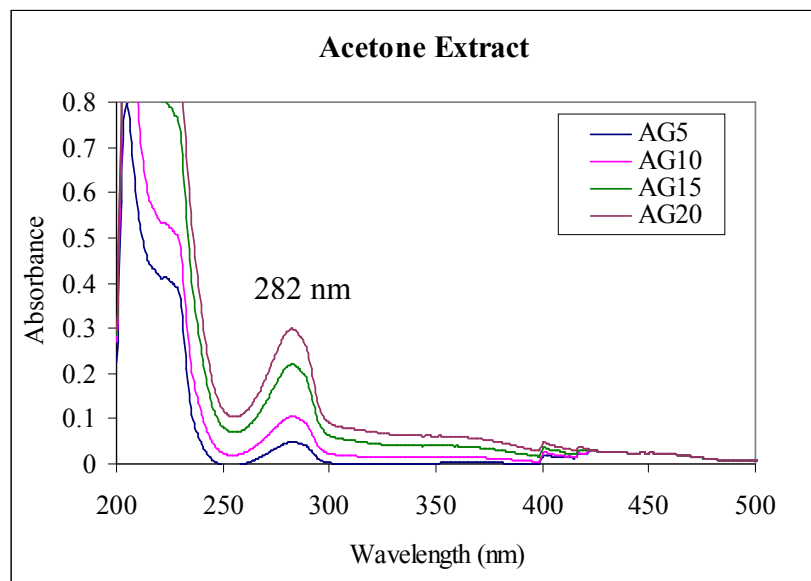
(b)

Figure A1 UV chromatogram of ginger extract (a) standard [6]-gingerol, (b) acetone extract, (c) 20% ethanol extract and (d) isolated [6]-gingerol
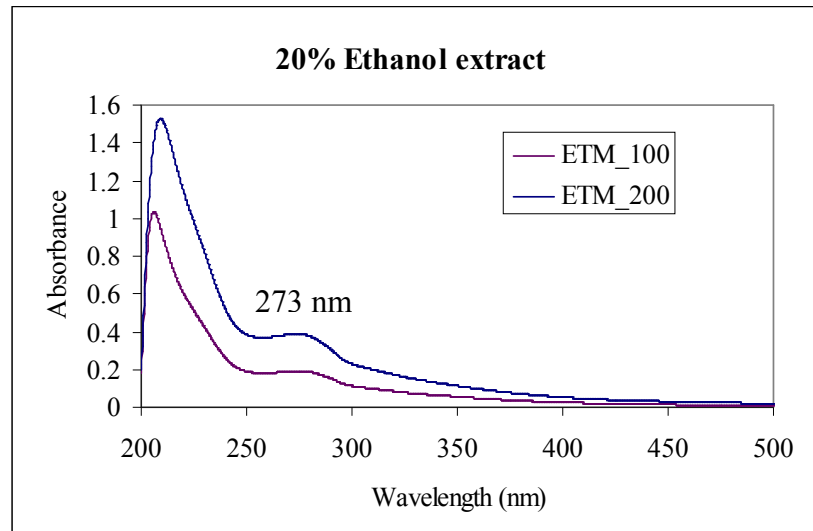
(c)
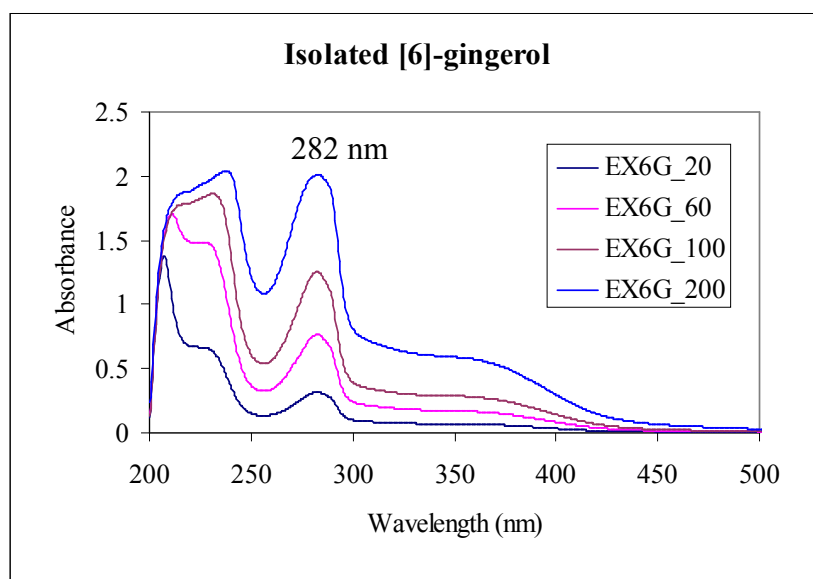
(d)

Figure A1 (continued)UV chromatogram of ginger extract (a) standard [6]-gingerol,
(b) acetone extract, (c) 20% ethanol extract and (d) isolated [6]-gingerol

Appendix B

Hydrogen-donating activity

(DPPH radical scavenging activity)

Table B1 DPPH radical inhibition of various ginger extracts compared to other antioxidants at different concentrations (Mean ± SD, n = 3)

Conc. (µg/ml)	Std. [6]-gingerol		Iso. [6]-gingerol		Acetone ext.		Ethanol Ext.		Vitamin C		Vitamin E	
	% Inh	SD	% Inh	SD	% Inh	SD	% Inh	SD	% Inh	SD	% Inh	SD
0	0.00	0.00	0.00	0.00	0.00	0.00	0.00	0.00	0.00	0.00	0.00	0.00
0.5	26.44	0.56	10.20	0.66	8.68	0.28	1.68	0.07	19.62	0.85	9.58	0.47
1.0	38.18	0.90	16.44	0.70	14.84	0.42	2.78	0.39	28.67	0.74	14.61	0.42
2.5	55.54	0.29	27.68	2.69	25.59	0.29	4.68	0.33	71.64	1.22	36.88	0.73
5.0	76.47	0.16	41.17	1.79	48.27	0.35	10.50	0.28	96.62	0.04	76.60	0.64
7.5	81.17	0.37	63.86	2.49	60.36	0.10	16.02	0.41	98.15	0.13	92.94	0.09
10	83.27	0.05	70.39	1.60	67.85	0.59	23.39	0.34	98.88	0.16	93.03	0.14
30	88.15	0.03	86.51	1.18	90.09	1.34	26.50	0.43	99.49	0.24	93.23	0.34
50	90.47	0.24	90.72	0.82	91.86	0.16	33.58	0.25	99.87	0.18	93.35	0.29
70	-	-	91.94	0.68	92.50	0.45	41.03	0.26	99.91	0.11	93.70	0.13
100	91.30	0.26	92.70	0.61	93.21	0.38	49.55	0.26	99.88	0.10	94.04	0.52
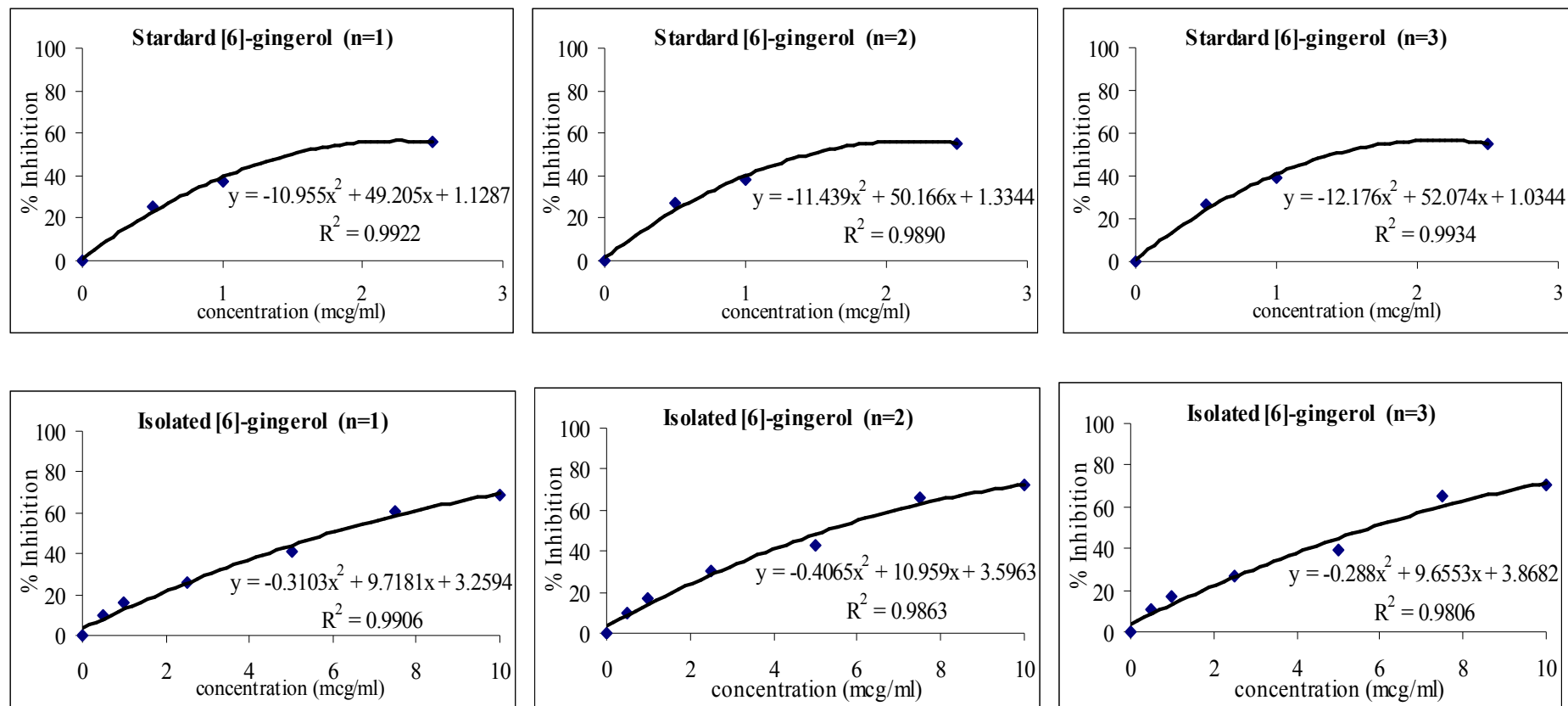
Figure B1 The relation of the % DPPH inhibition-concentration profile of the individual antioxidants.
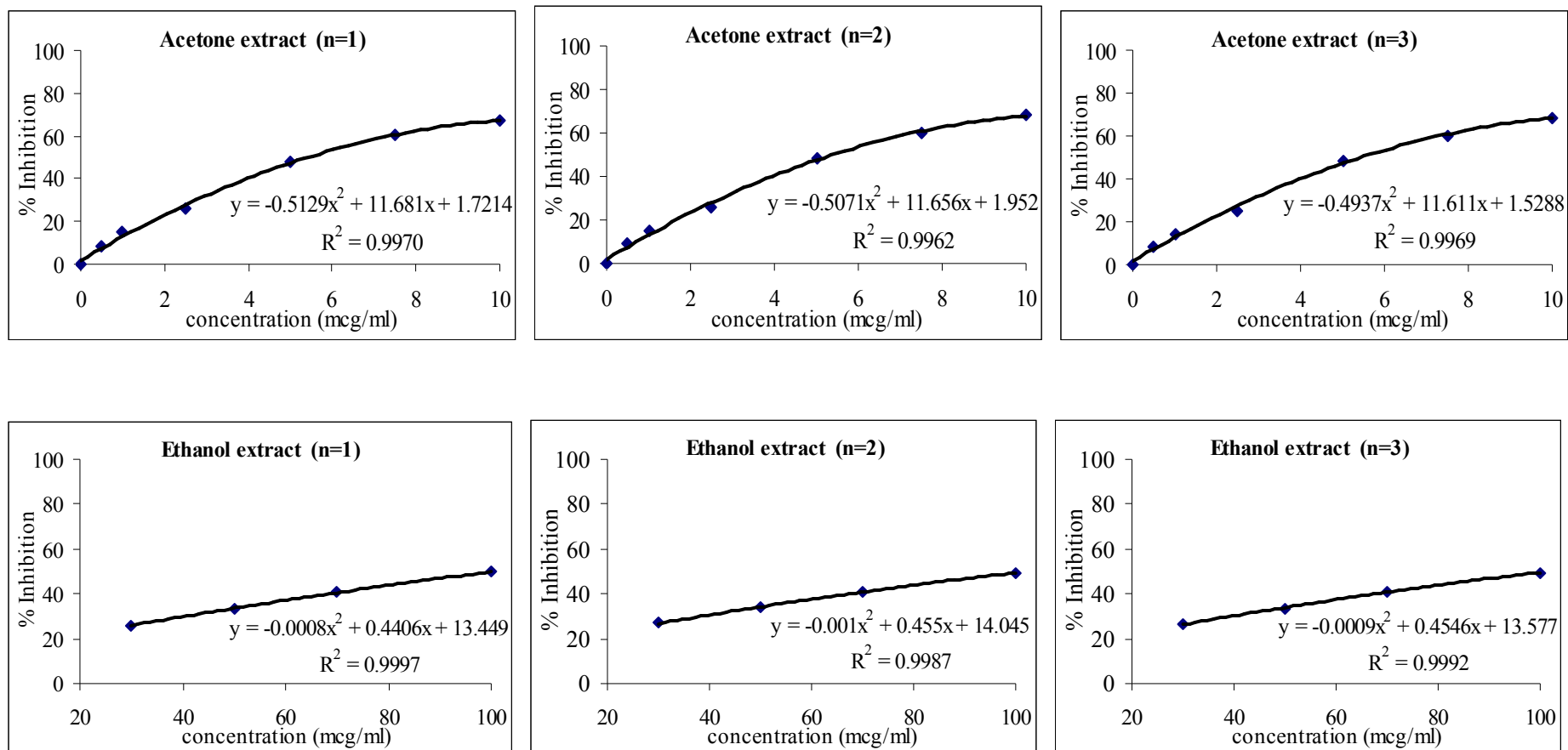
Figure B1 (continued) The relation of the % DPPH inhibition-concentration profile of the individual antioxidants.
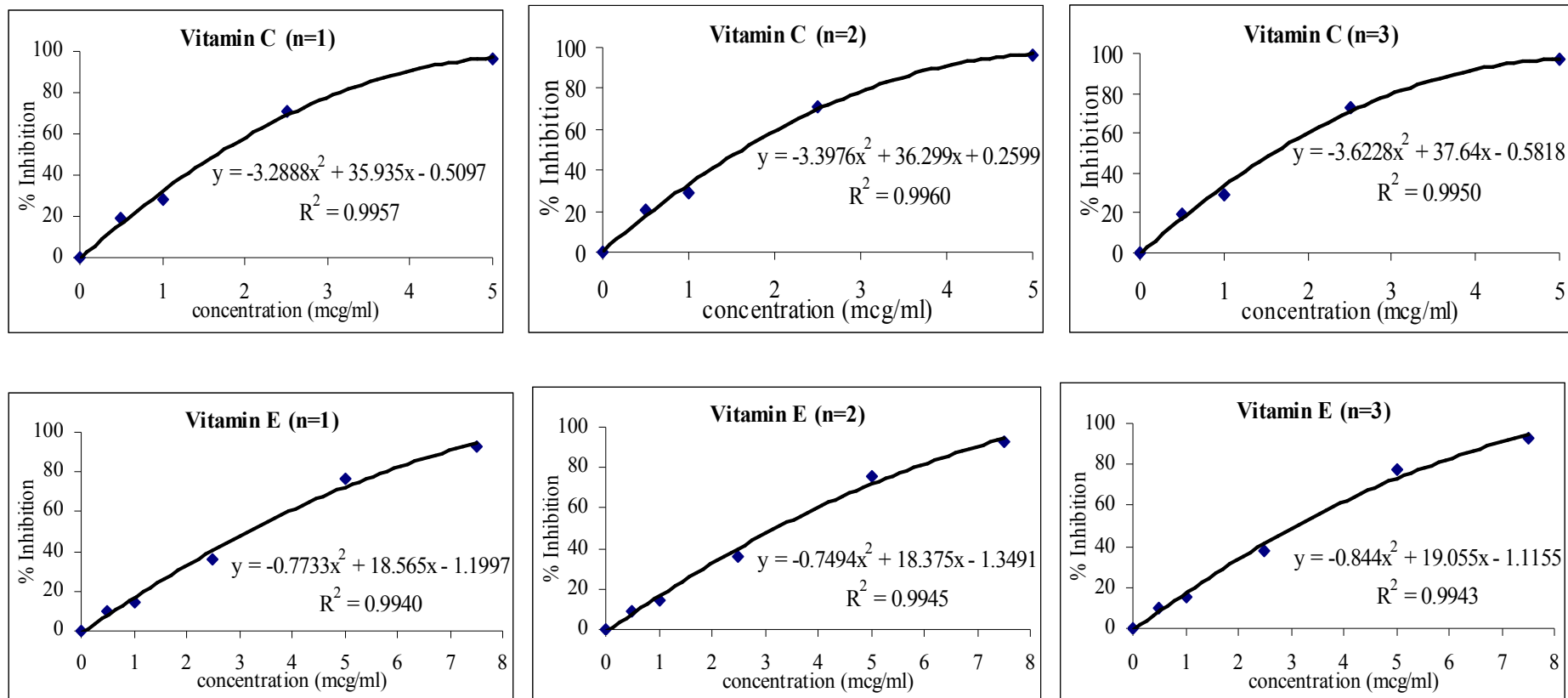
Figure B1 (continued) The relation of the % DPPH inhibition-concentration profile of the individual antioxidants.

Table B2 The raw data for DPPH radical inhibition percentages of Vitamin C

No	Conc. (μg/mL)	% Inhibition			mean	SD
		N 1	N 2	N 3		
1	0.00	0.0000	0.0000	0.0000	0.0000	0.0000
2	0.50	18.7702	20.4604	19.6310	19.6205	0.8451
3	1.00	27.8722	29.3511	28.7748	28.6660	0.7454
4	2.50	70.7322	71.1649	73.0299	71.6423	1.2210
5	5.00	96.6019	96.5866	96.6713	96.6199	0.0451
6	7.50	98.3010	98.0949	98.0549	98.1503	0.1321
7	10.00	99.0494	98.8490	98.7367	98.8784	0.1584
8	30.00	99.6561	99.2062	99.5990	99.4871	0.2449
9	50.00	99.9798	99.6626	99.9799	99.8741	0.1832
10	70.00	99.9798	99.7817	99.9799	99.9138	0.1144
11	100.00	99.9393	99.7619	99.9398	99.8803	0.1026

Table B3 The raw data for DPPH radical inhibition percentages of Vitamin E

No	Conc. (μg/mL)	% Inhibition			Mean	SD
		N 1	N 2	N 3		
1	0.00	0.0000	0.0000	0.0000	0.0000	0.0000
2	0.50	9.4632	9.1908	10.1014	9.5851	0.4674
3	1.00	14.8314	14.1263	14.8772	14.6116	0.4209
4	2.50	36.4763	36.4493	37.7255	36.8837	0.7291
5	5.00	76.6690	75.9330	77.2032	76.6017	0.6378
6	7.50	93.0489	92.8845	92.9050	92.9461	0.0896
7	10.00	93.0489	92.8845	93.1627	93.0320	0.1399
8	30.00	93.5478	92.8671	93.2658	93.2269	0.3420
9	50.00	93.4102	93.6170	93.0424	93.3565	0.2910
10	70.00	93.5994	93.6519	93.8499	93.7004	0.1321
11	100.00	93.5306	94.5762	94.0045	94.0371	0.5236

Table B4 The raw data for DPPH radical inhibition percentages of Acetone Extract

No	Conc. (μg/mL)	% Inhibition			Mean	SD
		N 1	N 2	N 3		
1	0.00	0.0000	0.0000	0.0000	0.0000	0.0000
2	0.50	8.7226	8.9309	8.3802	8.6779	0.2781
3	1.00	14.7810	15.2968	14.452	14.8433	0.4258
4	2.50	25.7299	25.8004	25.257	25.5958	0.2955
5	5.00	47.8832	48.5677	48.3802	48.2770	0.3537
6	7.50	60.4562	60.2509	60.3686	60.3586	0.1030
7	10.00	67.2080	68.0022	68.3608	67.8570	0.5900
8	30.00	89.4343	89.1968	91.6392	90.0901	1.3468
9	50.00	91.9343	91.9678	91.678	91.8600	0.1585
10	70.00	92.2993	92.1738	93.0165	92.4965	0.4547
11	100.00	92.9197	93.0725	93.6372	93.2098	0.3779

Table B5 The raw data for DPPH radical inhibition percentages of 6-gingerol

No	Conc. (µg/mL)	% Inhibition			Mean	SD
		N 1	N 2	N 3		
1	0.00	0.0000	0.0000	0.0000	0.0000	0.0000
2	0.50	25.8142	26.8939	26.6134	26.4405	0.5602
3	1.00	37.4977	37.8384	39.2084	38.1815	0.9055
4	2.50	55.8602	55.4820	55.2934	55.5452	0.2886
5	5.00	76.3201	76.631	76.4477	76.4663	0.1563
6	7.50	81.6007	80.9153	81.0099	81.1753	0.3714
7	10.00	83.2199	83.3301	83.2716	83.2739	0.0551
8	30.00	88.1141	88.1597	88.1843	88.1527	0.0356
9	50.00	90.7452	90.3408	90.3295	90.4718	0.2368
10	70.00	91.0028	91.4119	91.4798	91.2982	0.2580

Table B6 The raw data for DPPH radical inhibition percentages of Ethanol Extract

No	Conc. (µg/mL)	% Inhibition			Mean	SD
		N 1	N 2	N 3		
1	0.00	0.0000	0.0000	0.0000	0.0000	0.0000
2	0.50	1.7490	1.6032	1.6959	1.6827	0.0738
3	1.00	2.4144	3.1875	2.7485	2.7835	0.3877
4	2.50	4.3346	4.9981	4.7173	4.6833	0.3331
5	5.00	10.2091	10.7695	10.5263	10.5016	0.2810
6	7.50	15.8555	16.5032	15.731	16.0299	0.4146
7	10.00	23.0038	23.6326	23.5283	23.3882	0.3370
8	30.00	26.0646	26.9332	26.4912	26.4963	0.4343
9	50.00	33.3270	33.8174	33.6062	33.5835	0.2460
10	70.00	40.7414	41.2674	41.0721	41.0270	0.2659
11	100.00	49.8099	49.2833	49.5517	49.5483	0.2633

Table B7 The raw data for DPPH radical inhibition percentages of Isolated 6-gingerol

No	Conc. (µg/mL)	% Inhibition			Mean	SD
		N 1	N 2	N 3		
1	0.00	0.0000	0.0000	0.0000	0.0000	0.0000
2	0.50	9.5797	10.1312	10.8963	10.2024	0.6612
3	1.00	15.6822	17.0594	16.5843	16.4420	0.6995
4	2.50	25.7925	30.7605	26.4785	27.6772	2.6922
5	5.00	40.8183	43.1071	39.5766	41.1673	1.7909
6	7.50	61.0390	65.7542	64.7848	63.8593	2.4901
7	10.00	68.8591	72.0474	70.2611	70.3892	1.5980
8	30.00	85.8958	87.8792	85.7728	86.5159	1.1822
9	50.00	90.4902	91.6326	90.0353	90.7194	0.8229
10	70.00	92.0263	92.578	91.2209	91.9417	0.6825
11	100.00	92.8083	93.2553	92.0536	92.7057	0.6074

Table B8 One-way analysis of variance on the IC_{50} values of DPPH inhibition

ANOVA

%inhibition

	Sum of Squares	df	Mean Square	F	Sig.
Between Groups	23991.423		4798.285	19649.889	0.000
Within Groups	2.930	12	0.244		
Total	23994.353	17			

Table B9 Multiple Comparisons on the IC_{50} values of DPPH inhibition by LSD method

Dependent Variable: %inhibition

(I) type of antioxidant	(J) type of antioxidant	Mean Difference (I-J)	Std. Error	Sig.	95% Confidence Interval Lower Bound	95% Confidence Interval Upper Bound
Vitamin C	Vitamin E	-1.5700	0.40348	0.002	-2.4491	-.6909
	[6] - gingerol	0.1767	0.40348	0.669	-0.7024	1.0558
	Isolated [6] - gingerol	-4.0467	0.40348	0.000	-4.9258	-3.1676
	Acetone	-3.7967	0.40348	0.000	-4.6758	-2.9176
	Ethanol extract	-99.7100	0.40348	0.000	-100.5891	-98.8309
Vitamin E	Vitamin C	1.5700	0.40348	0.002	0.6909	2.4491
	[6] - gingerol	1.7467	0.40348	0.001	0.8676	2.6258
	Isolated [6] - gingerol	-2.4767	0.40348	0.000	-3.3558	-1.5976
	Acetone	-2.2267	0.40348	0.000	-3.1058	-1.3476
	Ethanol extract	-98.1400	0.40348	0.000	-99.0191	-97.2609
[6] - gingerol	Vitamin C	-0.1767	0.40348	0.669	-1.0558	0.7024
	Vitamin E	-1.7467	0.40348	0.001	-2.6258	-0.8676
	Isolated [6] - gingerol	-4.2233	0.40348	0.000	-5.1024	-3.3442
	Acetone	-3.9733	0.40348	0.000	-4.8524	-3.0942
	Ethanol extract	-99.8867	0.40348	0.000	-100.7658	-99.0076
Isolated [6] - gingerol	Vitamin C	4.0467	0.40348	0.000	3.1676	4.9258
	Vitamin E	2.4767	0.40348	0.000	1.5976	3.3558
	[6] - gingerol	4.2233	0.40348	0.000	3.3442	5.1024
	Acetone	0.2500	0.40348	0.547	-0.6291	1.1291
	Ethanol extract	-95.6633	0.40348	0.000	-96.5424	-94.7842
Acetone	Vitamin C	3.7967	0.40348	0.000	2.9176	4.6758
	Vitamin E	2.2267	0.40348	0.000	1.3476	3.1058
	[6] - gingerol	3.9733	0.40348	0.000	3.0942	4.8524
	Isolated [6] - gingerol	-0.2500	0.40348	0.547	-1.1291	0.6291
	Ethanol extract	-95.9133	0.40348	0.000	-96.7924	-95.0342

Table B9 (continued) Multiple Comparisons on the IC$_{50}$ values of DPPH inhibition by LSD method

Dependent Variable: %inhibition

(I) type of antioxidant	(J) type of antioxidant	Mean Difference (I-J)	Std. Error	Sig.	95% Confidence Interval	
					Lower Bound	Upper Bound
Ethanol extract	Vitamin C	99.7100	0.40348	0.000	98.8309	100.5891
	Vitamin E	98.1400	0.40348	0.000	97.2609	99.0191
	[6] - gingerol	99.8867	0.40348	0.000	99.0076	100.7658
	Isolated [6] - gingerol	95.6633	0.40348	0.000	94.7842	96.5424
	Acetone	95.9133	0.40348	0.000	95.0342	96.7924

* The mean difference is significant at the .05 level.

Table B10 Homogeneous subset on the IC$_{50}$ values of DPPH inhibition by Duncan method

%inhibition

type of antioxidant	N	Subset for alpha = 0.05			
		1	2	3	4
[6] - gingerol	3	1.4467			
Vitamin C	3	1.6233			
Vitamin E	3		3.1933		
Acetone	3			5.4200	
Isolated [6] - gingerol	3			5.6700	
Ethanol extract	3				101.3333
Sig.		0.669	1.000	0.547	1.000

Means for groups in homogeneous subsets are displayed.
a Uses Harmonic Mean Sample Size = 3.000.

Table C1 Hydroxyl radical inhibition of various ginger extracts compared to quercetin at different concentrations (Mean ± SD, n = 3)

Conc. (µg/ml)	Std. [6]-gingerol		Iso. [6]-gingerol		Acetone ext.		Ethanol Ext.		Quercetin	
	% Inh	SD	% Inh	SD	% Inh	SD	% Inh	SD	% Inh	SD
0	0.00	0.00	0.00	0.00	0.00	0.00	0.00	0.00	0.00	0.00
1	35.56	0.17	15.82	0.16	18.30	0.84	15.77	0.63	23.46	0.26
5	48.85	0.13	39.87	0.22	41.89	0.48	28.41	0.64	33.73	0.65
10	61.24	0.07	58.35	0.17	58.48	0.26	36.20	0.42	44.73	0.11
15	73.45	0.12	62.84	0.42	74.85	0.17	42.77	0.09	50.93	0.09
20	77.46	0.08	66.60	0.24	78.00	0.16	49.24	0.46	52.86	0.25
30	79.28	0.17	71.68	0.14	82.38	0.07	55.57	0.99	58.11	0.13
40	82.68	0.21	72.97	0.49	85.84	0.06	60.59	0.14	60.49	0.64

162
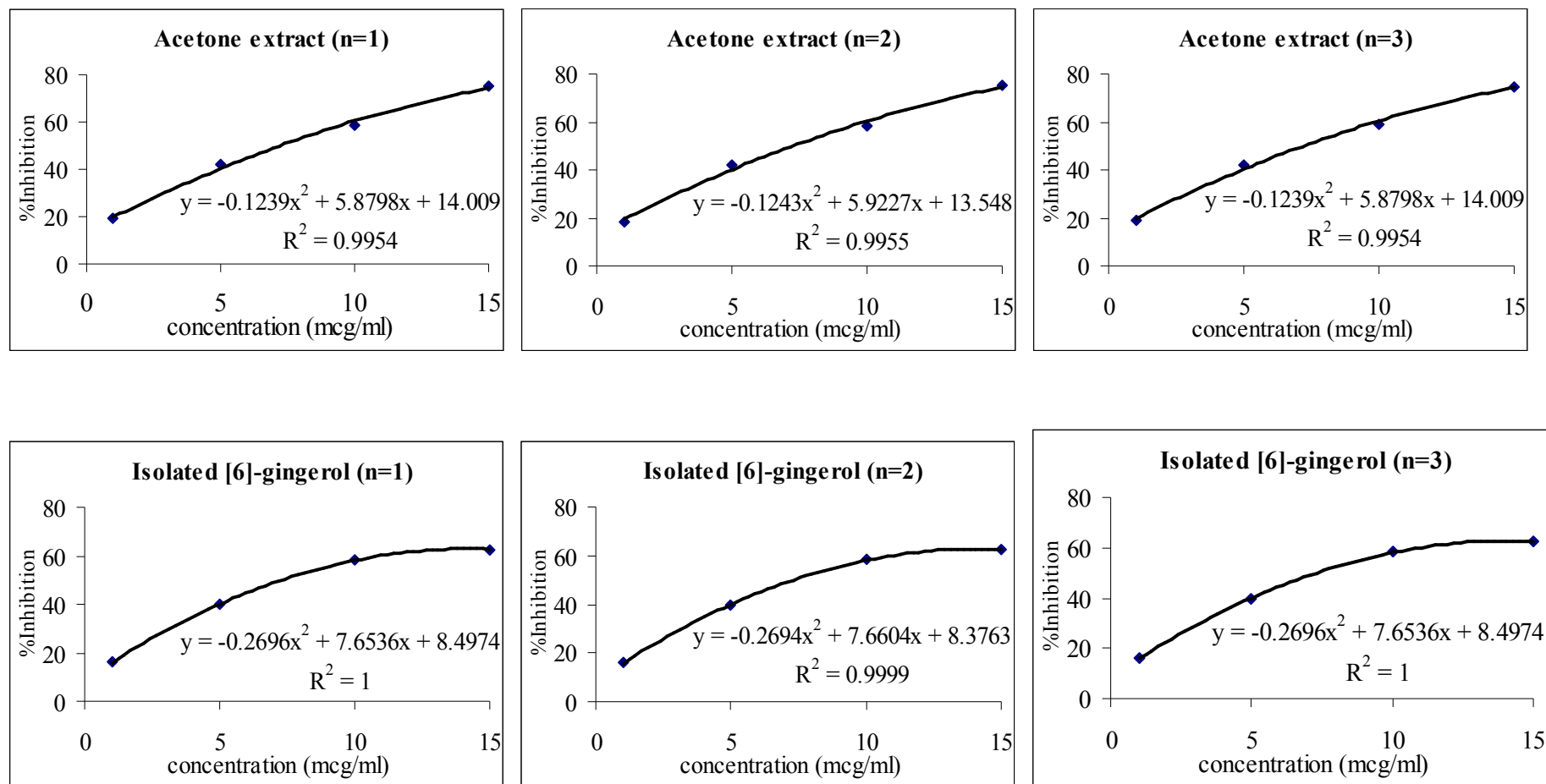
Figure C1 The relation of the % hydroxyl radical inhibition-concentration profile of the individual antioxidants.
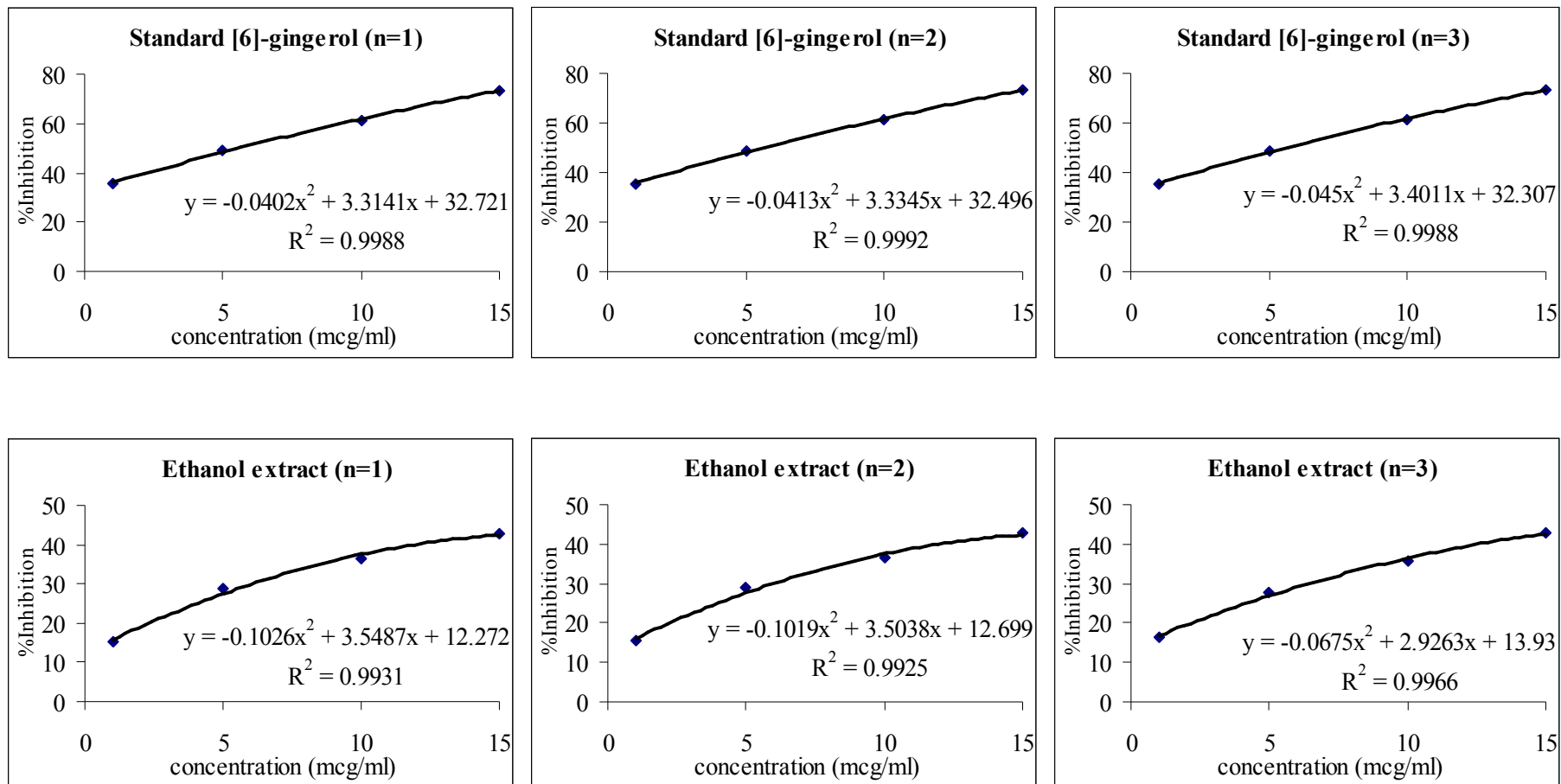
Figure C1 (continued) The relation of the % hydroxyl radical inhibition-concentration profile of the individual antioxidants.

Quercetin (n=1)

%Inhibition

$y = -0.0678x^2 + 3.0966x + 19.922$

$R^2 = 0.9986$

concentration (mcg/ml)

Quercetin (n=2)

%Inhibition

$y = -0.0697x^2 + 3.1007x + 20.315$

$R^2 = 0.9991$

concentration (mcg/ml)

Quercetin (n=3)

%Inhibition

$y = -0.0793x^2 + 3.2155x + 20.481$

$R^2 = 0.9999$

concentration (mcg/ml)
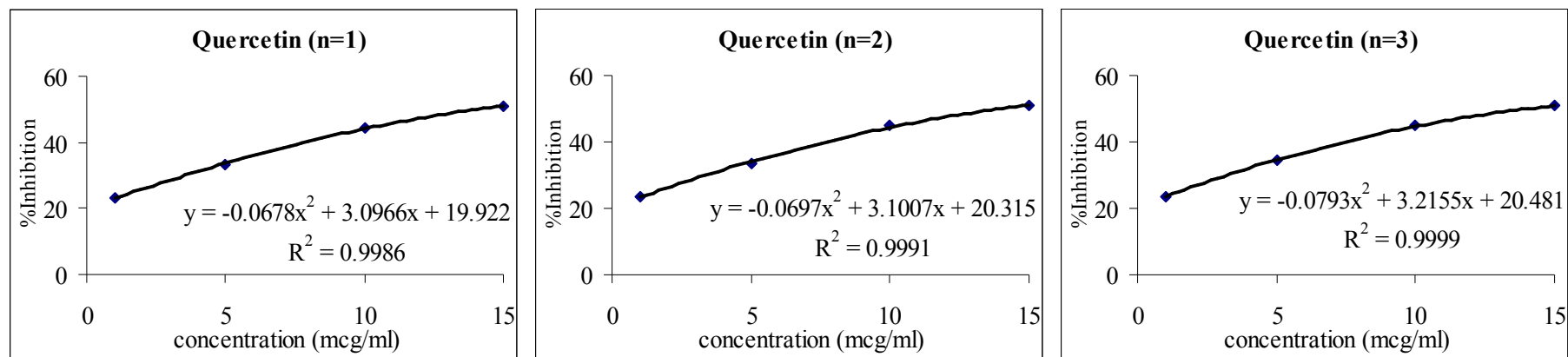
Figure C1 (continued) The relation of the % hydroxyl radical inhibition-concentration profile of the individual antioxidants.

Appendix C

Hydroxyl radical scavenging activity

Table C2 The raw data for hydroxyl (OH˙) radical inhibition percentages of Ginger Acetone extract

No	Conc. (µg/mL)	% Inhibition			mean	SD
		N 1	N 2	N 3		
1	0	0	0	0	0.0000	0.0000
2	1	18.9806	18.562	17.3645	18.3024	0.8388
3	5	42.2873	42.0299	41.3556	41.8909	0.4811
4	10	58.6604	58.5920	58.1846	58.4790	0.2572
5	15	74.8943	74.9933	74.6619	74.8498	0.1701
6	20	78.0157	78.1620	77.8481	78.0086	0.1571
7	30	82.3526	82.3387	82.4624	82.3846	0.0678
8	40	85.8328	85.9150	85.7892	85.8457	0.0639

Table C3 The raw data for hydroxyl (OH˙) radical inhibition percentages of [6]- gingerol

No	Conc. (µg/mL)	% Inhibition			mean	SD
		N1	N 2	N 3		
1	0	0	0	0	0.0000	0.0000
2	1	35.7233	35.5634	35.3869	35.5579	0.1683
3	5	48.9697	48.7036	48.8824	48.8519	0.1356
4	10	61.3249	61.2010	61.1968	61.2409	0.0728
5	15	73.5842	73.3734	73.3909	73.4495	0.1170
6	20	77.5652	77.4214	77.4084	77.4650	0.0870
7	30	79.1281	79.4631	79.2545	79.2819	0.1692
8	40	82.5414	82.9177	82.5859	82.6817	0.2056

Table C4 The raw data for hydroxyl (OH˙) radical inhibition percentages of Quercetin

No	Conc. (µg/mL)	% Inhibition			mean	SD
		N1	N 2	N 3		
1	0	0	0	0	0.0000	0.0000
2	1	23.1757	23.5266	23.6758	23.4594	0.2567
3	5	33.1443	33.6212	34.4262	33.7306	0.6479
4	10	44.6160	44.7523	44.8370	44.7351	0.1115
5	15	50.9634	51.0053	50.8262	50.9316	0.0937
6	20	52.6373	52.8156	53.1252	52.8594	0.2469
7	30	58.0213	58.046	58.2588	58.1087	0.1306
8	40	60.1257	60.1119	61.2240	60.4872	0.6381

Table C5 The raw data for hydroxyl (OH˙) radical inhibition percentages of Ginger 20 % ethanol extract

No	Conc. (μg/mL)	% Inhibition			mean	SD
		N 1	N 2	N 3		
1	0	0	0	0	0.0000	0.0000
2	1	15.2422	15.6145	16.4692	15.7753	0.6291
3	5	28.6516	28.8974	27.6785	28.4092	0.6446
4	10	36.4379	36.4546	35.7219	36.2048	0.4183
5	15	42.7716	42.6741	42.8562	42.7673	0.0911
6	20	48.9371	49.0186	49.7774	49.2444	0.4634
7	30	54.9841	55.0194	56.7237	55.5757	0.9943
8	40	60.5386	60.4888	60.7485	60.5920	0.1378

Table C6 The raw data for hydroxyl (OH˙) radical inhibition percentages of Isolated 6-gingerol

No	Conc. (μg/mL)	% Inhibition			mean	SD
		N 1	N 2	N 3		
1	0	0	0	0	0.0000	0.0000
2	1	15.9401	15.8858	15.6395	15.8218	0.1602
3	5	39.8785	39.6456	40.0931	39.8724	0.2238
4	10	58.2084	58.307	58.5418	58.3524	0.1713
5	15	62.6079	62.5853	63.3236	62.8389	0.4199
6	20	66.7518	66.7431	66.3221	66.6057	0.2456
7	30	71.5997	71.6064	71.8457	71.6839	0.1401
8	40	72.6726	72.7017	73.5343	72.9695	0.4893

Table C7 One-way analysis of variance on the IC_{50} values of hydroxyl (OH˙) radical inhibition

ANOVA

%inhibition

	Sum of Squares	df	Mean Square	F	Sig.
Between Groups	538.491	4	134.623	2285.874	0.000
Within Groups	0.589	10	0.059		
Total	539.080	14			

Table C8 Multiple Comparisons on the IC$_{50}$ values of hydroxyl (OH˙) radical inhibition by LSD method

Dependent Variable: %inhibition

(I) type of antioxidant	(J) type of antioxidant	Mean Difference (I-J)	Std. Error	Sig.	95% Confidence Interval	
					Lower Bound	Upper Bound
Quercetin	[6] - gingerol	8.6067	0.19815	0.000	8.1652	9.0482
	Isolated [6] - gingerol	7.3600	0.19815	0.000	6.9185	7.8015
	Acetone	6.9267	0.19815	0.000	6.4852	7.3682
	Ethanol extract	-7.2333	0.19815	0.000	-7.6748	-6.7918
[6] - gingerol	Quercetin	-8.6067	0.19815	0.000	-9.0482	-8.1652
	Isolated [6] - gingerol	-1.2467	0.19815	0.000	-1.6882	-0.8052
	Acetone	-1.6800	0.19815	0.000	-2.1215	-1.2385
	Ethanol extract	-15.8400	0.19815	0.000	-16.2815	-15.3985
Isolated [6] - gingerol	Quercetin	-7.3600	0.19815	0.000	-7.8015	-6.9185
	[6] - gingerol	1.2467	0.19815	0.000	0.8052	1.6882
	Acetone	-.4333	0.19815	0.054	-0.8748	0.0082
	Ethanol extract	-14.5933	0.19815	0.000	-15.0348	-14.1518
Acetone	Quercetin	-6.9267	0.19815	0.000	-7.3682	-6.4852
	[6] - gingerol	1.6800	0.19815	0.000	1.2385	2.1215
	Isolated [6] - gingerol	.4333	0.19815	0.054	-.0082	.8748
	Ethanol extract	-14.1600	0.19815	0.000	-14.6015	-13.7185
Ethanol extract	Quercetin	7.2333	0.19815	0.000	6.7918	7.6748
	[6] - gingerol	15.8400	0.19815	0.000	15.3985	16.2815
	Isolated [6] - gingerol	14.5933	0.19815	0.000	14.1518	15.0348
	Acetone	14.1600	0.19815	0.000	13.7185	14.6015

* The mean difference is significant at the .05 level.

Table C9 Homogeneous subsets on the IC_{50} values of hydroxyl (OH˙) radical inhibition by Duncan method

%inhibition

type of antioxidant	N	Subset for alpha = 0.05			
		1	2	3	4
[6] - gingerol	3	5.6267			
Isolated [6] - gingerol	3		6.8733		
Acetone	3		7.3067		
Quercetin	3			14.2333	
Ethanol extract	3				21.4667
Sig.		1.000	.054	1.000	1.000

Means for groups in homogeneous subsets are displayed.

a Uses Harmonic Mean Sample Size = 3.000.

Appendix D

Particle size and size distribution analysis

Table D1. The raw data of particle size and polydispersity index of GPP1 under storage condition

| | day 0 | | day 14 | | | | day 30 | | | | day 60 | | | |
| | | | 4 °C | | RT | | 4 °C | | RT | | 4 °C | | RT | |
No.	size	PI	size	PI	size	PI	size	PI	size	PI	size	PI	size	PI
1	224.3	0.113	227.3	0.282	225.0	0.191	235.9	0.244	243.9	0.108	228.8	0.292	343.6	0.354
2	243.9	0.207	226.8	0.153	217.5	0.222	229.4	0.021	255.3	0.108	222.1	0.279	355.4	0.366
3	245.5	0.288	233.7	0.288	222.7	0.152	231.4	0.025	256.8	0.133	226.6	0.256	351.8	0.350
4	227.6	0.258	223.0	0.076	221.9	0.214	229.3	0.147	254.4	0.133	225.6	0.287	346.6	0.336
5	227.4	0.259	224.7	0.281	220.1	0.158	227.8	0.122	255.3	0.281	227.8	0.251	354.2	0.356
6	228.5	0.257	226.4	0.199	218.6	0.221	229.3	0.147	254.8	0.281	229.3	0.268	353.3	0.346
7	234.8	0.302	230.3	0.258	217.7	0.234	229.9	0.048	255.7	0.303	229.9	0.288	358.3	0.303
8	220.5	0.279	228.2	0.239	220.7	0.241	226.1	0.042	253.4	0.289	230.9	0.311	350.6	0.386
9	219.2	0.388	227.0	0.264	220.8	0.163	227.5	0.044	255.0	0.286	227.9	0.242	346.6	0.397
mean	230.2	0.261	227.5	0.227	220.6	0.200	229.6	0.093	253.8	0.214	227.7	0.275	351.2	0.355
SD	9.4229	0.0739	3.0994	0.0718	2.4434	0.0344	2.8093	0.0761	3.8416	0.0890	2.6425	0.0223	4.7729	0.0274

Table D2. The raw data of particle size and polydispersity index of GPP3 under storage condition

| | day 0 | | day 14 | | | | day 30 | | | | day 60 | | | |
| | | | 4 °C | | RT | | 4 °C | | RT | | 4 °C | | RT | |
No.	size	PI	size	PI	size	PI	size	PI	size	PI	size	PI	size	PI
1	201.4	0.163	186.6	0.119	185.5	0.233	186.0	0.306	186.7	0.274	186.1	0.290	216.2	0.230
2	200.9	0.248	184.0	0.250	177.0	0.234	187.2	0.304	185.4	0.254	185.3	0.283	217.7	0.241
3	191.4	0.130	176.1	0.334	175.7	0.311	181.5	0.308	187.8	0.283	187.7	0.293	219.6	0.248
4	187.9	0.195	188.9	0.304	176.1	0.194	187.0	0.305	185.5	0.304	189.4	0.297	218.5	0.244
5	194.9	0.311	177.5	0.276	178.2	0.123	185.8	0.302	187.5	0.304	190.0	0.294	220.5	0.230
6	187.9	0.164	175.8	0.307	181.2	0.285	186.2	0.301	187.2	0.303	191.7	0.268	221.8	0.235
7	195.2	0.292	182.0	0.278	179.8	0.282	190.0	0.163	186.1	0.327	188.8	0.288	223.5	0.243
8	189.9	0.080	178.8	0.215	182.6	0.290	191.8	0.315	185.9	0.254	191.4	0.282	222.5	0.248
9	193.4	0.315	179.4	0.210	179.7	0.316	185.9	0.088	183.4	0.286	190.8	0.289	219.0	0.241
mean	193.7	0.211	181.0	0.255	179.5	0.252	186.8	0.266	186.2	0.288	189.0	0.287	219.9	0.240
SD	5.0237	0.0846	4.6700	0.0656	3.2125	0.0629	2.8796	0.0818	1.3491	0.0245	2.2714	0.0087	2.3737	0.0069

Table D3. The raw data of particle size and polydispersity index of GPP5 under storage condition

| | day 0 | | day 14 | | | | day 30 | | | | day 60 | | | |
| | | | 4 °C | | RT | | 4 °C | | RT | | 4 °C | | RT | |
No.	size	PI	size	PI	size	PI	size	PI	size	PI	size	PI	size	PI
1	217.9	0.285	210.4	0.350	218.7	0.215	223.4	0.277	238.3	0.244	239.7	0.293	248.3	0.217
2	224.9	0.298	210.9	0.313	219.3	0.310	227.9	0.332	238.8	0.205	235.3	0.297	247.3	0.196
3	228.5	0.316	222.1	0.334	213.2	0.289	222.0	0.280	240.2	0.210	232.2	0.258	244.2	0.197
4	236.7	0.332	210.9	0.299	217.7	0.321	231.6	0.304	239.6	0.154	235.4	0.275	248.5	0.209
5	229.6	0.265	233.6	0.325	212.6	0.324	237.4	0.318	239.0	0.219	225.5	0.299	247.9	0.204
6	234.9	0.231	213.8	0.340	222.5	0.309	221.9	0.307	229.2	0.217	239.6	0.328	251.3	0.215
7	228.7	0.201	212.8	0.299	214.5	0.305	228.9	0.316	238.3	0.221	227.9	0.285	244.1	0.221
8	224.0	0.303	212.7	0.285	215.1	0.282	223.5	0.280	232.7	0.213	223.6	0.290	250.2	0.212
9	231.8	0.323	212.9	0.321	219.9	0.286	236.0	0.312	241.3	0.260	234.6	0.262	248.3	0.216
mean	228.6	0.284	215.6	0.318	217.1	0.293	228.1	0.303	237.5	0.216	232.6	0.287	247.8	0.210
SD	5.7650	0.0440	7.6177	0.0214	3.3720	0.0330	5.9237	0.0196	3.9257	0.0291	5.8329	0.0212	2.3955	0.0089

Table D4. The raw data of particle size and polydispersity index of GPT1 under storage condition

	day 0		day 14				day 30				day 60			
			4 °C		RT		4 °C		RT		4 °C		RT	
No.	size	PI	size	PI	size	PI	size	PI	size	PI	size	PI	size	PI
1	207.7	0.264	206.2	0.151	212.4	0.279	212.0	0.253	223.4	0.277	202.1	0.223	229.4	0.298
2	211.6	0.279	204.3	0.268	214.7	0.247	211.3	0.251	227.9	0.332	203.4	0.236	239.4	0.289
3	207.6	0.281	196.4	0.224	201.4	0.213	214.9	0.255	222.0	0.280	204.0	0.246	240.8	0.282
4	200.3	0.263	188.0	0.294	200.8	0.067	213.4	0.249	231.6	0.304	202.7	0.225	239.0	0.296
5	199.5	0.245	188.4	0.262	198.7	0.173	212.5	0.240	237.4	0.318	205.0	0.232	238.1	0.289
6	208.5	0.252	187.1	0.224	201.0	0.265	213.3	0.272	221.9	0.307	201.1	0.249	241.3	0.280
7	197.0	0.274	199.2	0.263	199.0	0.270	211.4	0.299	228.9	0.316	204.9	0.259	223.4	0.285
8	194.5	0.173	189.7	0.287	202.8	0.249	210.8	0.213	223.5	0.280	208.4	0.243	239.1	0.275
9	195.2	0.257	188.9	0.293	196.5	0.112	210.4	0.272	236.0	0.312	209.3	0.247	250.6	0.277
mean	202.4	0.254	194.2	0.252	203.0	0.208	212.2	0.256	228.1	0.303	204.5	0.240	237.9	0.286
SD	6.4537	0.0328	7.4721	0.0460	6.2592	0.0756	1.4455	0.0238	5.9237	0.0196	2.7537	0.0119	7.6542	0.0080

Table D5. The raw data of particle size and polydispersity index of GPT3 under storage condition

| | day 0 | | day 14 | | | | day 30 | | | | day 60 | | | |
| | | | 4 °C | | RT | | 4 °C | | RT | | 4 °C | | RT | |
No.	size	PI	size	PI	size	PI	size	PI	size	PI	size	PI	size	PI
1	156.3	0.262	144.8	0.226	151.1	0.261	150.6	0.259	155.8	0.173	149.9	0.276	296.0	0.205
2	151.8	0.280	140.0	0.207	150.6	0.266	148.2	0.279	154.3	0.205	151.5	0.261	300.8	0.219
3	154.9	0.268	142.5	0.245	147.5	0.245	149.5	0.155	156.9	0.250	155.8	0.268	302.6	0.211
4	158.5	0.215	141.1	0.274	146.6	0.202	148.8	0.325	157.7	0.243	154.7	0.272	301.9	0.217
5	157.4	0.306	140.0	0.249	148.9	0.231	145.6	0.316	157.1	0.262	152.8	0.269	302.9	0.224
6	150.0	0.231	139.4	0.234	144.3	0.230	148.3	0.294	155.9	0.239	154.1	0.278	296.5	0.215
7	148.2	0.200	139.2	0.231	147.2	0.244	151.8	0.289	154.0	0.250	156.0	0.254	304.5	0.207
8	146.5	0.171	139.7	0.212	144.7	0.217	149.2	0.281	154.5	0.227	158.2	0.278	307.3	0.195
9	149.1	0.237	139.9	0.220	148.3	0.200	153.8	0.377	151.9	0.243	156.2	0.271	291.7	0.203
mean	152.5	0.241	140.7	0.233	147.7	0.233	149.5	0.286	155.3	0.232	154.4	0.270	300.5	0.211
SD	4.3732	0.0423	1.8289	0.0207	2.3406	0.0236	2.3425	0.0599	1.8386	0.0276	2.5880	0.0080	4.8495	0.0091

Table D6. The raw data of particle size and polydispersity index of GPT5 under storage condition

	day 0		day 14				day 30				day 60			
			4 °C		RT		4 °C		RT		4 °C		RT	
No.	size	PI	size	PI	size	PI	size	PI	size	PI	size	PI	size	PI
1	153.7	0.292	133.6	0.294	152.2	0.221	150.6	0.237	158.6	0.297	148.1	0.224	465.2	0.251
2	152.2	0.253	133.2	0.301	152.0	0.251	147.7	0.240	157.4	0.348	149.6	0.217	467.0	0.233
3	148.5	0.209	135.2	0.221	149.2	0.194	152.2	0.240	159.2	0.185	150.3	0.215	466.5	0.225
4	146.7	0.237	135.1	0.205	147.0	0.251	151.9	0.225	158.7	0.291	154.9	0.226	471.5	0.213
5	147.8	0.294	134.2	0.247	148.1	0.204	152.2	0.255	159.2	0.299	150.0	0.219	468.3	0.178
6	150.4	0.271	132.3	0.310	149.2	0.219	154.5	0.267	156.1	0.253	152.8	0.232	466.9	0.254
7	147.8	0.258	133.0	0.263	150.0	0.257	155.4	0.219	159.3	0.260	157.7	0.261	472.5	0.275
8	159.4	0.222	134.1	0.205	148.9	0.223	153.6	0.239	164.0	0.278	156.2	0.232	469.2	0.268
9	143.9	0.271	134.9	0.307	148.4	0.241	152.7	0.262	165.9	0.300	158.2	0.261	470.7	0.273
mean	150.0	0.256	134.0	0.261	149.4	0.229	152.3	0.243	159.8	0.279	153.1	0.232	468.6	0.241
SD	4.5698	0.0294	1.0113	0.0437	1.7220	0.0222	2.2508	0.0160	3.1208	0.0446	3.7883	0.0176	2.4971	0.0321

Table D7. The raw data of particle size and polydispersity index of GBP1 under storage condition

| | day 0 | | day 14 | | | | day 30 | | | | day 60 | | | |
| | | | 4 °C | | RT | | 4 °C | | RT | | 4 °C | | RT | |
No.	size	PI	size	PI	size	PI	size	PI	size	PI	size	PI	size	PI
1	341.7	0.005	378.7	0.005	391.9	0.005	379.0	0.005	397.1	0.005	405.1	0.379		
2	346.6	0.005	388.3	0.005	396.6	0.188	388.4	0.005	405.7	0.005	392.3	0.398		
3	356.7	0.005	383.1	0.005	398.3	0.005	387.5	0.005	404.7	0.005	390.0	0.367		
4	341.7	0.005	388.1	0.137	398.1	0.005	380.2	0.005	407.0	0.005	412.6	0.361		
5	357.4	0.005	380.7	0.005	390.2	0.048	381.3	0.005	403.6	0.005	410.3	0.362	Phase seperation	
6	344.9	0.005	388.1	0.005	410.0	0.005	385.4	0.005	405.5	0.005	396.6	0.343		
7	357.3	0.005	381.1	0.005	409.0	0.005	389.3	0.005	416.4	0.005	398.6	0.341		
8	356.7	0.005	386.3	0.151	406.8	0.005	378.1	0.005	409.1	0.005	397.4	0.374		
9	352.3	0.005	388.8	0.005	405.6	0.005	387.8	0.005	405.8	0.005	402.2	0.379		
mean	350.6	0.005	384.8	0.036	400.7	0.030	384.1	0.005	406.1	0.005	400.6	0.367		
SD	6.8497	0.0000	3.9192	0.0614	7.3622	0.0609	4.4375	0.0000	5.0710	0.0000	7.6842	0.0181		

Table D8. The raw data of particle size and polydispersity index of GBP3 under storage condition

| | day 0 | | day 14 | | | | day 30 | | | | day 60 | | | |
| | | | 4 °C | | RT | | 4 °C | | RT | | 4 °C | | RT | |
No.	size	PI	size	PI	size	PI	size	PI	size	PI	size	PI	size	PI
1	326.7	0.326	371.8	0.005	377.3	0.210	389.4	0.005	419.8	0.005	457.1	0.328		
2	311.6	0.005	363.6	0.005	377.7	0.005	416.8	0.005	414.7	0.005	451.8	0.364		
3	309.5	0.005	388.2	0.005	379.6	0.005	417.9	0.005	419.2	0.005	466.0	0.358		
4	311.4	0.005	390.3	0.005	368.8	0.005	416.6	0.005	420.0	0.005	434.4	0.376		
5	317.8	0.005	372.9	0.031	380.8	0.005	409.5	0.005	413.6	0.005	453.8	0.356	Phase seperation	
6	315.1	0.005	363.2	0.005	379.5	0.005	397.8	0.005	421.2	0.005	463.6	0.341		
7	307.6	0.005	386.4	0.041	385.2	0.043	407.3	0.005	418.3	0.005	466.6	0.335		
8	313.0	0.305	374.9	0.085	371.4	0.005	405.4	0.005	419.3	0.005	438.1	0.342		
9	307.1	0.005	386.7	0.051	381.3	0.005	403.6	0.005	422.1	0.005	462.2	0.356		
mean	313.3	0.074	377.6	0.026	378.0	0.032	407.1	0.005	418.7	0.005	454.8	0.351		
SD	6.0726	0.1370	10.6081	0.0286	5.0515	0.0679	9.4979	0.0000	2.8171	0.0000	11.7644	0.0152		

Table D9. The raw data of particle size and polydispersity index of GBP5 under storage condition

| | day 0 | | day 14 | | | | day 30 | | | | day 60 | | | |
| | | | 4 °C | | RT | | 4 °C | | RT | | 4 °C | | RT | |
No.	size	PI	size	PI	size	PI	size	PI	size	PI	size	PI	size	PI
1	318.7	0.005	382.3	0.407	376.7	0.469	392.2	0.005	396.6	0.005	393.5	0.217		
2	312.1	0.005	340.2	0.326	356.0	0.436	392.3	0.005	414.8	0.005	399.1	0.212		
3	305.3	0.005	341.2	0.080	391.0	0.005	389.8	0.005	386.7	0.005	397.7	0.206		
4	304.2	0.005	356.6	0.014	349.6	0.005	391.3	0.005	387.5	0.005	403.7	0.225		
5	315.6	0.005	362.3	0.350	383.2	0.005	389.6	0.005	408.9	0.005	402.2	0.282	Phase seperation	
6	304.1	0.005	359.9	0.005	379.4	0.438	387.2	0.005	414.4	0.005	401.7	0.247		
7	311.7	0.005	347.0	0.338	386.8	0.391	386.3	0.005	410.9	0.005	403.9	0.289		
8	304.2	0.177	350.7	0.441	377.6	0.005	397.4	0.005	392.7	0.005	402.8	0.306		
9	309.8	0.125	366.7	0.379	376.8	0.005	386.2	0.005	389.0	0.005	399.5	0.312		
mean	309.5	0.037	356.3	0.260	375.2	0.195	390.3	0.005	400.2	0.005	400.5	0.255		
SD	5.4373	0.0657	13.4084	0.1750	13.6949	0.2267	3.5736	0.0000	11.9539	0.0000	3.3764	0.0424		

Table D10. The raw data of particle size and polydispersity index of GBT1 under storage condition

| | day 0 | | day 14 | | | | day 30 | | | | day 60 | | | |
| | | | 4 °C | | RT | | 4 °C | | RT | | 4 °C | | RT | |
No.	size	PI	size	PI	size	PI	size	PI	size	PI	size	PI	size	PI
1	333.4	0.377	408.5	0.005	383.7	0.005	424.8	0.005	434.2	0.005	502.9	0.340		
2	335.8	0.005	410.2	0.445	407.9	0.005	418.2	0.005	438.8	0.005	503.3	0.344		
3	334.8	0.005	413.6	0.005	391.8	0.005	404.2	0.005	446.9	0.005	505.4	0.364		
4	332.5	0.277	425.3	0.005	389.9	0.057	421.5	0.005	446.2	0.005	506.1	0.387		
5	324.4	0.005	415.0	0.005	399.4	0.005	416.0	0.005	448.9	0.005	501.3	0.354	Phase seperation	
6	326.4	0.005	394.3	0.005	352.2	0.043	423.5	0.005	431.2	0.005	516.4	0.348		
7	327.5	0.005	392.7	0.005	393.7	0.047	417.2	0.005	424.0	0.005	495.8	0.329		
8	320.0	0.005	413.4	0.357	385.9	0.005	421.8	0.005	421.6	0.005	507.9	0.372		
9	316.9	0.005	413.3	0.005	408.0	0.054	423.5	0.005	448.9	0.005	504.3	0.355		
mean	328.0	0.077	409.6	0.093	390.3	0.025	419.0	0.005	437.9	0.005	504.8	0.355		
SD	6.7032	0.1442	10.2533	0.1760	16.7121	0.0242	6.3259	0.0000	10.6663	0.0000	5.5405	0.0176		

Table D11. The raw data of particle size and polydispersity index of GBT3 under storage condition

| | day 0 | | day 14 | | | | day 30 | | | | day 60 | | | |
| | | | 4 °C | | RT | | 4 °C | | RT | | 4 °C | | RT | |
No.	size	PI	size	PI	size	PI	size	PI	size	PI	size	PI	size	PI
1	296.5	0.005	382.9	0.417	325.1	0.071	445.8	0.005	370.5	0.005	452.0	0.227	363.1	0.276
2	293.0	0.459	380.2	0.050	330.7	0.005	436.6	0.005	385.0	0.005	445.4	0.392	360.3	0.255
3	291.7	0.005	385.4	0.005	337.5	0.005	449.0	0.005	382.5	0.005	454.2	0.227	370.1	0.231
4	288.5	0.005	380.3	0.005	332.0	0.051	456.4	0.005	369.9	0.005	450.0	0.342	361.3	0.262
5	293.6	0.196	382.5	0.230	341.9	0.005	456.0	0.005	377.9	0.005	457.2	0.373	359.7	0.213
6	304.0	0.341	382.6	0.394	329.8	0.005	461.0	0.005	372.4	0.005	450.2	0.386	387.4	0.243
7	298.9	0.005	362.7	0.479	331.9	0.005	455.0	0.005	373.4	0.005	455.9	0.390	386.1	0.344
8	300.7	0.005	383.0	0.352	323.7	0.005	445.0	0.005	373.5	0.005	443.5	0.389	363.7	0.323
9	296.2	0.505	393.1	0.392	315.9	0.005	454.4	0.005	375.4	0.005	460.4	0.349	361.4	0.342
mean	295.9	0.170	381.4	0.258	314.8	0.017	451.0	0.005	375.6	0.005	452.1	0.342	368.1	0.277
SD	4.7984	0.2127	8.0054	0.1909	7.6507	0.0252	7.5508	0.0000	5.2356	0.0000	5.4844	0.0675	10.9965	0.0486

Table D12. The raw data of particle size and polydispersity index of GBT5 under storage condition

| No. | day 0 | | day 14 | | | | day 30 | | | | day 60 | | | |
| | | | 4 °C | | RT | | 4 °C | | RT | | 4 °C | | RT | |
	size	PI	size	PI	size	PI	size	PI	size	PI	size	PI	size	PI
1	318.5	0.382	377.0	0.284	262.3	0.341	329.6	0.005	299.0	0.005	322.4	0.178	299.0	0.306
2	319.1	0.406	376.3	0.302	276.3	0.310	317.4	0.005	298.0	0.005	317.1	0.163	306.4	0.337
3	322.9	0.329	373.5	0.344	257.9	0.356	322.4	0.005	297.3	0.005	318.0	0.295	302.8	0.346
4	319.1	0.468	361.3	0.297	241.6	0.092	326.2	0.005	298.4	0.005	322.9	0.253	308.9	0.368
5	313.8	0.403	376.3	0.353	262.4	0.005	329.9	0.005	299.2	0.005	325.6	0.198	300.5	0.312
6	316.7	0.437	377.6	0.406	219.5	0.095	335.3	0.005	296.0	0.005	319.4	0.295	304.8	0.340
7	321.1	0.366	358.9	0.309	215.0	0.378	337.7	0.005	300.1	0.005	325.6	0.246	314.5	0.338
8	327.0	0.411	366.8	0.334	221.4	0.183	334.3	0.005	306.6	0.005	324.1	0.257	304.1	0.328
9	325.9	0.355	372.4	0.401	232.0	0.049	332.4	0.005	292.1	0.005	328.9	0.239	311.4	0.345
mean	320.5	0.395	371.1	0.337	314.8	0.201	329.5	0.005	298.5	0.005	322.7	0.236	305.8	0.336
SD	4.2539	0.0426	7.0883	0.0441	22.3755	0.1465	6.5211	0.0000	3.8376	0.0000	3.9000	0.0474	5.0527	0.0186

Table D13. The raw data of particle size and polydispersity index of GPPG1 under storage condition

| | day 0 | | day 14 | | | | day 30 | | | | day 60 | | | |
| | | | 4 °C | | RT | | 4 °C | | RT | | 4 °C | | RT | |
No.	size	PI	size	PI	size	PI	size	PI	size	PI	size	PI	size	PI
1	291.3	0.332	275.8	0.256	287.7	0.290	324.9	0.307	431.7	0.368				
2	294.4	0.349	273.2	0.263	286.4	0.311	334.8	0.338	444.1	0.362				
3	284.8	0.345	267.6	0.288	285.5	0.310	339.1	0.345	437.3	0.350				
4	287.7	0.347	260.1	0.274	286.1	0.307	352.0	0.347	446.9	0.356				
5	295.4	0.342	272.6	0.269	286.9	0.311	360.5	0.340	428.7	0.354	Phase seperation		Phase seperation	
6	299.4	0.348	274.5	0.271	286.7	0.304	329.5	0.333	425.1	0.360				
7	290.8	0.332	278.1	0.273	286.8	0.307	320.7	0.335	412.3	0.362				
8	285.1	0.348	275.4	0.249	284.6	0.308	326.5	0.338	421.5	0.368				
9	296.1	0.349	271.5	0.258	285.9	0.309	338.0	0.347	420.4	0.365				
mean	291.7	0.344	272.1	0.267	286.3	0.306	336.2	0.337	429.8	0.361				
SD	5.0961	0.0069	5.3899	0.0117	0.8992	0.0065	13.0415	0.0122	11.4212	0.0062				

Table D14. The raw data of particle size and polydispersity index of GPPG3 under storage condition

| | day 0 | | day 14 | | | | day 30 | | | | day 60 | | | |
| | | | 4 °C | | RT | | 4 °C | | RT | | 4 °C | | RT | |
No.	size	PI	size	PI	size	PI	size	PI	size	PI	size	PI	size	PI
1	194.7	0.332	188.0	0.276	201.2	0.294	183.9	0.307	186.9	0.267	193.8	0.270	197.2	0.255
2	203.7	0.270	183.9	0.260	200.7	0.240	182.5	0.300	186.2	0.260	192.7	0.265	198.4	0.246
3	201.7	0.290	188.1	0.278	197.6	0.262	183.0	0.291	187.5	0.272	190.8	0.289	201.2	0.264
4	222.5	0.279	187.3	0.282	199.1	0.240	184.9	0.271	190.5	0.251	191.1	0.282	203.1	0.282
5	205.9	0.342	184.7	0.256	193.1	0.272	183.8	0.286	190.4	0.252	189.0	0.266	200.7	0.248
6	204.7	0.341	188.7	0.281	202.8	0.283	182.6	0.278	198.6	0.252	188.5	0.267	206.8	0.253
7	214.0	0.334	190.5	0.274	199.4	0.268	182.6	0.289	189.2	0.212	189.3	0.272	202.9	0.251
8	211.1	0.298	186.0	0.277	197.7	0.279	184.5	0.277	190.2	0.213	192.8	0.276	208.3	0.245
9	206.3	0.134	188.2	0.278	199.9	0.218	186.7	0.284	190.9	0.260	191.2	0.288	207.0	0.244
mean	207.2	0.291	187.3	0.274	199.1	0.262	183.8	0.287	190.0	0.249	191.0	0.275	202.8	0.254
SD	7.9297	0.0651	2.0658	0.0092	2.7745	0.0245	1.3838	0.0114	3.6425	0.0217	1.8438	0.0093	3.8997	0.0121

Table D15. The raw data of particle size and polydispersity index of GPPG5 under storage condition

| | day 0 | | day 14 | | | | day 30 | | | | day 60 | | | |
| | | | 4 °C | | RT | | 4 °C | | RT | | 4 °C | | RT | |
No.	size	PI	size	PI	size	PI	size	PI	size	PI	size	PI	size	PI
1	197.8	0.216	197.3	0.057	216.1	0.005	207.0	0.209	220.3	0.155	196.2	0.254	227.3	0.264
2	217.1	0.261	196.0	0.299	212.7	0.317	208.1	0.294	221.3	0.136	202.9	0.263	229.4	0.275
3	196.2	0.244	192.8	0.166	203.6	0.168	203.0	0.301	223.7	0.169	199.5	0.267	225.2	0.268
4	215.3	0.160	194.6	0.197	205.1	0.227	208.7	0.303	225.7	0.172	204.1	0.274	228.4	0.272
5	226.3	0.067	189.2	0.225	205.3	0.249	204.6	0.218	223.2	0.248	207.5	0.286	231.0	0.270
6	205.5	0.165	188.8	0.188	207.0	0.187	202.7	0.230	221.2	0.283	205.3	0.279	227.3	0.284
7	210.0	0.153	193.1	0.136	216.5	0.334	206.1	0.244	226.0	0.212	203.5	0.263	227.8	0.269
8	214.7	0.121	193.6	0.258	209.4	0.300	209.8	0.325	226.9	0.159	209.7	0.275	236.3	0.271
9	206.3	0.219	192.8	0.209	212.4	0.303	209.1	0.296	212.9	0.258	209.7	0.286	237.6	0.264
mean	209.9	0.178	193.1	0.193	209.8	0.232	206.6	0.269	222.4	0.199	204.3	0.272	230.0	0.271
SD	9.6140	0.0623	2.7933	0.0700	4.8545	0.1032	2.6391	0.0433	4.2385	0.0527	4.4839	0.0110	4.2400	0.0061

Table D16. The raw data of particle size and polydispersity index of GPTG1 under storage condition

| | day 0 | | day 14 | | | | day 30 | | | | day 60 | | | |
| | | | 4 °C | | RT | | 4 °C | | RT | | 4 °C | | RT | |
No.	size	PI	size	PI	size	PI	size	PI	size	PI	size	PI	size	PI
1	216.4	0.248	180.3	0.150	219.5	0.281	213.4	0.228	208.2	0.299	685.8	0.408		
2	220.8	0.250	183.6	0.162	217.3	0.288	209.8	0.226	206.0	0.269	655.9	0.477		
3	219.1	0.260	194.2	0.217	215.3	0.278	210.3	0.221	202.4	0.302	674.7	0.352		
4	219.5	0.266	197.2	0.200	206.3	0.301	211.3	0.239	203.2	0.313	696.7	0.347		
5	215.8	0.253	197.5	0.196	218.4	0.304	212.0	0.249	204.1	0.305	682.3	0.366	Phase seperation	
6	220.4	0.259	196.7	0.194	203.6	0.309	209.5	0.258	206.2	0.299	696.7	0.347		
7	219.0	0.260	194.8	0.192	204.9	0.285	212.1	0.260	205.7	0.298	708.4	0.364		
8	216.8	0.270	196.0	0.199	202.6	0.302	206.8	0.264	203.6	0.208	707.8	0.318		
9	217.2	0.272	198.2	0.223	205.2	0.310	209.5	0.223	205.0	0.282	689.5	0.329		
mean	218.3	0.260	193.2	0.193	210.3	0.295	210.5	0.241	204.9	0.286	688.6	0.368		
SD	1.8214	0.0085	6.5355	0.0234	7.0674	0.0123	1.9389	0.0172	1.7993	0.0320	16.5934	0.0483		

Table D17. The raw data of particle size and polydispersity index of GPTG3 under storage condition

| | day 0 | | day 14 | | | | day 30 | | | | day 60 | | | |
| | | | 4 °C | | RT | | 4 °C | | RT | | 4 °C | | RT | |
No.	size	PI	size	PI	size	PI	size	PI	size	PI	size	PI	size	PI
1	154.8	0.223	149.0	0.184	145.3	0.184	157.0	0.214	262.2	0.213	162.6	0.322	279.8	0.192
2	136.5	0.280	155.5	0.244	147.9	0.209	161.0	0.257	260.4	0.221	175.6	0.257	274.8	0.197
3	138.1	0.296	143.4	0.152	146.5	0.209	160.8	0.249	257.1	0.213	174.6	0.318	275.5	0.192
4	144.5	0.266	142.5	0.265	146.2	0.256	155.8	0.208	254.4	0.215	176.7	0.208	276.5	0.196
5	153.4	0.259	146.1	0.152	144.4	0.209	159.3	0.255	252.8	0.150	178.9	0.319	275.4	0.199
6	152.9	0.273	145.4	0.248	145.5	0.234	158.3	0.254	250.5	0.270	181.8	0.254	269.4	0.277
7	145.2	0.232	148.0	0.246	143.4	0.146	154.2	0.240	246.3	0.147	182.3	0.320	267.6	0.237
8	146.6	0.197	147.3	0.287	148.9	0.223	154.3	0.246	261.9	0.157	184.2	0.314	276.0	0.194
9	149.5	0.258	141.7	0.206	143.0	0.126	154.9	0.247	247.1	0.152	181.6	0.247	267.8	0.262
mean	146.8	0.254	146.5	0.220	145.7	0.200	157.3	0.241	254.7	0.193	177.6	0.284	273.6	0.216
SD	6.5357	0.0310	4.1854	0.0491	1.9505	0.0414	2.6844	0.0179	6.0826	0.0432	6.5172	0.0430	4.3035	0.0335

Table D18. The raw data of particle size and polydispersity index of GPTG5 under storage condition

| | day 0 | | day 14 | | | | day 30 | | | | day 60 | | | |
| | | | 4 °C | | RT | | 4 °C | | RT | | 4 °C | | RT | |
No.	size	PI	size	PI	size	PI	size	PI	size	PI	size	PI	size	PI
1	159.4	0.185	171.3	0.192	168.3	0.302	193.0	0.285	200.8	0.229	199.0	0.275	230.1	0.277
2	157.1	0.240	166.8	0.229	165.6	0.181	192.0	0.280	202.1	0.232	201.2	0.227	229.5	0.257
3	174.7	0.139	166.5	0.267	166.0	0.254	189.8	0.267	207.7	0.234	206.8	0.298	228.1	0.270
4	175.0	0.200	168.5	0.172	168.5	0.086	190.8	0.275	205.6	0.237	196.5	0.260	225.7	0.264
5	164.2	0.223	175.7	0.318	170.1	0.237	191.3	0.267	204.8	0.229	194.2	0.257	228.8	0.274
6	171.2	0.219	170.9	0.289	170.1	0.292	186.6	0.253	208.2	0.278	198.9	0.254	222.5	0.283
7	165.1	0.245	170.6	0.221	160.2	0.228	188.0	0.203	203.6	0.247	206.4	0.310	223.5	0.232
8	157.0	0.246	176.0	0.102	169.8	0.265	189.8	0.267	207.5	0.240	213.5	0.314	229.2	0.262
9	169.4	0.253	176.7	0.165	177.6	0.296	191.7	0.268	204.0	0.233	193.8	0.278	217.2	0.198
mean	165.9	0.217	171.4	0.217	168.5	0.238	190.3	0.263	204.9	0.240	201.1	0.275	226.1	0.257
SD	7.0977	0.0369	3.9084	0.0677	4.6530	0.0688	2.0267	0.0242	2.5772	0.0154	6.5731	0.0287	4.2945	0.0267

Table D19. The raw data of particle size and polydispersity index of GBPG1 under storage condition

| | day 0 | | day 14 | | | | | | | | | | | | |
| | | | 4 °C | | RT | | 4 °C | | RT | | 4 °C | | RT | | |
No.	size	PI	size	PI	size	PI	size	PI	size	PI	size	PI	size	PI
1	443.4	0.162	364.6	0.326										
2	441.9	0.166	367.0	0.331										
3	436.9	0.110	369.2	0.221										
4	438.7	0.172	368.4	0.232										
5	427.6	0.182	373.6	0.244	Phase seperation		Phase seperation		Phase seperation		Phase seperation		Phase seperation	
6	433.4	0.174	359.0	0.230										
7	432.1	0.177	367.0	0.244										
8	438.2	0.214	354.1	0.231										
9	437.7	0.221	369.8	0.224										
mean	436.7	0.175	365.9	0.254										
SD	4.9252	0.0320	5.9433	0.0431										

Table D20. The raw data of particle size and polydispersity index of GBPG3 under storage condition

| | day 0 | | day 14 | | | | day 30 | | | | day 60 | | | |
| | | | 4 °C | | RT | | 4 °C | | RT | | 4 °C | | RT | |
No.	size	PI	size	PI	size	PI	size	PI	size	PI	size	PI	size	PI
1	362.1	0.005	339.5	0.175	370.5	0.215	394.6	0.411						
2	319.8	0.005	395.3	0.123	397.5	0.365	401.7	0.423						
3	374.7	0.005	396.9	0.315	379.3	0.111	398.3	0.367						
4	342.8	0.005	397.2	0.005	390.8	0.252	405.1	0.342						
5	363.4	0.005	381.6	0.474	389.2	0.173	401.4	0.514	Phase seperation		Phase seperation		Phase seperation	
6	333.0	0.005	368.2	0.196	390.6	0.297	398.8	0.456						
7	347.0	0.121	335.5	0.005	379.0	0.301	386.7	0.344						
8	346.6	0.116	334.6	0.678	378.2	0.145	403.4	0.367						
9	348.3	0.134	354.0	0.354	373.8	0.374	399.4	0.371						
mean	348.6	0.045	367.0	0.258	383.2	0.248	398.8	0.399						
SD	16.5665	0.0595	26.8998	0.2215	9.0865	0.0941	5.4849	0.0573						

Table D21. The raw data of particle size and polydispersity index of GBPG5 under storage condition

| | day 0 | | day 14 | | | | day 30 | | | | day 60 | | | |
| | | | 4 °C | | RT | | 4 °C | | RT | | 4 °C | | RT | |
No.	size	PI	size	PI	size	PI	size	PI	size	PI	size	PI	size	PI
1	346.0	0.005	314.4	0.175	392.6	0.145	356.6	0.305						
2	321.5	0.005	315.5	0.237	355.8	0.075	350.3	0.312						
3	324.5	0.005	326.2	0.327	344.7	0.235	359.5	0.323						
4	317.5	0.005	337.9	0.137	353.9	0.041	351.6	0.419						
5	343.7	0.005	322.5	0.074	362.6	0.314	362.1	0.343	Phase seperation		Phase seperation		Phase seperation	
6	339.8	0.005	330.7	0.096	346.3	0.306	353.5	0.296						
7	329.2	0.005	329.4	0.312	335.7	0.133	365.9	0.287						
8	327.5	0.005	321.2	0.278	336.9	0.254	362.6	0.354						
9	343.8	0.005	319.9	0.154	365.7	0.177	352.1	0.246						
mean	332.6	0.005	324.2	0.199	354.9	0.187	357.1	0.321						
SD	10.8077	0.0000	7.6083	0.0932	17.5701	0.0973	5.6252	0.0486						

Table D22. The raw data of particle size and polydispersity index of GBTG1 under storage condition

	day 0		day 14											
			4 °C		RT		4 °C		RT		4 °C		RT	
							day 30				day 60			
No.	size	PI	size	PI	size	PI	size	PI	size	PI	size	PI	size	PI
1	359.5	0.280	495.1	0.226										
2	357.5	0.246	490.9	0.214										
3	341.3	0.230	485.4	0.334										
4	352.1	0.256	472.5	0.336										
5	340.4	0.214	477.8	0.309	Phase seperation		Phase seperation		Phase seperation		Phase seperation		Phase seperation	
6	358.4	0.200	494.9	0.261										
7	352.1	0.208	500.7	0.245										
8	347.8	0.204	487.8	0.220										
9	331.5	0.229	496.6	0.206										
mean	349.0	0.230	489.1	0.261										
SD	9.5590	0.0268	9.2352	0.0520										

Table D23. The raw data of particle size and polydispersity index of GBTG3 under storage condition

No.	day 0 size	day 0 PI	day 14 4 °C size	day 14 4 °C PI	day 14 RT size	day 14 RT PI	day 30 4 °C size	day 30 4 °C PI	day 30 RT size	day 30 RT PI	day 60 4 °C size	day 60 4 °C PI	day 60 RT size	day 60 RT PI
1	299.0	0.075	341.8	0.211	331.8	0.345	326.0	0.215	325.5	0.435	356.5	0.305	386.6	0.332
2	289.8	0.434	332.4	0.125	321.2	0.167	324.4	0.254	321.9	0.415	354.0	0.325	389.0	0.334
3	297.4	0.403	345.1	0.231	340.2	0.351	330.7	0.235	328.2	0.418	340.3	0.318	383.9	0.327
4	292.4	0.005	331.0	0.143	341.8	0.296	324.7	0.312	336.7	0.404	366.7	0.330	386.7	0.362
5	273.7	0.029	339.3	0.354	326.0	0.179	326.9	0.287	337.1	0.417	358.5	0.327	391.8	0.329
6	299.8	0.057	336.3	0.267	336.5	0.211	324.1	0.324	334.1	0.400	352.2	0.285	365.8	0.355
7	293.9	0.160	343.5	0.147	332.2	0.278	323.2	0.253	329.3	0.398	355.7	0.293	370.3	0.336
8	291.2	0.013	327.6	0.466	327.6	0.322	321.9	0.314	328.0	0.395	356.1	0.306	366.5	0.327
9	286.9	0.079	345.6	0.372	331.5	0.324	320.8	0.243	334.9	0.328	361.0	0.309	371.8	0.332
mean	291.6	0.139	338.1	0.257	332.1	0.275	324.7	0.271	330.6	0.401	355.7	0.311	379.2	0.337
SD	7.9645	0.1649	6.5757	0.1182	6.6689	0.0713	2.9211	0.0394	5.3162	0.0302	7.1591	0.0155	10.3845	0.0126

Table D24. The raw data of particle size and polydispersity index of GBTG5 under storage condition

| | day 0 | | day 14 | | | | day 30 | | | | day 60 | | | |
| | | | 4 °C | | RT | | 4 °C | | RT | | 4 °C | | RT | |
No.	size	PI	size	PI	size	PI	size	PI	size	PI	size	PI	size	PI
1	302.5	0.259	317.4	0.393	302.3	0.129	344.5	0.196	340.9	0.294	379.4	0.250	330.0	0.301
2	296.6	0.309	316.4	0.390	300.8	0.312	344.1	0.180	340.4	0.306	383.7	0.248	332.6	0.316
3	295.1	0.277	315.8	0.332	299.8	0.145	345.4	0.173	336.3	0.255	380.0	0.269	335.1	0.312
4	314.1	0.097	321.8	0.353	299.6	0.134	334.8	0.369	338.0	0.247	375.7	0.265	328.9	0.310
5	313.0	0.277	316.2	0.317	309.5	0.143	342.4	0.354	336.2	0.340	363.2	0.283	328.1	0.312
6	300.7	0.005	317.0	0.267	304.1	0.321	347.9	0.325	343.2	0.272	362.9	0.272	326.3	0.327
7	296.9	0.005	321.2	0.279	302.2	0.342	345.2	0.319	345.7	0.283	371.6	0.248	322.5	0.302
8	309.6	0.233	326.3	0.167	303.0	0.179	347.9	0.327	341.5	0.215	363.9	0.253	328.2	0.310
9	313.7	0.033	316.8	0.135	304.3	0.134	345.2	0.325	338.9	0.247	368.4	0.261	326.3	0.314
mean	304.7	0.166	318.8	0.293	302.8	0.204	344.2	0.285	340.1	0.273	372.1	0.261	328.7	0.312
SD	7.9192	0.1287	3.5658	0.0914	3.0146	0.0920	3.9132	0.0786	3.1455	0.0373	7.9706	0.0123	3.6821	0.0077

Appendix E

Entrapment efficiency study

Table E1 The raw data for entrapment efficiency study (% entrapment) of SLN dispersions at day 0

SLN	N 1	N 2	N 3	N 4	N 5	Mean	SD
GPTG3	95.56	96.42	97.28	96.67	95.43	96.27	0.7766
GPTG5	89.32	91.57	88.83	91.07	90.88	90.33	1.1893
GBTG3	94.05	96.88	94.23	97.07	95.27	95.50	1.4263
GBTG5	88.42	90.28	91.41	90.8	91.26	90.43	1.2092
GPPG3	88.83	89.19	86.85	89.85	88.21	88.59	1.1377
GPPG5	83.59	85.51	84.95	83.96	84.58	84.52	0.7660

Table E2 The raw data for entrapment efficiency study (% entrapment) of SLN dispersions at day 30

SLN	N 1	N 2	N 3	N 4	N 5	Mean	SD
GPTG3	95.82	95.78	97.71	96.94	94.93	96.24	0.9752
GPTG5	88.67	91.54	88.91	90.38	91.10	90.12	1.1499
GBTG3	94.22	96.80	94.03	96.41	94.88	95.27	1.1343
GBTG5	89.09	90.26	90.91	90.83	90.92	90.40	0.7002
GPPG3	88.53	89.09	87.90	89.22	88.55	88.66	0.4701
GPPG5	83.62	85.06	84.41	84.02	84.67	84.36	0.5003

Table E3 The raw data for entrapment efficiency study (% entrapment) of SLN dispersions at day 60

SLN	N 1	N 2	N 3	N 4	N 5	Mean	SD
GPTG3	93.28	93.34	93.01	93.46	93.21	93.26	0.1495
GPTG5	87.29	89.10	87.64	89.72	88.72	88.49	0.9056
GBTG3	91.80	93.99	96.67	92.14	91.81	93.28	1.8787
GBTG5	86.66	87.40	86.39	88.42	87.35	87.24	0.7055
GPPG3	86.32	87.80	85.27	86.12	85.74	86.25	0.8538
GPPG5	79.51	80.72	77.21	78.68	78.45	78.91	1.1654

Table E4 The raw data for entrapment efficiency study (%free [6] - gingerol) of SLN dispersions at day 0

SLN	N 1	N 2	N 3	N 4	N 5	Mean	SD
GPTG3	3.76	3.18	2.86	2.91	3.16	3.17	0.3200
GPTG5	9.58	9.55	10.24	9.34	9.07	9.56	0.3876
GBTG3	4.05	3.04	4.1	2.94	3.79	3.58	0.4973
GBTG5	10.72	9.88	9.47	9.38	8.98	9.69	0.5909
GPPG3	11.03	10.99	11.06	10.52	10.65	10.85	0.2214
GPPG5	14.76	13.88	13.74	14.33	13.96	14.13	0.3689

Table E5 The raw data for entrapment efficiency study (%free [6] - gingerol) of SLN
dispersions at day 30

SLN	N 1	N 2	N 3	N 4	N 5	Mean	SD
GPTG3	3.63	3.09	3.01	3.03	3.44	3.24	0.2496
GPTG5	9.39	9.40	9.58	9.60	9.39	9.47	0.0966
GBTG3	5.74	4.92	5.80	4.40	5.65	5.30	0.5514
GBTG5	10.04	9.89	9.96	9.90	9.40	9.84	0.2254
GPPG3	9.52	9.40	9.54	9.60	9.90	9.59	0.1671
GPPG5	15.59	15.50	15.58	15.85	15.88	15.68	0.1545

Table E6 The raw data for entrapment efficiency study (%free [6] - gingerol) of SLN
dispersions at day 60

SLN	N 1	N 2	N 3	N 4	N 5	Mean	SD
GPTG3	3.74	5.85	5.84	5.92	6.17	5.50	0.8900
GPTG5	11.37	11.53	11.20	11.56	11.48	11.43	0.1311
GBTG3	7.30	7.21	8.25	8.27	7.33	7.67	0.4818
GBTG5	16.22	13.07	12.70	12.02	12.71	13.34	1.4776
GPPG3	12.51	12.68	12.69	18.84	13.09	13.96	2.4464
GPPG5	16.69	17.14	18.65	18.89	19.22	18.12	1.0089

Table E7 One-way analysis of variance on the percentages of entrapped [6] – gingerol
at day 0

ANOVA

% Entrapment

	Sum of Squares	df	Mean Square	F	Sig.
Between Groups	480.869	5	96.174	46.286	0.000
Within Groups	49.867	24	2.078		
Total	530.736	29			

Table E8 Homogeneous subset on the percentages of entrapped [6] – gingerol
at day 0 by Duncan method

% Entrapment

type of formulation	N	Subset for alpha = .05			
		1	2	3	4
GPPG5	5	84.5160			
GPPG3	5		88.5860		
GBTG5	5		90.4340	90.4340	
GPTG5	5			91.2080	
GBTG3	5				95.4980
GPTG3	5				96.2680
Sig.		1.000	0.054	0.404	0.407

Means for groups in homogeneous subsets are displayed.
a Uses Harmonic Mean Sample Size = 5.000.

Table E9. One-way analysis of variance on the percentages of entrapped [6] – gingerol at day 30

ANOVA

% Entrapment

	Sum of Squares	df	Mean Square	F	Sig.
Between Groups	480.451	5	96.090	102.106	0.000
Within Groups	22.586	24	0.941		
Total	503.037	29			

Table E10 Homogeneous subset on the percentages of entrapped [6] – gingerol at day 30 by Duncan method

% Entrapment

type of formulation	N	Subset for alpha = 0.05			
		1	2	3	4
GPPG5	5	84.3560			
GPPG3	5		88.6920		
GPTG5	5			90.1200	
GBTG5	5			90.4020	
GBTG3	5				95.2680
GPTG3	5				96.2360
Sig.		1.000	1.000	0.650	0.128

Means for groups in homogeneous subsets are displayed.
a Uses Harmonic Mean Sample Size = 5.000.

Table E11 One-way analysis of variance on the percentages of entrapped [6] – gingerol at day 60

ANOVA

% Entrapment

	Sum of Squares	df	Mean Square	F	Sig.
Between Groups	649.019	5	129.804	132.243	0.000
Within Groups	23.557	24	0.982		
Total	672.577	29			

Table E12 Homogeneous subset on the percentages of entrapped [6] – gingerol at day 60 by Duncan method

% Entrapment

type of formulation	N	Subset for alpha = 0.05			
		1	2	3	4
GPPG5	5	78.9140			
GPPG3	5		86.2500		
GBTG5	5		87.2380	87.2380	
GPTG5	5			88.4980	
GBTG3	5				92.0320
GPTG3	5				93.2580
Sig.		1.000	0.128	0.056	0.062

Means for groups in homogeneous subsets are displayed.
a Uses Harmonic Mean Sample Size = 5.000.

Table E13 One-way analysis of variance on the percentages of entrapped [6] – gingerol of GPTG3

ANOVA

% Entrapment

	Sum of Squares	df	Mean Square	F	Sig.
Between Groups	29.883	2	14.942	24.648	0.000
Within Groups	7.274	12	0.606		
Total	37.157	14			

Table E14 Homogeneous subset on the percentages of entrapped [6] – gingerol of GPTG3 by Duncan method

% Entrapment

DAY	N	Subset for alpha = 0.05	
		1	2
60	5	93.2580	
30	5		96.2360
0	5		96.2680
Sig.		1.000	0.949

Means for groups in homogeneous subsets are displayed.
a Uses Harmonic Mean Sample Size = 5.000.

Table E15 One-way analysis of variance on the percentages of entrapped [6] – gingerol GPTG5

ANOVA

% Entrapment

	Sum of Squares	df	Mean Square	F	Sig.
Between Groups	18.598	2	9.299	3.040	0.085
Within Groups	36.703	12	3.059		
Total	55.301	14			

Table E16 Homogeneous subset on the percentages of entrapped [6] – gingerol of GPTG5 by Duncan method

% Entrapment

DAY	N	Subset for alpha = 0.05	
		1	2
60	5	88.4980	
30	5	90.1200	90.1200
0	5		91.2080
Sig.		0.168	0.345

Means for groups in homogeneous subsets are displayed.
a Uses Harmonic Mean Sample Size = 5.000.

Table E17 One-way analysis of variance on the percentages of entrapped [6] – gingerol GBTG3

ANOVA

% Entrapment

	Sum of Squares	df	Mean Square	F	Sig.
Between Groups	37.563	2	18.781	10.725	0.002
Within Groups	21.014	12	1.751		
Total	58.577	14			

Table E18 Homogeneous subset on the percentages of entrapped [6] – gingerol of GBTG3 by Duncan method

% Entrapment

DAY	N	Subset for alpha = 0.05	
		1	2
60	5	92.0320	
30	5		95.2680
0	5		95.4980
Sig.		1.000	0.788

Means for groups in homogeneous subsets are displayed.
a Uses Harmonic Mean Sample Size = 5.000.

Table E19 One-way analysis of variance on the percentages of entrapped [6] – gingerol GBTG5

ANOVA

% Entrapment

	Sum of Squares	df	Mean Square	F	Sig.
Between Groups	33.711	2	16.855	18.772	0.000
Within Groups	10.775	12	0.898		
Total	44.485	14			

Table E20 Homogeneous subset on the percentages of entrapped [6] – gingerol of GBTG5 by Duncan method

% Entrapment

DAY	N	Subset for alpha = 0.05	
		1	2
60	5	87.2380	
30	5		90.4020
0	5		90.4340
Sig.		1.000	0.958

Means for groups in homogeneous subsets are displayed.
a Uses Harmonic Mean Sample Size = 5.000.

Table E21 One-way analysis of variance on the percentages of entrapped [6] – gingerol GPPG3

ANOVA

% Entrapment

	Sum of Squares	df	Mean Square	F	Sig.
Between Groups	19.052	2	9.526	11.539	0.002
Within Groups	9.907	12	0.826		
Total	28.959	14			

Table E22 Homogeneous subset on the percentages of entrapped [6] – gingerol of GPPG3 by Duncan method

% Entrapment

DAY	N	Subset for alpha = 0.05	
		1	2
60	5	86.2500	
0	5		88.5860
30	5		88.6920
Sig.		1.000	0.857

Means for groups in homogeneous subsets are displayed.
a Uses Harmonic Mean Sample Size = 5.000.

Table E23 One-way analysis of variance on the percentages of entrapped [6] – gingerol GPPG5

ANOVA

% Entrapment

	Sum of Squares	df	Mean Square	F	Sig.
Between Groups	101.706	2	50.853	59.028	0.000
Within Groups	10.338	12	0.861		
Total	112.044	14			

Table E24 Homogeneous subset on the percentages of entrapped [6] – gingerol of GPPG5 by Duncan method

% Entrapment

DAY	N	Subset for alpha = 0.05	
		1	2
60	5	78.9140	
30	5		84.3560
0	5		84.5160
Sig.		1.000	0.790

Means for groups in homogeneous subsets are displayed.
a Uses Harmonic Mean Sample Size = 5.000.

APPENDIX F

Validation of Analytical Method

Analysis of [6]-gingerol by high performance liquid chromatographic (HPLC) method

1. The determination of [6]-gingerol content in 20% isopropanol in PBS buffer pH 7.4

The determination of [6]-gingerol content in 20% isopropanol in PBS buffer pH 7.4 was performed for analysis of [6]-gingerol content in receiver medium of Franz cell in release study.

The validation of analytical method is the process by which it is established that the performance characteristics of the method meet the requirements for the intended analytical applications. The performance characteristics are expressed in term of analytical parameters. For HPLC assay validation, these include specificity, linearity, accuracy and precision.

1.1 Specificity

The specificity of an analytical method is the ability to measure the analyses accurately and with specificity in the presence of other components in the sample. Figures F1 were shown typical chromatogram of [6]-gingerol standard solution, internal standard solution, ginger extract solution, respectively. The chromatograms demonstrated that the HPLC condition used in the study had a suitable specificity.
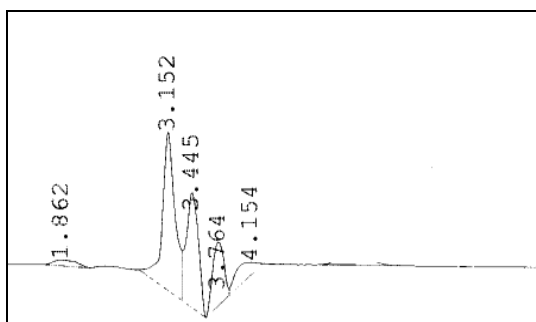
(a)
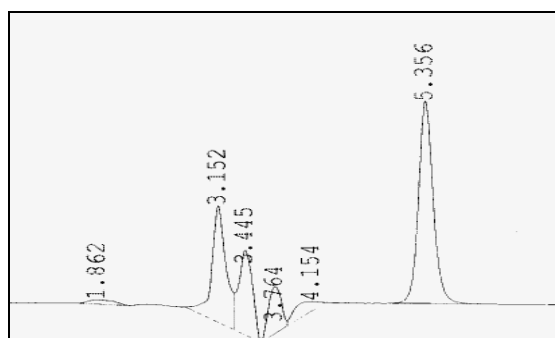
(b)
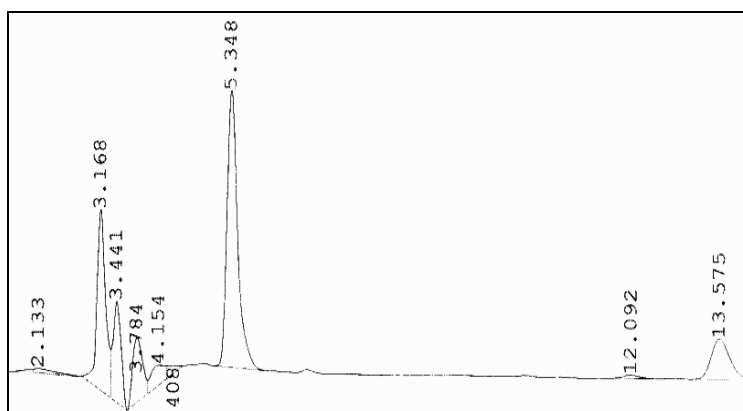
(c)

Figure F1 HPLC chromatograms of in HPLC validation

    (a) Phosphate buffer pH 7.4

    (b) prednisolone solution

    (c) prednisolone solution and [6]-gingerol standard
       solution

1.2 Linearity

Table F1 Data for calibration curve of [6]-gingerol in 20% IPA in PBS pH 7.4

Concentration (µg/ml)	Peak height ratio			Mean	SD	%CV
	Set1	Set2	Set3			
0.25	0.3338	0.3358	0.3327	0.3341	0.0016	0.4704
0.5	0.4625	0.4664	0.4613	0.4634	0.0027	0.5754
1	0.666	0.6699	0.6660	0.6673	0.0023	0.3374
3	1.3359	1.3375	1.3351	1.3362	0.0012	0.0915
5	2.0556	2.0451	2.0526	2.0511	0.0054	0.2637
7	2.7163	2.7127	2.7180	2.7157	0.0027	0.0997
9	3.3841	3.3948	3.3867	3.3885	0.0056	0.1647
R2	**0.9995**	**0.9996**	**0.9995**	**0.9995**	**-**	**-**

$$y = 0.3464x + 0.2911$$
$$R^2 = 0.9995$$
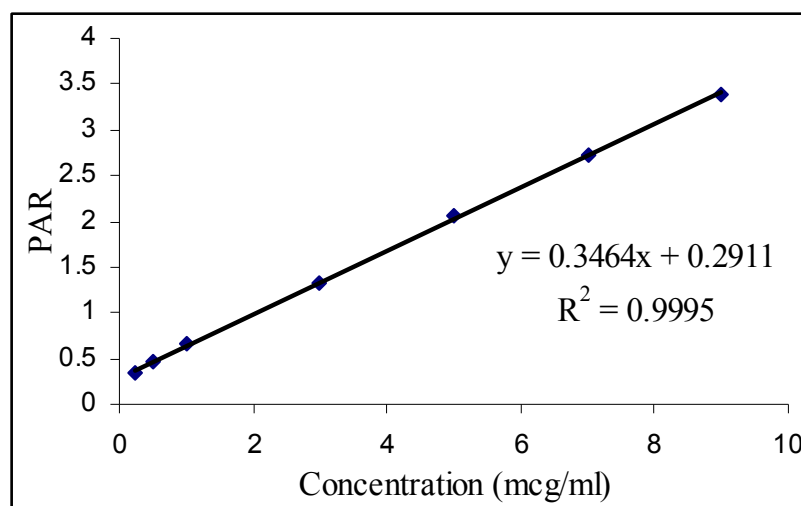
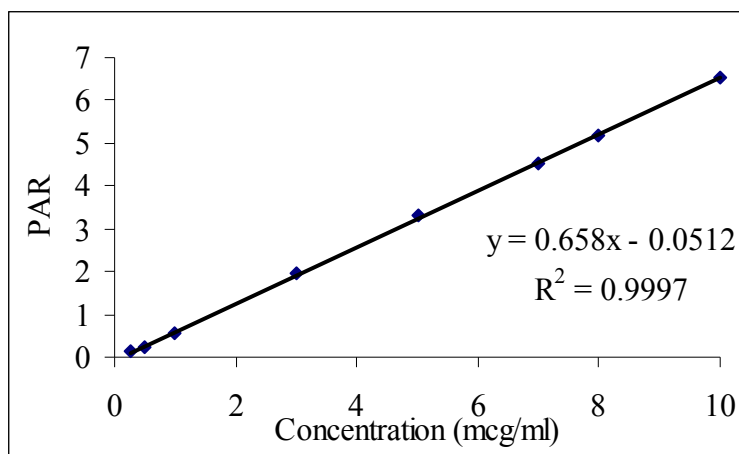Figure F2 Calibration curve of [6]-gingerol in 20% IPA in PBS pH 7.4 by HPLC method

1.3 Accuracy

The accuracy of an analytical method is the closeness of test results obtained by the method to the true value. Accuracy is calculated as percent recovery by the assay of known added amount of analyses. The percentages of analytical recovery of [6]-gingerol solution are showed in Table F2. The percentages analytical

recovery of [6]-gingerol was in the range of 100.63-100.95% which indicated that this method could be used for analysis in all concentrations studied with a high accuracy.

Table F2 The percentages of analytical recovery of [6]-gingerol solution in 20% IPA in PBS buffer pH 7.4 by HPLC method

Concentration (µg/ml)	%Analytical recovery					Mean ± SD
	1	2	3	4	5	
0.75	100.22	101.68	99.49	98.83	101.99	100.95±1.37
2	99.75	101.62	99.36	100.74	99.05	100.68±0.65
6	99.75	101.51	100.84	100.71	99.49	100.63±0.83

1.4 Precision

The precision of [6]-gingerol analyzed by HPLC method were determined both within run precision and between run precision as illustrated in Tables F3 and Table F4. All coefficients of variation values were small, as 0.64-0.74% and 0.21-0.75%, respectively. The coefficient of variation of an analytical method should generally be less than 2%. Therefore, the HPLC method was precise for quantitative analysis of [6]-gingerol in the range studied.

Table F3 Data of within run precision of [6]-gingerol in 20% IPA in PBS pH 7.4

Concentration (µg/ml)	Peak area ratio					Mean	SD	%CV
	Set1	Set2	Set3	Set4	Set5			
0.75	0.5526	0.5564	0.5507	0.5490	0.5572	0.5532	0.0036	0.64
2	0.9832	0.9961	0.9805	0.9900	0.9783	0.9856	0.0073	0.74
6	2.3649	2.4015	2.3875	2.3849	2.3595	2.3797	0.0172	0.72

Table F4 Data of between run precision of [6]-gingerol in 20% IPA in PBS pH 7.4

Concentration (µg/ml)	Peak area ratio					Mean	SD	%CV
	Set1	Set2	Set3	Set4	Set5			
0.75	0.5526	0.5496	0.5470	0.5580	0.5504	0.5515	0.0041	0.75
2	0.9832	0.9883	0.9855	0.9856	0.9832	0.9852	0.0021	0.21
6	2.3649	2.3763	2.3578	2.3577	2.3547	2.3623	0.0087	0.37

2. The determination of [6]-gingerol content in PBS buffer pH 7.4

The determination of [6]-gingerol content in PBS buffer pH 7.4 was performed for analysis of [6]-gingerol content in receiver medium of Franz cell in permeation study.

Table F5 Data for calibration curve of [6]-gingerol in PBS pH 7.4 by HPLC method

Concentration (μg/ml)	Peak height ratio			Mean	SD	%CV
	Set1	Set2	Set3			
0.25	0.1217	0.1247	0.1232	0.1232	0.0015	1.2175
0.5	0.2576	0.2507	0.2544	0.2542	0.0035	1.3582
1	0.5657	0.5703	0.5611	0.5657	0.0046	0.8132
3	1.9591	1.9628	1.9245	1.9488	0.0211	1.0840
5	3.3133	3.3504	3.3421	3.3353	0.0195	0.5838
7	4.4929	4.4968	4.5431	4.5109	0.0279	0.6191
8	5.2029	5.1751	5.2055	5.1945	0.0169	0.3244
10	6.5475	6.4469	6.5442	6.5129	0.0572	0.8775
R^2	0.9997	0.9994	0.9997	0.9997	-	-

Figure F3 Calibration curve of [6]-gingerol in PBS pH 7.4 by HPLC method

1.1.3 Accuracy

The accuracy of an analytical method is the closeness of test results obtained by the method to the true value. Accuracy is calculated as percent recovery by the assay of known added amount of analyses. The percentages of analytical

Table F8 Data of between run precision of [6]-gingerol in PBS pH 7.4 by HPLC method

Concentration (µg/ml)	Peak area ratio					Mean	SD	%CV
	Set1	Set2	Set3	Set4	Set5			
2	1.2560	1.2632	1.2574	1.2584	1.2445	1.2559	0.0069	0.55
4	2.5842	2.5506	2.611	2.5736	2.5609	2.5761	0.0233	0.90
6	3.9041	3.9267	3.9294	3.8952	3.8943	3.9099	0.0170	0.43

3. The determination of [6]-gingerol content in methanol

The determination of [6]-gingerol content in methanol was performed for analysis of [6]-gingerol content in new born pig skin in permeation study.

Table F9 Data for calibration curve of [6]-gingerol in methanol by HPLC method

| Concentration (µg/ml)	Peak height ratio			Mean	SD	%CV
	Set1	Set2	Set3			
2	2.1976	2.2050	2.1925	2.1984	0.0063	0.2859
4	2.8858	2.8749	2.8771	2.8793	0.0058	0.2002
6	3.7269	3.7313	3.7327	3.7303	0.0030	0.0811
8	4.4463	4.451	4.4756	4.4576	0.0157	0.3530
10	5.3830	5.3884	5.3833	5.3849	0.0030	0.0564
12	6.1412	6.1064	6.1431	6.1302	0.0207	0.3371
14	6.8851	6.8712	6.8926	6.8830	0.0109	0.1578
16	7.5695	7.6296	7.6243	7.6078	0.0333	0.4374
R2	**0.9990**	**0.9992**	**0.9993**	**0.9992**	-	-
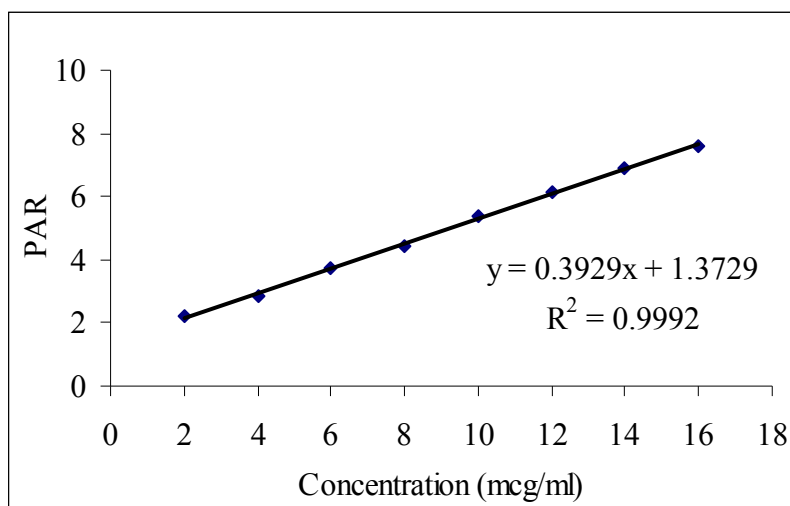
Figure F4 Calibration curve of [6]-gingerol in methanol by HPLC method

1.1.4 Accuracy

The accuracy of an analytical method is the closeness of test results obtained by the method to the true value. Accuracy is calculated as percent recovery by the assay of known added amount of analyses. The percentages of analytical recovery of [6]-gingerol solution are showed in Table F10. The percentages analytical recovery of [6]-gingerol was in the range of 98.61-99.66% which indicated that this method could be used for analysis in all concentrations studied with a high accuracy.

Table F10 The percentages of analytical recovery of [6]-gingerol solution in methanol by HPLC method

Concentration (μg/ml)	%Analytical recovery					Mean ± SD
	1	2	3	4	5	
3	98.58	98.49	98.64	98.70	99.91	98.86±0.59
9	100.23	100.16	99.99	99.75	98.16	99.66 ±0.86
13	98.61	98.68	98.55	98.68	98.54	98.61±0.17

1.4.2 Precision

The precision of [6]-gingerol analyzed by HPLC method were determined both within run precision and between run precision as illustrated in Tables F11 and Table F12. All coefficients of variation values were small, as 0.29-0.78% and 0.55-0.90%, respectively. The coefficient of variation of an analytical method should generally be less than 2%. Therefore, the HPLC method was precise for quantitative analysis of [6]-gingerol in the range studied.

Table F11 Data of within run precision of [6]-gingerol in methanol by HPLC method

Concentration (µg/ml)	Peak area ratio					Mean	SD	%CV
	Set1	Set2	Set3	Set4	Set5			
3	2.4714	2.4703	2.4722	2.4729	2.4878	2.4749	0.0073	0.29
9	4.9581	4.9554	4.9492	4.9403	4.8817	4.9369	0.0316	0.64
13	6.5157	6.5194	6.5128	6.5197	6.5119	6.5159	0.0036	0.16

Table F12 Data of between run precision of [6]-gingerol in methanol by HPLC method

Concentration (µg/ml)	Peak area ratio					Mean	SD	%CV
	Set1	Set2	Set3	Set4	Set5			
3	2.4612	2.4714	2.4627	2.4543	2.4465	2.4592	0.0094	0.38
9	4.8631	4.9581	4.9341	4.9279	4.9141	4.9195	0.0353	0.72
13	6.4601	6.5157	6.4933	6.4726	6.4624	6.4808	0.0235	0.36

Appendix G

The release study

Table G1 The percentage of cumulative release of [6]-gingerol from acetone extract solution

Time	% Cumulative release of [6]-gingerol					mean	SD
	N1	N2	N3	N4	N5		
2	0.203	0.095	0.812	3.882	0.543	1.107	1.725
4	73.171	72.901	74.365	81.018	83.684	77.028	5.184
6	94.802	97.308	96.965	95.091	96.678	96.169	0.981
8	101.073	99.764	99.931	100.755	100.755	100.339	0.433
10	101.073	100.719	99.931	100.755	100.755	100.339	1.707
12	101.073	100.719	99.931	100.755	100.755	100.339	2.020
14	101.073	100.719	99.931	100.755	100.755	100.339	5.536
16	101.073	100.719	99.931	100.755	100.755	100.339	5.339
20	101.073	100.719	99.931	100.755	100.755	100.339	1.510
24	101.073	100.719	99.931	100.755	100.755	100.339	2.940

Table G2 The percentage of cumulative release of [6]-gingerol from GPTG3

Time	% Cumulative release of [6]-gingerol					mean	SD
	N1	N2	N3	N4	N5		
2	2.6396	2.0510	2.54743	2.54751	1.3439	2.2259	0.5446
4	6.7766	6.8326	6.87294	4.98077	8.7804	6.8487	1.34414
6	9.8505	10.7644	9.96204	9.20287	11.7794	10.3119	0.99042
8	13.0959	12.3713	13.2622	12.3205	13.4437	12.8987	0.51975
10	15.7896	15.3563	15.9243	15.517	15.4139	15.6002	0.24598
12	17.4540	17.5621	17.4922	17.207	17.9070	17.5245	0.25226
14	19.5131	18.0294	19.6267	18.4342	19.3380	18.9883	0.71273
16	22.8247	20.2725	23.7505	23.3848	20.6507	22.1766	1.60554
20	21.5419	22.4508	24.8585	24.8021	23.0859	23.3478	1.46046
24	22.1956	23.0988	26.0349	25.5157	28.4974	25.0685	2.50121

Table G3 The percentage of cumulative release of [6]-gingerol from GPTG5

Time	% Cumulative release of [6]-gingerol					mean	SD
	N1	N2	N3	N4	N5		
2	0.0459	0.1467	0.0785	0.1683	0.9593	0.2797	0.3831
4	3.4615	2.8194	3.4161	2.0358	3.9640	3.1393	0.7383
6	5.1479	5.8387	5.0449	4.3108	8.0768	5.6838	1.4432
8	9.3085	9.1277	9.0088	8.7641	10.9492	9.4317	0.8711
10	10.4908	11.6892	10.3014	9.8909	12.6823	11.0109	1.1491
12	11.9305	11.7084	12.3569	11.9327	12.4112	12.0679	0.3032
14	13.0296	12.7683	13.6154	13.5846	15.2707	13.6537	0.9740
16	14.2285	14.0547	14.3781	14.6268	15.9365	14.6449	0.7519
20	14.8729	16.5182	15.1439	15.2504	17.4082	15.8387	1.0824
24	15.4016	15.0794	15.6951	15.7536	19.4159	16.2691	1.7794

Table G4 The percentage of cumulative release of [6]-gingerol from GPPG3

Time	% Cumulative release of [6]-gingerol					mean	SD
	N1	N2	N3	N4	N5		
2	11.4639	7.6884	11.6927	11.2707	8.5019	10.1235	1.8798
4	17.3058	14.5838	17.4241	14.4455	15.2201	15.7959	1.4625
6	21.9924	18.4147	21.2742	18.1214	18.9834	19.7572	1.7589
8	26.4443	21.4943	26.4939	24.0898	22.4906	24.2026	2.2668
10	29.4699	24.1015	29.7374	27.2613	24.9912	27.1122	2.5513
12	31.5243	28.2441	32.1926	27.8356	29.4596	29.8512	1.9417
14	33.3692	29.8352	33.2407	30.8584	30.4678	31.5543	1.6400
16	35.7414	28.4807	34.2563	32.1970	28.8098	31.8970	3.2264
20	29.9891	33.4873	31.7814	30.7756	34.1615	32.0390	1.7654
24	34.7907	34.9496	31.3175	28.8587	36.8222	33.3477	3.2013

Table G5 The percentage of cumulative release of [6]-gingerol from GBTG3

Time	% Cumulative release of [6]-gingerol					mean	SD
	N1	N2	N3	N4	N5		
2	2.2652	0.0782	2.5008	2.7537	0.2410	1.5678	1.2983
4	6.8899	2.5016	6.5901	7.9719	3.4233	5.4754	2.3733
6	10.3143	5.0389	10.4242	11.0914	9.2006	9.2139	2.4306
8	13.2994	8.3388	13.1559	13.4983	9.4204	11.5426	2.4638
10	14.8472	10.6958	14.2380	14.1379	11.4290	13.0696	1.8704
12	16.1258	11.1547	15.7833	16.8214	12.7171	14.5205	2.4519
14	17.6339	15.9757	17.3726	17.7215	13.4867	16.4381	1.7941
16	19.0312	16.3775	19.1036	19.0833	16.7653	18.0722	1.3771
20	18.5147	18.9905	19.4113	19.2859	18.8927	19.0190	0.3522
24	21.9010	20.2033	20.9852	19.6830	21.3465	20.8238	0.8868

Table G6 The percentage of cumulative release of [6]-gingerol from GBTG5

Time	% Cumulative release of [6]-gingerol					mean	SD
	N1	N2	N3	N4	N5		
2	0.8887	1.2370	0.9709	0.7702	0.1290	0.1290	0.4120
4	4.0603	4.7821	3.8598	5.2614	4.4525	4.4525	0.5620
6	6.9636	7.8138	7.0899	8.0789	8.6702	8.6702	0.7088
8	10.0901	10.4880	10.2666	10.6043	11.6667	11.6667	0.6162
10	12.7155	12.2864	12.1597	12.4865	13.0088	13.0088	0.3398
12	13.8414	15.5165	13.6765	13.7479	15.4022	15.4022	0.9360
14	16.2897	13.7329	15.9534	15.1603	16.0707	16.0707	1.0459
16	17.6488	18.9765	17.5770	18.1349	18.4059	18.8880	0.5763
20	18.5161	21.0432	18.6232	18.7373	19.5213	19.5558	1.0579
24	22.7859	22.7465	18.7628	18.4817	19.2398	20.2189	2.1740

Table G7 The release constant of [6]-gingerol from SLN formulations

Formulation	N1	N2	N3	N4	N5	mean	SD
GPTG3	3.7776	3.4425	3.8842	3.9144	3.4951	3.7028	0.2203
GPTG5	2.7998	2.7903	2.8804	2.9980	2.9404	2.8818	0.0895
GPPG5	4.6576	4.4673	4.8836	4.3037	4.7168	4.6058	0.2251
GBTG3	3.1794	3.2868	3.1224	3.0284	2.9717	3.1177	0.1242
GBPG5	3.3316	3.2349	3.2595	3.1413	3.4592	3.2853	0.1187

Table G8 One-way analysis of variance on the release rate constant of [6] – gingerol from SLN formulation

ANOVA

Release rate constant

	Sum of Squares	df	Mean Square	F	Sig.
Between Groups	9.185	4	2.296	83.931	0.000
Within Groups	0.547	20	2.736E-02		
Total	9.733	24			

Table G9 Homogeneous subset on the release rate constant of [6] – gingerol from SLN formulation by Duncan method

Release rate constant

Type of formulation	N	Subset for alpha = 0.05			
		1	2	3	4
GPTG5	5	2.8813			
GBTG3	5		3.1177		
GBTG5	5		3.2853		
GPTG3	5			3.7027	
GPPG3	5				4.6058
Sig.		1.000	0.125	1.000	1.000

Means for groups in homogeneous subsets are displayed.
a Uses Harmonic Mean Sample Size = 5.000.
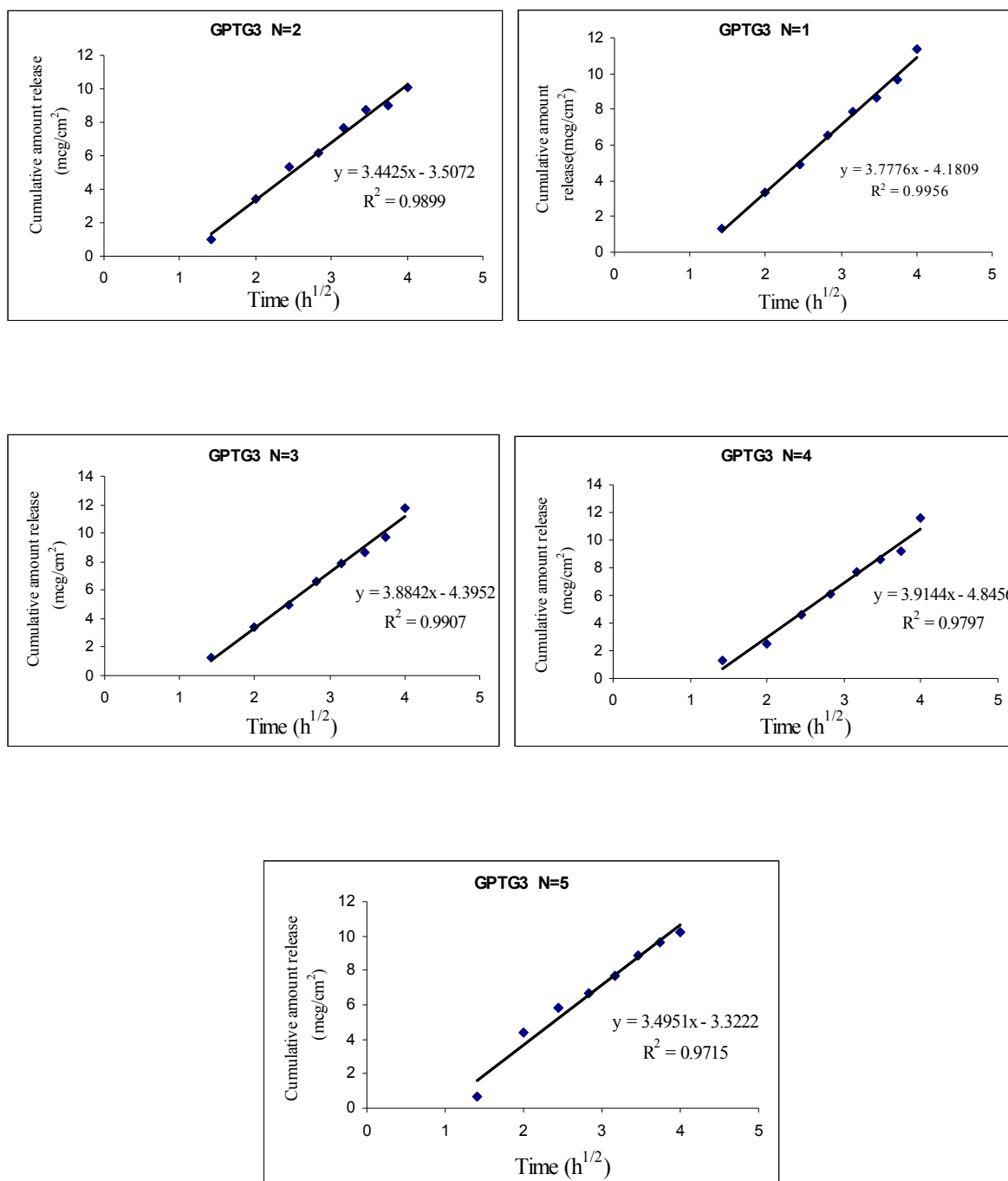
Figure G1 Cumulative releases of [6]-gingerol per unit area as a function of square root of time from GPTG3 formulations (n=5).
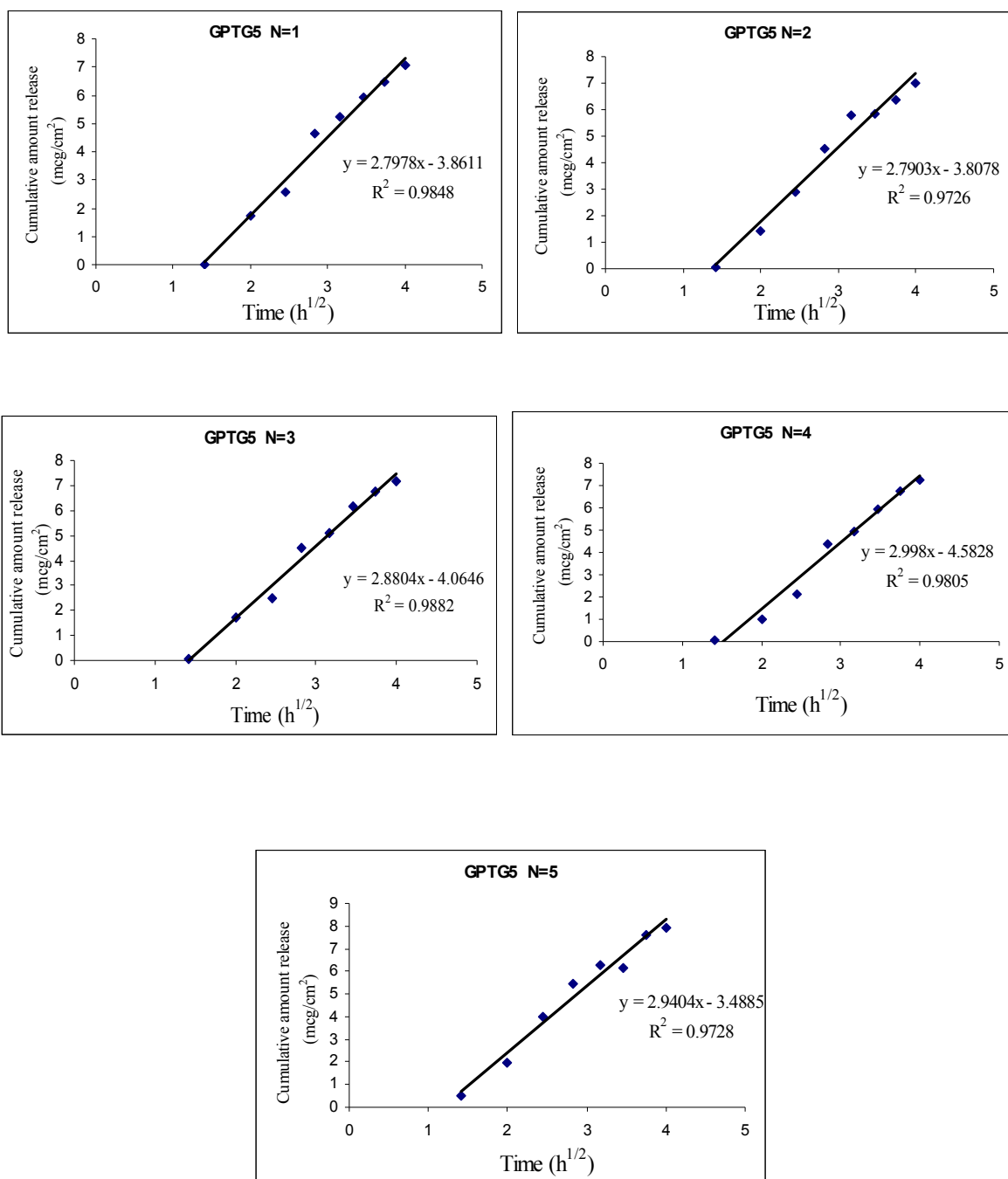
Figure G2 Cumulative releases of [6]-gingerol per unit area as a function of square root of time from GPTG5 formulations (n=5).
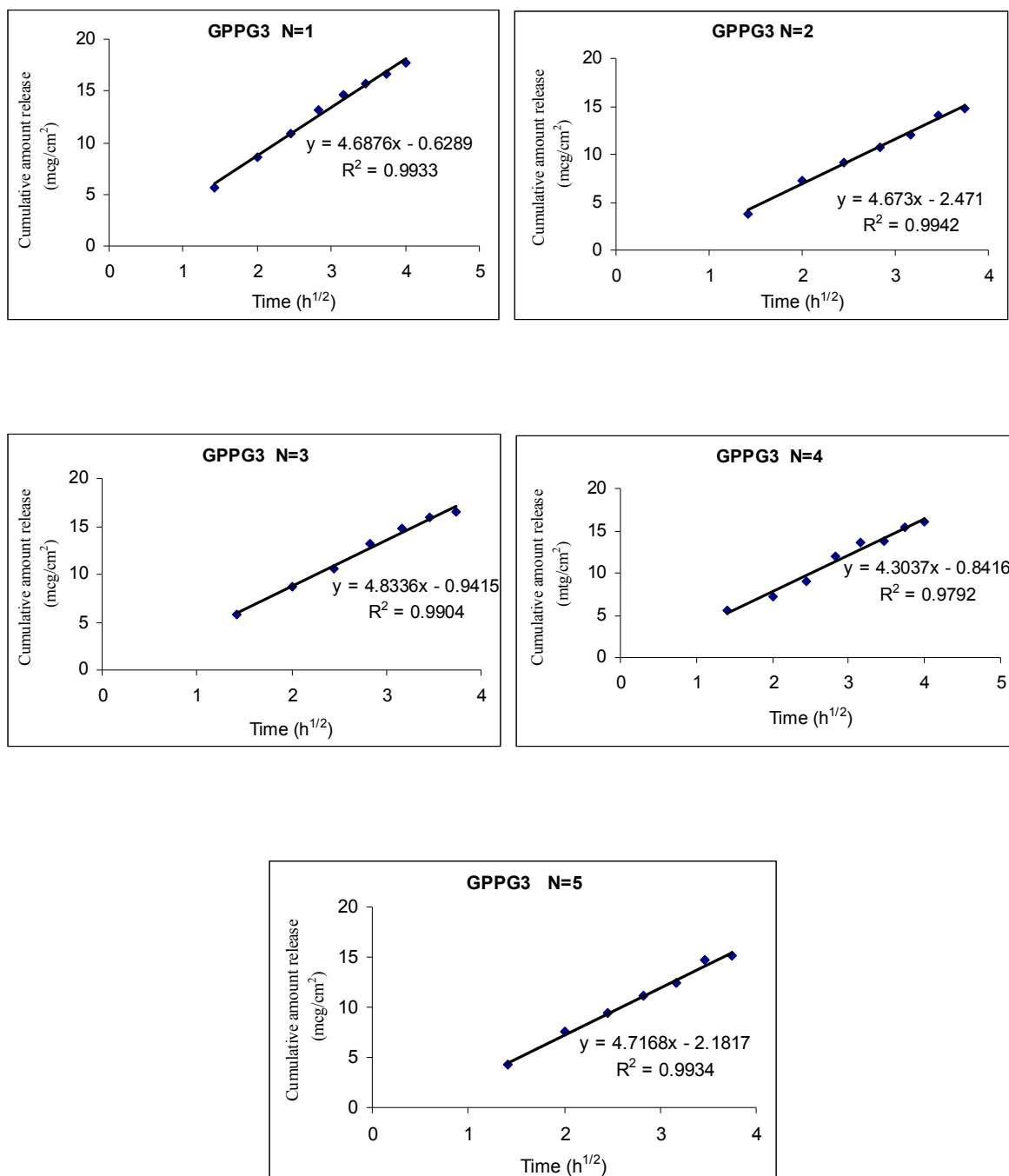
Figure G3 Cumulative releases of [6]-gingerol per unit area as a function of square root of time from GPPG3 formulations (n=5).
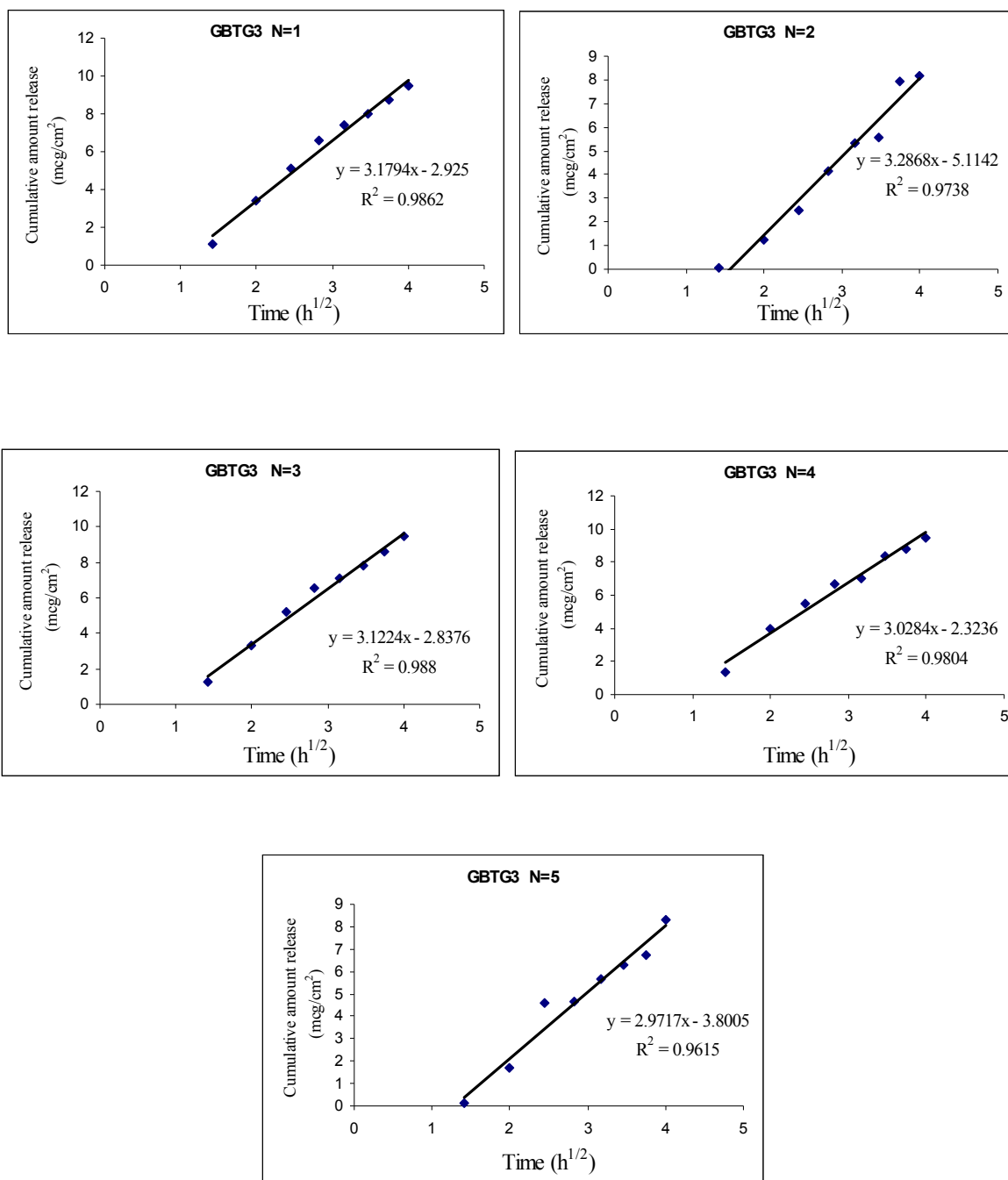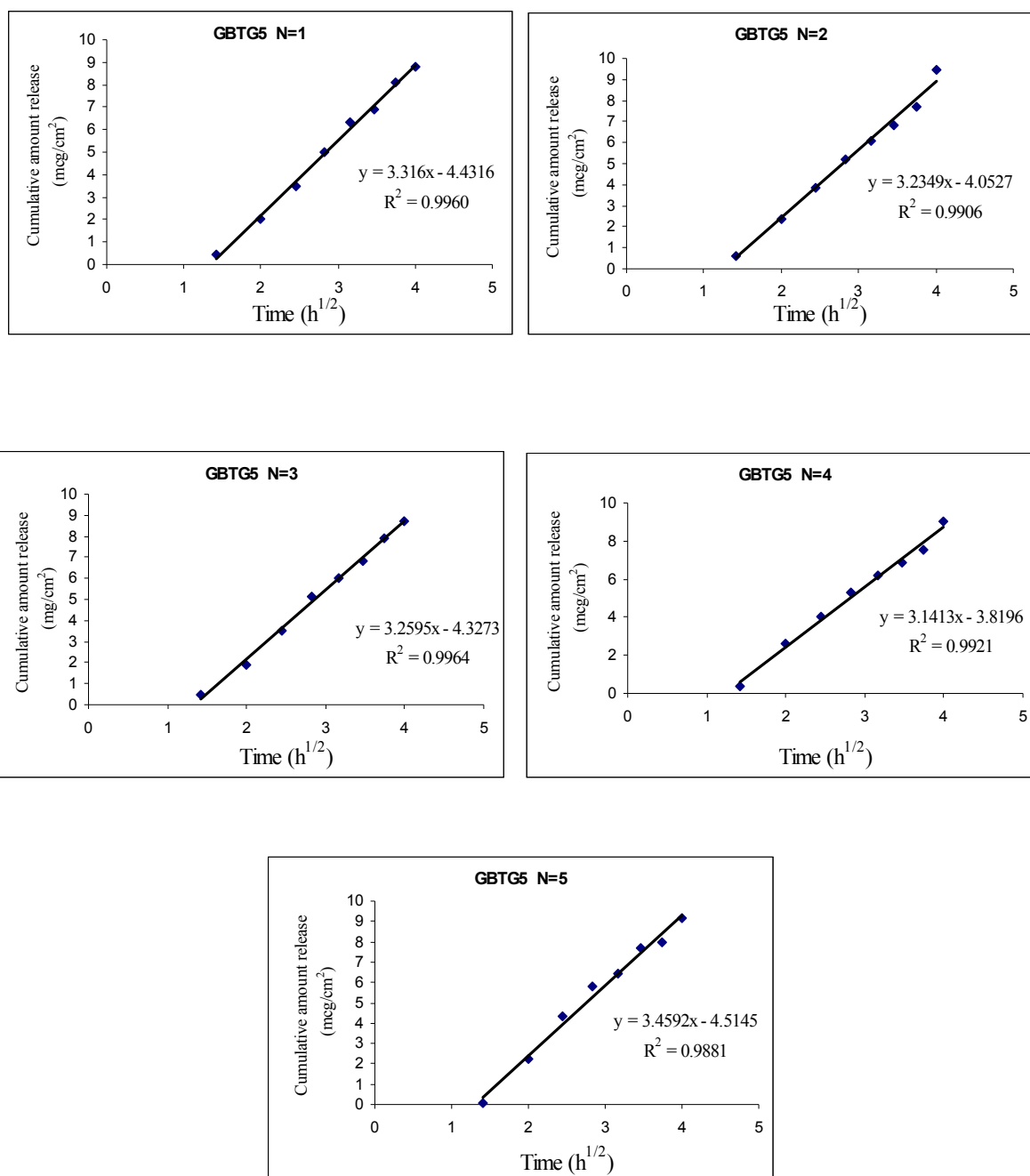
Figure G4 Cumulative releases of [6]-gingerol per unit area as a function of square root of time from GBTG3 formulations (n=5).

Figure G5 Cumulative releases of [6]-gingerol per unit area as a function of square root of time from GBTG5 formulations (n=5).

Appendix H

Permeation study

Table H1 The percentage of cumulative permeation of [6]-gingerol from GP+3TW80

Time	% Cumulative permeation of [6]-gingerol					mean	SD
	N1	N2	N3	N4	N5		
2	1.5662	1.3893	0.1981	0.4774	0.4774	0.8217	0.6129
4	1.7414	1.1012	1.8363	1.8976	1.5910	1.6335	0.3192
6	1.9621	1.4744	2.4308	2.7007	1.5883	2.0313	0.5288
8	2.3541	1.7277	3.1333	3.0547	1.9170	2.4374	0.6416
10	2.5772	1.8621	3.3593	3.1670	1.8566	2.5644	0.7052
12	2.6868	1.8621	3.4639	3.3217	2.8213	2.8312	0.6326
14	2.6868	1.8621	3.4601	4.8535	3.4050	3.2535	1.1048
16	2.6868	1.8621	4.5512	4.8535	3.4050	3.4717	1.2536
20	2.6868	1.8621	4.5512	4.8535	3.4050	3.4717	1.2536
24	2.6868	1.8621	4.5512	4.8535	3.4050	3.4717	1.2536

Table H2 The percentage of cumulative permeation of [6]-gingerol from GP+5TW80

Time	% Cumulative permeation of [6]-gingerol					mean	SD
	N1	N2	N3	N4	N5		
2	0.7636	0.6947	0.0638	0.4708	0.4774	0.4940	0.2733
4	1.0695	0.6251	1.6397	1.3781	1.2888	1.2002	0.3809
6	1.5443	1.1057	1.8445	1.8026	1.6259	1.5846	0.2949
8	1.9081	1.2508	2.5508	2.8374	1.3303	1.9755	0.7106
10	2.2236	1.3620	2.8871	2.5537	1.6365	2.1326	0.6314
12	2.2236	1.3620	3.2028	3.0752	1.7401	2.3207	0.8082
14	2.2236	1.3620	3.2028	3.6077	2.8449	2.6482	0.8805
16	2.2236	1.3620	3.2028	3.8547	2.8449	2.6976	0.9519
20	2.2236	1.3620	3.2028	3.8547	2.8449	2.6976	0.9519
24	2.2236	1.3620	3.2028	3.8547	2.8449	2.6976	0.9519

Table H3 The percentage of cumulative permeation of [6]-gingerol from GP+5P188

	% Cumulative permeation of [6]-gingerol						
Time	N1	N2	N3	N4	N5	mean	SD
2	1.6947	1.6016	0.4709	0.9722	1.1737	1.1826	0.4972
4	1.9238	1.7831	2.9033	2.6117	2.9524	2.4349	0.5488
6	2.1364	1.9674	3.2029	3.1393	3.2076	2.7307	0.6231
8	2.9639	2.2626	3.4081	4.6419	3.8059	3.4165	0.8930
10	2.9639	2.2626	5.4591	5.8758	4.2875	4.1698	1.5555
12	2.9639	2.2626	5.4827	5.9415	5.6581	4.4618	1.7134
14	2.9639	2.2626	5.1292	5.9415	5.6581	4.3911	1.6674
16	2.9639	2.2626	6.4617	5.9415	5.6581	4.6576	1.9045
20	2.9639	2.2626	6.4617	5.9415	5.6581	4.6576	1.9045
24	2.9639	2.2626	6.4617	5.9415	5.6581	4.6576	1.9045

Table H4 The percentage of cumulative permeation of [6]-gingerol from acetone extract solution

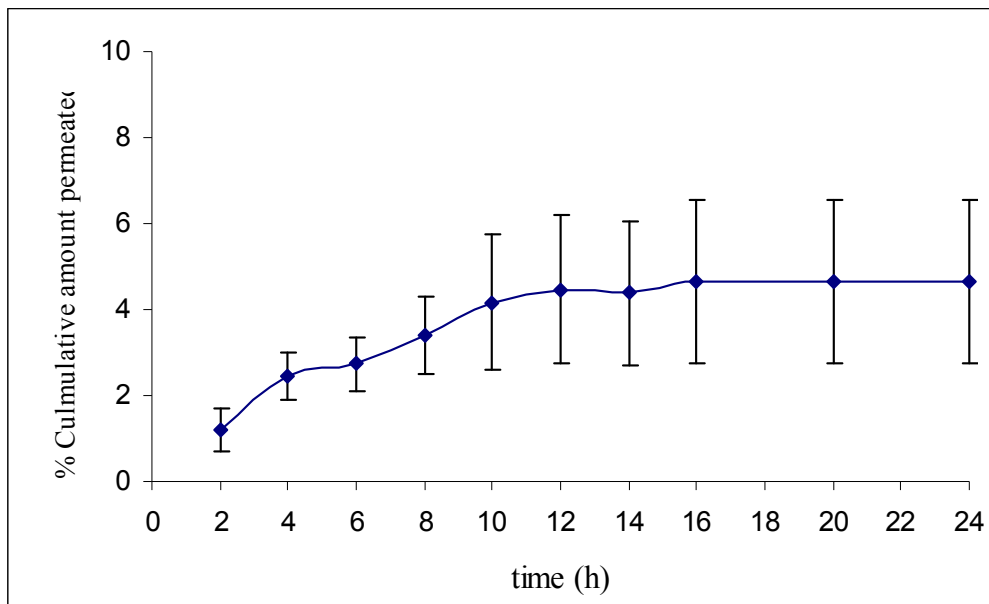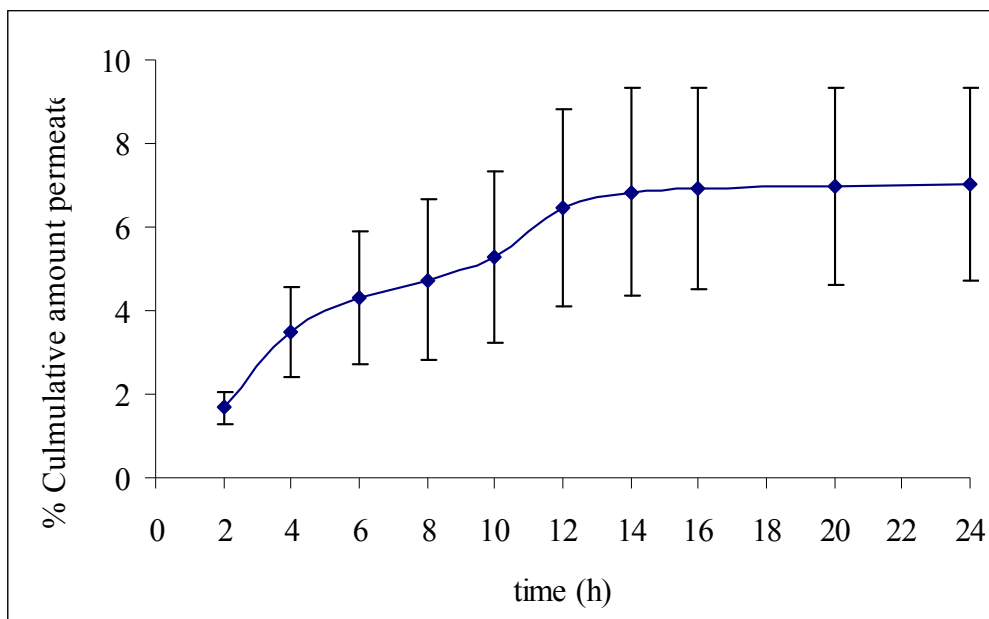|	% Cumulative permeation of [6]-gingerol						
Time	N1	N2	N3	N4	N5	mean	SD
2	2.1398	1.9666	1.2258	1.3730	1.6949	1.6800	0.3855
4	2.4156	2.2393	4.2138	4.6199	3.9268	3.4831	1.0851
6	2.6014	2.5401	5.3448	5.7465	5.3110	4.3088	1.5959
8	2.5245	2.8219	6.0272	6.4947	5.8441	4.7425	1.9067
10	2.9128	3.2389	6.8937	7.1423	6.2478	5.2871	2.0480
12	3.8734	3.9213	8.1669	8.3369	8.1039	6.4805	2.3597
14	4.0324	4.2238	8.9493	8.3369	8.6627	6.8410	2.4869
16	4.3508	4.2238	8.9493	8.3369	8.7941	6.9310	2.4242
20	4.5742	4.2238	8.9493	8.3369	8.7941	6.9757	2.3662
24	4.7975	4.2238	8.9493	8.3369	8.7941	7.0203	2.3109
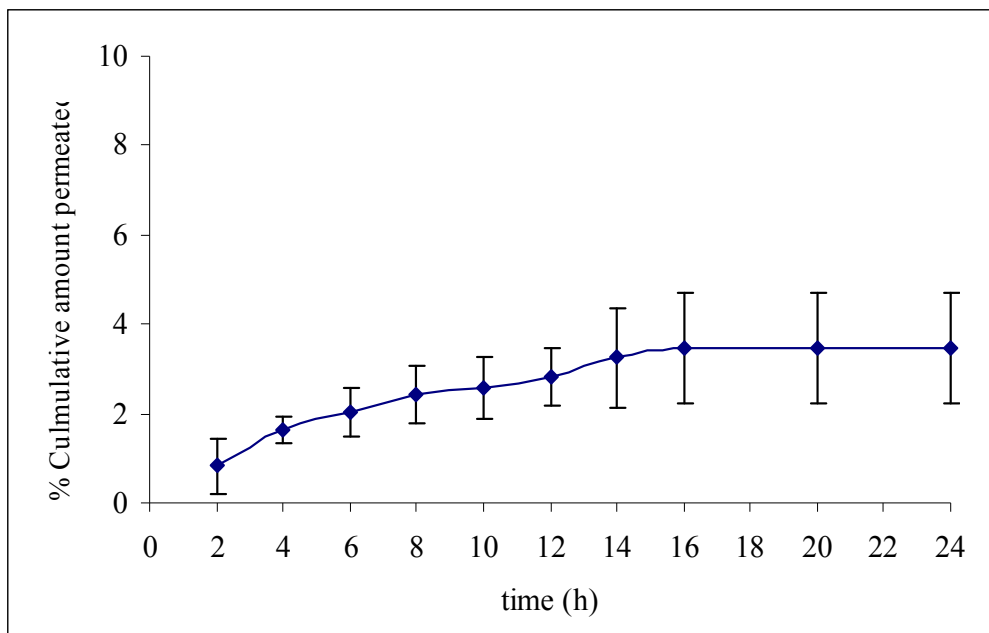
(a)
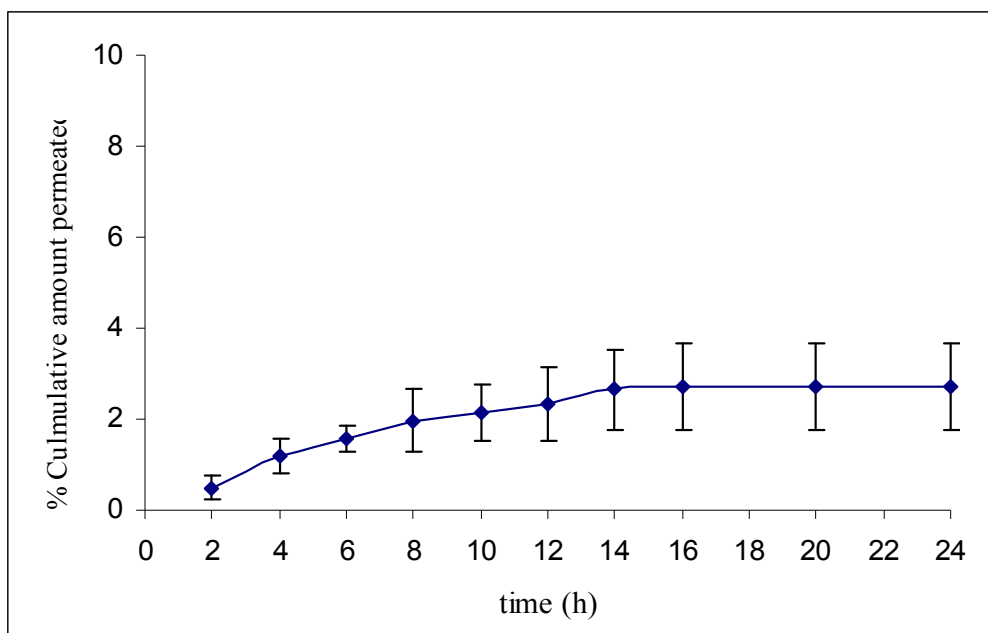
(b)

Figure H1 The permeation profile of [6]-gingerol from (a) GP+3Tw80,

(b) GP+5Tw80, (c) GP+3P188 and (d) acetone extract solution, (mean ± SD, n=5)

(c)

(d)

Figure H1 (continued) The permeation profile of [6]-gingerol from (a) GP+3Tw80, (b) GP+5Tw80, (c) GP+3P188 and (d) acetone extract solution, (mean ± SD, n=5)
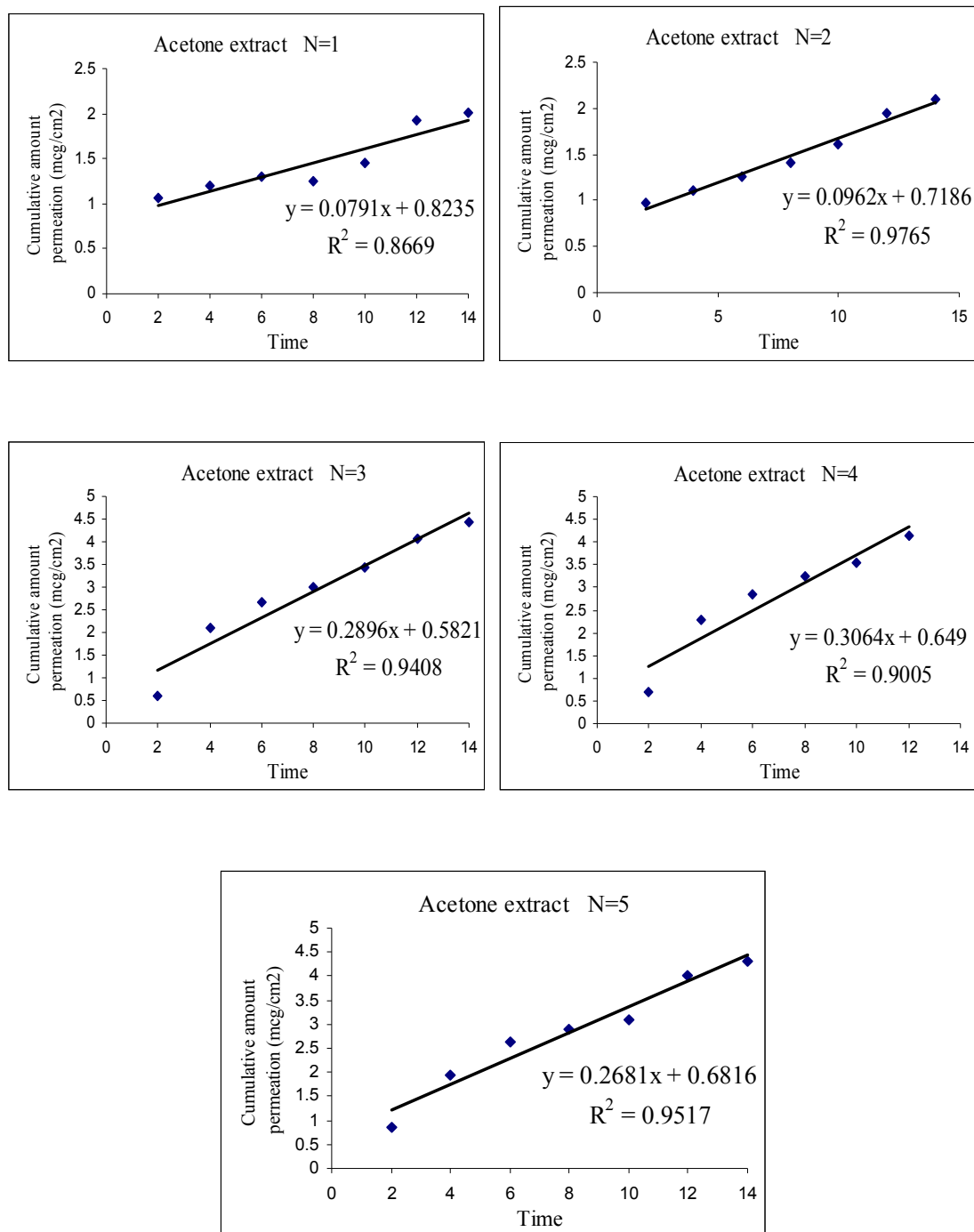
Figure H2 Cumulative permeation of [6]-gingerol per unit area as a function of time from acetone extract solution (n=5)
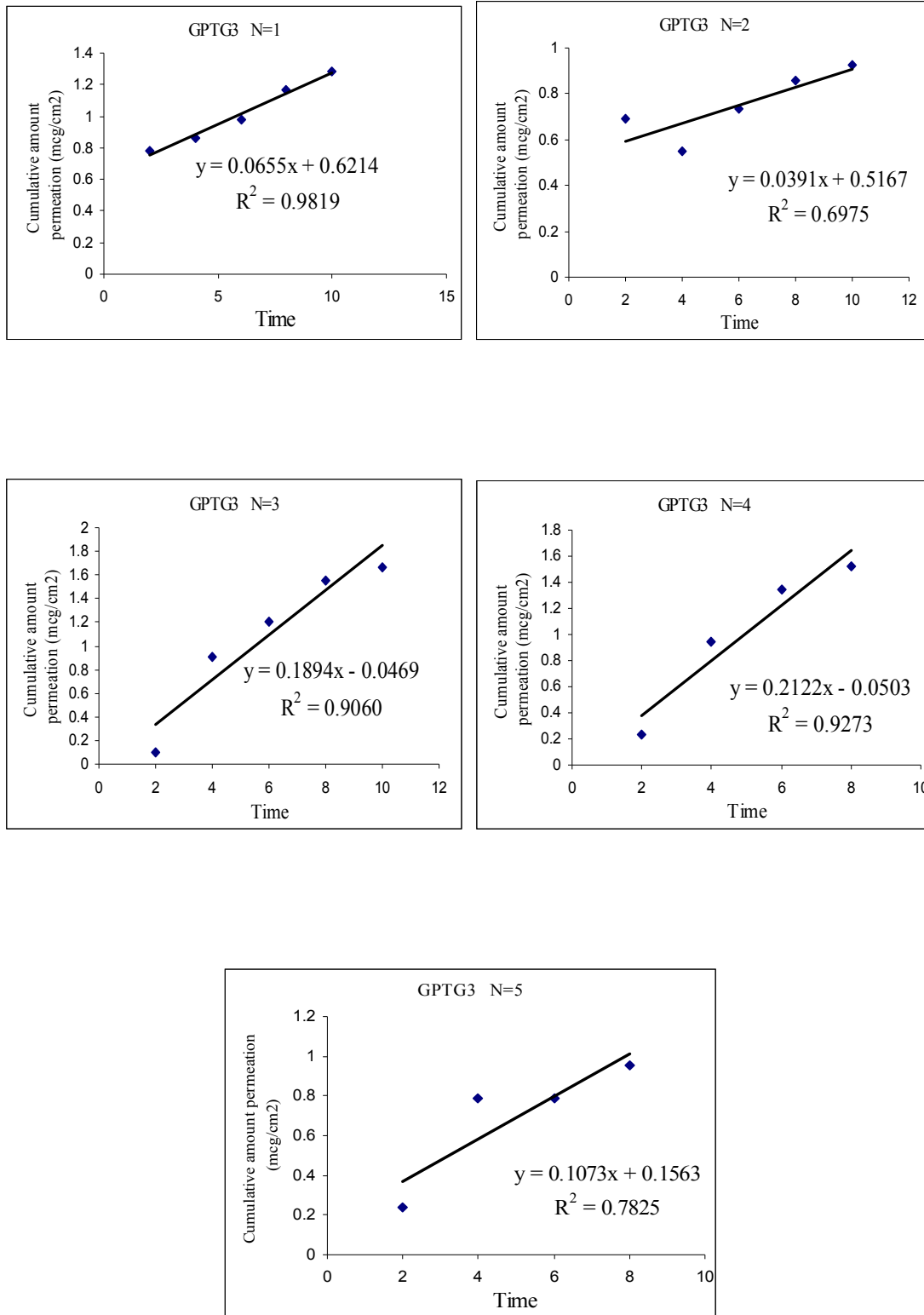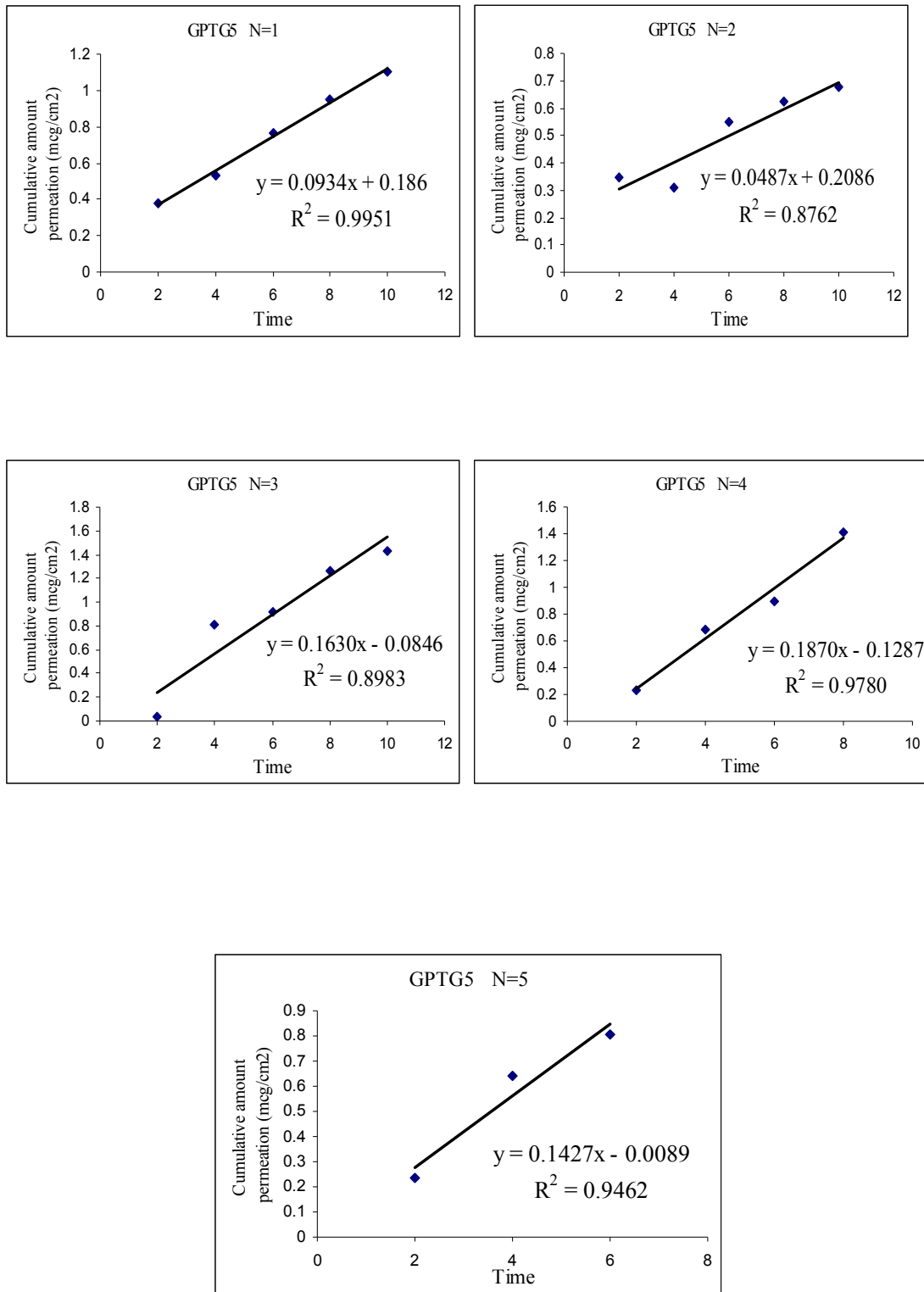
227

Figure H3 Cumulative permeation of [6]-gingerol per unit area as a function of time
from GPPTG3 formulations (n=5)

Figure H4 Cumulative permeation of [6]-gingerol per unit area as a function of time
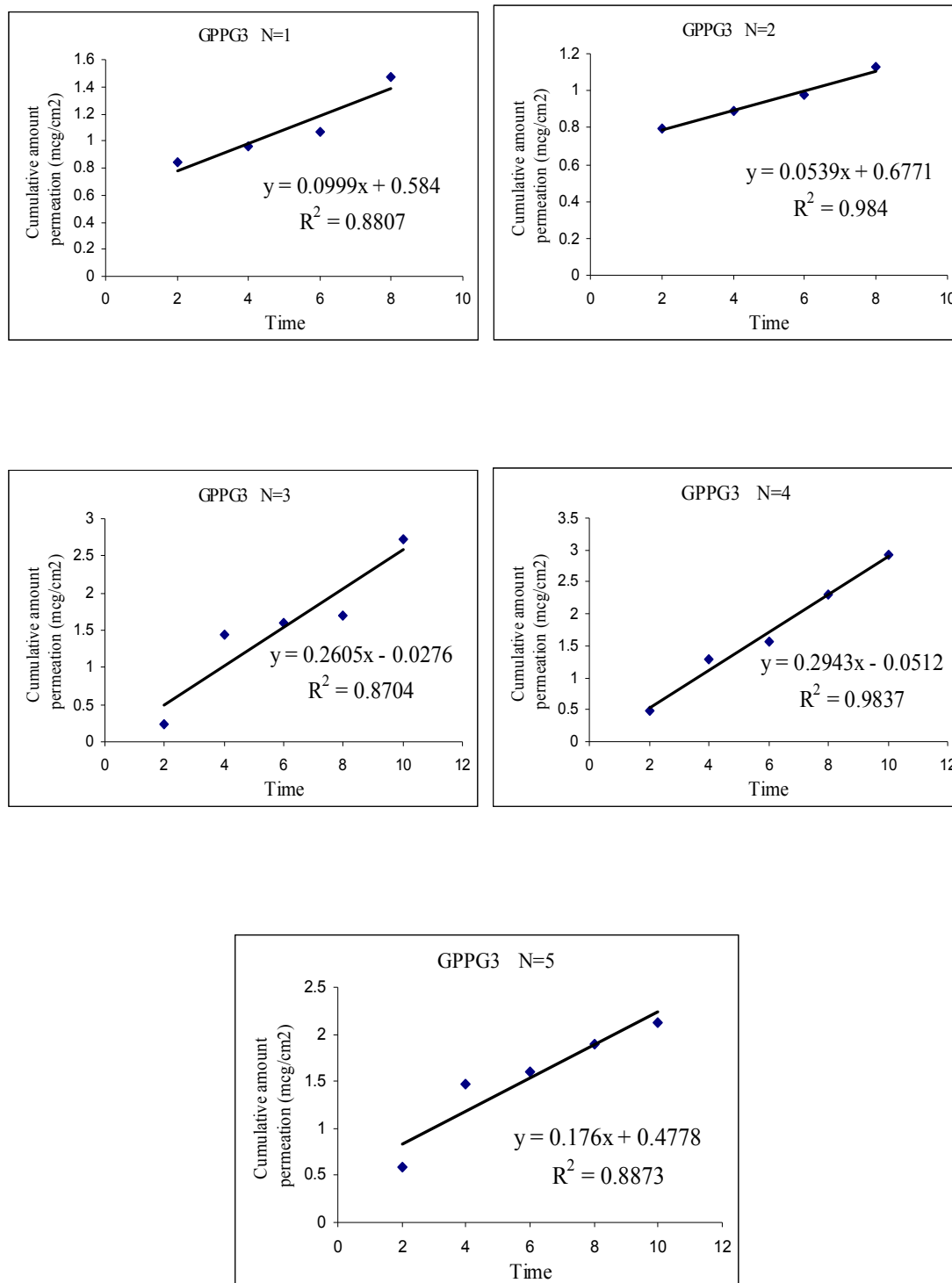from GPPTG5 formulations (n=5)

Figure H5 Cumulative permeation of [6]-gingerol per unit area as a function of time from GPPPG3 formulations (n=5)

ANOVA

Table H5 One-way analysis of variance on the permeation rate constant of
[6] – gingerol from SLN formulations

ANOVA

Permeation rate constant

	Sum of Squares	df	Mean Square	F	Sig.
Between Groups	2.527E-02	3	8.423E-03	1.067	0.391
Within Groups	0.126	16	7.891E-03		
Total	0.152	19			

Appendix I

Materials for SLN formulation

1. Glyceryl palmitostearate (Kibbe, A.H., 2000)

1.1 Chemical name

Octadecanoic acid, 2, 3-dihydroxylpropyl ester mixed with 3-hydroxy-2-[(1-oxohexadecyl)-oxyl] propyl octadecanoate, 2-[1-oxohexadecyl)-oxy]-1,3-propanediyl dioctadecanoate and 1,2,3-propane triol

1.2 Empirical formula

Glyceryl palmitostearate is a mixture of mono-, di-, tri-glycerides of C_{16} and C_{18} fatty acids.

1.3 Appearance

Glyceryl palmitostearate is fine powder with a faint odor.

1.4 Typical properties

Melting point   : 52-55 ˚C

Saponification vale : 1745-195

Solubility   : freely soluble in chloroform and dichloromethane; practically insoluble in ethanol (95%), mineral oil, and water.

1.5 Stability

Glyceryl palmitostearate should not be stored at temperature above 35˚C in an airtight container, protected from light and moisture.

1.6 Safety

Glyceryl palmitostearate is generally regarded as an essential nontoxic and nonirritant material.

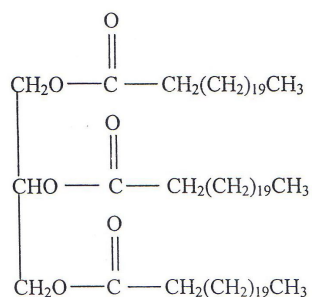**2. Glyceryl behenate** (The Council of Europe, 2001; Kibbe, A.H., 2000)

2.1 Chemical name

Glycerobehenate

Glycerol dibehenate

2.2 Empirical formula

Glyceryl behenate is a mixture of mono-, di-, and tri-glycerides of C_{20} fatty acid ($C_{69}H_{134}O_6$)

2.3 Structural formula

2.4 Appearance

Glyceryl behenate is fine powder or white or almost white with a faint odor.

2.5 Typical properties

Melting point : 65-77°C

Saponification value : 145-164

Solubility : glyceryl behenate is insoluble in water, soluble in methylene chloride and partly soluble in alcohol.

2.6 Stability

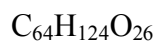Glyceryl behenate should be store in an airtight container, protected from light and moisture.

2.7 Safety

Glyceryl behenate is generally regarded as an essential nontoxic and nonirritant material.

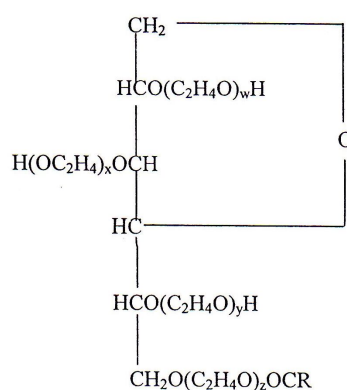**3. Tween®80** (Kibbe, A.H., 2000)

3.1 Chemical name

Polyoxyethylene 20 sorbitan monooleate

3.2 Emperical formula

$C_{64}H_{124}O_{26}$

3.3 Structural formula

$$\begin{array}{c}
CH_2 \\
HCO(C_2H_4O)_wH \\
H(OC_2H_4)_xOCH \\
HC \\
HCO(C_2H_4O)_yH \\
CH_2O(C_2H_4O)_zOCR
\end{array} \quad O$$

Polyoxyethylene sorbitan monoester

$w+x+y+z = 20$

R = oleic acid

3.4 Appearance

Tween®80 is a clear yellowish or brownish-yellow oily liquid with a faint characteristics odor, somewhat bitter taste. It has a HLB value of 15.0

3.5 Typical properties

HLB value : 15.0

Specific gravity at 25°C : 1.08

Viscosity : 425 mPa s

Solubility   : Tween®80 is miscible with water, alcohol, dehydrate alcohol, ethylacetate, and methyl alcohol; practically insoluble in liquid paraffin and fixed oils.

3.6 Stability

Tween®80 is stable to electolytes and weak acids and bases. It should be stored in a well-closed container, protected from light, in a cool, dry place.

3.7 Safety

Tween®80 is widely used in cosmetics, food products, parenteral and topical pharmaceutical formulations and is generally well tolerated, practically nonirritating and of very low toxicity. The WHO has set an estimated acceptable daily intake for Tween®80, calculated as total polysorbate esters, at up to 25 mg/kg.

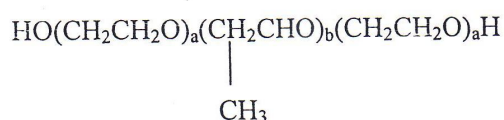## 4. Poloxamer 188 (Kibbe, A.H., 2000)

4.1 Chemical name

α- Hydro-ω-hydroxypropoly-(oxyethylene)-poly-(oxypropylene)-poly-(oxyethylene) block copolymer

4.2 Empirical formula

$HO\ (C_2H_4O)_a(C_3H_6O)_b(C_2H_4O)_aH$

4.3 Structural formula

$$HO(CH_2CH_2O)_a(\underset{\underset{CH_3}{|}}{CH_2CHO})_b(CH_2CH_2O)_aH$$

The poloxamer polyols are series of closely related block copolymers of ethylene oxide and propylene oxide.

Poloxamer   : 188
a   : 80
b   : 27
Average molecular weight : 7680-9510

4.4 Apperance

Poloxamer 118 generally occurs as white-colored, waxy, free flowing prilled granules or as cast solids. It is practically odorless and tasteless.

4.5 Typical properties

Melting point   : 52°C

HLB value   : 29

Solubility   : Poloxamer is freely soluble in water, ethanol, and isopropyl alcohol.

4.6 Stability

Poloxamer is stable material. Aqueous solution is stable in the presence of acid, alkali, and metal ion. However, aqueous solution does support mold growth. The bulk material should be stored in a well-closed container in a cool, dry place.

4.7 Safety

Poloxamer is used in variety of oral, parenteral and topical pharmaceutical formulations and is generally regarded ad nontoxic and nonirritant material. Poloxamer is not metabolized in the body.

VITA

Miss Petchompoo Siriphan was born on January 22, 1982 in Bangkok, Thailand. She received her Bachelor Degree in Pharmacy from the Faculty of Pharmaceutical Sciences, Chulalongkorn University in 2005. She continued the enrollment to the Master degree program in Pharmacy at Chulalongkorn University in the same year.